EVALUATION OF OPTICAL COHERENCE TOMOGRAPHY IN DETECTING INITIAL ENAMEL EROSION: *IN VITRO* AND *IN VIVO* STUDIES

AZWATEE ABDUL AZIZ

FACULTY OF DENTISTRY
UNIVERSITY OF MALAYA
KUALA LUMPUR

2019

EVALUATION OF OPTICAL COHERENCE TOMOGRAPHY IN DETECTING INITIAL ENAMEL EROSION: *IN VITRO* AND *IN VIVO* STUDIES

AZWATEE ABDUL AZIZ

THESIS SUBMITTED IN FULFILMENT OF THE REQUIREMENTS FOR THE DEGREE OF DOCTOR OF PHILOSOPHY

FACULTY OF DENTISTRY
UNIVERSITY OF MALAYA
KUALA LUMPUR

2019

UNIVERSITY OF MALAYA

ORIGINAL LITERARY WORK DECLARATION

Name of Candidate: **AZWATEE ABDUL AZIZ**

Matric No: **DHA 120006**

Name of Degree: **DOCTOR OF PHILOSOPHY**

Title of Thesis: **EVALUATION OF OPTICAL COHERENCE TOMOGRAPHY IN DETECTING INITIAL ENAMEL EROSION: *IN VITRO* AND *IN VIVO* STUDIES**

Field of Study: **CARIOLOGY**

I do solemnly and sincerely declare that:

(1) I am the sole author/writer of this Work;

(2) This Work is original;

(3) Any use of any work in which copyright exists was done by way of fair dealing and for permitted purposes and any excerpt or extract from, or reference to or reproduction of any copyright work has been disclosed expressly and sufficiently and the title of the Work and its authorship have been acknowledged in this Work;

(4) I do not have any actual knowledge, nor do I ought reasonably to know that the making of this work constitutes an infringement of any copyright work;

(5) I hereby assign all and every right in the copyright to this Work to the University of Malaya ("UM"), who henceforth shall be owner of the copyright in this Work and that any reproduction or use in any form or by any means whatsoever is prohibited without the written consent of UM having been first had and obtained;

(6) I am fully aware that if in the course of making this Work I have infringed any copyright whether intentionally or otherwise, I may be subject to legal action or any other action as may be determined by UM.

Candidate's Signature Date:

Subscribed and solemnly declared before,

Witness's Signature Date:

Name:

Designation:

ABSTRACT

Introduction: Enamel erosion is a problem of increasing clinical concern and early detection is difficult. A reliable tool that is able to detect minute changes on the enamel surface is indispensable. Optical Coherence Tomography (OCT) has significant potential for non-invasive, non-ionizing detection of the earliest signs of enamel erosion. Hence, the overarching goal of this study is to assess the potential of OCT to detect initial enamel erosion that could be used in clinical trials and oral health survey.

Aims: For the *in vitro* study, to evaluate the effect of early dental biofilm on OCT backscattered intensity, and to evaluate the effect of dental water-jet on acid-induced softened human enamel surfaces. For the *in vivo* study, to explore the utility of OCT in detecting initial enamel erosion, *in vivo*.

Methods: *In vitro* study, 80 enamel specimens were prepared, exposing 2 x 4mm^2 window. At baseline (t_1), specimens were subjected to acid challenge (citric acid for 30 min) and divided into four groups; (1) Control (immersed in de-ionised water for 3-days), (2) 1-Day_Biofilm, (3) 2-Day_Biofilm, and (4) 3-Day_Biofilm. Specimens from group 2, 3 and 4 were inoculated to produce early laboratory-cultivated biofilm for 1, 2 and 3 days, respectively. All specimens were then subjected to water-jet (WJ) for 20 sec. Swept Source OCT (SS-OCT) was used to scan the specimens at baseline (t_1), post-erosion (t_2), with biofilm (t_3) and post-WJ (t_4) time points. Surface Microhardness (SMH) was measured at t_1 and t_2. Repeated measures ANOVA was used to compare the data between time points, within each group. The *in vivo* study involved a two-phase (A and B) study with 22 subjects. In Phase-A, subjects were instructed to swish a total of 250 ml orange juice for 10 min, three times per day with three-hour interval for three consecutive days. In Phase B, the same protocol was followed with an addition of gum chewing for 15 min

after each swishing. OCT measurements were taken before and after each swishing, totalling of six time points per day ($t_1 – t_6$). Data was analysed using repeated measures ANOVA and paired t-test. The level of significance was set at $p<0.05$ for all studies.

Results: The *in vitro* results showed statistically significant increase ($p<0.05$) in Supra-surface integrated reflectivity ($IR_{biofilm}$) between t_2 and t_3 for all groups. Subsurface integrated reflectivity (IR_{sub}) results showed significant decrease ($p<0.05$) in 2-Day Biofilm group, however, a significant increase ($p<0.05$) was shown in 3-Day Biofilm group, between t_2 and t_3. Results also showed a significant reduction in SMH ($p<0.05$) at t_2, however, the reduction in enamel thickness (D) was not statistically significant. $IR_{biofilm}$ mean values showed no significant differences at t_4 ($p>0.05$) amongst all groups. The *in vivo* results revealed that there was a statistically significant increase in *IR* after repeated acid challenge ($p<0.05$) in day-1 of Phase B, at t_1, t_2 and t_3.

Conclusions: *In vitro*, biofilm on the enamel surface showed some effects on the OCT backscattered intensity. Results also showed that WJ application did not cause surface loss of softened enamel and the biofilm was not adequately removed. *In vivo* results showed higher intensities observed from the B-scans following acid challenges indicated that OCT could detect initial enamel erosion, however, quantitatively there was no significant difference. Thus, this study provides support for further development of OCT to be used as a tool to detect minute changes of the initially eroded enamel surface.

Keywords: *In vivo*, initial erosion, optical coherence tomography, biofilm, dental water jet.

ABSTRAK

Pengenalan: Hakisan enamel adalah masalah klinikal yang semakin meningkat dan pengesanan awal adalah sukar. Alat yang boleh digunakan untuk mengesan perubahan kecil pada permukaan enamel adalah amat diperlukan. Tomografi Koheren Optik (OCT) berpotensi tinggi untuk pengesanan tanpa invasi, tanpa ionisasi bagi mengesan tanda-tanda awal hakisan enamel. Oleh itu, tujuan utama kajian ini adalah untuk menilai potensi OCT untuk mengesan hakisan enamel di peringkat awal yang mungkin boleh digunakan dalam percubaan klinikal dan juga bagi tujuan kaji selidik dalam bidang kesihatan mulut. **Tujuan:** Untuk kajian *in vitro*, pertamanya adalah untuk menilai kesan biofilm awal pergigian pada intensiti *backscattered* bagi OCT. Kedua, untuk menilai kesan jet air pergigian pada permukaan enamel gigi manusia yang dicerna oleh asid. Tujuan kajian *in vivo* pula adalah untuk meneroka kebolehan penggunaan OCT dalam mengesan hakisan awal enamel.

Kaedah: Dalam kajian *in vitro*, 80 spesimen enamel disediakan, mendedahkan tingkap berukuran 2 x 4 mm^2. Pada bacaan dasar (t_1), spesimen didedahkan pada cabaran asid (asid sitrik selama 30 minit) dan dibahagikan kepada empat kumpulan; (1) kawalan (direndam di dalam air terionisasi selama 3 hari), (2) 1-hari Biofilm 1 hari, (3) 2-hari Biofilm, dan (4) 3-hari Biofilm. Spesimen dari kumpulan 2, 3 dan 4 diinokulasikan bagi menghasilkan biofilm awal yang dikultur di makmal untuk 1, 2 dan 3 hari, masing-masing. Semua spesimen kemudiannya tertakluk kepada jet-air (WJ) selama 20 saat. Swept-Source OCT (SS-OCT) digunakan bagi mengimbas spesimen pada garis dasar (t_1), selepas-hakisan (t_2), dengan biofilm (t_3) dan selepas WJ (t_4). *Surface Microhardness* (SMH) diukur pada t_1 dan t_2. *Repeated measures* ANOVA digunakan bagi membandingkan data antara titik-titik masa, dalam setiap kumpulan. Kajian *in vivo* pula melibatkan dua fasa (A dan B) di mana 22 subjek terlibat dalam setiap. Dalam Fasa A,

subjek dikehendaki berkumur dengan sejumlah 250 ml jus oren selama 10 minit, tiga kali sehari, setiap tiga jam selama tiga hari berturut-turut. Dalam Fasa B, protokol yang sama diikuti dengan penambahan gula-gula getah selama 15 minit selepas setiap kumuran. Pengukuran OCT telah diambil sebelum dan selepas setiap kumuran, berjumlah enam kali sehari (t_1 - t_6). Data dianalisa menggunakan *Repeated measures* ANOVA dan *paired t-test*. Tahap signifikan ditetapkan pada $p < 0.05$ untuk semua kajian.

Keputusan: Keputusan kajian *in vitro* menunjukkan peningkatan ketara secara statistik ($p<0.05$) dalam refleksiviti bersepadu Supra-permukaan ($IR_{biofilm}$) antara t2 dan t3 untuk semua kumpulan. Bagi sub-permukaan refleksiviti bersepadu (IR_{sub}), hasil kajian menunjukkan penurunan ketara ($p < 0.05$) dalam kumpulan 2-hari Biofilm, tetapi peningkatan yang ketara ($p < 0.05$) ditunjukkan dalam kumpulan 3-hari Biofilm, antara t_2 dan t_3. Keputusan juga menunjukkan pengurangan ketara dalam SMH ($p < 0.05$) pada t_2, namun begitu, pengurangan ketebalan enamel (*D*) adalah tidak signifikan secara statistik. Purata nilai $IR_{biofilm}$ menunjukkan tiada perbezaan yang signifikan pada t_4 ($p>0.05$) di antara semua kumpulan. Hasil kajin *in vivo* menunjukkan bahawa terdapat perbezaan signifikan secara statistik bagi nilai *IR* selepas cabaran asid ($p < 0.05$) hanya pada hari pertama Fasa B, di t_1, t_2 dan t_3.

Kesimpulan: Dalam kajian *in vitro*, biofilm pada permukaan enamel menunjukkan beberapa kesan terhadap intensiti *backscattered* OCT. Keputusan kajian juga menunjukkan bahawa aplikasi WJ tidak menyebabkan kehilangan permukaan lembut enamel dan biofilm tidak disingkirkan dengan secukupnya. Hasil kajian *in vivo* menunjukkan intensiti yang lebih tinggi yang dilihat dari *B-scan* selepas cabaran asid menunjukkan bahawa OCT dapat mengesan hakisan enamel awal, namun secara kuantitatif tidak terdapat perbezaan yang signifikan. Oleh itu, kajian ini memberi

sokongan untuk pembangunan lanjut OCT untuk digunakan sebagai alat untuk mengesan perubahan awal permukaan enamel yang terhakis.

Kata kunci: *In vivo*, hakisan awal, tomografi koheren optik, biofilm, jet-air pergigian.

ACKNOWLEDGEMENT

This thesis would not have been possible without the help of my family, friends and people at the Faculty of Dentistry, University of Malaya. There are too many to name individually however a certain few deserve special thanks.

Assoc. Prof. Dr Chew Hooi Pin, Dr Maria Angela Gonzalez; and Prof. Noor Hayaty Abu Kasim, I owe the biggest thanks to my supervisors. They guided and helped me through the process impeccably and have always provided amazing advice and encouragement. Without them this thesis would not be possible. They have given me the strongest foundations to further my scientific career and helped me grow academically, professionally and personally.

Dr Christian Zakian; I also owe a big thank you who has helped me along the process of data analysis.

Pn. Faraliza, En. Anuar, Pn Zarina, Pn Helen and En. Hassan for their advice, ideas and help with all laboratory related matters.

All my colleagues and friends; whom I have shared this journey more closely than others and whom have endured the ups and downs but always provided sound advice and encouragement when I needed it most.

My beloved parents, Abdul Aziz and Shamsina; my two dearest sisters, Azleen and Azureen; they have been with me through the whole journey. They have always given me emotional support and help.

My husband, Mazli and dearest kids; Alif, Arif and Alya, they are my pillars of strength, without them, I may not reach this far.

I am forever grateful to the people mentioned above and also the ones that are not. I thank them again for their patience and help during this process that has had its many hurdles and tears. THANK YOU….

Funding:

The work was supported by

1. The University of Malaya and High Impact Research Grant, Ministry of Higher Education, Malaysia (UM-MOHE HIR Grant UM.C/HIR/MOHE/DENT/11, no. H-18001-00-C000011).
2. Postgraduate Research Grant (PPP) - PG188-2015B.

TABLE OF CONTENTS

LIST OF FIGURES

LIST OF TABLES

LIST OF SYMBOLS AND ABBREVIATIONS

BHI	:	Brain Heart Infusion
D	:	Enamel thickness
DEJ	:	Dentine-enamel junction
FC	:	Fractional change
IR	:	Integrated Reflectivity
$IR_{biofilm}$	:	Supra-surface Integrated Reflectivity
IR_{sub}	:	Subsurface Integrated Reflectivity
KHN	:	Knoop Hardness Number
ROI	:	Region of interest
SMH	:	Surface Microhardness
OCT	:	Optical Coherence Tomography
ΔSMH	:	Fractional change of Surface Microhardness
$\Delta\ IR_{biofilm}$	:	Fractional change of the Integrated Reflectivity (supra-surface)
$\Delta\ IR_{sub}$	:	Fractional change of the Integrated Reflectivity (subsurface)

LIST OF APPENDICES

CHAPTER 1: INTRODUCTION

1.1 Preface

The thesis consists of six chapters. It begins with the first chapter which includes an overview and a general introduction of the whole study, followed by the second chapter which is a review of the literature. Chapters three and four are the experimental chapters which follow a similar layout. Each chapter has an introduction which includes clinical relevance and aim and objectives, followed by literature review specific to that chapter. The materials and methods directly related to that chapter and its experiments are then presented followed by the results and discussion.

Chapter three investigates the effect of early biofilm on the measurement of initial enamel erosion using Optical Coherence Tomography (OCT) on *in vitro* erosive wear. Chapter four investigates the effect of dental water jet application on softened human enamel surfaces on *in vitro* erosive wear.

Chapter five uses the knowledge gained from the previous two chapters to appropriately design the protocol for the *in vivo* study. The first part describes a pilot investigation for the subsequent *in vivo* evaluation of initial enamel erosion using OCT. The second part of Chapter five describes the actual clinical study with the protocol modified from the results gained from the pilot study. The *in vivo* study aimed to assess the potential of optical coherence tomography in the detection of initial enamel erosion *in vivo* for a clinical trial. Lastly, Chapter six includes final conclusions and suggestions for future work.

1.2 Background

Dental erosion is a process where acid is responsible in dissolving enamel and dentine surfaces, which involves a chemical process, and the source of acid is other than bacteria (Stenhagen, Hove, Holme, & Tveit, 2013). Sources of acid exposure can be extrinsic (from outside the body) or intrinsic (from within the body). Extrinsic acid can be found in many everyday drinks and foods, such as fruit juice, carbonated drinks, sports drinks and citrus fruit. Also, medications or supplements such as Vitamin C, aspirin and some iron preparations may also contribute to the acid exposure. People who suffers from gastric reflux or recurrent vomiting are the ones with high risk of intrinsic exposure (Zero & Lussi, 2005).

In the initial stage of enamel erosion, a superficial dissolution of the enamel surface will occur which is due to the initial acid attacks. The process involves histological changes and also modifications of the mechanical and physical properties (surface softening) of the tooth where minerals are released to the erosive acid (Schlueter, Hara, Shellis, & Ganss, 2011). At this stage of erosion, it involves the softening and loss of some mineral content from the enamel surface, but the condition is totally reversible due to the presence of saliva where enamel can be re-mineralised and re-hardened. Furthermore, no surface loss will be observed yet at this early stage. However, if the exposure to acid continues, the softened layer may eventually be lost or worn away (Cheng, Wang, Cui, Ge, & Yan, 2009; Eisenburger, Hughes, West, Jandt, & Addy, 2000). Therefore, detection of erosion at this stage is critical because the remaining softened enamel can serve as a scaffold for new mineral. Prolongation of the challenge may result in further dissolution, ultimately leading to tissue loss that require complex restorations (Addy & Shellis, 2006).

1.3 Clinical Problem

The clinical diagnosis of dental erosion is best to distinguish acid-induced hard tissue loss from different forms of tooth wear, such as attrition, abrasion or abfraction. The diagnostic procedure aims to classify tooth wear based on clinically observed morphological features (Ganss & Lussi, 2014). A number of indices have been proposed to diagnose and quantify dental erosion, but there is a need for standardization of indices and for the development of practical diagnostic tools (Ganss & Lussi, 2014).

Currently, dental professionals normally estimate the progression of tooth wear of the patients by comparing consecutive study casts taken over long period of time (Pretty, Edgar, & Higham, 2004). This method may satisfy most clinical needs in deciding the patient's appropriate management which can be limited to restoration or prevention counselling. However, more accurate methods may be useful where detection of initial tooth erosion is possible so that preventive treatment can be decided immediately. Thus, it was realised that, an early detection and accurate diagnosis of enamel erosion is very important in arresting the progression of the lesions.

Quantitative methods such as ultrasonication (Eisenburger et al., 2000), profilometry (Ramos-Oliveira et al., 2017) and quantitative light-induced fluorescence (QLF) (Chew, Zakian, Pretty, & Ellwood, 2014) have been reported by different researchers as potential tools for diagnosing dental erosion more accurately. However, most of these methods have not yet been tested clinically or *in vivo*. Further research will determine whether they are suitable for measurement of tooth wear *in vivo* and thus, whether they should be recommended for use under clinical settings. At present, the clinical trials involving dental erosion are of the '*in situ*' design where subjects have to wear appliances with embedded enamel or dentine. The '*in situ*' design has added cost,

is uncomfortable to the subject and affects the salivary flow rate of the subjects due to the presence of an appliance in the mouth.

Given the lack of reliable methods to detect minute changes in tooth wear *in vivo*, current understanding of erosive tooth wear is primarily based on *in vitro* research. To date, a tool that can measure and monitor initial enamel erosion for *in vivo* assessment for erosion clinical trial has not yet been found, thus emphasizing the need for early detection of such lesion. Clinical trials are important that would provide information that is more relevant as it is done in an intra oral environment. Therefore, the possibilities for the quantitative *in vivo* diagnosis of initial enamel erosion and monitoring of the treatment efficiencies *in vivo* are very attractive long-term goals in dentistry.

Optical coherence tomography (OCT) is a relatively new non-invasive imaging technique that allows the acquisition of high-resolution, cross-sectional images of biological tissue based on the detection of backscattered light. OCT uses an optical signal to capture images using near-infrared light, which allows for high-resolution analysis of the tissue in question. In ophthalmology, for example, OCT is used to obtain images that can aid in assessing macular degeneration. Cardiology is also taking full advantage of this high-resolution analysis, as its imaging has provided the ability to image coronary arteries and the amount of biofilm within them (D. Huang et al., 1991). While this use is applicable in nearly all areas of the body, this study is mainly focusing its value in monitoring very early stage of enamel erosion.

This study may provide useful information regarding the potential and sensitivity of OCT in the diagnosis and monitoring of initial enamel erosion *in vivo*. If the results are positive, this will contribute to the availability of an objective tool for clinical trials which aim to evaluate the efficacy of anti-erosive products or the erosiveness of certain types of food and beverage. At present, the clinical trials involving dental erosion are of the '*in situ'* design where subjects had to wear appliances with embedded enamel or dentine. The

'*in situ*' design has added cost, is uncomfortable to the subjects and affects the salivary flow rate of the subjects due to the presence of an appliance in the mouth. Therefore, the overarching goal of this study is to assess the potential of OCT to detect initial enamel erosion that could be used in clinical trials and oral health survey.

1.4 Research Questions

1. Does Optical Coherence Tomography (OCT) has the potential to be used as a tool to detect initial enamel erosion in a clinical trial?
2. Does early dental biofilm has an effect on data captured by OCT?
3. What is the effect of dental water jet on initial enamel erosion?

1.5 Aims and Objectives

In alignment with the above research questions, this study is divided into three interrelated aims:

1.5.1 Aim 1 (Chapter 3)

To evaluate the effect of early dental biofilm on OCT backscattered intensity.

Objectives:

1. To cultivate early dental biofilm in a laboratory setting.
2 To study the attenuation of OCT signal through laboratory-cultivated oral biofilm of different intervals.
3. To study the change in OCT backscattering at the immediate tooth subsurface, with and without oral biofilm cultivated at different intervals.

Null hypotheses

1. OCT signals is not affected by laboratory-cultivated biofilm.
2. No changes in OCT backscattering at the immediate tooth subsurface, with and without oral biofilm cultivated at different intervals.

1.5.2 Aim 2 (Chapter 4)

To evaluate the effect of dental water jet on acid-induced softened human enamel surfaces and on the removal of biofilm.

Objectives:

1. To determine the enamel thickness of acid-induced softened human enamel following the application of dental water jet.
2. To evaluate the ability of dental water jet in removing laboratory-cultivated biofilm on acid-induced softened human enamel surface.

Null hypothesis:

1. The application of dental water jet has no effect on the enamel thickness of acid-induced softened human enamel.
2. The dental water jet is unable to remove laboratory-cultivated biofilm on acid-induced softened human enamel surface.

1.5.3 Aim 3 (Chapter 5)

To explore the utility of OCT in detecting initial enamel erosion, *in vivo*.

Objectives:

1. To induce initial enamel erosion *in vivo* without causing enamel surface loss.
2. To assess the ability of OCT in the detection of initial enamel erosion following acid challenge.
3. To evaluate the ability of OCT to detect the change in enamel backscattering after gum chewing.

Null hypothesis:

1. Initial enamel erosion *in vivo* will not result in enamel surface loss.
2. OCT is unable to detect initial enamel erosion following acid challenge.
3. OCT is unable to detect the change in enamel backscattering after gum chewing.

CHAPTER 2: LITERATURE REVIEW

2.1 Tooth wear

The term ‘tooth wear’ describes all types of non-carious tooth substance loss (B. G. Smith & Knight, 1984). It is commonly noted as the gradual loss of dental hard tissues other than by dental caries or trauma. Importantly, tooth wear may be as a direct result of complex process involving abrasion (wear produced by interaction between teeth and other materials), attrition (wear through tooth–tooth contact) and erosion (dissolution of hard tissue by acidic substances) (Addy & Shellis, 2006). It has been postulated that in a fourth wear related process (abfraction), abnormal occlusal loading predisposes cervical enamel to mechanical and chemical wear (Grippo, 1991). Summary of types of tooth wear is shown in **Table 2.1**.

Table 2.1: Types of tooth wear.

Abrasion	The physical wear of tooth surface through a mechanical process caused by factors other than tooth to tooth contact.
Attrition	The physiological wearing of teeth resulting from tooth to tooth contact with or without the presence of an abrasive substance between the teeth.
Erosion	The progressive loss of hard dental tissues by a chemical process not involving bacterial action.
Abfraction	Wedge-shaped defect at the cementoenamel junction of a tooth caused by eccentrically applied occlusal forces leading to tooth flexure.

2.2 Dental Erosion

Dental erosion is currently considered a near surface demineralisation, comprising two developmental stages. The initial erosive stage, termed dental erosion, corresponds to enamel softening, which results in losses of mechanical resistance and structural integrity (Ganss, Lussi, & Schlueter, 2014; Lussi, Schlueter, Rakhmatullina, & Ganss, 2011). The following process, so-called erosive tooth wear, occurs by either prolonged demineralisation of tooth surface or the action of mechanical factors such as abrasion and attrition, results in accelerated, pathological wear of the teeth that can lead to irreversible dental enamel loss (Ganss et al., 2014; Huysmans, Chew, & Ellwood, 2011; Lussi et al., 2011). Erosive tooth wear is a term used to describe the interaction of acids with mechanical tooth wear. It has recently been defined as the "chemical-mechanical process resulting in a cumulative loss of hard dental tissue not caused by bacteria" (Carvalho et al., 2015).

Although the terms dental erosion and dental erosive wear are often considered synonymous, in this thesis, this erosion-facilitated wear will be referred as "erosive tooth wear", reserving the term erosion only for the chemical process as defined above. Clinically, erosion does not often happen in isolation. Thus, the clinical condition of erosive tooth wear is recognised to have a multi-factorial aetiology rather than due to acid alone (Young et al., 2008).

2.2.1 Aetiology of dental erosion

Dental erosion is caused by constant contact between tooth surfaces and acidic substances. It has long been recognized that once the pH in the intra-oral environment reaches the critical threshold of 5.5, demineralisation of dental enamel will occur (Hicks, Garcia-Godoy, & Flaitz, 2004). According to Yan-Fang and Ren (2011), intra-oral acids can be originated from three main sources: produced *in situ* by acidogenic bacteria,

extrinsic acids from dietary components and intrinsic acids from the backflow f gastric contents. It is well known that extrinsic and intrinsic acids are the cause of dental erosion while acids of bacterial origin cause dental caries. Clearance of these acids from the oral cavity is, to a large extent, dependent on the saliva flow rate and the saliva buffering capacity. Furthermore, low saliva flow rate and poor buffering capacity allow prolonged retention of extrinsic and intrinsic acids in the mouth, which will increase the rate of the erosive process.

2.2.1.1 Extrinsic factors

Extrinsic acid can be found in many everyday foods and drinks, such as fruit juice (Lussi, Jaeggi, & Jaeggi-Scharer, 1995; Ren, Amin, & Malmstrom, 2009; West et al., 1998; Willershausen, Callaway, Azrak, & Duschner, 2008), carbonated soft drinks (Devlin, Bassiouny, & Boston, 2006; Kitchens & Owens, 2007; Maupome, Diez-de-Bonilla, Torres-Villasenor, Andrade-Delgado, & Castano, 1998; Moazzez, Smith, & Bartlett, 2000), sports drinks (Coombes, 2005; Milosevic, 1997; Rees, Loyn, & McAndrew, 2005) and wines (Chehal, Pate, Cohen, & Bhattacharyya, 2009; Mandel, 2005; Rees, Hughes, & Innes, 2002). Also, medications or supplements such as Vitamin C, aspirin and some iron preparations may also contribute to the acid exposure (Thomas, Vivekananda Pai, & Yadav, 2015).

Individuals who are in day-to-day exposure to acids at their work place are at a greater risk of increased dental erosion as a direct result of environmental factors. Examples of such professionals are battery factory workers, fertilizer factory workers, galvanizing factory workers, and workers exposed to etching and cleaning processes with the use of acids (Zero, 1996). Moreover, swimmers (Buczkowska-Radlinska, Lagocka, Kaczmarek, Gorski, & Nowicka, 2013) professional wine tasters (George, Chell, Chen, Undery, & Ahmed, 2014) or staff within the chemical industry, are also known to be at

greater risk of experiencing some degree of erosion as a direct result of the increased exposure of teeth to the acidic environment (Wiegand & Attin, 2007).

2.2.1.2 Intrinsic factors

Any disorder or behaviour known to cause acid backflow from the gastrointestinal tract into the oral cavity and subsequently making contact with teeth is recognised as an intrinsic factor. This acidic stomach content tends to backflow into the oral cavity due to malfunction of the oesophageal sphincter. Thus, the presence of the highly acidic gastric juice (pH 1.0-3.0) in the oral environment may lead to dental erosion. Thus, those who experience gastric reflux or recurrent vomiting are people who are at risk from intrinsic acid exposure (Zero & Lussi, 2005). Gastric juice consists mainly of hydrochloric acid, produced by the parietal cells in the stomach. Gastroesophageal reflux disease (GERD), bulimia and rumination are the main conditions associated with the backflow of gastric juice into the mouth (Picos, Chisnoiu, & Dumitrasc, 2013; Wilder-Smith, Materna, Martig, & Lussi, 2017).

Patients suffering from bulimia may ruminate multiple times daily over a prolonged period of time, which may cause typical dental hard tissue loss on the palatal aspect of the maxillary teeth. The prevalence of dental erosion is higher in bulimic patients than in non-bulimic controls (Rytomaa, Jarvinen, Kanerva, & Heinonen, 1998). Dental erosion in these patients is most likely associated with oral retention of regurgitated gastric contents. Furthermore, their dietary habits may include binging on high-energy foods and foods with high erosive potential, which may further exacerbate erosion (Rosten & Newton, 2017).

Chronic alcohol abuse is also associated with frequent vomiting and can cause gastrointestinal reflux. In addition, alcoholics may also consume potentially erosive alcoholic beverages on a regular basis. Thus, several studies reported an increased

prevalence of dental erosion in alcohol-dependent patients (Hede, 1996; B. G. Smith & Robb, 1989).

2.2.2 Erosion risk assessment

As mentioned earlier, extrinsic and intrinsic acids are the main aetiological factors for dental erosion. Therefore, erosion risk assessment mainly involves identification of these factors in a specific patient and an evaluation of their roles in the development of dental erosion. Established risk indicators of erosive wear according to the recent studies include frequent or high consumption of acidic drinks and dietary products (Bartlett et al., 2013; El Aidi, Bronkhorst, Huysmans, & Truin, 2011; Hasselkvist, Johansson, & Johansson, 2016; Muller-Bolla, Courson, Smail-Faugeron, Bernardin, & Lupi-Pegurier, 2015) as well as acidic reflux (Bartlett et al., 2013; Mulic, Skudutyte-Rysstad, Tveit, & Skaare, 2012) and hyposalivation (Buzalaf, Hannas, & Kato, 2012). However, it seems unlikely that one or two isolated factors are responsible for a multifactorial condition like erosive wear, instead, an interaction between chemical, mechanical and biological processes seems to be crucial (Lussi & Carvalho, 2014). Some of the risk indicators of erosive tooth wear are consistent with dental caries (i.e. frequent use of sweetened soft drinks and acidic candies) but interestingly, the role of some factors, such as socio-demographics (Al-Dlaigan, Shaw, & Smith, 2001; Muller-Bolla et al., 2015; van Rijkom et al., 2002) and tooth brushing habits (Bardolia et al., 2010; Bartlett et al., 2013) were also reported.

2.2.3 Clinical presentation

Dental erosion occurs on all tooth surfaces; however, it has some distinctive characteristics in terms of its location, appearance and morphology. The surfaces of teeth most commonly affected is common are the palatal of maxillary anterior teeth and on

occlusal surfaces of mandibular first molars (El Aidi, Bronkhorst, & Truin, 2008; Jaeggi & Lussi, 2006).

Due to differential wear, cupping lesions on the cusp tips of the occlusal surfaces of posterior teeth may occur as the dentine is lost more quickly than the surrounding enamel (Bishop, Kelleher, Briggs, & Joshi, 1997; Yip, Smales, & Kaidonis, 2002). The lesions may also present as a central area of exposed dentine surrounded by sound enamel at the gingival margin, and this is attributed to the buffering capacity of the gingival crevicular fluid that constantly bathes that area (Bishop et al., 1997). Moreover, the teeth are often sensitive to touch and to temperature changes and the loss of tooth surface is disproportionate to the age of the patient (Yip et al., 2002). Advanced erosion can lead to pulpal, functional and aesthetic problems (Yip et al., 2002). Furthermore, it is usually evident that amalgam restorations are not affected by erosion and therefore appear "raised" compared to the surrounding dental tissues (Barron, Carmichael, Marcon, & Sandor, 2003).

Cervical and incisal grooves are typical erosive lesions in premolars, canines and incisors. Shallow defects with a broad base on facial surfaces above the cemento-enamel junction (CEJ) have been found to be associated with acidic dietary habits but not with abrasive diets (Ganss, Klimek, & Borkowski, 2002).

2.2.4 Prevalence and incidence of tooth wear

The prevalence and incidence of tooth wear, especially acid erosion, is increasingly being reported. Tooth wear prevalence varies around the world. Epidemiological evidence suggests that the prevalence and incidence rate of erosive tooth wear has been increasing in the last 10-20 years, particularly in younger age groups (Jaeggi & Lussi, 2014). In Malaysia, the first tooth wear study was conducted in Sabah in 1996, with 148 subjects from a wide range of age (14–77-years), using the Tooth Wear

Index (TWI) (Milosevic & Lo, 1996). They reported that, out of 148 individuals examined, 95 had tooth wear with moderate dentine exposure and 41 had severely worn dentition. Furtnermore, tooth wear into dentine was a common occurrence, especially among the Kadazan subjects and least among the Chinese subjects, however, they concluded that the aetiological factors associated with this tooth wear are different from those encountered in Western cultures. Tobacco chewing was positively associated with both moderate and severe tooth wear, as was the habit of crushing/eating bones. Neither carbonated beverages nor fresh fruit intake, which had low consumption, were associated with tooth wear. A second study by Saerah, Ismail NM, L, and AR (2006), reported that in the State of Kelantan, tooth wear was becoming an alarming problem where amongst 16 years old children, it was found that 100% of the children had tooth wear mainly on enamel. These studies were conducted at least 10 years ago on subjects with different age, sociodemographic and geographical backgrounds in Malaysia.

Tooth wear results from erosion, attrition, abrasion or abfraction, as well as a combination of the abovementioned causes. Thus, reported data on pure dental erosion in Malaysia is still limited. Furthermore, the reported prevalence of dental erosion varies greatly in the literature, which can be partially explained by age, country and different evaluation standards. However, in general, the prevalence of dental erosion or erosive wear has been reported to be increasing (Jaeggi & Lussi, 2006), mainly in children (El Aidi et al., 2011; Kreulen et al., 2010) . Thus, early diagnosis and adequate prevention are essential to minimize the risk of tooth erosion.

2.2.5 Dental caries vs dental erosion

Dental caries occurs as a result of irreversible solubilization of tooth mineral by acid produced by certain bacteria. The acid is produced when sugars (mainly sucrose) in

foods or drinks react with bacteria which adhere to the tooth surface within the bacterial communities known as dental plaque (Selwitz, Ismail, & Pitts, 2007).

Dental enamel consists of 96% inorganic minerals and up to 4% organic material and water by weight. The inorganic component is hydroxyapatite, a calcium phosphate crystal. Hydroxyapatite crystals are organised in rods close to each other to form the dental enamel. However, small spaces exist between the crystals which are microscopically seen as pores. All these microscopic gaps allow penetration of bacterial products and, under certain circumstances, make the enamel surface susceptible to dental caries (Chiego, 2018).

The first stage of the carious process is characterised by increased intercrystalline porosity which is usually still not detectable clinically. The mineral loss is very superficial and constricted to only few micrometres from the external surface. As the lesion progresses, level of porosity increases at the enamel subsurface region and the first visual change appears on the tooth in the form of a white spot lesion. With time, porosity increases further and, as a result, mineral loss underneath the surface enamel progresses. At this stage, the visual changes of the tooth surface become more apparent (Fejerskov & Kidd, 2009). Currently, cariogenesis is thought to occur when the four factors, which are host (teeth); microorganisms, substrate and time are all present (Hayashi, Chiba, Shimoda, & Momoi, 2016). The two dynamic mechanisms that cause onset and progression of enamel caries have been identified in the interface between enamel surface and saliva; demineralisation and remineralisation (Silverstone & Poole, 1969).

Caries and dental erosion are two of the primary conditions that cause human enamel to dissolve. The processes involved in dental erosion are very different than those involved in dental caries. Acids in dental caries are produced as a result of fermentation of sugars by bacteria in dental biofilm over time, and surfaces affected by caries are commonly covered with dental biofilm, whereas on the other hand, dental erosion results

when acids, either from food, drinks or what is regurgitated or vomited from the stomach come in contact with the tooth surface. In this process no bacteria are involved, and the tooth surfaces are usually biofilm-free and clean. **Table 2.2,** adapted from (Faller & Noble, 2018) shows the main differences between dental caries and erosion.

Table 2.2: Main differences between dental caries and erosion (Faller & Noble, 2018).

	Dental Caries	**Dental Erosion**
Aetiology	Bacterial acids	Non-bacterial acids, e.g. Dietary, gastric acids.
Site	Surfaces covered with dental plaque	Usually plaque-free surfaces
Conditions	Prolonged exposure to weak acids, usually pH > 5.5	Repeated exposure to strong dietary acids, usually pH < 4.5, for shorter time
Outcome	Subsurface phenomenon with intact enamel surface	Surface softening leading to enamel loss

2.2.5.1 Demineralisation-Remineralisation of enamel

Tooth demineralisation is a chemical process by which minerals (mainly calcium) are removed from any of the hard tissues—enamel, dentine, and cementum (X. Li, Wang, Joiner, & Chang, 2014). Erosion and carious lesions are the two main consequences of demineralisation. The process of demineralisation begins at the crystal surface found inside the hard tooth tissue and may progress into cavitation unless arrested or overridden by remineralisation. The effect of demineralisation can be reversed if there is sufficient time to allow remineralisation to occur to counteract the acids in the oral cavity (Garcia-Godoy & Hicks, 2008).

Tooth remineralisation is a naturally occurring process in the oral cavity (Fejerskov & Kidd, 2009). Remineralisation of enamel occurs by the deposition of ions from saliva, since enamel has no capability to repair itself as it has no cells. It is defined as a process in which calcium and phosphate ions diffuses into the demineralised enamel, with the help of fluoride, builds on existing crystal remnants rather than the formation of new crystals (Featherstone, 2000). This process remains imperative towards the management of non-cavitated carious lesions and prevention of disease progression within the oral cavity and eventually contributing towards restoring strength and function within tooth structure (Cochrane, Cai, Huq, Burrow, & Reynolds, 2010).

The entire process of erosive tooth wear is not straight forward where there is a complex interaction of various factors that could lead to tissue loss. Demineralisation and softening of the tooth surface occur as a result of acid attack on the enamel surface. This is referred to as "initial erosion," and at this stage the process is still reversible and remineralisation or re-hardening is possible. If the process continues, the softened surface will eventually be removed, and this process can be accelerated by attrition or abrasion (Addy & Shellis, 2006; Amaechi, Higham, & Edgar, 2003; Shellis, Ganss, Ren, Zero, & Lussi, 2011).

The most important factors in the repair of softened enamel are saliva and fluoride (S. M. Hooper, Hughes, Newcombe, Addy, & West, 2005). Acid softened enamel can reharden after exposure to saliva, remineralisation solution, dietary substances and fluoride may enhance the remineralisation process (Amaechi & Higham, 2001a; Ganss, Klimek, Schaffer, & Spall, 2001; Gedalia, Dakuar, et al., 1991). Saliva and pellicle play a major role in providing natural protection against demineralisation and facilitate remineralisation.

Current research and thinking have focused on prevention of demineralisation and facilitation of remineralisation/re-hardening to prevent the process from starting or

reverse it once it has started. The reversal of the process can happen either through natural, inherent biological defence mechanisms or through products intervention.

i. **Role of saliva**

Saliva is able of impacting both the remineralisation and demineralisation processes. The process of remineralisation occurs on a daily basis after an acid challenge with the presence of saliva (Garcia-Godoy & Hicks, 2008). Saliva contains calcium, phosphate and fluoride, which are required for effective remineralisation and maintenance of the enamel surface integrity. Thus, as saliva is rich in calcium and phosphate ions, it can act as a natural buffer where acid can be neutralised and allow remineralisation of demineralised tooth tissues (X. Li et al., 2014). However, saliva, as a natural source of calcium and phosphorus ions for remineralisation, is not a very effective remineralisation environment in the absence of fluoride. An increase in the fluoride concentration of saliva is associated with an increase in remineralisation and a decrease in caries rate (Schemehorn, Orban, Wood, Fischer, & Winston, 1999). Moreover, if there is reduction in salivary flow or quality, this will increase the risk of demineralisation and thus, create the need for treatment in order to prevent demineralisation progression (X. Li et al., 2014).

ii. **Fluoride**

The presence of fluoride in saliva and biofilm fluid play an important role in remineralisation process and thus exerts a topical or surface effect. When fluoride is present in oral fluids, fluorapatite, rather than hydroxyapatite, forms during the remineralization process. Technically, this fluoride controls the rate of tooth substance loss. When fluoride ions are present in biofilm fluid together with dissolved hydroxyapatite, and the pH is higher than 4.5 (Cury & Tenuta, 2008), the fluoride ions (F^-) replace the hydroxyl groups (OH^-) and form the apatite crystal lattice layer. This

remineralised layer which is formed over the remaining surface of the enamel is more acid-resistant compared to the original hydroxyapatite, and is formed more quickly than ordinary remineralised enamel would be (Featherstone, 2008). The cavity-prevention effect of fluoride is partly due to these surface effects, which occur during and after tooth eruption (Hellwig & Lennon, 2004).

Fluoride interferes with the process of tooth decay via fluoride intake during the period of enamel development for up to seven years of age; the fluoride then alters the structure of the developing enamel making it more resistant to acid attack. In children and adults when teeth are subjected to the alternating stages of demineralisation and remineralisation, the presence of fluoride intake encourages remineralisation and ensures that the laid down enamel crystals that are of improved quality (Robinson et al., 2004).

Fluoride is commonly found in toothpastes so that it can be delivered to many parts of the oral cavity during brushing, including the tooth surface, saliva, soft tissues and remaining biofilm (X. Li et al., 2014). Furthermore, a person living in an area with fluoridated water may experience rises of fluoride concentration in saliva to about 0.04 mg/L several times during a day (Pizzo, Piscopo, Pizzo, & Giuliana, 2007).

2.2.6 Acid erosion mechanisms

When exposed to acid, teeth become softer as the hydroxyapatite (HA) is solubilized, and therefore, more susceptible to mechanical wear. The two chemical methods by which this can occur are either direct acid attack or chelation (Lussi & Jaeggi, 2008; Wiegand & Attin, 2007).

When hydronium ions are formed from an acid in solution, they bind with carbonate or phosphate in HA, releasing the anions into solution in a form of chemical etching. Carbonate is more reactive than phosphate and requires a lower concentration of

hydronium to react with, and is therefore why HA is weaker with excess carbonate (Wiegand & Attin, 2007).

Three phases of attack have been identified, based on the pH of the acid (Lussi, von Salis-Marincek, et al., 2012). Acids with pH < 1 can cause surface etching when exposed to teeth for very short period. Nanoscale surface softening occurs with short exposure at pH 2–4, but this does not extend to the macroscale (Barbour et al., 2006; Zheng et al., 2011). The third and most common form of acid attack is through weak acid (pH 4.5–6.9) subsurface dissolution. This along with bacteria can lead to the formation of carious lesions.

2.2.6.1 Enamel softening

The very first stage is softening of the surface. Shellis, Barbour, Jesani, and Lussi (2013) described this process as "near-surface" demineralisation, emphasizing that softening is not only a phenomenon that occurs at the interface between the acidic solution and the enamel surface but also within the thin (only a few micrometres), partly demineralised softened enamel layer. The stage of enamel softening is followed by a continuous layer-by layer dissolution of enamel crystals. This leads to, either a permanent loss of tooth volume or the development of a softened layer at the surface of the remaining dental tissue (Lussi et al., 2011). This softened tooth surface becomes more susceptible to mechanical forces, such as hard foods, bruxing, and toothbrushing (Voronets & Lussi, 2010).

Initially, the erosive process involves enamel dissolution, which is associated with a softening of the surface due to weakening of the enamel structure. At this stage the mechanical and physical properties of the tooth are modified, as minerals are released to the erosive acid. Enamel and dentine are affected differently because of the very high mineral content in enamel. Erosion of enamel is initially manifested as partial

demineralisation at the surface leading to softening and increased roughness, whereas dentine contains less mineral and more organic material, and shows mineral loss initially at the border between the peri- and inter-tubular dentine (Lussi et al., 2011).

The softening process of enamel happens when the enamel layer loses minerals from a layer extending a few microns below the surface (Addy & Shellis, 2006). Some reports showed that the early stages of initial enamel erosion resulted in the softening of the enamel surface up to less than 1–10 μm in depth (Imfeld, 1996), however, Finke (2001) reported a depth of less than 1 μm and no bulk material loss takes place at this early stage. With time, as softening progresses further into the enamel, dissolution in the enamel will reach the point where enamel is permanently lost, exposing the dentine layer (Addy & Shellis, 2006).

2.2.6.2 Enamel surface loss

Persistent acidic impact induces further demineralisation and contributes to a gradual loss of the enamel tissue (Ganss & Lussi, 2014). However, tooth surfaces that are covered with a thick saliva protein pellicle (Amaechi, Higham, Edgar, & Milosevic, 1999) or dental biofilm (Honorio et al., 2008) may have the 'protective' effect against acid-induced softening compared to newly cleaned enamel surfaces . Therefore, tooth brushing before an intake of acidic foods may cause a problem where the protective effect will be reduced. On the other hand, the habit of tooth brushing immediately after acid exposure is not good either where this softened enamel layer is highly vulnerable to abrasion and can be easily removed by tooth brushing (Voronets, Jaeggi, Buergin, & Lussi, 2008; Voronets & Lussi, 2010).

In more advanced stages, continuing exposure to acids and to mechanical and chemical challenges leads to surface loss, either through dissolution or abrasion of the fragile softened enamel surface. Like other wear processes, dental erosion is a progressive

loss of tooth surface (Amaechi & Higham, 2001a) that may expose the dentine if the acidic exposure is frequent and continues over a period of time. Furthermore, an eroded tooth surface is highly susceptible to abrasion and mechanical impacts. The interplay between erosion and abrasion (specifically oral hygiene practices) may be the main driver leading to the clinical manifestation of this disorder (Attin et al., 1997).

2.3 Clinical diagnosis of dental erosion

Early diagnosis of dental erosion is important. Clinicians can diagnose erosive lesions from any deviations from the original tooth morphology, however, they may miss or fail to diagnose this very early stages of dental erosion, and thus not requiring any specific intervention. Usually, only at the later stages of the process where dentine is exposed, the clinical condition becomes more obvious during routine examination. Apparently, there is currently no device available for the specific detection of dental erosion and thus, clinical feature is currently the most important diagnostic feature.

Visual inspection of tooth surfaces and wear patterns provides direct evidence of dental erosion. However, accurate diagnosis of erosion begins with an in-depth assessment of risk factors for erosion and of medical and dental histories. Diagnosis of erosive tooth wear includes not only information about patients' complaints and concerns, but also includes thorough investigation of their lifestyle. Since a severely worn dentition represents a great challenge in terms of its management, it is crucial to recognize the risk factors early, preferably before any sign of erosive tooth wear is present in order to facilitate early intervention.

2.3.1 Clinical erosion indices

Currently, there are no established clinical evaluation tool available to detect and monitor dental erosion. Visual identification is still the main way of detection by the clinicians. Many different clinical erosion and tooth surface loss indices had been developed and used mainly for epidemiological and clinical studies to simplify and enhance the diagnosis.

Tooth wear indices are commonly employed to score dental wear based on severity, appearance and location of lesions. These indices can be broadly divided into quantitative and qualitative in nature. The qualitative criteria describe terms like slight, mild, moderate and severe or descriptions of the surface texture of enamel which are more subjective and need a high level of training and calibration to render them useful. Quantitative methods tend to rely on objective physical measurements, such as depth of groove, area of facet or height of crown; and is typically associated to a gradation of numerical value, but although these indices may be useful for statistical and descriptive purposes, they are an imperfect tool. Furthermore, in a clinical intra-oral examination, there will be an inclination towards descriptive assessment measures, such as mild, moderate or severe, rather than quantitative measurement, which is easier to perform reliably on a model or in the laboratory.

A number of indices for the clinical diagnosis of erosive tooth wear have been proposed (Al-Malik, Holt, & Bedi, 2002; Arnadottir, Saemundsson, & Holbrook, 2003; Harding, Whelton, O'Mullane, & Cronin, 2003; I. B. Larsen et al., 2000; Linkosalo & Markkanen, 1985; Lussi, 1996; O'Sullivan, 2000), which more or less are modifications or combinations of the indices published by Eccles (Eccles, 1979) and Smith and Knight (B. G. Smith & Knight, 1984).

Eccles (1978) originally classified lesions broadly as early, small and advanced, with no strict criteria definitions, thus allowing wide interpretation. Later, the index was refined and expanded, with greater emphasis on the descriptive criteria (Eccles, 1979). It graded both the severity and site of erosion and was as a comprehensive qualitative index and is considered as one of the cardinal indices from which others have evolved (**Table 2.1**).

Smith and Knight B. G. Smith and Knight (1984) took Eccles' ideas a stage further, producing the tooth wear index (TWI), a comprehensive system whereby all four visible surfaces (buccal, cervical, lingual and occlusal–incisal) of all teeth present were scored for wear, regardless of its aetiology (**Table 2.4**). Linkosalo and Markkanen (1985) utilized a qualitative index with listed diagnostic criteria to confirm lesions as erosive and a four-scale grading of severity, relating to involvement of dentine. Their scoring system was then modified by Lussi, Schaffner, Hotz, and Suter (1991) to create an erosive index that has been used widely by European workers to score the facial, lingual and occlusal surfaces of all teeth except the third molars.

Oilo, Dahl, Hatle, and Gad (1987) concentrated on a different type of scoring system, with criteria based on treatment need. They criticized the use of indices that used a nonlinear scoring method, claiming calculated mean wear scores can be misleading. Their index was based on Ryge and Snyder's system (Ryge & Snyder, 1973) for evaluating the quality of restorations and had five categories divided into two broad camps; Romeo, Sierra and Mike were satisfactory, whilst Tango and Victor indicated unacceptable levels of wear requiring treatment. All groups except Romeo were subdivided according to degree of dentine exposed and clinical findings such as pain, sensitivity and fracture of restorations, giving the impression of a complicated system.

Dahl, Oilo, Andersen, and Bruaset (1989) modified it with the introduction of even more categories, with an aim to establish subjective dental criteria for present and

future evaluations of tooth wear and the need for treatment. In practice, these indices require experience for reliable use, individuals with differing clinical backgrounds will not get consistent, objective results.

There have also been attempts to visualise, measure and monitor the amount of worn enamel or exposed dentine indirectly on serial study casts. Fareed, Johansson, and Omar (1990), (Schlueter, Ganss, De Sanctis, & Klimek, 2005) and I. B. Larsen et al. (2000) recommended a new clinical index based on a combination of clinical examination, photographs and study casts with complicated qualitative and quantitative criteria.

Due to the huge number of indices reported for tooth wear with different qualifiers and scores for different aetiologies, it was accepted among researchers of tooth wear and erosion that comparisons of reported incidences and prevalence of erosion was almost impossible (Young et al., 2008). Therefore, Bartlett, Ganss, and Lussi (2008) published the Basic Erosive Wear Examination (BEWE), which ranks tooth wear (by sextant from 0 to 3), summing up the total area of tooth loss (on a scale that goes to 18), and ranking the extent of risk from none to high (**Table 2.5**). It was designed to provide a simple tool for use in general practice and to allow comparison to other more discriminative indices. It is a partial scoring system recording the most severely affected surface in a sextant with a four-level score and the cumulative score classified and matched to risk levels which guide towards the management of the condition. The BEWE allows re-analysis and integration of results from existing studies and it was hoped that it would avoid the continued proliferation of indices. The BEWE further aims to increase the awareness of tooth erosion amongst clinicians and general dental practitioners and to provide a guide as to its management (Bartlett et al., 2008).

Table 2.3: Eccles index for dental erosion of non-industrial origin (Eccles, 1979).

Class	Surface	Criteria
Class I		Early stages of erosion, absence of developmental ridges, smooth, surfaces of maxillary incisors and canines.
Class II	Facial	Dentine involved for less than one third surface; two types Type 1(commonest): ovoid-crescentic in outline, concave in cross differentiate from wedge shaped abrasion lesions Type 2: irregular lesion entirely within crown. Punched out.
Class IIIa	Facial	More extensive destruction of dentine, affecting anterior teeth part of the surface, but some are localised and hollowed out.
Class IIIb	Lingual or palatal	Dentine eroded for more than one third of the surface area. Gingival white, etched appearance. Incisal edges translucent due to loss of is flat or hollowed out, often extending into secondary dentine.
Class IIIc	Incisal or occlusal	Surfaces involved into dentine, appearing flattened or with cupping. Undermined enamel; restorations are raised above surrounding.
Class IIId	All	Severely affected teeth, where both labial and lingual surfaces are may be affected; teeth are shortened.

Table 2.4: The Tooth wear index as described by B. G. Smith and Knight (1984).

Score	Surface	Criteria
0	B/L/O/I C	No loss of enamel surface characteristics. No loss of contour.
1	B/L/O/I C	Loos of enamel surface characteristics. Minimal loss of contour.
2	B/L/O I C	Loss of enamel exposing dentine for less than one third of surface. Loss of enamel just exposing dentine. Defect less than 1 mm deep.
3	B/L/O I C	Loss of enamel exposing dentine for more than one third of surface. Loss of enamel and substantial loss of dentine. Defect less than 1-2 mm deep.
4	B/L/O I C	Complete enamel loss - pulp exposure - secondary dentin exposure. Pulp exposure or exposure of secondary dentine. Defect more than 2mm deep - pulp exposure - secondary dentine exposure.

B: buccal; L: lingual; O: occlusal; I: incisal; C: cervical.

Table 2.5: The Basic Erosive Wear Examination (BEWE) index (Bartlett et al., 2008).

Sextant scoring of 0 to 3 for loss of tooth surface.
0 = no erosive too wear **1 = initial loss of surface texture** **2 = distinct defect, hard tissue loss < 50% of the surface area** **3 = hard tissue loss > 50%of the surface area**
Total mouth score **0 to 2 = no risk** **3 to 8 = low risk** **9 to 13 = medium risk** **14+ = high risk with a document provided for follow-up care and management.**

Review of the literature on indices for tooth wear (or erosion) is confusing; there are too many indices proposed and utilized, with lack of standardisation in terminology. The indices described above may not be sensitive enough to monitor all changes in dental erosion and therefore may not be suitable to evaluate the progression of erosion measure the rate of wear due to the distinctions between the various levels of scores are generally too crude. To date, there is no one ideal index that meets all the requirements of all purposes of epidemiological study, clinical staging and longitudinal monitoring of the effect of interventions on dental erosion or erosive wear.

2.4 Methods of assessing enamel erosion

Methods for assessing enamel erosion have been reviewed previously (Attin & Wegehaupt, 2014; Azzopardi, Bartlett, Watson, & Smith, 2000; Barbour & Rees, 2004; Field, Waterhouse, & German, 2010; Grenby, 1996; Joshi, Joshi, Kathariya, Angadi, & Raikar, 2016; Schlueter et al., 2011).

Erosive alterations of dental hard tissues are mostly investigated either in *in vitro* or *in situ* studies. Various *in vitro* methods are used to assess the hard tissue surface loss caused by erosive tooth wear at an initial stage, where it ranges from nanometres to a maximum of a few micrometres. It is highly important to be able to detect even a minor enamel loss in order to diagnose this initial stage or erosion. *In vitro* investigations in dental research are important as they allow for tooth erosion conditions to be extensively studied in controlled environments for product development and testing. These techniques achieve greater sensitivity, specificity, and accuracy in measuring tooth loss compared to the *in vivo* techniques. Furthermore, *in vitro* models are less expensive, can be executed in a shorter time and require fewer staff compared to *in situ* studies, and do not require real live subjects, thus, no issue of compliance involved. However, the main

disadvantage of the *in vitro* models is that they can only mimic but not able to duplicate actual intra-oral conditions with all the biological variations known to influence erosion.

In situ means that the enamel or dentine specimens are prepared extra-orally, placed or embedded in intra-oral appliances and worn in the oral cavity. Specimens are subjected to acid challenges either extra-orally (Ablal, Milosevic, Preston, & Higham, 2017) or intra-orally (West et al., 2017) depending on the study protocol, and finally all measurements for hard tissue loss or surface alterations are done extra-orally i.e. in a laboratory setting, where direct measurement may not be possible.

In vitro and *in situ* study designs have been developed in attempts to overcome the challenges that hinder *in vivo* studies whilst still providing meaningful data that reflect what actually happens in the oral cavity. The main advantages of such models are that strict standardised controls can be implemented, one variable at a time can be examined, new variables can be introduced stepwise, and accurate measurement technologies over defined time periods can be used to determine loss of tooth tissue. *In situ* models offer the advantage that they allow control of the acid challenge but also expose the specimens to the oral environment.

The earliest *in situ* models used small gold cups (Bunting, 1928) and gold plates (Nygaard Östby, Mörch, & Hals, 1958) to study demineralisation in vital teeth. In 1964, Koulourides and Volker introduced a new *in situ* model (intra-oral cariogenicity/ICT model) to assess the cariogenicity of different types of foods. They suggested that this model was suitable to determine the ability of topically applied. Furthermore, *in situ* models are particularly suitable to assess erosion due to acidic drinks and testing numerous interventions that can offer protection with regard to a number of acid challenges. They enable the entire process of erosion to be monitored over time in a more or less entirely natural environment comprising pellicle development, routine oral care, and saliva flow (Koulourides & Volker, 1964).

2.4.1 Chemical analysis of dissolved minerals

Chemical analysis has been used widely by measuring the concentrations of calcium and phosphate released into the dissolving solution, as well as the pH and uptake or release of minor constituents of enamel such as fluoride or magnesium. Calcium analysis is typically carried out using atomic absorption spectroscopy and phosphate concentration is usually determined using spectrophotometry of a coloured phosphate complex (Barbour & Rees, 2004).

The pH stat is a technique frequently applied to studies of chemically pure hydroxyapatite dissolution (Shellis, Wahab, & Heywood, 1993) but is readily applicable to the investigation of real time enamel erosion (Barbour & Rees, 2004). It is a chemical analysis device, which measures the hydroxyapatite and enamel release hydroxyl (OH^-) ions on enamel dissolution. Thus, the rate of release of OH^- ions is determined by measuring the pH change of a solution, and from this the rate of enamel dissolution can be calculated. The pH stat includes a feedback loop, which acts to hold the pH at a stationary value. When the enamel specimen is immersed in the acid, it starts to dissolve and releasing OH^- ions which neutralise H+ ions and cause the pH to increase. The pH stat equipment automatically adds acid to compensate for this neutralisation of H+ ions and maintains the pH at the initial value. By measuring the rate at which it is necessary to add acid to maintain a constant pH, it is possible to calculate the dissolution rate of the enamel at a chosen pH.

These chemical analysis techniques are well established, sensitive and accurate but provide information only on the net concentrations of ions released. Additional techniques are necessary to visualise the crystal surfaces and deposition or nucleation of new material, and only *in vitro* processes can be investigated (Arends & ten Bosch, 1992). However, chemical techniques do have the advantage that erosion of natural enamel surfaces can be investigated, without prior surface polishing of specimens.

2.4.2 Surface hardness measurements

Hardness is generally defined as a materials resistance to permanent or plastic deformation. In many materials, hardness is a measure of resistance to an indentation where a ball, diamond pyramid or cone is forced into the material being tested under an applied load (typically 1kg to 50kg) for a given time.

There are several methods of indentation hardness testing being used which are the Rockwell, Vickers, Knoop and Brinell. The principle of measurement in indentation-based methods is that the surface of the material being tested is put into contact with an indenter of specified shape and dimensions, which during a specified time interval applies pressure of a specified intensity of force, after which the hardness is calculated based on the dimensions of the indenter. Furthermore, all tests use the relationship between total applied force and area or depth of impression to provide a measure of hardness.

For measurement of thin foils, surface treatments, enamel layer, anodised layers, thin solid films, or microstructural constituents, the microhardness test and the nanohardness Test can be employed. This is based on the Vickers and Knoop test but produces a smaller impression due to the lighter loads used (loads below 1kg are generally termed as Microhardness.

Hardness changes on enamel surface are a common symptom of carious lesions or erosion, thus assessing it provides some information about the lesion's severity and progression (Tantbirojn, Huang, Ericson, & Poolthong, 2008). For determining the enamel surface hardness, microhardness and nanoindentation techniques are often used. With hardness measurements, early stages of enamel and dentine dissolution, which are associated with weakening of the surface, can be determined. The basic method of micro- and nanoindentation involves the indentation of a diamond tip of known geometrical dimensions for a given load and duration.

2.4.2.1 Microhardness

There are two common types of microhardness measurements being used in dental erosion studies are Vickers and Knoop. The technique produces data in arbitrary units, usually Knoop hardness number (KHN) or Vickers hardness number (VHN). In this test, a pyramid shaped fine diamond tip of known geometry is pushed into the enamel or dentin surface with a defined load. This results in an indentation in the surface of the tooth, and the measure of the diameter of the indentation indicates the microhardness, which is measured with a micrometer scale incorporated into the ocular part of the microscope. The difference between the Vickers and Knoop is the shape of the diamond indenter. The Vickers microhardness test leaves a tetra-pyramidal indentation mark while the Knoop microhardness indenter leaves a rhomboid indentation mark. For a given indentation length, the Vickers indenter penetrates 4.5 times deeper than the Knoop indenter (Knoop, Peters, & Emerson, 1939). The Knoop microhardness test has been reported to be more sensitive to surface hardness than many other conventional hardness tests and it is suitable for the measurement materials such as hydroxyapatite, the main component of dental enamel (Jandt, 2006).

For microhardness assessments of eroded tooth surfaces, the diamond indenter such as Knoop or Vickers are used on polished surfaces. Polished surfaces are recommended to produce well-defined indentations. The lengths of the indentations on the surface are measured under a microscope requiring indentations lengths of about 30–40 μm length for accurate measurements. The gold standard for the measurement of early stage surface softening is micro-hardness testing (Schlueter et al., 2011). However, this is typically an *in vitro* technique, reliant upon physical indentation of the specimen.

2.4.2.2 Nanohardness

The nanohardness test is an ultra-micro indentation system for testing hard materials, which measures the hardness and elastic modulus of a material on an extremely small surface scale of 50 nm (C. Machado, Lacefield, & Catledge, 2008). Nanoindentations in sound enamel have sub-micrometre indentation depths, typically around 200 nm (Finke, 2001) and are only affecting the material to a depth of a few micrometres (Barbour & Rees, 2004). The indentations made are too small to be seen unless viewed under a high power optical or atomic force microscope, thus making it a non-destructive method (Xu et al., 1998).

Despite the broad use of the nanoindentation technique in engineering and physics, its use in dentistry has not been popular. A related study in which *in vitro* erosion by soft drinks was investigated using 'ultra-microindentation' apparatus also indicated different degrees of softening by different drinks (Mahoney, Beattie, Swain, & Kilpatrick, 2003). In a preliminary study, another group observed changes in the mechanical properties of enamel after storage in deionised water and saline solution, and advised caution in the choice of storage medium for tooth specimens (Habelitz, Marshall, Balooch, & Marshall, 2002). Furthermore, a series of investigations of *in vitro* enamel erosion has previously demonstrated unknown features of the dependence of enamel erosion on the calcium and phosphate concentrations, degree of saturation and pH of acidic solutions (Barbour, Parker, Allen, & Jandt, 2003a, 2005; Barbour, Parker, & Jandt, 2003). Moreover, authors like Barbour et al. (2006) used nanoindentation hardness and AFM to correlate soft drink consumption with softening of human enamel. These studies used exposure times of 30 s – 10 min, which is comparable to the clearance times of acids in the mouth. This demonstrates that nanoindentation is extremely sensitive to changes in the mechanical properties of the enamel surface and is likely to find increasing application in enamel erosion research.

Advantages: With a typical nanoindentation apparatus, the displacement of the tip as a function of the applied load, is continually monitored during indentation, and as such the plastic and elastic deformation of the surface can be determined. In practical terms, both the hardness (plastic, permanent deformation) and the elastic modulus (or Young's modulus) may be readily calculated from nanoindentation load–displacement data. Elastic modulus data may be useful in erosion experiments, since it has been shown in studies of thin films and of enamel erosion (Barbour, Parker, Allen, & Jandt, 2003b) to be more sensitive than hardness to the presence of underlying hard material (intact enamel in the case of erosion).

Disadvantages: A drawback of this technique is that the enamel surface must be polished to provide a flat substrate prior to erosion. The outer layer of the enamel, which contains much greater concentrations of fluoride and lower concentrations of magnesium and carbonate than enamel, is thus removed. Since the solubility of inner enamel is known to be higher than that of surface enamel, erosion proceeds more quickly in polished specimens.

2.4.3 Microradiography

Microradiography is a tool for quantification of mineral loss based on the attenuation of X-ray irradiation transmitting dental hard tissue. X-ray photons transmitting a dental hard tissue specimen can be recorded by photon-counting X-ray detectors or X-ray sensitive photographic plates or film. The mineral mass can be calculated from the photon counts or grey values of photographic plates or film knowing the appropriate mass attenuation coefficient or by determining photographic density measurements calibrated by an aluminium step wedge (Anderson & Elliott, 2000; E. D. J. De Jong, van der Linden, & Ten Bosch, 1987; E De Josselin De Jong, Van Der Linden, Borsboom, & Ten Bosch, 1988).

Microradiography has been predominantly used in the investigation of caries, and for the detection of erosive mineral loss *in vitro* and has the potential to assess both material loss and the extent of softening. Microradiography is a technique where a photographic plate (Arends & ten Bosch, 1992) or a photon counter (Anderson, Levinkind, & Elliot, 1998) is used to record the penetrating radiation of a beam of X-rays incident on an enamel section. The degree of blackening of the film or the photon density, together with a calibration specimen, provides a map of the mineral density of the enamel.

This technique is usually divided into one of three 'generations' of microradiography. These are: transverse microradiography (TMR), used for thin sections (50–200 μm) and radiographed perpendicular to the specimen; longitudinal microradiography (LMR), used for thick sections of teeth; and wavelength-independent microradiography, which is used to quantify mineral content in whole teeth (Arends, Ruben, & Inaba, 1997).

2.4.4 Transverse microradiography (TMR)

TMR is the gold standard for quantitative assessment of the mineral content as a function of depth from the surface for caries and caries-like lesions (Arends & ten Bosch, 1992). It has been adopted for detecting erosive mineral loss *in vitro* and has the potential of assessing both material loss, and the extent of softening. From the in-depth profiles, the lesion depth and mineral loss integrated over the entire depth of the lesion can be calculated. Lesion depth is usually defined up to the point, where the mineral content reaches 95% of the mineral content of sound enamel or dentine. Hall et al. (1997) found a strong correlation between mineral loss determined by either TMR or profilometry even for discrimination of early erosive lesions caused by erosion times of less than 1 h.

2.4.5 Surface Profilometry

Surface profilometry has been extensively used to characterise enamel loss caused by erosion *in vitro*. The surface of a specimen is scanned to produce a two-dimensional or three-dimensional profile, using either a contact or a non-contact measuring device (Gracia, Rees, Brown, & Fowler, 2010). In contact profilometry, the surface is scanned using a stylus with a diamond or steel tip (Paice, Vowles, West, & Hooper, 2011; Ren, Zhao, Malmstrom, Barnes, & Xu, 2009). It is the most applied method to measure tooth loss, despite its main limitation of potential tissue damage (Schlueter et al., 2011). Non-contact profilometry on the other hand uses a laser light probe, thus there is no direct physical contact between the probe and the surface and no damage occurs to the soft eroded surface. In order to measure tooth surface loss due to erosion, both contact and non-contact profilometry require a reference area that is not affected by erosion. Tapes or varnish has been used to cover parts of the tooth surface from the acid and the step height between the unaffected reference area and the eroded area is then measured. However, sometimes the covered area may still be affected through seepage of the acid underneath the tape or the deterioration of the varnish during acid challenge.

In profilometry studies, polished surfaces are commonly utilised due to the fact that dentine surface and/or native enamel provide an intrinsic coarseness render impossible the detection of small changes as a result of abrasion/erosion. Nevertheless, in natural enamel, the measurement of natural enamel extended depths reaching at least 50 μm of erosive grooves can be measured without there being any call for the surface to be polished (Ganss, Klimek, & Schwarz, 2000). However, Eisenburger, Hughes, West, Shellis, and Addy (2001) used contact profilometry together with ultrasonication to evaluate erosion depths and the extent of surface softening. The softened surface was removed with ultrasonication and the resulting crater was measured with a contact or non-contact profilometer. This has provided an estimate of the thickness of the softened layer

of approximately 2–5 μm. This method has since been used to assess the influence of liquid temperature and flow rate on surface softening (Eisenburger & Addy, 2003), the effects of modification of soft drinks on its erosive potential (Hughes et al., 2002) and to compare the effects of tooth brushing relative to ultrasonication.

Profilometry has the advantage of being a simple and fast assessment method over a relatively wide area of enamel. However, similar to indentation techniques, the enamel specimen has to be ground flat prior to use.

2.4.6 Ultrasonication measurement of enamel thickness

With ultrasonic pulse-echo measurements, the time interval between the transmission of an ultrasound pulse on the enamel surface and the echo produced by the dentine-enamel junction (DEJ) is determined by a light stereomicroscope and the thickness of the enamel layer can be calculated (Attin & Wegehaupt, 2014). This method is non-destructive and can be used for both early diagnosis of dental erosion and longitudinal measurement of progressive enamel loss (Eisenburger et al., 2000; Hughes et al., 2002; Huysmans & Thijssen, 2000). However, its use in erosion studies is limited because of poor probe tip positioning and repeatability and poor reliability in measurement of enamel thickness changes of less than 300μm (Louwerse, Kjaeldgaard, & Huysmans, 2004).

2.4.7 Scanning Electron Microscopy (SEM)

Changes in tooth structure due to extrinsic factors have been widely investigated using SEM. This method requires proper specimen preparation where the surface has to be coated with a material that is electrically conductive, to prevent the accumulation of electrostatic charge. This material is usually gold, and the specimens will undoubtedly be irreversibly altered during the desiccation and sputtering process. Thus, these procedures

change the natural condition and/or part of the specimen structure (Poggio, Lombardini, Vigorelli, & Ceci, 2013). Despite all the preparation procedures, it is still one of the most frequently used devices for qualitatively assessment of ultramicroscopic surface alterations associated with erosion on both enamel and dentine (Azzopardi, Bartlett, Watson, & Sherriff, 2004; Cheng et al., 2009). Moreover, this method is commonly used as an adjunct investigation tool to other quantitative methods.

SEM evaluation allowed to qualitatively understand the process of demineralisation of enamel surface through the observation of specific morphological and structural features, for example, Ceci et al. (2016) reported on SEM observations showed a remarkable increase of enamel roughness after the exposure to coke, which causes a loss of material from the surface. The etching process involves mainly the inner area of the prism creating a honeycomb like structure.

2.4.8 Atomic Force Microscopy (AFM) and AFM Nanoindentation

Atomic Force Microscopy (AFM) has been applied to measure the early stages of enamel loss (Barbour et al., 2005; Finke, 2001). It is capable of providing a three-dimensional surface profile with high resolutions, with minimal specimen preparation, thus, this technique has been widely used to characterize the erosion of enamel and dentine (Parker et al., 2014). There are two types of AFM scanning: tapping mode and contact mode; whereby the tapping mode AFM has been successfully applied to study alterations in enamel (N. C. Santos & Castanho, 2004).

AFM nanoindentation allows for the measurement of nanomechanical properties, such as surface hardness and reduced elastic modulus, and for indentation depths of less than 100 nm. It has been shown useful for studying the mechanical properties of surface softened enamel (Barbour et al., 2006; Lippert, Parker, & Jandt, 2004). Therefore, AFM

and nanoindentation have revolutionized the investigation on the development of new soft drinks with reduced erosive potential.

2.4.9 Confocal Laser Scanning Microscopy (CLSM)

CLSM is a technique for obtaining high-resolution 3-D optical images with depth selectivity from specimens. A laser beam passes through a light source aperture and focused by an objective lens into a small focal volume within or on the surface of a specimen. Only the in-focus light is recorded to acquire the images and all the out-of-focus light is suppressed by confocal apertures, resulting in sharper images. Topography is recorded by a series of consecutive images in both the x-y and x-z planes including depth measurement in the z-direction. CLSM allows for the study of un-sectioned, naturally moist teeth, hence, no specimen preparation is required while visualizing the outermost surface or subsurface areas. It has the advantage of high resolution and fast recording of the surface topography (Al-Salihi & Tarmidzi, 2009). Though it is mostly used to obtain qualitative information, it is also used for quantifying erosive tissue loss and softening depth (Heurich et al., 2010; Schlueter et al., 2011).

2.4.10 Laser speckle imaging

Koshoji et al. (2015) reported on the use of laser speckle imaging to detect dental erosion using coherent visible light. The different intensity of the backscattered light on the eroded tissue compared to sound enamel showed that the effects are related to the heterogeneity induced in the microstructure of the enamel by the demineralisation process, which increases the interprismatic spaces, exposing the top of the prism, which has greater porosity (S. L. Zhou et al., 2012).

It was reported that this method is possible to acquire information on the microstructure of the enamel and detect minimal changes in early erosion lesions, where

it has been proven sensitive to 10 min of acid challenge on tooth enamel, which is a lesion so incipient that is unlikely to be detected in clinical practice even by a trained dentist. Furthermore, it is also sensitive to the erosion progression. However, this method has not been tested in a clinical trial (Koshoji et al., 2015).

2.4.11 Nanoscratch testing

Over the past decade, nanohardness testing (using a nanoindenter) has been applied to detect enamel softening from acidic diet during early stages of erosion (Mahoney et al., 2003; A. J. White et al., 2010). Nanohardness testing provides indirect information regarding wear resistance of a bioceramic material, such as enamel (Jeng, Lin, Wong, Chang, & Shieh, 2008), whereas nanoscratch testing provides site specific, accurate understanding of its micro- or nanotribological behaviour when conducted under appropriate conditions (Guidoni, Swain, & Jäger, 2009; Jeng, Lin, & Shieh, 2009). Thus, it is likely to clarify fundamental mechanisms involved with tooth softening during the early stages of dental erosion,

Furthermore, nanoscratch testing has been reported to be having the potential to provide tribological data more accurately and efficiently compared with existing models of tooth wear using machines in which a tooth specimen is worn against an opposing tooth specimen or a toothbrush at a macro- or micro-scale under various loads and lubricants (Kaidonis, Richards, Townsend, & Tansley, 1998; Ranjitkar, Kaidonis, Townsend, Vu, & Richards, 2008).

2.4.12 Quantitative Light-Induced Fluorescence (QLF)

Quantitative light-induced fluorescence (QLF) has been reported that it can be used for the detection of early enamel caries and for the evaluation of deep dentine caries (Jun et al., 2016). (Lee, Lee, & Kim, 2018) reported that this technology can also provide

evidences for determining the extent of caries removal non-invasively, besides detecting dentine caries. From the QLF technology , the fluorescence loss is an indication of minerals loss (Elbert de Josselin de Jong, Higham, Smith, van Daelen, & van der Veen, 2009), and an increase in red fluorescence is an indication of bacterial activity, and these two changes in fluorescence provide useful optical information for the diagnosis of caries (Volgenant, van der Veen, de Soet, & ten Cate, 2013). Furthermore, QLF also allows detection of the early enamel demineralisation based on the change of its auto-fluorescence signal, and the fluorescence image of enamel lesions can be digitised, and the fluorescence loss in the lesion quantified in comparison to the fluorescence radiance level of the surrounding sound enamel. When tooth surface is irradiated with blue-green light, it emits fluorescence with a wavelength of 540 nm caused by chromophores, which are predominately located at the dentino-enamel junction (DEJ) and in the dentine. Demineralised areas appear darker permitting quantification of the erosion (Angmar-Mansson & ten Bosch, 2001). The most important result parameters reported are lesion size, depth and volume. This method can be used for the longitudinal assessment and detection of very early mineral changes in enamel (Angmar-Mansson & ten Bosch, 2001; Pretty et al., 2004; Van der Veen & de Jong, 2000).

Chew et al. (2014) reported that OCT and QLF were able to detect demineralisation after 10 min of acid challenge and could be used to monitor the progression of demineralisation of initial enamel erosion *in vitro.* The technique can be used *in vitro*, *in situ* and *in vivo* to monitor mineral changes (Van der Veen & de Jong, 2000) and it is often preferred due to less safety concerns and portable units have now been developed for safe chair-side use

Although all existing methods have limitations, in combination they can adequately fulfil most of the needs of research in dental erosion. For initial erosion, chemical analyses of mineral release and enamel surface hardness have been used.

Advanced erosion has been mostly analysed using surface profilometry and microradiography (Schlueter et al., 2011).

2.4.13 Optical coherence tomography (OCT)

OCT is an optical imaging tool which produces high resolution, cross-sectional topographic images of the microstructure of substance and biological tissues by computing backscattered light. OCT is also often referred to as an optical analogue of ultrasound. It has an imaging range of 1-15 mm and an axial resolution better than 5μm. It is capable of constructing cross-sectional and 3D tomographic images for oral screening and diagnosis. OCT is considered to fill a niche between ultrasound and confocal microscopy. The imaging can be achieved in a non-destructive optical approach *in situ* or in real time mode (D. Huang et al., 1991).

OCT is a high resolution, Low Coherence Interferometric (LIC) technique that generates subsurface images of enamel specimens using near infrared light (820nm). It is non-invasive and can potentially measure both surface characteristics and quantitative loss of tooth structure (Ando et al., 1997). This method provides cross-sectional imaging by measuring the magnitude and echo time delay of backscattered light. The increased porosity of demineralised enamel as in erosion compared to sound enamel results in a change in optical properties, permitting the difference in intensity of the reflected light to be quantified and analysed (Ando et al., 1997; Huysmans et al., 2011; Popescu, Sowa, Hewko, & Choo-Smith, 2008). There have been reports that OCT could be used to assess enamel thickness, reflectivity, and absorbance, which can then be related to the amount of mineral loss (Ando et al., 1997; Field et al., 2010).

Typically, techniques for *in vitro* longitudinal erosion measurement require specimens to be removed from the acidic solution and dehydrated prior to measurement. Such an approach may disrupt the softened region (Shellis & Addy, 2014) and introduce

variations in specimen hydration (Nazari et al., 2013), that in OCT has been shown to reduce sensitivity to demineralisation and therefore contributes to experimental uncertainty. Repositioning accuracy has previously been addressed by placing control markings to aid realignment of successive measurements (Chew et al., 2014). Nevertheless, manual repositioning limits the accuracy of longitudinal measurements because successive B-Scans are not guaranteed to be spatially co-registered. This can be a significant limitation where only single B-Scans are acquired for analysis at each time point and becomes increasingly important for detecting small changes such as in initial erosion stage (Attin & Wegehaupt, 2014).

2.4.14 Clinical Examination and use of photographs

In epidemiology, photographs are valuable in measuring dental erosion whereby photographs can be selected, arranged and rearranged and reassessed without clinically re-examining the patient. They have potential in developing national and international comparisons in measuring erosion (Al-Malik, Holt, & Bedi, 2001). Photographs give results similar to those from visual examination of erosion but, may underestimate the extent of the condition (Al-Malik, Holt, & Bedi, 2001; Al-Malik, Holt, Bedi, & Speight, 2001). The quality of the outcome depends on the dexterity of the photographer and ambient conditions such as light reflectivity. Though clinical photographs are useful for monitoring erosive wear, factors like proficiency of the operator or photographer and the general setting may affect the precision of erosion estimates, especially of early lesions (Al-Malik, Holt, & Bedi, 2001).

Advantages and disadvantages of these methods are summarized in **Table 2.6**.

Table 2.6: Advantages and disadvantages of diagnostic methods for detecting enamel erosion.

	Diagnostic Methods	Advantages	Disadvantages
1.	**Chemical analysis of dissolved minerals.** (Barbour & Rees, 2004)	Mostly easy and well-established methods.	No information about structural changes.
2.	**Surface hardness measurements.** (Tantbirojn et al., 2008)	• Relatively low costs. • Well-established method. • Can be combined with determination. • of surface loss due to abrasion.	• Measurement of surface hardness is influenced by non-demineralised deeper layers. • Polished, flat surfaces needed.
3.	**Microradiography.** (Anderson & Elliott, 2000)	Determination of both mineral loss and demineralization possible.	• Limited resolution. • Demanding sample preparation.
4.	**Transverse microradiography (TMR).** (Arends & ten Bosch, 1992)	Gold standard for quantitative assessment of the mineral content as a function of depth.	Imaging precision at the sample edge is limited.
5.	**Surface Profilometry.** (Gracia et al., 2010)	Applicable for measurement in natural dentition (replica technique)	• Time consuming when complete mapping of surfaces. • Stylus could damage surface
6.	**Ultrasonication measurement of enamel thickness.** (Attin & Wegehaupt, 2014)	Allows non-destructive analysis without extensive sample preparation.	Low resolution.
7.	**Scanning Electron Microscopy (SEM).** (Poggio et al., 2013)	Very high-resolution images of less than 1nm in size of a sample surface can be visualized.	• Requires sample preparation • Only qualitative assessment. • High cost.

8.	**Atomic Force Microscopy (AFM) and AFM Nanoindentation.** (Barbour et al., 2005)	• High resolution • Nearly non-destructive	• Time-consuming measurement. • Only limited areas of about 250 × 250 μm could be scanned. • High costs.
9.	**Confocal Laser Scanning Microscopy (CLSM).** (Al-Salihi & Tarmidzi, 2009)	High resolution and fast recording of the surface topography.	Only qualitative assessment.
10.	**Laser speckle imaging.** (Koshoji et al., 2015)	• Possible to acquire information on the microstructure of the enamel. • Can detect minimal changes in early erosion lesions.	Has not been tested in a clinical trial.
11.	**Nanoscratch testing.** (A. J. White et al., 2010)	Is likely to clarify fundamental mechanisms involved with tooth softening during the early stages of dental erosion.	Polished, flat surfaces needed.
12.	**Quantitative Light-Induced Fluorescence (QLF).** (Lee et al., 2018)	Surface scan is not time consuming.	• Limited resolution. • Low experience in erosion studies. • Exact repositioning of samples for comparative measurements is difficult.
13.	**Optical coherence tomography (OCT).** (D. Huang et al., 1991)	• Non-destructive analysis. • Allows for characterization of early erosive lesions.	• High costs. • Limited penetration depth.
14.	**Clinical Examination and use of photographs.** (Al-Malik, Holt, & Bedi, 2001)	Potential in developing national and international comparisons in measuring erosion.	Proficiency of the operator or photographer and the general setting may affect the precision of erosion estimates, especially of early lesions.

2.5 Management of dental erosion

The effects of erosion have traditionally been monitored until sufficient tooth structure was missing, and then restorative intervention has occurred. It is difficult to guide patients toward responsible management of the early stages of dental erosion because it is often asymptomatic, subtle, requires behavioural change, and has an aetiology and progression the patient is unfamiliar with and many have doubts about.

The first step in the management of dental erosion is to determine the aetiology and to identify the associated risk factors which should be eliminated whenever possible. Management of dental erosion includes prevention, tooth remineralisation, and active treatment by restoring the involved teeth. Contemporary approaches to the treatment of enamel erosion are based on the idea of ‘‘demineralisation and remineralisation’’ in a microphase to retain healthy teeth (Malterud, 2006; Murdoch-Kinch & McLean, 2003). The management of dental erosion mainly involves elements of prevention and restorations.

2.5.1 Primary prevention

Primary prevention aims to prevent disease or to prevent loss of tooth surface due to erosion. The first step in the management of dental erosion is to determine the cause of the dental erosion and to identify the associated risk factors and where possible eliminated.

2.5.1.1 Dietary counselling

Dietary counselling is important in educating and creating awareness on the long-term effect of erosion and it should be given after a thorough analysis of the diet. Furthermore, prevention of ongoing erosion can be undertaken by emphasizing on

reducing the exposures to acidic or erosive substance such as fruit juices, carbonated drinks or any natural acid or acid-flavoured food items, and enhance the ability of the oral cavity to overcome and resist the effect of the acidic environment (Kilpatrick & Mahoney, 2004).

Patient education is one of the ways to create awareness regarding the potential progression of erosion. Studies have shown that the technique of motivational interviewing can improve patient compliance toward behavioural changes necessary in managing the early stages of dental erosion (W. R. Miller & Rose, 2009).

When eating-disorders, vomiting or gastric reflux are parts of the risk complex, psychological counselling, lifestyle changes and medication are essential components for the management of the condition (Twetman, 2015).

2.5.1.2 Modification of products

In response to the increasing concern on dental erosion, relevant products have been modified in order to minimize the negative effect of the condition. Kilpatrick and Mahoney (2004) reported three approaches related to this issue. The first involves raising the pH, reducing the titratable acidity and adding calcium to soft drinks. There were also reports on adding hydrocolloid food gum to original product. An example of this product is Ribena ToothKind drink (Ribena®, Glaxo Smithkline, UK). The second approach was to add a large amount of calcium fluoride into soft drinks with the aim to supersaturate the environment surrounding the tooth. Unfortunately, this technique is less effective compared to the first approach. Finally, minimal amounts of caseine phosphopeptide-amorphous calcium phosphate (CPP-ACP) has been added to products such as; sports drinks (e.g. Powerade®), chewing gum (A. F. de Oliveira et al., 2017), toothpaste (Soares et al., 2017) and fluoride varnish (Savas, Kavrik, & Kucukyilmaz, 2016).

2.5.2 Secondary prevention

Secondary prevention aims to reduce the impact of a disease or injury that has already occurred. Secondary prevention of dental erosion includes clinical interventions. (Li, 2014)

2.5.2.1 Fluoride and calcium for enamel mineralisation

The use of fluoride in the protection and treatment of erosive lesions is a well discussed subject. The preventive effect of fluoride is mainly due to the formation of a calcium fluoride (CaF_2) layer on the enamel, which acts as a reservoir for fluoride. During an acid attack, fluoride released from the reservoir is incorporated into the outer surface of enamel by forming fluorapatite crystal resulting in a reduced susceptibility to acid (Lagerweij et al., 2006; Wiegand, Bichsel, Magalhaes, Becker, & Attin, 2009). Studies have shown that fluoride application in low or moderate concentrations, as in regular fluoride toothpastes, has little or no preventive effect against erosive lesions, however, high-concentration acidic fluorides, especially stannous fluorides, can have preventive effect against erosive lesions (Huysmans, Young, & Ganss, 2014).

Fluoride therapy is often used to promote remineralisation. This produces the stronger and more acid-resistant fluorapatite, rather than the natural hydroxyapatite. Some studies have shown that treatment with fluoride containing toothpastes helps protect enamel from acid-mediated surface softening and promotes hardness restoration after erosive attack (Barlow, Sufi, & Mason, 2009; Fowler, Willson, & Rees, 2006; Magalhaes, Wiegand, Rios, Buzalaf, & Lussi, 2011; Turssi et al., 2011). However, while some clinical and laboratory studies demonstrate fluoride may be able to help manage dental erosion, there were studies that showed fluoride efficacy is insufficient (M. J. Larsen & Richards, 2002; X. Wang, Klocke, Mihailova, Tosheva, & Bismayer, 2008).

Apart from fluoride, studies have also shown that products containing calcium compounds can significantly increase the hardness of enamel softened by erosive substances, while reducing erosion and abrasive wear (Panich & Poolthong, 2009; Piekarz, Ranjitkar, Hunt, & McIntyre, 2008; Ranjitkar et al., 2009; Tantbirojn et al., 2008; C. P. Wang, Huang, Liu, Li, & Yu, 2014). However, a pH cycling study found that, when acid challenges were alternated with applications of dentifrices containing Casein Phosphopeptide–Amorphous Calcium Phosphate (CPP-ACP or Tooth Mousse) or calcium and sodium phosphosilicate, the use of these products offered no advantage over conventional fluoride toothpaste (Rehder Neto, Maeda, Turssi, & Serra, 2009).

2.5.2.2 Calcium-phosphate product (CPP-ACP)

CPP-ACP has also been used to mitigate dental erosion and can be use primary or secondary preventive measures. This compound seems to cause the formation of a layer that fills the enamel interprism cavities (Cassimiro-Silva, Maia, Monteiro, & Gomes, 2016; Poggio, Lombardini, Dagna, Chiesa, & Bianchi, 2009). When placed on the tooth surface, CPP-ACP interacts with hydrogen ions and form calcium hydrogen phosphate which releases calcium and phosphate ions, thus aid in remineralisation. Furthermore, CPP-ACP containing fluoride (CPP-ACPF or Tooth Mousse Plus) provides additional advantage where fluoride, together with calcium and phosphate ions may enhance the remineralisation process (Cochrane et al., 2010).

Vanichvatana and Auychai (2013) have reported the remineralisation effect of CPP-ACPF and beta tricalcium phosphate (β-TCP) and sodium lauryl sulphate. Furthermore, an *in-situ* study showed that the use of a chewing gum containing CPP-ACP improved the mineral precipitation of eroded enamel (Prestes et al., 2013).

2.5.2.3 Bioactive material for enamel mineralisation - Bioactive glass

Bioactive glass (BAG 45S5) was originally invented by Hench as a bone regenerative material. Bioactive glasses form hydroxycarbonate (HCA) apatite following immersion in body fluids. This glass has shown positive results in inducing apatite formation when brought into contact with saliva or any physiological fluid. These apatites constitute either hydroxyapatites (Hench, 1991), or fluorapatites (Delia S. Brauer, Karpukhina, Law, & Hill, 2009), if fluoride was incorporated into the chemical composition of the glass structure.

Bioactive glasses have unique remineralising properties and are generally introduced into various dentifrices as very fine particles to provide calcium and phosphorus to the tooth surface (Madan, Madan, Sharma, Pardal, & Madan, 2011). Fluoride-containing glasses have 'smart' properties, with increased remineralisation activity in low pH environments (D. S. Brauer, Karpukhina, O'Donnell, Law, & Hill, 2010). Consequently, it has variously been added to tooth-paste, prophylactic gels and dental materials to treat enamel demineralisation (D. S. Brauer et al., 2010; Litkowski, Hack, Sheaffer, & Greenspan, 1997).

The SEM observation of sound enamel surfaces submitted to pH-cycling or to bleaching procedure and treated with BAG paste revealed mineral precipitations attached to the surfaces (E. Gjorgievska & Nicholson, 2011; E. S. Gjorgievska & Nicholson, 2010). Treating the surface of bovine enamel with BAG 45S5 during bleaching procedures reduced the microhardness loss and the ultra-structural changes of the bleached surface (Deng et al., 2013). In addition, the application of 45S5 BAG paste significantly improved the microhardness of the sub-surface of the eroded enamel surface (Bakry, Marghalani, Amin, & Tagami, 2014). In another in-vitro study, the use of toothpaste containing BAG 45S5 exhibited no significant remineralisation effect on eroded enamel surfaces when compared to the control group, assessed using

nanohardness (X. Wang, Megert, Hellwig, Neuhaus, & Lussi, 2011). Overall, the previous investigations explored the potential role of BAG in enamel remineralisation and presented promising result.

2.5.2.4 Calcium silicate

Calcium silicate and sodium phosphate salts toothpaste and a dual phase booster gel have also been developed to provide additional enamel remineralisation benefits. The toothpaste has been shown to form hydroxyapatite on enamel surface by depositing calcium silicate, which then releases calcium ions into oral fluids to help nucleate hydroxyapatite. Recent studies have shown that toothpaste containing calcium silicate/phosphate reduces enamel demineralisation and enhances remineralisation compared to the fluoride and non-fluoride controls (Joiner, Schafer, Naeeni, Gupta, & Zero, 2014; S. B. Jones et al., 2014; Parker et al., 2014).

2.5.2.5 Saliva flow and buffering capacity

Once acidic substances enter the oral cavity, salivary glands will reflectively increase secretion of saliva which will accelerate in clearing the acids from the mouth. Since human saliva contains bicarbonates and urea, it rapidly neutralizes the acidic remnants and returns the oral pH to normal – which is known as the buffering capacity of saliva, an important mechanism for oral pH regulation. Many factors affect saliva flow rate and buffering capacity, including autoimmune diseases (e.g., Sjögren's syndrome), medications (e.g., antidepressants and antipsychotics) and aging. When saliva flow rate is reduced, its clearance and buffering capacity will be negatively impacted, resulting in abnormal acid retention in the mouth, which, in turn, may contribute to dental erosion. Saliva flow rate and buffering capacity are therefore important etiological factors for erosion (Brand, Tjoe Fat, & Veerman, 2009; Piangprach, Hengtrakool, Kukiattrakoon, &

Kedjarune-Leggat, 2009). Low saliva flow rate and poor buffering capacity are often found to be associated with the development of dental erosion (Jarvinen, Rytomaa, & Heinonen, 1991; O'Sullivan & Curzon, 2000b). Furthermore, factors that increase salivary flow such as gum chewing will likely increase pH, buffering capacity, lubrication, and remineralisation potential (Amaechi & Higham, 2001a; Gedalia, Dakuar, et al., 1991). Gum chewing is usually useful due to good compliance compared to other approaches.

2.5.3 Restorative treatment

Any restorative treatment should be ideally delayed until the effect of the preventive measures on the rate of tooth wear is assessed. In cases where extensive erosive damages have occurred, restorative treatment may be necessary with the use of composites, laminates or crowns, in conjunction with preventive strategies. The purpose is to relief symptoms, protect the pulp, and replace lost tooth substance to improve function and aesthetics. If possible, the least invasive restorative therapy should be used, for example, direct composite restorations (Carvalho et al., 2016).

Depending on the degree of tooth wear, restorative treatment can range from minimally invasive and adhesive dentistry, to full mouth rehabilitation, to restoring the lost vertical height. However, regardless of the type of restorative therapy provided, prevention of the progression of erosion should be the basis of management of the patient with erosion. This will increase the likelihood of successful, long-term outcomes of the restorative treatment.

2.6 Optical Coherence Tomography (OCT)

2.6.1 Background

Optical coherence tomography (OCT) is a more recent imaging modality that has been developed since the early 1990s. OCT is an emerging 'non-destructive' biomedical imaging technology based on the same concept as for ultrasound imaging but uses light instead of sound. Furthermore, OCT is comparable to ultrasound as in both techniques, an incident beam is used, and a backscattered signal is measured (Gimbel, 2008; Schuman, 2008). The general principle of using reflections to create the images is the same for OCT and ultrasound but the methods for detecting these reflections are different.

Using light as the medium in OCT offers it the benefit of being a non-contact optical imaging technique, whereas ultrasound needs a coupling medium, such as water along its path between transmitter and tissue to pass the sound waves. As light is faster than sound, the time delays between reflections from different layers cannot be measured directly, the differences would be on the order of femtosec, hence, OCT uses low-coherence interferometry to see the difference in time, corresponding to the distances between structures (Schuman, 2008).

OCT is an imaging system, based on a Michelson Interferometer for creating cross- sectional imaging of internal biological structures due to the scattering and absorption of coherent or incoherent light (J. Fujimoto & Drexler, 2008; D. Huang et al., 1991). It is capable of measuring the intensities of the backscattered reflections as a function of their axial and transverse positions in the tissue. The typical light sources used are near-IR lasers or broadband low coherent radiation sources, from 780 nm to 1550 nm. The light source and wavelength used offers great potential for optical imaging modalities in dentistry, due to the weak scattering and absorption in dental hard tissue (Robert S Jones, Huynh, Jones, & Fried, 2003). Moreover, oral cavity is suitable for OCT imaging

because they are easily accessible by the fibre-optic OCT device (Otis, Colston, Everett, & Nathel, 2000).

OCT imaging has the potential to detect and diagnose very early stages of demineralisation, remineralisation, recurrent caries, restorative failures, root canals, periodontal disease, soft tissue dysplasias and precancerous lesions in real time (Gimbel, 2008). Initially, OCT was developed to image transparent tissue, such as the eye. Recently it has been used to image non-transparent tissues, such as enamel. Therefore, this added advantage has been utilized in imaging the oral cavity as they have both transparent and non-transparent tissues (Podoleanu et al, 2005). Furthermore, while many of these technologies improved retinal imaging, they also allowed for the application of OCT to many new clinical areas. As a result, OCT has been clinically demonstrated in a diverse set of medical and surgical specialties, including gastroenterology, dermatology, cardiology, and oncology, among others.

When measuring the backscattered signal from a surface, an A-scan is obtained which is basically a signal intensity as a function of its axial position (depth) within the tissue (Fried et al., 2002). In some studies that have used polarisation sensitive OCT (PS-OCT), a type of OCT where the backscattered light is polarised (Hee, Swanson, Fujimoto, & Huang, 1992; Manesh, Darling, & Fried, 2009), this backscattered intensity signal was shown as a colour-coded scale.

2.6.2 Principles of OCT

OCT was developed based on the concept of low-coherence interferometry. In simple words, a laser source is projected over a specimen, and the backscattered signal intensity from within the scattering medium reveals depth-resolved information about scattering and reflection of the light in the specimen. The signal from serial scans can be

transformed into an image by a software, or in other words, the frequency information of the backscattered light is used to generate an image (D. Huang et al., 1991).

OCT is analogous to ultrasound imaging but uses light instead of sound. Cross-sectional images are generated by measuring the echo time delay and intensity of light that is reflected or backscattered from the inner structures. The echo time delay cannot be measured directly because the velocity of light is extremely high. Instead, it is necessary to use correlation or interferometry techniques. One method for measuring the echo time delay of light is to use low-coherence interferometry (Singh, Singh, Nagpal, & Laller, 2015).

An OCT system is characterized by several parameters such as imaging speed, lateral and axial resolutions, and penetration depth (Schmitt, Xiang, & Yung, 1999). Although imaging depths are not as deep as ultrasound, the resolution of OCT is more than 10 to 100 times more detail than standard clinical ultrasound (J. G. Fujimoto, 2003). The nomenclature in OCT is however analogous to the one used in ultrasound tomography. Single depth scans and cross-sections are classified as A- and B-scans, respectively (**Table 2.7**). OCT produces two-dimensional (2D) optical tomographic (XZ), cross-sectional depth images which are the B-scans. When multiple B-scan images are taken in the Y-plane direction, a three-dimensional (3D) image (in the XYZ dimensions) can be obtained.

Table 2.7: Scanning modes in OCT imaging (Aggarwal et al., 2013).

A-Scan	• also known as axial scan. • a single depth scan obtained by focusing the light beam to a point on the surface of the specimens and recombining the reflected light with the reference. • information obtained corresponds to the depth of the tissue which is determined by the optical reflectance of the tissue.
B-Scan	• also known as longitudinal scan. • a cross-section scan generated by collecting many single axial scans linearly across the tissue and in subsequent transverse position. • images obtained will have both depth axis and lateral or angular axis.

2.6.3 OCT development

Since the first publication of OCT in the early nineties (D. Huang et al., 1991), the technology has evolved substantially with enhancements both in imaging method and image analysis. There are 2 main types of OCT: time domain (TD-OCT) and spectral domain (SD-OCT) (Leitgeb, Hitzenberger, & Fercher, 2003). SD-OCT, also known as Fourier-domain OCT (FD-OCT), is a newer technology in which the scan rate is faster, has better penetration depth and signal-to-noise ratio, compared to TD-OCT. These characteristics are further improved in swept-source OCT (SS-OCT), in which diminishes the likelihood of motion artefacts and thus results in better image contrast and reduces the chance of missing pathology (Avanaki et al., 2013; de Boer et al., 2003).

The developmental path started with time-domain (TD-OCT), followed by spectral-domain (SD-OCT) and other OCT techniques with higher scan acquisition speed (Potsaid et al., 2010; Potsaid et al., 2008) and higher axial and transverse resolution (Godara, Dubis, Roorda, Duncan, & Carroll, 2010; Wong, Koizumi, & Lai, 2011). The conventional OCT imaging system was based on the principles of TD-OCT, where a mirror mechanically scans a distance at the reference arm to enable resolving of the depth information. Later, SD-OCT systems were developed, in which the mechanical scanning at the reference mirror had been eliminated and the images were obtained in a shorter time (Yamanari, Lim, Makita, & Yasuno, 2009). Simplification of this system by encoding the spectral components (wavenumber) in time, generated the swept-source OCT (SS-OCT). In this technology, the laser source sweeps near-infrared wavelength within milliseconds of scan delays at kilohertz rates in order to achieve real-time imaging. SS-OCT is the latest implementation of imaging technology with a promising prospect as a chair-side diagnostic modality in dentistry, due to its enhanced two-dimensional (2-D) and three-dimensional (3-D) scanning speed and image resolution. This modality has been validated to score carious lesion extent and detect cracks and dental restoration

defects (Bakhsh, Sadr, Shimada, Tagami, & Sumi, 2011; Imai, Shimada, Sadr, Sumi, & Tagami, 2012; Makishi, Shimada, Sadr, Tagami, & Sumi, 2011; Shimada et al., 2010).

OCT has been widely used in assessment of demineralisation based on two main principles; increased light scattering in the porous demineralised tissue, and depolarization of the incident light by the demineralised tissue. The latter necessitates a polarization- sensitive OCT (PS-OCT) or cross-polarization OCT (CP-OCT) setup (R. S. Jones & Fried, 2006; H. Kang, Darling, & Fried, 2012; Le, Darling, & Fried, 2010), but the former phenomenon can be observed as increased signal intensity by both conventional and polarized sensitive OCT systems. Furthermore, image analysis techniques in correlative OCT studies have been mainly based on the increased signal intensity values to quantify parameters such as depth (as a cut-off point) and mineral loss (dB values integrated over depth) in demineralised lesions (Natsume et al., 2011), however, there are fewer studies on the assessment of remineralisation by conventional OCT.

During demineralisation, minerals are partially dissolved and a porous structure with different optical properties is formed (Fried et al., 2002). In dental literature, several studies have utilized OCT to assess enamel demineralisation and remineralisation (R. Jones et al., 2012; Shimamura et al., 2011). However, most of them have used PS-OCT. It has been shown that PS-OCT can remove the confounding influence of surface reflections and native birefringence to enhance resolution of the surface structure of caries lesions (Amaechi, Higham, Podoleanu, Rogers, & Jackson, 2001; Baumgartner et al., 2000; Fried et al., 2002; R. S. Jones, Darling, Featherstone, & Fried, 2006a; R. S. Jones & Fried, 2006; Le et al., 2010). On the other hand, the potential of non-polarization sensitive OCT systems in this field has been underestimated.

Quantitative measurement of other optical properties that are based on light propagation in tissue may potentially provide a repeatable means of the tissue

characterization. Among those properties, the attenuation coefficient has shown promising results in discriminating between healthy and diseased states of various tissues including the epithelial tissues, arteries, skin, and lymph nodes (Scolaro et al., 2012; van der Meer et al., 2005). This parameter was noted in relation to enamel demineralisation and remineralisation (Popescu et al., 2008; Sadr et al., 2013). However, few studies have investigated the parameter at the 1300-nm OCT wavelength range against mechanical properties of enamel in a wide range of lesion conditions.

The illustration about the differences between TD-OCT, SD-OCT, and SS-OCT is shown in **Table 2.8**.

Table 2.8: Comparison of Time-Domain Optical Coherence Tomography (TD-OCT), Spectral-Domain OCT, and Swept-Source OCT

Adapted from (Rimayanti, Kiuchi, & Maulidia, 2014).

Parameter	TD-OCT	SD-OCT	SS-OCT
Working Principle	Measure the wavelengths of reflected light	Measure the wavelengths of reflected light	Measure the wavelengths of reflected light
Light Source	Broadband and continuous wave	Broadband and continuous wave	Narrow instantaneous line width, rapidly swept wave
Central Wavelength	830 nm	830 nm	1300 nm
Axial resolution / transverse resolution	~10 μm/20-25 μm	~5 to 7 μm/10-25 μm	~5 to 7 μm/~12.5 μm
Scan Speed	400 A-scans/s	~55,000 A-scans/s	~400,000 A-scans/s

2.6.4 Medical applications

It has been reported in the literature that the first application of low-coherence interferometry in the biomedical optics field was for the eye length measurement by Fercher, Mengedoht, and Werner (1988). Nowadays, OCT is being used as a clinical diagnostic modality in various medical fields (Fercher et al., 1988).

OCT enables real-time imaging of tissues without the need for biopsy, histological procedures, or the use of X-rays, so it can be used in many fields of medicine. OCT was first introduced as an imaging technique in biological systems by D. Huang et al. (1991), who recorded the *ex vivo* images of retina. The first *in vivo* OCT images, displaying retinal structures were published in 1993 (Fercher, Hitzenberger, Drexler, Kamp, & Sattmann, 1993). It has had significant impact in the ophthalmic field, specifically with the imaging of posterior eye segments including the retina, macula, and the optic nerve, allowing for the diagnosis and monitoring of relevant diseases (Adhi & Duker, 2013).

The OCT is used in ophthalmology, in the diagnosis of all layers of the retina, and is increasingly being used in cardiology, gastroenterology, pulmonology, oncology, and dermatology. The basic properties of OCT, that is, non-invasiveness and low wattage of the used light, have also been appreciated in analytical technology by conservators, who use it to identify the quality and age of paintings, ceramics, or glass. Recently, the OCT technique of visualization is being tested in different fields of dentistry.

OCT was first applied *in vitro* in human retina and in atherosclerotic biofilm (D. Huang et al., 1991). It is an optical imaging technique that enables cross-sectional imaging of microstructures of tissue *in situ*. OCT can provide “optical biopsy” without the need for excision and processing of specimens as in conventional biopsy and histopathology. With improvement of optical specifications and system capabilities, OCT demonstrates great potentials in research topics and clinical applications to date.

OCT was first reported by Fujimoto *et al.* in 1995 for *in vivo* imaging of the human eye (J. G. Fujimoto et al., 1995). OCT has also been widely used in numerous clinical applications, including gastroenterology (Evans et al., 2006; Poneros et al., 2001; P. Wilder-Smith et al., 2009), ophthalmology (Hangai et al., 2007; Y. Wang, Bower, Izatt, Tan, & Huang, 2008; Yasuno et al., 2007), dermatology (Olsen, Themstrup, & Jemec, 2015; Pierce, Strasswimmer, Park, Cense, & de Boer, 2004), and dentistry (Machoy et al., 2017).

2.6.5 Dental applications

In 1998, Colston *et al*. were the first to image dental hard and soft tissue both *in vitro* and *in vivo* using OCT (B. Colston et al., 1998). Since then with the advancement of spectral domain OCT, many studies were done in the dental field, specifically with imaging teeth. *In vitro* investigation in the area of enamel demineralisation, providing insight into the causes, timing, and what features can be detected with OCT. Furthermore, efforts have been made to remineralise the enamel and the success of these developments can be assessed through OCT, permitting product validation.

In vivo evaluation of demineralisation has been less extensively investigated (Fried, Staninec, Darling, Chan, & Pelzner, 2013; Ibusuki et al., 2015; Lenton et al., 2012; Nakajima et al., 2014; Nee et al., 2014). OCT was applied for the *in vivo* quantification of advanced dental erosion in patients with gastroesophageal reflux disease (C. H. Wilder-Smith et al., 2009). Shimada et al. (2014) published the first paper using SS-OCT for detection of proximal caries *in vivo* where the SS-OCT results were compared with dental X-ray. They found that the SS-OCT appeared to be a more reliable and accurate method than bitewing radiographs for the detection and estimation of the depth of proximal lesions in a clinical environment.

Shimada, Sadr, Sumi, and Tagami (2015) reviewed the various applications of OCT in dentistry, including the detection of demineralisation as well as the diagnoses of cracks, caries, and restoration defects. The presence and extent of caries can be detected with OCT through increased scattering, and the dentino-enamel junction (DEJ) also becomes highly reflective and distinctive once caries has penetrated this juncture and can help determine the depth of demineralisation and the progression of caries into the dentine. Furthermore, several studies have also focused on imaging caries *in vivo* as an alternative means of diagnosis, identifying these lesions as brighter enamel regions in the OCT images (Ibusuki et al., 2015; Lenton et al., 2012; Nakajima et al., 2014; Shimada et al., 2014; Shimada et al., 2015). Other researchers have investigated how OCT can be used to assess how certain products affect enamel erosion, whether it be orthodontic brackets contributing to demineralisation (Nee et al., 2014) 41 or treatments, such as fluoride, to prevent or reverse demineralisation damage (Fried et al., 2013).

OCT could measure the changes in the intensity of the backscattered light from different level of depth. It could obtain cross-sectional imaging by measuring the magnitude and echo time delay of the backscattered light by using a broad-band light source. OCT intensity is high at the air-enamel or air-root interface but signal will rapidly dying out with certain depth into the tooth (Choo-Smith, Dong, Cleghorn, & Hewko, 2008). It could also produce qualitative morphological cross-section images of near surface tissue structures. OCT has been used to study *in vitro*, the progression of demineralisation of initial enamel erosion (Chew et al., 2014), and it has the potential of being used for *in vivo* initial erosion studies. The principle of this method is that after erosion, the tooth surface is roughened and porous. This creates open spaces within the enamel matrix and therefore, more light will be scattered and less will be transmitted compared to sound tissue. Furthermore, OCT had shown potential as a quantitative

method tool which allows non-destructive and safe measurements of dental erosion for clinical evaluation (Chan, Chan, Darling, & Fried, 2013).

2.6.6 Factors affecting OCT signal

The optical system focuses the light beam (incident light) onto the specimen and collects backscattered or reflected light back to the interferometer, where the magnitude and the echo time delay of the backscattered light are analysed. Hence, OCT images show light-scattering intensity from different layers of tissue. Because healthy sound enamel and demineralised tissue have different scattering properties, the OCT images are able to provide information regarding the enamel thickness, morphology and porosity. For example, demineralised eroded areas of enamel have higher porosity than the healthy hard tissue which causes higher light scattering in the eroded enamel and a reduced depth of light penetration. As a result, demineralised areas appear on the OCT images with increased signal intensity/reflectivity compared to the sound tissue. Analogously, remineralisation can be detected as an area with reduced light scattering, i.e. reduced signal intensity compared to the demineralised enamel (Attin & Wegehaupt, 2014).

2.6.6.1 Hydration of substrate

Under dry conditions, higher brightness was observed at enamel surface as but generally a clear boundary was not observed. In other words, a visual border between the brighter and darker parts of enamel could not be found. Likewise, on hydrated specimens, demineralised enamel appeared to be brighter as the demineralisation period increased; however, a boundary could be observed in some specimens (Nazari et al., 2013).

2.6.6.2 Biofilm

But the full nature of its influence is unknown and would be best to be removed before scanning with OCT. One of the methods is to use water jet. However, if water jet is not able to fully remove the biofilm, it would be necessary to know how its presence affects the OCT signal.

2.6.7 Limitations of OCT

There are also limitations for clinical use of OCT in dentistry and future perspectives from latest research. The main issues are cost and lack of commercial availability. OCT machines are costly when produced for commercialization due to the high cost of the component parts, thus, limits sales and discourages manufacturers in promoting the machines for clinical use. Future research should be directed toward increasing the optical penetration of OCT, thus allowing accurate diagnosis of proximal caries lesions, lesions underneath and around restorations, and more deeply located occlusal caries; developing imaging software and algorithms for image analysis, contrast measurement, and image registration for real-time simultaneous processing and analysis of images; and also increasing the contrast between sound and eroded or carious tissues.

CHAPTER 3: THE EFFECT OF EARLY BIOFILM ON THE MEASUREMENT OF INITIAL ENAMEL EROSION USING OPTICAL COHERENCE TOMOGRAPHY (OCT): AN *IN VITRO* STUDY

3.1 Introduction

Because the prevalence of dental erosion is growing steadily and shifting toward young age groups (Jaeggi & Lussi, 2014), it is important to diagnose it at its initial stage for the timely application of preventive measures and to delay the process of tooth wear. Detection method for initial enamel erosion is emerging. The gold standard for the measurement of early stage surface softening is microhardness testing (Schlueter et al., 2011). However, this is typically an *in vitro* technique, reliant upon physical indentation of the specimen. Clinically, erosion can be measured on casts obtained from dental impressions (Zou, Cherukara, Hao, Seymour, & Samarawickrama, 2009) using surface profilometry or visually at the chairside using an ordinal scoring system (Maupome & Ray, 2000). Nevertheless, these techniques are only sensitive to bulk mineral loss that is beyond remineralisation. Therefore, various techniques have been proposed for detecting, imaging, monitoring and quantifying dental hard tissue mineralisation dynamics, both *in vitro* and *in vivo* (Elton, Cooper, Higham, & Pender, 2009). Among these techniques, optical coherence tomography (OCT) has been explored for caries detection (Amaechi et al., 2001; Baumgartner et al., 2000; Chen, Otis, Piao, & Zhu, 2005; B. W. Colston, Jr. et al., 1998; Nakagawa, Sadr, Shimada, Tagami, & Sumi, 2013; Shimada et al., 2014; X. J. Wang et al., 1999) and to a lesser extent for erosion measurement (Austin et al., 2017; Chew et al., 2014; C. H. Wilder-Smith et al., 2009).

OCT is able to detect demineralisation after a 10 min acid challenge and could be used to monitor the progression of demineralisation of initial enamel erosion *in vitro*. In addition, it can also distinguish sound enamel from enamel erosion lesions *in vitro* (Chew

et al., 2014). However, the measurements obtained from this tool may be compromised by natural components of the oral environment. The presence of dental biofilm may interfere with the clinical measurements of enamel using OCT. From a previous study (Chew, 2013), it was thought that biofilm on the enamel surface could be a confounding factor in acquired 'noisy' results in OCT readings *in situ.* Thus, this study was conducted to determine whether oral biofilm of different stages of maturation can affect OCT sub-surface measurements.

To date, the effect of the dental biofilm on this technique has not yet been examined. Therefore, there is a need to conduct further studies to explore how this parameter may affect the ability of OCT to detect and monitor erosive lesion progression.

3.2 Literature Review

3.2.1 Dental plaque as a biofilm

Dental plaque has been defined as the diverse microbial community found on the tooth surface as a biofilm, embedded in an extracellular matrix of polymers of host and microbial origin (Marsh, 2004). In recent years, dental plaque has been identified as a biofilm, and the structure, microbiology, and pathophysiology of dental biofilms have been described. Biofilms are naturally found in all wet environments including the oral structures of nearly all species.

Dental biofilm which is also termed as “oral biofilm” may be defined as the soft tenacious material found on tooth surfaces that is not readily removed by rinsing with water, but more specifically, it is an organized matrix derived from salivary glycoproteins and extracellular microbial products in the form of a biofilm that forms on the hard, non-shedding surfaces in the mouth (N. C. Claydon, 2008). Biofilms are held together by sugary molecular strands known as EPS or “extracellular polymeric substances”. The cells that secreted the EPS are protected by the formation of the resulting biofilm.

The nature of the biofilm enhances the component bacteria's resistance to both the host's defence system and antimicrobials. If not removed regularly, the biofilm undergoes maturation, and the resulting pathogenic bacterial complex can lead to dental caries, gingivitis, and periodontitis. In addition, dental biofilm, especially subgingival plaque in patients with periodontitis, has been associated with various systemic diseases and disorders, including cardiovascular disease, diabetes mellitus, respiratory disease, and adverse pregnancy outcomes (Gurenlian, 2007).

In the oral cavity, there are different types of bacteria that normally present in the mouth. These bacteria and leukocytes, neutrophils, macrophages, and lymphocytes are part of the normal oral cavity and contribute to the individual's health (Darby & Walsh,

2014). Approximately 80–90% of the weight of biofilm is water. While 70% of the dry weight is bacteria, the remaining 30% consists of polysaccharides and glycoproteins (Marsh & Bradshaw, 1995). *Strep. mutans* and anaerobes are the initial colonisers of the tooth surface, and play a major role in the establishment of the early biofilm community (Kolenbrander, 2000). These microorganisms present in dental biofilm are all naturally present in the oral cavity and are normally harmless. However, failure to remove biofilm by regular tooth brushing means that they are allowed to build up in a thick layer and cause dental disease. Those microorganisms nearest the tooth surface ferment dietary sucrose; it is in this state that they start to produce acids.

3.2.2 Stages of biofilm formation

Formation of the biofilm involves a series of steps beginning with the initial colonization of the pellicle and ending with a complex formation of a mature biofilm (**Figure 3.1**). As the biofilm matures, the microbial composition changes from one that is primarily gram-positive and streptococcus-rich to a structure filled with gram-negative anaerobes (Xie et al., 2000). The process of biofilm formation can be divided into three major stages (Nield-Gehrig, 2005).

3.2.2.1 Stage 1: Formation of dental pellicle

The first stage of the biofilm development involved the formation of the acquired saliva pellicle. The acquired pellicle is an amorphous acellular layer covering the surface of the tooth in the presence of saliva. It is a thin layer of saliva that is composed of mainly glycoproteins and forms shortly after cleaning of the teeth or exposure of new teeth (Kreth, Merritt, & Qi, 2009).

Electrostatic attractive forces contribute to the formation of the acquired pellicle. According to Bernardi, Giro, and Gaillard (1972), the hydroxyapatite of the enamel and

its various chemical groups are arranged so that their negatively charged phosphate groups lie close to the surface, and in doing so effectively 'shield' the positively charged calcium groups, which gives the hydroxyapatite surface a net negative charge. The study notes that, when water is present, the hydroxyapatite attracts ions of the opposite charge, and these ions form a layer over the surface. This layer of oppositely charged ions-counter ions-is referred to as the hydration layer or Stern layer, and in the case of the enamel surface effectively neutralizes the negative charge. When enamel is immersed in saliva the hydration layer has been estimated to consist of 90% calcium and 10% phosphate (Bernardi et al., 1972).

When the enamel is precoated with pellicle, adherence of early bacterial species will be enhanced. The resulting pellicle acts like an adhesive, causing bacteria to adhere to the tooth surface protects the surface of the tooth by regulating the mineral ions exchanged between the tooth and saliva. This directly influences the initial bacterial colonization, and additional bacteria continue to adsorb to the tooth surface.

3.2.2.2 Stage 2: Initial colonization of bacteria

The second stage is the initial bacterial colonisation which occurs within minutes to hours after deposition of the acquired pellicle. The colonisation process starts with the adhesion of pioneer bacteria, known as early colonizers, to the salivary pellicle on the tooth surface, as well as on the existing dental restoration. In the very early stages, the predominant tooth colonisers were found to be *actinomyces sp*. (J. Li et al., 2004; Onisei, Onisei, Feier, Rusu, & Stratul, 2008). These species are called the early colonisers followed by the late colonisers. J. Li et al. (2004) demonstrated that *actinomyces* were the prominent colonisers in biofilm which were formed within 6 h on dental enamel surfaces. Their data showed that the relative proportion of streptococci, in particular, *Strep. mitis*

and *Strep. oralis*, become more predominant than *actinomyces* within the first 6 h of biofilm formation.

The bacterial adhesion occurs via specific receptors located in the salivary pellicle layer (Marsh, 2004) and this stage refers to the stage where the pellicle is populated with bacteria. Furthermore, they are able to withstand the mechanical forces of the intra-oral activities such as chewing, tongue movements, and salivary flow, due to the attachment of oral bacteria via specific molecular interactions (J. Li et al., 2004). This stage of bacterial colonisation is expected to be the stage observed on the enamel surface in this *in vitro* study.

- **Early colonisers**

Streptococcus sp. and *Actinomyces sp.* have been recognized as dominant species in a healthy oral environment. They were observed *in vivo* as the bacteria attaching directly to the tooth surface (Zijnge et al., 2010), where they are able to bind directly to the salivary pellicle (Kolenbrander, Palmer, Periasamy, & Jakubovics, 2010).

- <u>*Streptococccus sanguinis (Strep. Sanguinis)*</u>

Strep. Sanguinis, previously known as *Strep. Sanguis* is one of the early colonisers of dental biofilm (Razak & Rahim, 2003) and is one of the first bacteria to attach to the pellicle glycoproteins and is a normal inhabitant of the healthy human mouth. These bacteria are able to replicate in the oxygen rich environment of the oral cavity and form micro-colonies within minutes after attachment. Other bacteria including *Strep. mutans* are able to grow in these colonies. *Strep. mutans* is important because it is associated with dental caries (Y. H. Li et al., 2002). These bacteria produce an enzyme known as glucosyltransferase. Glucosyltransferase converts sucrose into exopolysaccharides. These exopolysaccharides create a sticky environment that allows other bacteria to attach

to the initial colonies and protect them from acidic environments. As the biofilm begins to develop and expand, oxygen can no longer diffuse into the colonies.

After a few days, anaerobic gram-negative cocci, rods, and filaments begin to colonize the biofilm. After several weeks the cocci, rods, and filaments grow together forming colonies known as corncobs. This anaerobic environment causes facultative anaerobes such as *Strep. mutans* and *Lactobacilli* to break down sucrose through fermentation pathways. These bacteria produce lactic acid as a metabolic by product (C. H. Miller & Palenik, 2014). If the concentration of lactic acid becomes high enough it can cause the pH around the biofilm to drop below 5.5 and demineralisation will occur (Roberson, Heymann, & Swift Jr, 2006).

- *Streptococcus mitis (Strep. mitis)*

Strep. mitis is a common species in the mouth and frequently predominates with *Strep. sanguinis* during the initial colonization of the tooth surface. *Strep. mitis* group, were dominant in the early bacterial flora on human enamel surfaces (Nyvad & Kilian, 1990).

- *Actinomyces*

The bacterial distribution in biofilm specimens was distinct from that in saliva, confirming the selectivity of the adhesion process. In the very early stages, the predominant tooth colonisers were found to be *Actinomyces* species. The relative proportion of streptococci, in particular *Strep. mitis* and *Strep. oralis,* increased at the expense of *Actinomyces* species between two and six hours. Furthermore, early dental biofilm, assessed for 40 strains of bacteria, has been found to consist mainly of *Actinomyces* until between two and six hours after the formation begins, where at this point, the number of *Streptococci* increased when compared to *Actinomyces*, especially *Strep. mitis* and *Strep. oralis* (Listgarten, 1994).

3.2.2.3 Stage 3: Biofilm maturation

The subsequent stage is the development of complex flora or biofilm maturation where the early biofilm changes from simple gram-positive coccal bacteria to a complex flora with gram-positive and gram-negative rods and spirochetes (Chapple & Gilbert, 2002). The early colonizers become established which leads to increased dental biofilm complexity due to factors, such as oxygen consumption within the biofilm, creating anaerobic zones, food chains becoming established, and an increased range of receptor sites for bacterial attachments. Cell division and recruitment of new bacteria also allows the bacterial population to increase. Furthermore, the presence of gram-positive bacteria enhances the colonisation of other species such as the gram-negative rods by co-aggregation. Biofilm reaches the mature stage after seven to 14 days and becomes relatively stable around the 21st day.

Table 3.1 and **Figure 3.1** summarise the phases of biofilm formation.

Table 3.1: Description of the phases of biofilm formation (Chetrus & Ion, 2013).

1.	Pellicle formation	A thin bacteria free layer forms within minutes on cleaned tooth surface.
2.	Attachment	Within hours, bacteria attach to the pellicle and a slime layer is formed around the attached bacteria.
3.	Young supra-gingival biofilm	Young supra-gingival biofilm consists mainly of gram-positive cocci and rods, some gram-negative cocci and rods.
4.	Aged supra-gingival biofilm	In aged supra-gingival biofilm, there is an increase in the percentage of gram-negative anaerobic bacteria.
5.	Sub-gingival biofilm formation	Tooth-attached biofilm, mostly gram-positive bacteria, with some gram-negative cocci and rods. Epithelial attachment and unattached biofilm, mostly gram-negative rods and spirochetes.

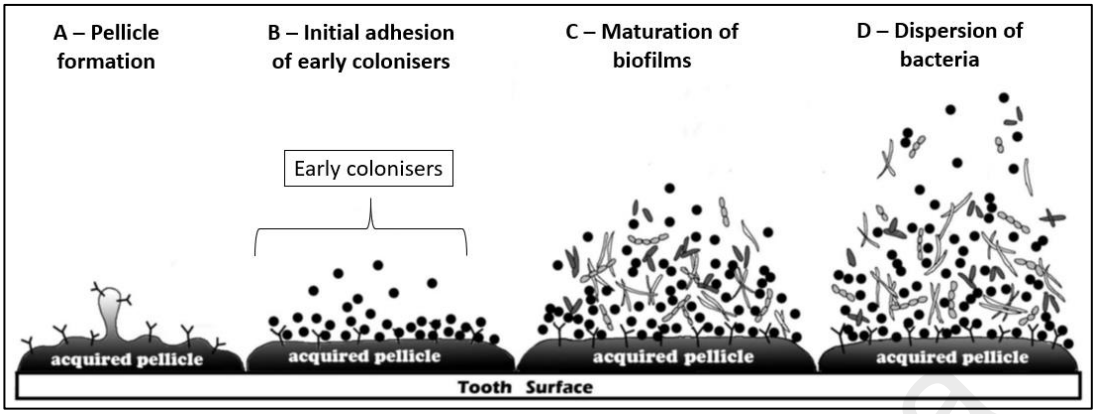

Figure 3.1: Formation of a biofilm and its dispersal to other sites.

Adapted from (R. Huang, Li, & Gregory, 2011)

Figure 3.1 represents stage of oral biofilm formation.

(A) Pellicle formation: The pellicle is a thin layer derived from salivary glycoproteins attached to a clean tooth surface.

(B) Initial adhesion: Early colonizers in saliva recognize the binding proteins in acquired pellicle and attach to them. This adhesion is reversible.

(C) Maturation: Different bacterial species coaggregate and mature biofilm forms.

(D) Dispersion: Bacteria disperse from the biofilm surface and spread to colonise a new site.

3.2.3 *In vitro* biofilm cultivation

When developing an orally relevant biofilm model, the closer it can be to the *in situ* scenario, the more representative of the *in vivo* effects can be investigated, *in vitro*. Most studies of biofilm structure in relation to microbial metabolism and ecology have been restricted to *in vitro* model systems. Various culture systems such as constant-depth fermenters, chemostats, and flow cells have all been used to generate both single- and mixed-species biofilms *in vitro* (Sissons, 1997). An investigation of naturally found biofilms is difficult to perform due to the lack of well-defined environmental conditions that support the biofilm growth. Therefore, biofilms are generally cultivated in laboratories under defined conditions for research purposes.

The basis of any study that requires an artificial mouth model is to have a continuous or intermittent supply of nutrients to growing biofilms within an environment, which can possibly mimic the *in vivo* oral niches. However, artificial systems could never entirely imitate human parameters. Nevertheless, every attempt should be made to close the gap and achieve a more realistic simulation of what actually happens in real-life scenarios. The complexity of the oral environment, and ethical problems associated with *in vivo* studies of oral diseases such as caries and periodontal diseases in humans have inevitably led to the development of laboratory models, which simulate the oral environment *in vitro*.

These model systems are usually termed ‘artificial mouth’. The basis of an artificial mouth model is to provide a continuous or intermittent supply of nutrients to bacterial plaque or biofilms growing within an environment, which mimics the *in vivo* oral niches and habitats. During such experimental procedures, real-time growth and development of dental biofilm can be observed with various microscopy tools or analysed using microbiological, biochemical and molecular methods.

The artificial mouth model developed by Sissons, Cutress, Hoffman, and Wakefield (1991), allows the long-term growth and development of dental plaque, derived either from clinical plaque or saliva specimens. The methodology permits the addition of different nutrients and modification to the environment to understand their effects on the developing biofilm. The biofilm was grown on a cover-slip, where nutrients and test agents can be added via entry ports. Utilising this methodology, Sissons et al. (1991) was able to show similarities in responses to changes in pH with addition of sucrose and urea, and mineralisation as measured by the deposition of Ca^{3+}, PO^{4-} and F^{-} to that of natural dental plaques. As noted by the authors, although the system was running for 6-weeks, after just 3-weeks, the biomass was too large for the cover-slip. A key feature of this "artificial mouth" model is the capacity to monitor the metabolism and environmental changes within the biomass formed. This model has been widely used to evaluate caries development (Shu, Wong, Miller, & Sissons, 2000; Tang, Yip, Cutress, & Samaranayake, 2003); and biofilm viability (Filoche, Coleman, Angker, & Sissons, 2007).

In the early days, the artificial mouth model was designed using glass cylindrical funnel (Pigman, Elliott, & Laffre, 1952; Pigman & Newbrun, 1962). This was later replaced by glass incubation chamber (Russell & Coulter, 1975). Subsequently, artificial mouth models called the Column System using pyrex glass tube (Sudo, 1977) and a culture vessel were designed (M. H. De Jong & Van der Hoeven, 1987).

From 1990 onward, a complex artificial mouth model was developed, called the Multi-Plaque Artificial Mouth, which consisted of a glass cylinder containing five stations for plaque growth (Sissons et al., 1991). This complex artificial mouth model can be used to monitor long-term growth of plaque.

3.2.4 Assessment of biofilm

Various optical and non-optical techniques have been reported for the quantification and monitoring of biofilms. Any techniques used have to be performed non-destructively in order to characterize the biofilm growth in terms of structural organization. Non-optical methods include the structural monitoring of the biofilms using magnetic resonance imaging (MRI), and investigation using scanning transmission x-ray and transmission electron microscopy (TEM) (Lawrence et al., 2003; Manz, Volke, Goll, & Horn, 2005). However, most of these techniques use ionization radiation which affects the biofilm growth. Moreover, applicability of these techniques is limited because of the poor image resolution and inability to provide real-time monitoring.

Alternatively, optical imaging techniques are identified as promising tool for investigation of biological specimens since they use non-ionization radiation and offer excellent resolution (Balas, 2009). On account of this, optical imaging techniques such as time resolved photo acoustic spectroscopy, light microscopy and confocal laser scanning microscopy (CLSM) are widely used for investigating biofilms (Mueller, de Brouwer, Almeida, Stal, & Xavier, 2006).

3.2.4.1 Confocal Laser Scanning Microscopy (CLSM)

Confocal laser scanning microscopy (CLSM) is a non-destructive and non-invasive method with the capability to provide time-resolved three-dimensional images of biofilms, and it has been an important method for the study of biofilm structure. Since its first application (Lawrence, Korber, Hoyle, Costerton, & Caldwell, 1991), CLSM has become widely used to improve the understanding of the biofilm architecture (Lawrence & Neu, 1999).

CLSM is an optical microscope equipped with a laser beam, particularly useful in biology and life sciences in studying biofilm. This technology makes it possible to scan

a thick biofilm, e.g. a microbial biofilm, by processing images, line by line, in X, Y and Z axes. Biological samples are often stained with specific fluorescent dye so that the fluorescent light from the illuminated spot is collected into the objective and transformed by a photodiode in electrical signal processed by a computer. The optical reconstruction of all the pixel information is assembled yielding a high contrast and high-resolution three-dimensional image. This technique has been widely used in the study of biofilm, especially to study extra cellular polymeric substances (EPS) components (Karygianni et al., 2012; Lawrence et al., 1991).

The major limitation of CLSM is that the imaging can be performed only with staining. Furthermore, CLSM is not efficient in mapping of the EPS (Ratheesh Kumar, Murukeshan, Seah, & Shearwood, 2015). The light microscopy-based biofilm assessment always demands vertical displacement of the specimen in order to move the focal plane of the microscope from the water–biofilm interface to the biofilm–substratum interface. The requirement of moving the specimen often obstructs the live monitoring of the biofilm. Moreover, light microscopy-based monitoring scheme offers less working distance by keeping the specimen very close to objective lens, which is often undesirable when conducting biofilm experiments (Ratheesh Kumar et al., 2015).

i. **Principles of CLSM**

CLSM is made up of the optical system, the laser light source, the detection system, and the scanning device. The optics behind this type of imaging is a laser emitted from the light source that becomes a parallel beam of expanded diameter when it passes through the pinhole aperture, encounters the dichromatic mirror, and is reflected onto the objective lens. The light beam is reflected 90° when it hits the dichromatic mirror and is focused onto the desired focal plane on the sample when it passes through the objective lens. The fluorescence-emitting sample fluoresces in all directions under excitation from

the laser. Part of the fluorescence becomes focused at the focal point of the objective once it passes through the objective lens, dichromatic mirror, and focusing lens. The fluorescent light passes through a pinhole at the focal point and can then be picked up by the detector. When a laser scans the sample point by point, the photomultiplier tube behind the pinhole receives the corresponding point-by-point confocal optical image. Accordingly, different focal planes within the sample and optical cross-sectional images (also known as optical sectioning) can be analysed one by one. Using computer image processing and three-dimensional image reconstruction software, a high-resolution three-dimensional image can be obtained from the sample. Cell structure, cell content, and dynamic changes can be analysed by continuous scanning on the same plane.

ii. **Application in dental biofilm research**

Dental biofilm, in its natural hydration status, can be studied directly through special fluorescent staining. Through this process, dead and viable bacteria in dental plaque can be observed in situ, and the relationship between bacteria during the formation of dental plaque can be observed as well. Images of a single cell, a group of cells, or different levels within tissues can be obtained by scanning biofilm of a given thickness continuously using CLSM. Compared with SEM, CLSM requires fewer sample preparation steps before the composition and structure of dental plaque can be studied. During sample preparation in SEM, structural damage to the sample can accumulate during steps such as dehydration, fixing, embedding, and dyeing (X. Zhou & Li, 2015).

Moreover, CLSM can be used to observe structures, specific molecules, and biological ionic changes in living cells. The technique can also be used to track structural changes and physiological processes within living cells over time to detect changes under the natural state or after stimulation by certain factors. Quantitative and qualitative measurements can be made regarding the perimeter or area of a sample, average

fluorescence intensity of cells, in situ determination of cellular contents, composition and distribution of lysosomes, mitochondria, endoplasmic reticulum, cytoskeleton, structural proteins, DNA, RNA, enzymes and cellular receptors among others (X. Zhou & Li, 2015).

The major limitation of CLSM is that the imaging can be performed only with staining, and only few fluorescent stains can be employed simultaneously showing just a couple of components in the same image. A few types of staining solutions and techniques have been used for CLSM imaging in dental biofilm research:

1. **LIVE/DEAD® BacLight™ Bacterial viability Kits.**

The manufacturer indicates that LIVE/DEAD® BacLight™ fluorescence solution can be used to differentiate vital cells from non-vital ones based on membrane integrity. Vital cells are stained with SYTO9 which fluoresces green, while the non-vital ones are stained with Propidium Iodide which fluoresces red. However, the mechanism was not that straight forward and proved to be quite complex (Stocks, 2004). The main drawback of this method is the need to observe statistically relevant portion of the sample, representative of the total population. In any case, as it is impossible to get a total count of bacterial cells, the method provides only semi-quantitative results (Howlin et al., 2015; Thurnheer, Rohrer, Belibasakis, Attin, & Schmidlin, 2014).

2. **Fluorescent *In Situ* Hybridization (FISH).**

This technique is a genetic approach using oligonucleotide probes labelled with fluorescent dyes. These probes can be specifically designed to bind rRNA, particularly abundant in viable cells or to a specific molecule representative of a specific target of interest. Because of the genetic approach, this method can also be adopted for studies on multispecies biofilm. It is worthy to note that FISH can detect viable but not cultivable bacteria or bacteria with low metabolism (dormant) in biofilm (Pantanella, Valenti, Natalizi, Passeri, & Berlutti, 2013).

Combining FISH technique with CLSM makes it possible to identify and topographical visualise different species in a multispecies biofilm. The principal limitations are related to the complex preparation procedure and that the technique is time consuming and expensive. (F. C. Machado, Cesar, Assis, Diniz, & Ribeiro, 2012; Thurnheer, Gmur, & Guggenheim, 2004).

3. **Fluorescein Diacetate / Ethidium Bromide (FD/EB)**

FDA/EB vital fluorescence staining is routinely used together with CLSM to establish the three-dimensional vitality pattern of the (early) dental biofilm or to document the antibacterial effects of dental materials, mouthrinse solutions as well as food preservatives (Arweiler et al., 2014; Auschill et al., 2002; Auschill et al., 2005; Zaura-Arite, van Marle, & ten Cate, 2001). Due to easy handling and to the independency of calibration procedures, as well as concentration and other physical and chemical parameters, the results obtained via FDA/EB staining can be compared between different studies (Netuschil, Auschill, Sculean, & Arweiler, 2014).

3.2.4.2 OCT in biofilm research

OCT is the emerging imaging technique of the last decade in biofilm research. Its remarkable features are the fast – up to real-time – acquisition of multi-dimensional datasets, *in situ* application, involving no specimen preparation, allowing for a non-invasive and complete characterization of an unaltered biofilm structure. Additional advantages are the compact dimensions and mobility of on OCT device, which allows investigating biofilms directly inside the cultivation device (e.g., biofilm reactor) under operational conditions (e.g., flow). Hence, biofilms in various systems are analysed, which are not accessible by other, established imaging modalities. 2-D and 3-D datasets contain a representative description of the overall biofilm structure.

The earlier version of this technique, time–domain OCT (TD-OCT), relies on the scanning of the reference arm of the interferometer to acquire the depth resolved images. In this technique, the temporal gating is achieved by using a spectrally broadened, incoherent source (D. Huang et al., 1991). Another technique, Fourier–domain OCT (FD-OCT), was demonstrated in which the depth information is retrieved from the spectral contents of the interferogram without the translatory motion of the reference arm. FD-OCT is further classified into spectral domain OCT (SD-OCT) and swept source OCT (SS-OCT), based on the scheme through which the spectral components are resolved and detected. The SD-OCT uses a spectrally broadened source similar to the TD-OCT for illumination and the spectral components are spatially resolved by an optical grating followed by the detection using a line scan camera (Yaqoob, Wu, & Yang, 2005). In the case of SS-OCT, a rapidly sweeping narrow bandwidth laser source is used for lighting the system and the spectral fringes are detected sequentially by a photodetector (S. Yun, Tearney, de Boer, Iftimia, & Bouma, 2003).

Research in OCT was more focused on FD-OCT systems because of their capability of imaging with improved speed and sensitivity (Choma, Sarunic, Yang, & Izatt, 2003; Leitgeb et al., 2003). Of these FD-OCT schemes, the swept source based OCT (SS-OCT) has been identified as superior than spectral domain OCT (SD-OCT) in performance because of major advantages such as the reduced sensitivity fall-off and lower fringe washout effect caused by the specimen motion (Hendargo, McNabb, Dhalla, Shepherd, & Izatt, 2011; S. H. Yun, Tearney, de Boer, & Bouma, 2004). Furthermore, the availability of extremely narrow linewidth tuneable light sources with higher sweeping rate in association with the balanced detection and sophisticated data acquisition enables high speed and deeper imaging, making it more attractive for many bio-imaging applications.

Images obtained by OCT can be evaluated qualitatively by identification of structures, dimensions, and proportions (de Oliveira Mota et al., 2013; Nakagawa et al., 2013), and quantitatively, for example by analysing the reflectivity (R. S. Jones & Fried, 2006) or the total optical attenuation (Hariri, Sadr, Shimada, Tagami, & Sumi, 2012). Using OCT, it has been demonstrated in several studies that demineralised enamel shows stronger optical backscattering (Mandurah et al., 2013), and different authors have extensively studied the characteristics and the dynamic of the remineralisation of enamel, for teeth submitted to different periods of pH cycling (Fried et al., 2002; H.; Kang, Chan, Darling, & Fried, 2013).

The intensity of backscattered light is measured as a function of its axial position (depth) in the tissue. Low coherence interferometry is used to acquire the intensity of backscattered light and reflected as a function of position within the tissue with a resolution of 20– 30 mm. Lateral scanning of the probe beam across the tooth is then used to generate a two-dimensional intensity plot, similar to ultrasound images, called a 'B-scan' (Fried et al., 2002).

The versatility of OCT became obvious. However, in addition to a pure visualization of the biofilm structure, quantitative measures are required allowing for the objective comparison of imaging datasets as well as a statistical treatment applied to available data. A step forward in biofilm research has been achieved by monitoring the deformation (e.g., compaction, relaxation) of the biofilm structure at real-time in a series of B-scans (Blauert, Horn, & Wagner, 2015). In defined deformation experiments performed directly within the cultivation device (e.g., micro-fluidic flow channel), mechanical properties such as shear and Young's modulus have thereby been determined non-invasively (Blauert et al., 2015). However, OCT suffers from limitations, similar to any other visualisation tools. For example, the changing refractive indices along the z-axis, artefacts created by moving structures, or the signal-to-noise drop-off along an A-

scan of SD-OCT device. Although, OCT provides extraordinary penetration capabilities even in highly scattering biofilm specimens, optical clearing agents might be necessary to be added in some experiments. Analysis of OCT datasets is affected more or less by one or more of these issues. Therefore, a common image analysis protocol is still lacking, and individual biofilm research groups develop custom procedures. In future, software developers for OCT devices may consider this fact.

Imaging of biofilm systems have used to monitor the biofilm development, biofilm structure changes in complex/sophisticated cultivation setups, as well as to understand its dynamic behaviour. However, to date, no report has been published on how biofilm affects OCT backscattering behaviour during imaging of underlying structure such as, the enamel surface. Thus, the measurement of initially eroded enamel using OCT in the presence of dental biofilm on the tooth surface is not well understood. Thus, this study aimed to determine how biofilm would affect the OCT reading during imaging.

3.2.5 Aim and Objectives

Aim: To evaluate the effect of early dental biofilm on OCT backscattered intensity.

Objectives:

1. To cultivate early dental biofilm in a laboratory setting.
2. To study the attenuation of OCT signal through cultivated oral biofilm of different intervals.
3. To study the change in OCT scattering at the immediate tooth subsurface, with and without oral biofilm cultivated at different intervals.

Null hypotheses:

1. OCT signals are not affected by laboratory-cultivated biofilm.
2. No changes of OCT scattering at the immediate tooth subsurface, with and without oral biofilm cultivated at different intervals.

.

3.3 Materials and Methods

3.3.1 Ethics and collection of specimens

Ethical approval was obtained from the Medical Ethics Committee, Faculty of Dentistry, University of Malaya (DF RD1518/0062(P)). Extracted human premolar teeth were collected within six months, by the local dentists and were stored in 2% Chloramine-T solution for two weeks to inhibit bacterial growth and later, they were stored in distilled water at 4 °C until further use to ensure hydration.

3.3.2 Preparation of enamel specimens

Forty sound human extracted premolars were used in this study. All soft deposits on the teeth were removed with a scaler. Subsequently, the crowns were separated from the roots by using a diamond abrasion wheel (Isomet, 11-1,180 Low Speed Saw, Buehler Ltd., USA). The crowns were sectioned into buccal and lingual halves with a water-cooled diamond saw. Eighty sound buccal or lingual enamel surfaces were embedded in cold-cure epoxy resin (Mirapox 950-230 A/B, Miracon Sdn Bhd, Malaysia) in a custom-made rubber moulds to form a 15 mm x 12 mm x 6 mm rectangular-shaped disc, exposing an enamel area of approximately (X, Y) 2 mm x 4 mm in the centre (**Figure 3.2**).

The exposed enamel areas were polished on a Buehler Isomat II polishing machine using 600 grade silicon carbide paper (Buehler, Lake Bluff, IL, USA), followed by six, three, and one μm diamond abrasive (Buehler, Metadi diamond spray) on Buehler polishing cloth under constant cooling (D. J. White & Featherstone, 1987). Polishing was continued until an enamel area measuring 2 mm x 4 mm was exposed in order to match the area for OCT scanning. After polishing, the specimens were rinsed with distilled water for one min and baseline OCT scanning were performed.

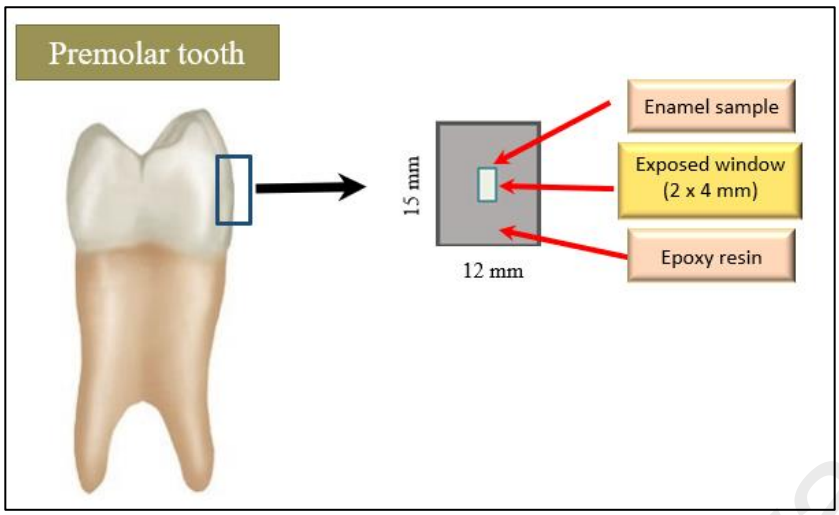

Figure 3.2: Schematic illustration of the preparation of enamel specimen.

3.3.3 Acid challenge

The rectangular shaped resin blocks containing the enamel specimens were then immersed into a beaker containing 150 ml of 0.003 M citric acid at pH 3.2. The beaker was placed on a magnetic stirrer (IKA RCT basic) which was set to stir the acid solution at 275 rpm (Gravelle et al., 2015). The pH of the acid was monitored with a pH meter (Eutech ION 2700, Eutech Instruments) and the temperature of the solution was kept constant at 36°C throughout the experiment. After 30 min, the specimens were removed from the acid and rinsed under running water for one min to remove excess acid from the specimens. Post-erosion OCT scanning were performed. In this chapter, post-erosion data for all groups were termed 'without biofilm'.

3.3.4 Specimens allocation

After being subjected to acid challenge, the specimens were randomly allocated into four groups; Control group, Group 1-Day biofilm, 2-Day Biofilm and 3-Day Biofilm, with twenty specimens in each group (n=20). Specimens from group 2, 3 and 4 were inoculated with early laboratory-cultivated biofilm for 1, 2 and 3 days, respectively (**Table 3.2**). Specimens from group 1 (control group) were stored in de-ionised water for

three days after the acid challenge and were not inoculated with laboratory-cultivated biofilm. Swept Source OCT (SS-OCT) was used to scan all the specimens from all groups at baseline (t_1), post-erosion (t_2) and with biofilm (or without biofilm from control group) (t_3) time points (**Table 3.3)**

Surface Microhardness (SMH) was measured at all time points except at t_3. However, the SMH measurements were not releveant for this chapter, therefore the mesurements were described in Chapter 4 (pg. 146).

The summary of the study design is shown in **Figure 3.13** (pg. 103).

Table 3.2: Experimental groups.

Groups		N=80	
1	Control Group	n=20	Specimens not containing biofilm.
2	1-Day Biofilm Group	n=20	Specimens containing 1-day old biofilm.
3	2-Day Biofilm Group	n=20	Specimens containing 2-day old biofilm.
4	3-Day Biofilm Group	n=20	Specimens containing 3-day old biofilm.

Table 3.3: Measurement time points.

Time points		**Measurements**
Baseline	t_1	~~SMH_1~~ OCT
Post-erosion	t_2	~~SMH_2~~ OCT_2
Biofilm	t_3	OCT_3

3.3.5 Artificial Mouth Model

3.3.5.1 Preparation of Brain Heart Infusion (BHI) Broth

Brain Heart Infusion (BHI) broth (Oxoid Ltd) was prepared according to the manufacturer's instruction. Thirty-seven grams of BHI powder was dissolved in one litre of distilled water, mixed well and distributed into a sterile container. The mixture was then sterilized by autoclaving at 121°C for 15 min. This media was used as a reservoir for the bacteria.

3.3.5.2 Preparation of Brain Heart Infusion Agar (BHI Agar) Media

BHI agar (Oxoid Ltd) was prepared according to the manufacturer's instruction. 47g of BHI agar powder was suspended in 1 litre of distilled water. The mixture was boiled until completely dissolved and sterilized by autoclaving at 121°C for 15 min. The liquefied agar was then poured into sterile Petri dish until it completely covered the bottom part, and the lid was placed immediately on the top. After all of the Petri dishes were poured, they were allowed to cool down and set. They were then stored in the refrigerator at 4°C until further use.

3.3.5.3 Inoculation of bacteria onto agar plates

The following protocol was adopted from (Razak & Rahim, 2003). *Strep sanguinis, Strep mitis* and *Actinomyces sp*. were used in this study as the representatives of bacteria that exist in the early dental biofilm (Razak & Rahim, 2003). Stocks of bacteria: *Strep. Sanguinis* (ATCC BAA-1455), *Strep. mitis* (ATCC 49456D) and *Actinomyces sp*. (ATCC 43146) were thawed separately and inoculated onto the agar plates.

Inoculation of bacteria onto agar plates was done using the streak technique. The inoculating loop was flamed until it was red hot and then allowed to cool down. A small amount of bacterial growth was removed with the sterile inoculating loop from an agar plate containing a single colony. One loopful of bacteria was made as a primary inoculum and was then distributed thinly over a quarter of the plate by streaking the loop in a series of parallel lines using a back and forth motion (**Figure 3.3**). The loop was again flamed and cooled between the different sets of streaks in different segments of the plate. The steps were repeated, and the final streak was done in the untouched area of the plate.

Plates were then incubated at 37 °C for 24 hours. They were placed upside down (agar up), to prevent the condensation from dripping down on to the agar's surface and interfere with the developing bacteria.

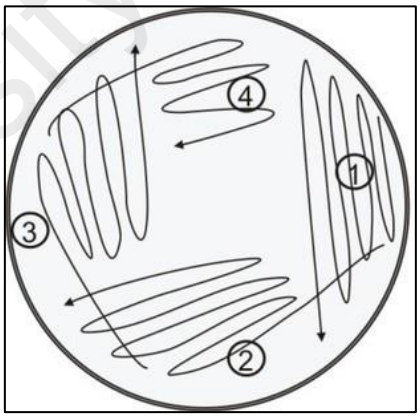

Figure 3.3: Diagram of plate streaking technique. Spreading of inoculum on agar plate following the sequence 1-4.

3.3.5.4 Preparation of bacterial suspensions

The colonies of each type of bacteria were then harvested and dispersed into 30 ml of sterilised BHI broth without sucrose. The concentration of the bacteria used in the study was adjusted to give an absorbance of 0.144 at 550 nm wavelength (equivalent of McFarland Standard # 0.5, BioMerieux, France) using a spectrophotometer. A spectrophotometer measures the fraction of the incident light transmitted through a solution. In other words, it is used to measure the amount of light that passes through a solution, and by comparing it to the initial intensity of light reaching the specimens, it indirectly measures the amount of light absorbed by that specimens. At this absorbance, the concentration of cell is standardised to about 108 cells/ml (Razak & Rahim, 2003). The mixture was then kept at 4 °C until further use. This media was used as a reservoir for the bacteria.

The summary of the procedure is shown in **Figure 3.4**.

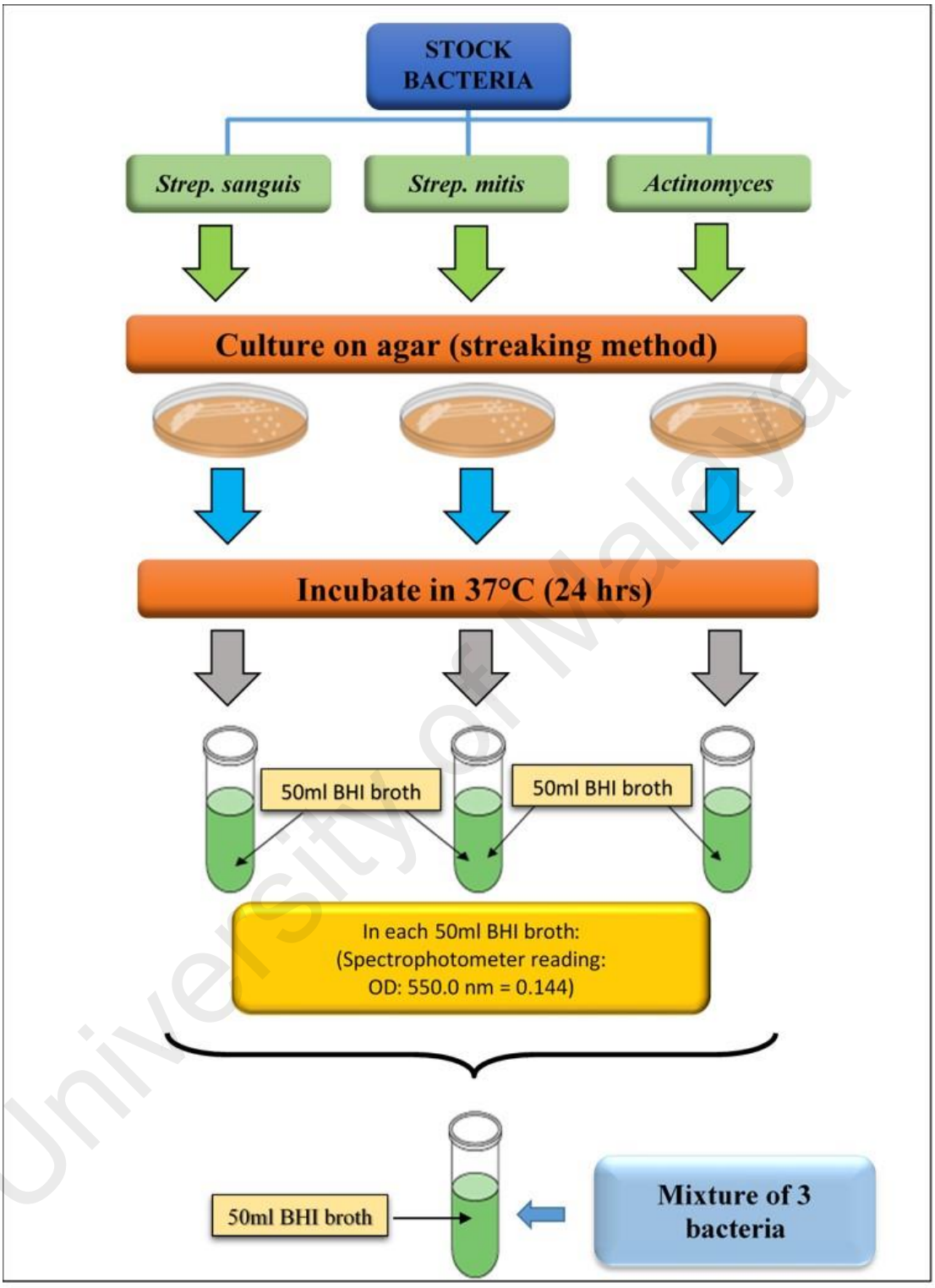

Figure 3.4: Flowchart of preparation of bacterial suspensions.

3.3.5.5 Modified Nordini's Artificial Mouth (MNAM)

For this study, laboratory-cultivated biofilm was 'harvested' using the "NAM model" (Rahim, Fathilah, Irwan, & Wan Nordini Hasnor, 2008) with some modifications. This model was used for simulation of the oral cavity (**Figure 3.5**).

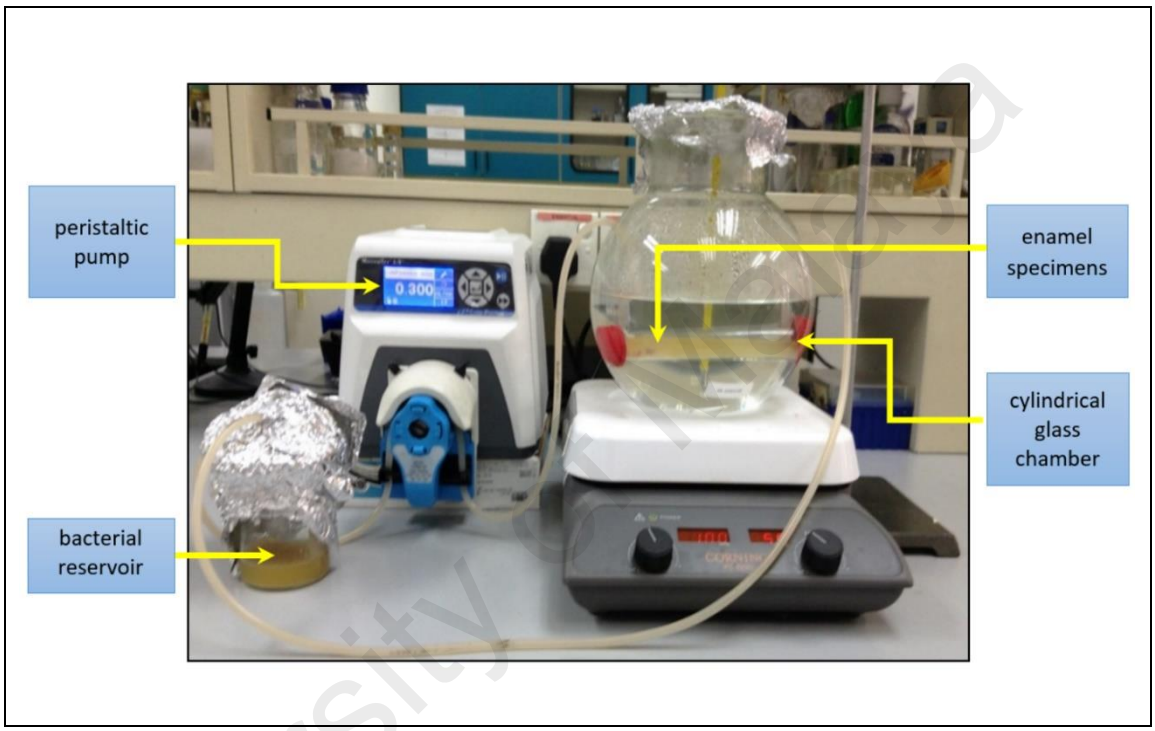

Figure 3.5: Modified 'NAM Model' – enamel specimens placed in a cylindrical glass chamber (mimicking the oral cavity) in a water bath connected to bacterial reservoir via peristaltic pump.

3.3.5.6 Setting up of Modified 'NAM Model' (MNAM model)

The water bath and a glass cylindrical chamber used as a receptacle for the enamel specimens in the water bath were designed and custom made to suit the dimensions of the enamel specimens. The original NAM model (Rahim et al., 2008) consisted of a glass chamber (1 cm x 6 cm) where six glass beads of 3 mm in diameter each were placed in the small chamber which served as substrata for biofilm formation (Rahim et al., 2008). In this study, the size of the chamber had to be modified in order to position the rectangular shaped specimens (15 mm x 12 mm) along the tube as the substrata for biofilm formation.

Referring to **Figure 3.5**, the two ends of the cylindrical glass chamber were connected with rubber tubes to a bacterial reservoir via a peristaltic pump. The chamber was immersed in a water bath, which functions as an incubator with temperature fixed at 37 °C to mimic the intra-oral temperature. A thermometer was fitted into the incubator to monitor the temperature of the system. This was to ensure that the biofilm develops in an environment that mimics that of the mouth. A peristaltic pump (Masterflex, Cole Palmer, Vernon Hills, USA) was used to maintain the flow rate that represents the flow rate of saliva in the oral cavity, of fluids coming from and fluids flowing back to the bacterial reservoir after passing through the NAM model.

3.3.5.7 Preparation of sterile saliva

Sterile saliva was prepared following the method described by Rahim et al. (2008). Approximately 25 ml of stimulated saliva was collected from a single volunteer. The volunteer was asked to chew on a sugar-free gum in order to stimulate saliva production and the saliva was then collected using a test tube. The aggregation of protein in the saliva specimen was minimized by adding 1,4-Dithio-D,L-threitol (DTT) to a concentration of 2.5 mM. Upon addition of DTT, the saliva was stirred slowly for 10 min

before it was centrifuged at 864 g for 30 min. the supernatant obtained was then filter-sterilized through a disposable 0.2 μm (Supor membrane) low protein-binding filter (Aerodise syringe filters, Pall Corp, USA) into sterile tubes. The sterile stimulated saliva was then stored at -20ºC. Prior to use, the sterile saliva was thawed and centrifuged once again to remove any precipitate.

3.3.5.8 Development of biofilm

In the development of the biofilm, the enamel specimens placed in the cylindrical glass chamber needed to be coated with saliva to form the acquired pellicle. This was done by allowing the sterilized saliva to flow into the cylindrical glass chamber of the 'modified NAM model' (MNAM) for two min at a rate of 0.3 mL min^{-1}, with the enamel specimens facing upwards. Following this, sterile distilled water was allowed to run into the system to rinse excess saliva from the enamel surface (Rahim et al., 2008). Bacterial inoculum (*Strep sanguinis*, *Strep mitis* and *Actinomyces sp*.) from the bacterial reservoir was pumped into the system at a rate of 0.3 mL min^{1} for 24 hr, 48 hr, or 72 hr depending on the specimen group. In this chapter, measurement at this time point is referred to as 'with biofilm'.

The bacterial reservoir was renewed daily. For flow rate, it was pre-set at 0.3 mL min^{-1} to represent the flowrate of saliva in the oral cavity under unstimulated saliva (Edgar, O'Mullane, & Dawes, 2004).

3.3.6 Confocal Laser Scanning Microscopy (CLSM)

The staining solution for fluorescence analysis was prepared as described by Netuschil and co-workers (1998). A stock solution of Fluorescin Diacetate (FDA) was prepared by mixing 5 mg/ml of FDA in cold acetone. FDA is a non-fluorescent cell-permeable dye that is converted to fluorescein (green) by intracellular esterases. The

solution was then stored at -20°C. The stock solution of Ethidium Bromide (EB) containing 10mg/ml of EB in saline was stored at 5°C. EB is a red fluorescing nucleic acid stain that penetrates damaged membranes of bacteria (Zaura-Arite et al., 2001). Five specimens from each group (n=5) were selected and viewed under CLSM for assessment of biofilm.

Just prior to staining procedure, 6 µl of the FDA stock solution and 3 µl of the EB solution were mixed together in 1 ml of cold saline and stored at 5°C. 3.5 µl of the final mixture were carefully pipetted into the on the surface of the enamel specimens containing the laboratory-cultivated biofilm. The stained specimens were then viewed under Confocal Laser Scanning Microscope (CLSM) (Leica TCS SP5 II) with a wavelength of 450-490 nm (Netuschil, Weiger, Preisler, & Brecx, 1995). The representative site was within the 1 mm x 2 mm window chosen for visualisation under the microscope on each specimen. Confocal Z-series stacks were acquired on a Leica SP5 confocal, using a 63x 1.3NA Oil immersion objective, and spectral detection, adjusted for the emission of the Alexam 488 and Alexa 568 flurochromes.

3.3.7 Measurement of specimens

3.3.7.1 OCT

i. **OCT Data acquisition**

A commercially available SS-OCT system (OCS1300SS, Thorlabs Ltd., UK) was used to capture cross-sectional images of the enamel specimens. The instrument incorporates a broad-band, frequency-swept near infra-red source centred at 1325 μm. The imaging probe was attached to a stand and the specimens were placed in a customised positioning jig (**Figure 3.6**) which was attached to on a translational stage that allows X, Y translation and Y, Z rotation. The jig was used to obtain a reproducible specimen

positioning during each scan at each measuring time point. The YZ plane with the least specular reflection was determined and recorded for replication at consecutive measuring time points.

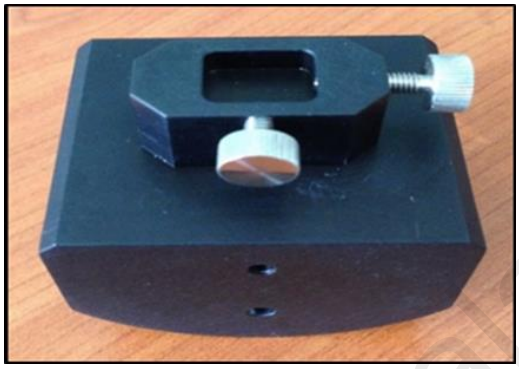

Figure 3.6: Customised repositioning jig used to provide a consistent positioning to all imaged specimens for OCT measurement.

The Thorlabs OCT capturing software (Swept Source OCT Imaging System Version 2.3.1, Thorlabs) was used to capture the image, configure the OCT settings and guide the light beam. The light beam was configured to scan an area of 2 mm x 4 mm window in the X-Y direction and at a depth of 3 mm in air, corresponding to an axial physical depth of 1.85 mm (Z-axis) in enamel (refractive index = 1.62), with a resolution of 1024, 512 and 512 pixels at the X, Y and Z axis respectively (**Figure 3.7**). Immediately before scanning with OCT, each specimen with no biofilm was dried with oil-free compressed air at a pressure of 29 psi administered from a point 5 cm from the tooth surface using a three-way syringe for 10 s (Shimamura et al., 2011). Specimens with cultured biofilm were not dried with compressed air. The specimens were scanned immediately after removal from the cylindrical glass chamber. OCT images were acquired, and backscattered light intensity as a function of depth was analysed for each time point.

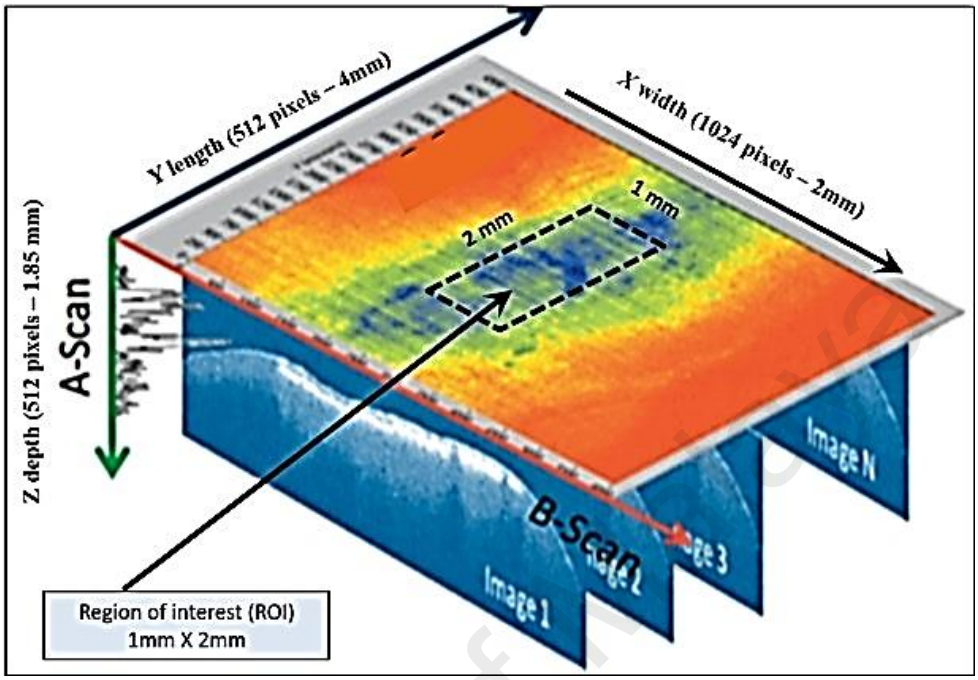

Figure 3.7: 3D representation of OCT scans. (Modified from Figure 1(b) in (Maia, de Freitas, de, Gomes, & Karlsson, 2016) . With permission from author.

ii. **OCT Data processing**

A customized, 2D OCT Analytics software was developed in Matlab (MathWorks Inc.) to load the OCT B-scan images (**Figure 3.8** (a)). A similar region of interest (ROI) was selected for each specimen for all time points. The ROIs have a dimension of 1 mm X 2 mm (X, Y) and were located in the middle of the exposed area, as shown in **Figure 3.7**, which was modified from Figure 1(b) of (Maia et al., 2016). The ROIs were then subjected to a surface determination and alignment algorithm and a mean depth-resolved intensity profile (A-scan) for each specimen was generated, and the intensity values were exported automatically to excel sheets (**Figure 3.8**).

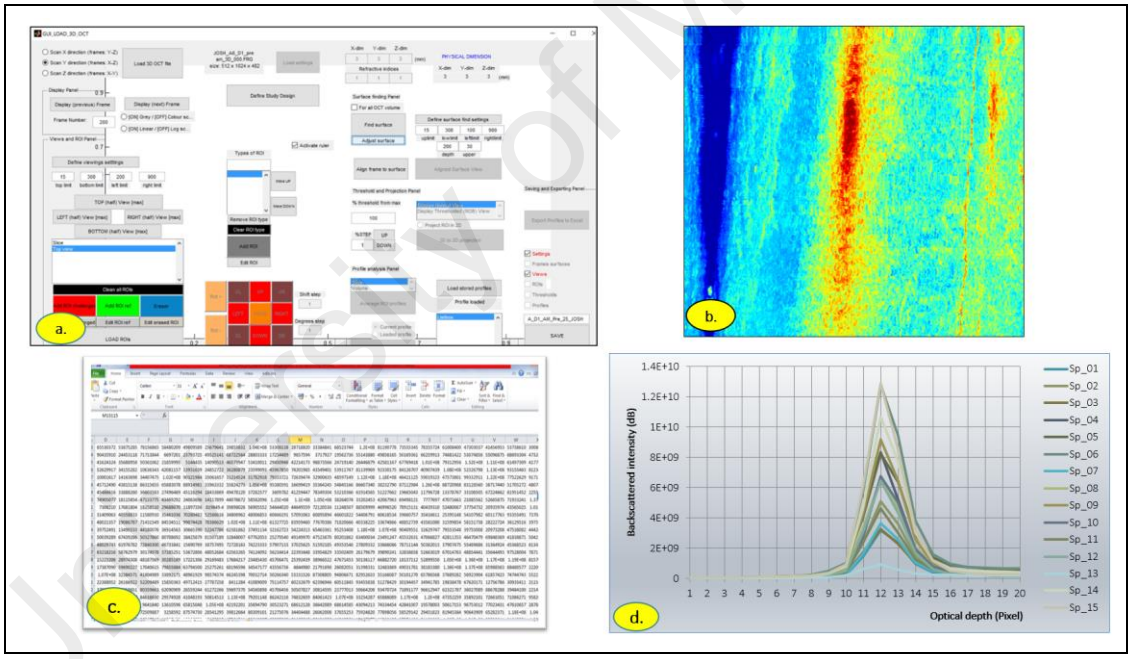

Figure 3.8: Sequence of OCT data processing.

Data processing of OCT images (a) Graphic User Interface (GUI) of Matlab programme for uploading and processing of data. (b) ROI - aligned surface view of one image at one time point. (c) data from mean A-scan for one B-scan exported to excel files. (d) depth-resolved intensity profile (A-scan) for all specimens in one group at one time point

iii. **Integrated Reflectivity (*IR*)**

The area under the curve or integrated reflectivity (*IR*) was calculated and values were used to analyse the OCT signals at different time points (Tezuka et al., 2016). Line profiles were taken from the A-scans and the reflectivity was integrated from the enamel surface to various depths, yielding the *IR*, and was expressed by an arbitrary unit (a.u.).

The chosen height on the surface for this study were pixel-4 (biofilm-air interface) and pixel-10 (biofilm-tooth interface). Assuming that the refractive index of biofilm is similar to that of water (refractive index of water = 1.33) (Bakke, Kommedal, & Kalvenes, 2001), the optical depth of pixel-4 translated to the physical depth of 17.62 μm measured from the biofilm-tooth interface; or in other words, this area with biofilm was expected to be approximately 26.43 μm between the biofilm-air interface and the biofilm-tooth interface. The intensity of the backscattered light at pixel-50 was the intensity where the A-scans had reached a plateau and was assumed not affected by the acid challenge. For this study, pixel-50 was observed to be at the sub-surface at the physical depth of 176.22 μm measured from the biofilm-tooth interface (**Figure 3.11**).

The *IR* was calculated using the formula stated in **Figure 3.9**. *IR* between pixel-4 and pixel-10 is called Supra-Surface Integrated Reflectivity ($IR_{biofilm}$) (**Figure 3.10** and **Figure 3.11**). In this study, $IR_{biofilm}$ represented the area of backscattered light intensity as it travels from the light source into the biofilm, prior to hitting the tooth surface and it is proportional to the biofilm accumulated over the tooth surface (i.e. the total amount of biofilm accumulated on the tooth surface); and the *IR* between pixel-10 and pixel-50 (plateau) is called Sub-Surface Integrated Reflectivity (IR_{sub}), which is the amount of backscattered intensity as it travels into the tooth which indicates demineralisation changes (**Figure 3.12**). **Table 3.4** shows the summary of the explanation above.

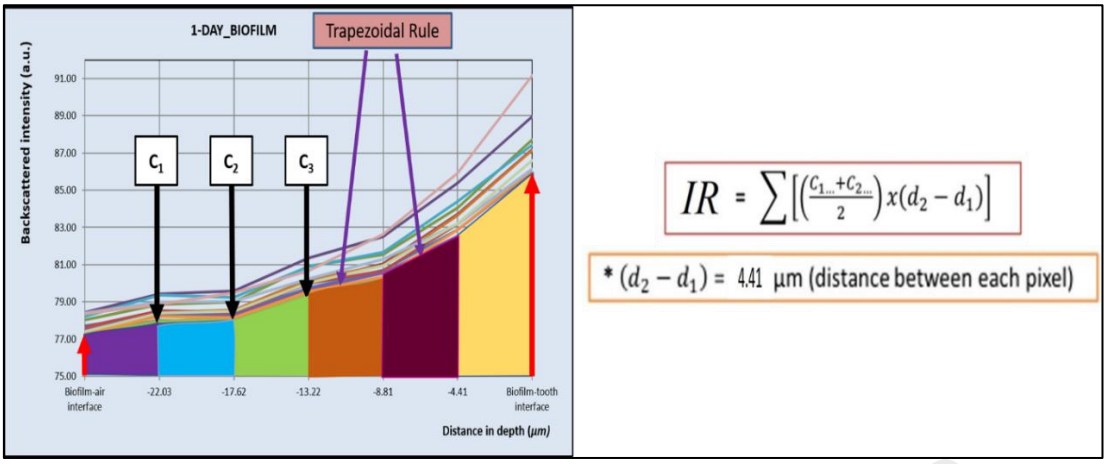

Figure 3.9: Calculation of Integrated Reflectivity (*IR*).

Integrated reflectivity (*IR*) is calculated using the trapezoidal rule and it is representing the area under the curve of an A-scan (backscattered intensity vs depth).

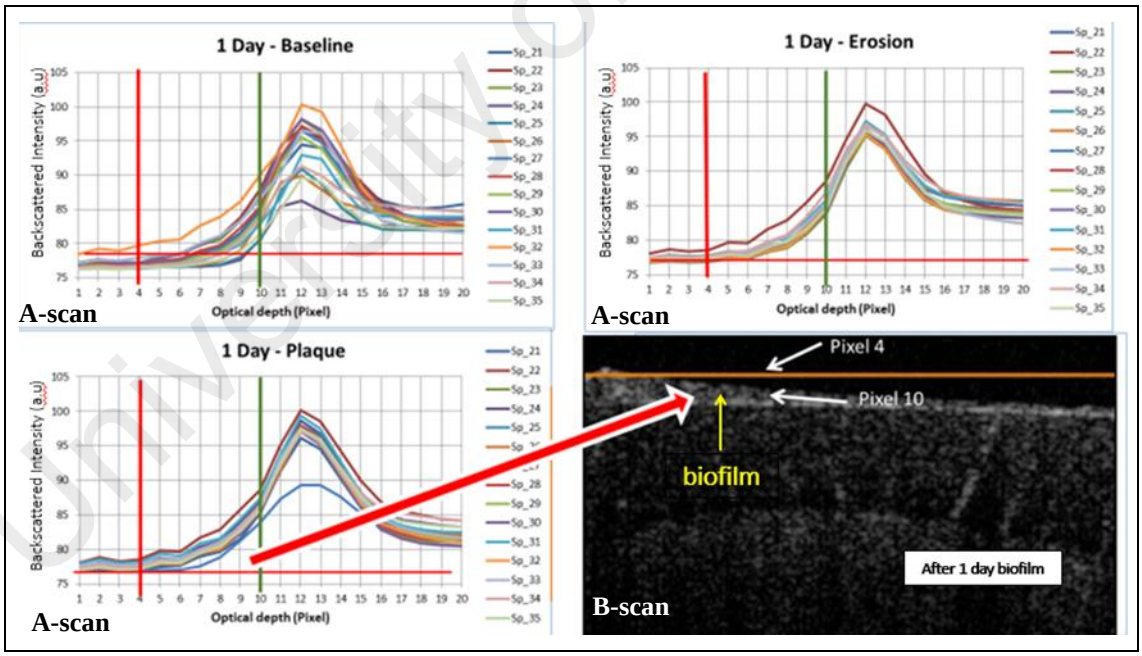

Figure 3.10: A-Scans of all the specimens in 1_Day Biofilm group. A representative B-scan shows evidence of biofilm with higher backscattering intensities on the enamel surface.

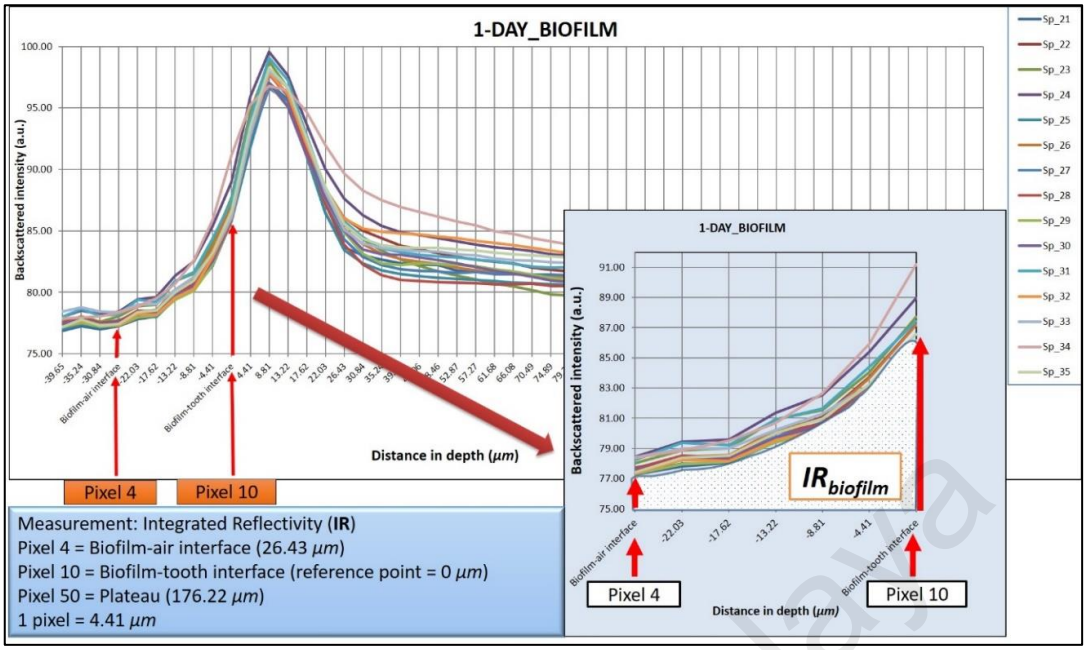

Figure 3.11: Area for $IR_{biofilm}$ is enlarged to show the area for measurement on an A-scan.

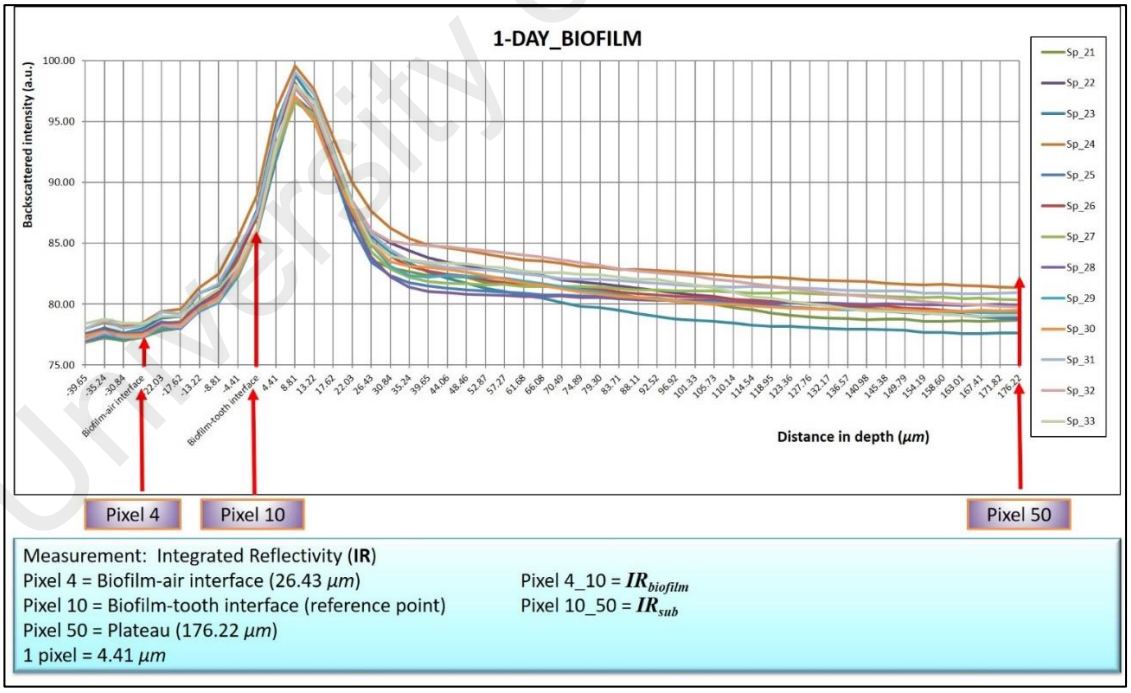

Figure 3.12: Areas for calculations of $IR_{biofilm}$ and IR_{sub}.

Table 3.4: Summary of the chosen depths for the study.

Pixel	Physical depth (μm)	Description
Pixel 4	26.43	Biofilm-air interface.
Pixel 10	0 (Reference point)	Biofilm-tooth interface.
Pixel 50	176.22	Where the backscattered intensity reached a plateau.
*1 pixel = 4.41 μm (physical depth)		

3.3.8 Outcome measures

The outcome measure used for OCT was the fractional change of the integrated reflectivity (ΔIR), which is the difference of backscattered intensity of the same specimen, before and after biofilm accumulation. This value should provide a value that corrects for any compositional variations and therefore produce comparable results. Without biofilm time point was actually the same as post-erosion time point. The value was calculated for all the specimens using the formula below:

$$\Delta\ IR = \left[\frac{IR\ (t_3) - IR\ (t_2)}{IR\ (t_2)}\right]$$

$IR\ (t_2)$ = IR (without biofilm)
$IR\ (t_3)$ = IR (with biofilm)

3.3.9 Statistical Analysis

The data of integrated reflectivity (*IR*) were subjected to statistical analysis using the statistic package for social study (SPSS) version 25.0 (SPSS Inc., Chicago, USA). The paired sample t-test was used to analyse the difference between specimens with and without biofilm within each group. One-way ANOVA was used to assess the differences in *IR* and fractional change of *IR* among the four groups (Control, 1-Day Biofilm, 2-Day Biofilm and 3-Day Biofilm). Tukey's post hoc test was applied, when necessary, in cases where ANOVA revealed significant differences.

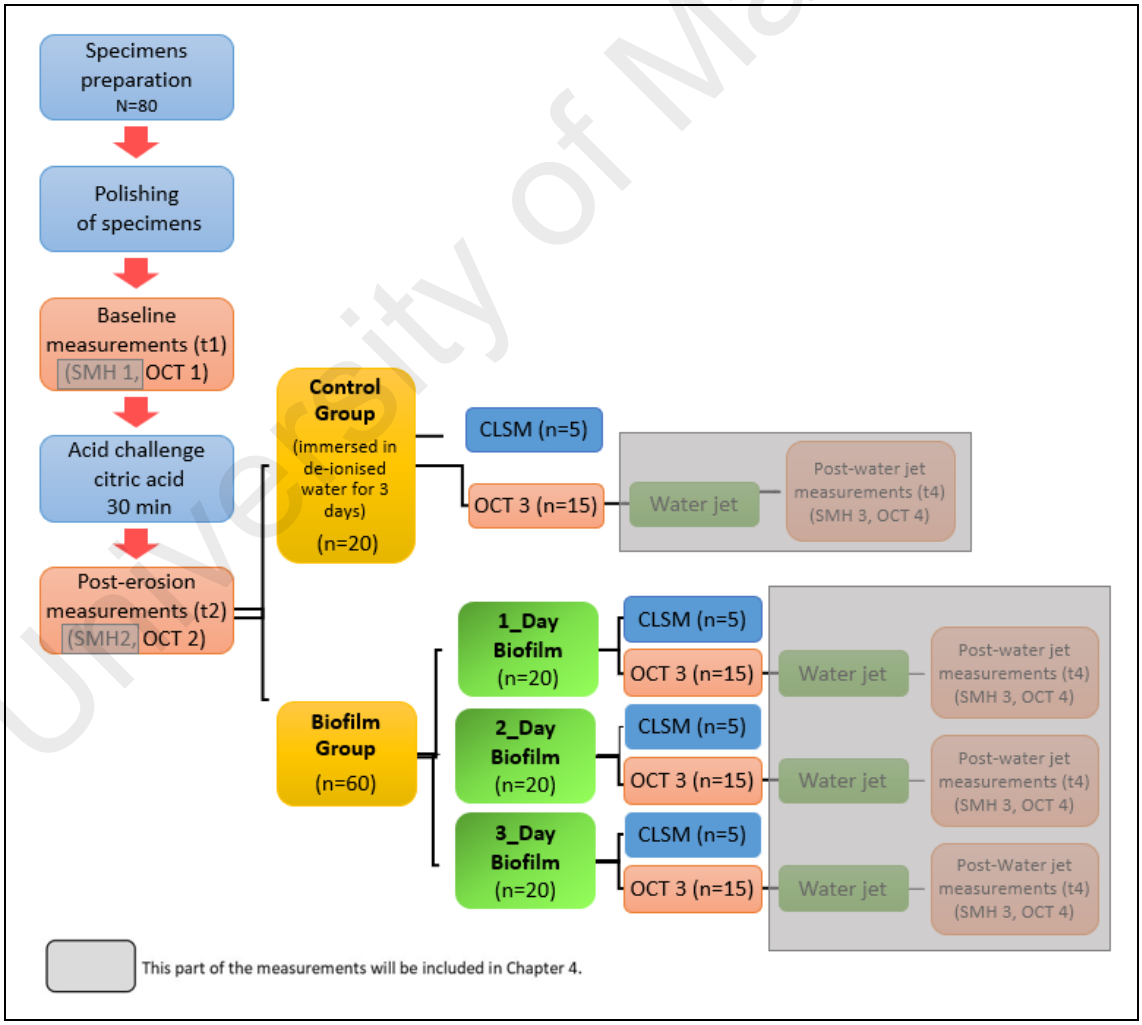

Figure 3.13: Flowchart of the study design.

3.4 Results

3.4.1 Confocal Laser Scanning Microscope (CLSM) - Qualitative observations

The CLSM images of the biofilm formed on enamel surfaces at 1-day, 2-day and 3-day periods were taken to show the formation of early biofilm on the enamel surfaces. Representative examples of the enamel specimens with early biofilm for each group are shown in **Figure 3.14** a, b, and c.

The topography of sparse bacteria colonies could be observed on the surfaces and the amounts of the adhered bacterial cells were seen to increase with time. At 1-day, surface area was occupied by microorganisms and at 3-day, it appears to be more densely covered with microorganisms. green colour indicates live cells.

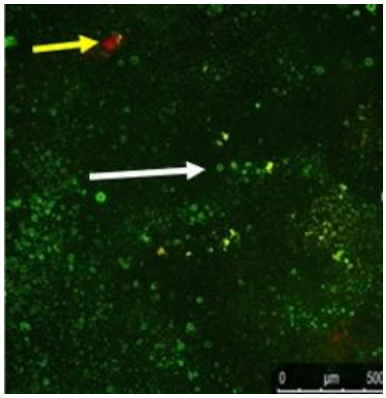

(a)

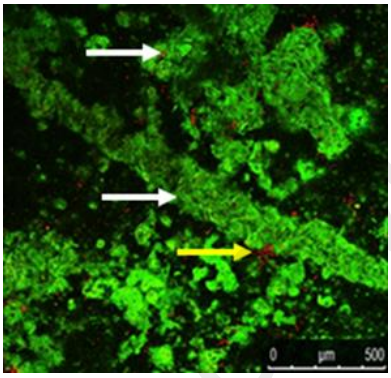

(b)

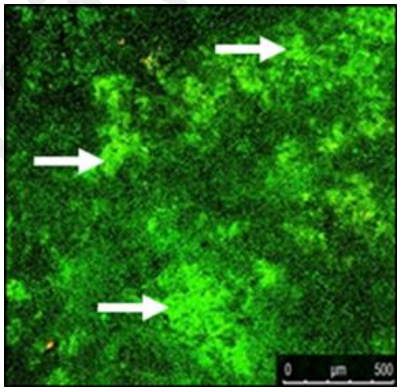

(c)

Figure 3.14: CLSM images of the biofilm formed on enamel surfaces at 1-Day (a), 2-Day (b) and 3-Day (c) (Mag. x 600).

White arrows pointing to green elements representing vital bacterial cells.
Yellow arrow pointing to red elements representing non-vital bacterial cells.

3.4.2 The attenuation of OCT intensity within the biofilm.

OCT B-scan images of one representative enamel specimen in 3-day biofilm group are presented in **Figure 3.15**. There was a noticeable distinction of the initially eroded enamel surface shown in the OCT images at post-erosion (without biofilm), with a high reflectivity within a certain depth of enamel (subsurface). Then, with a 3-day biofilm on the enamel surface, there were higher reflectivity but limited to the supra-surface of the enamel, which indicated a layer of biofilm.

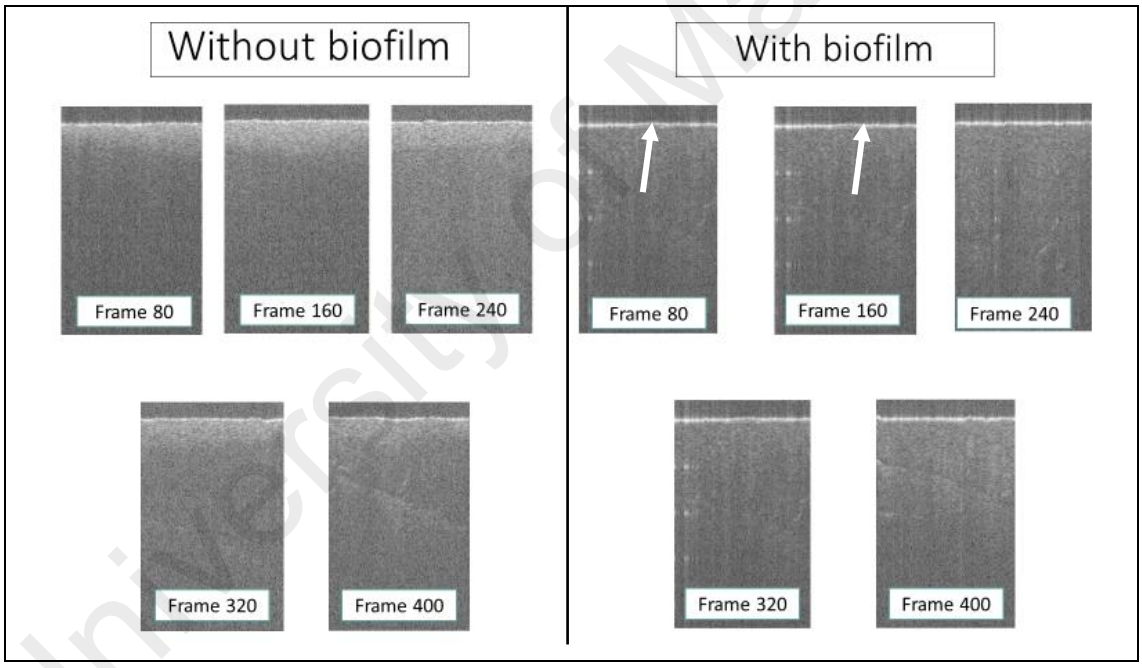

Figure 3.15: B-scan images of a specimen in 3-day biofilm group.

Five frames of the B-scans of a representative sample were selected at two time points; without (t_2) and with biofilm (t_3). Images with biofilm showed higher scattering at the outer layer of the enamel (white arrows).

3.4.2.1 OCT - $IR_{biofilm}$

In order to explore the attenuation of OCT intensity in the presence of biofilm, the integrated reflectivity ($IR_{biofilm}$) was evaluated. Data from integrated reflectivity (IR) presented normal distribution. The graph showing the mean values of $IR_{biofilm}$ without (t_2) and with biofilm (t_3) for the three biofilm groups are shown in **Figure 3.16**.

Repeated measure ANOVA showed that the mean increase in $IR_{biofilm}$ were statistically significant ($p < 0.05$), comparing between time points, t_2 and t_3 time points for all groups (**Table 3.5 - Table 3.10**).

Graph in **Figure 3.16** shows a statistically significant different between the mean values of $IR_{biofilm}$ of 3-Day Biofilm group and the control group at t_3.

Table 3.11 and **Table 3.12** show the output of the one-way ANOVA analysis and whether there was a statistically significant difference between the mean change. There was a statistically significant difference between groups as determined by one-way ANOVA ($F(3,56) = 6.828$, $p \leqslant 0.05$). Post hoc comparisons using the Tukey HSD test revealed that the mean of $IR_{biofilm}$ was statistically significantly higher in 3-Day Biofilm group (1745.43 ± 11.35 a.u., $p < 0.05$) compared to the control group (**Table 3.13**).

Table 3.14 and **Table 3.15** show the output of the one-way ANOVA analysis. There was a statistically significant difference between groups as determined by one-way ANOVA ($F(3,56) = 5.455$, $p \leqslant 0.05$). Post hoc comparisons using the Tukey HSD test revealed that the fractional change of $IR_{biofilm}$ ($\Delta\ IR_{biofilm}$) was statistically significantly higher in 3-Day Biofilm group (0.027 ± 0.008, $p = 0.002$) compared to the other three groups (**Table 3.16**).

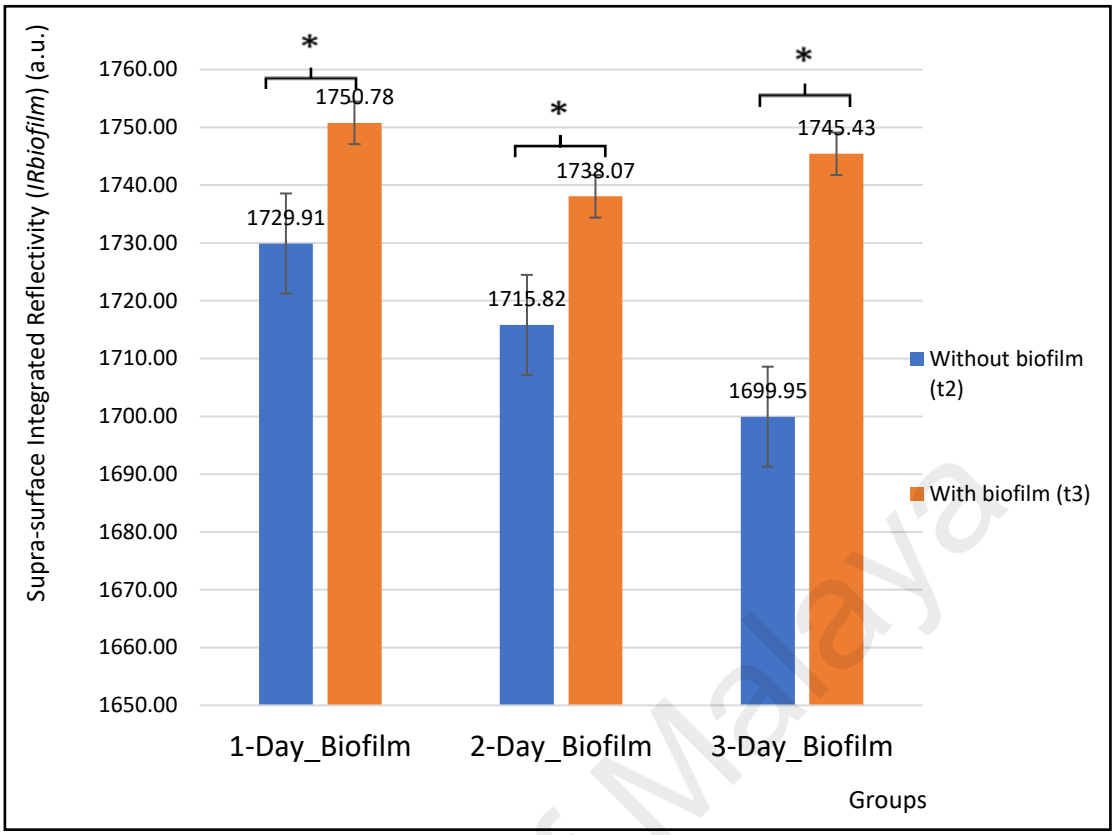

Figure 3.16: Mean $IR_{biofilm}$ ± SD, without biofilm (t_2) and with biofilm (t_3) for three experimental groups (n=15). (* sig. difference at p<0.05)

Mean values of IR_{sub} ± SD, for enamel specimens for three experimental groups (n=15) at t_2 and t_3. Repeated measures ANOVA showed statistically significant different between t_2 and t_3 in 1-Day, 2-Day and 3-Day Biofilm groups (**Table 3.5 - Table 3.10)**.

Table 3.5: Tests of Within-Subjects Effects Table - 1-Day Biofilm group

Tests of Within-Subjects Effects

Measure: MEASURE_1

Source		Type III Sum of Squares	df	Mean Square	F	Sig.	Partial Eta Squared
Time	Sphericity Assumed	11548.347	3	3849.449	8.089	.000	.366
	Greenhouse-Geisser	11548.347	1.675	6896.048	8.089	.003	.366
	Huynh-Feldt	11548.347	1.876	6156.607	8.089	.002	.366
	Lower-bound	11548.347	1.000	11548.347	8.089	.013	.366
Error(Time)	Sphericity Assumed	19986.645	42	475.873			
	Greenhouse-Geisser	19986.645	23.445	852.496			
	Huynh-Feldt	19986.645	26.261	761.086			
	Lower-bound	19986.645	14.000	1427.618			

A repeated measures ANOVA with a Greenhouse-Geisser correction showed that the mean scores for $IR_{biofilm}$ was statistically significantly different ($F(1.675, 23.445) = 8.089$, $p < 0.05$) for 1-Day Biofilm group.

Table 3.6: Pairwise Comparisons Table – 1-Day Biofilm group

Pairwise Comparisons

Measure: MEASURE_1

(I) Time	(J) Time	Mean Difference (I-J)	Std. Error	Sig.[b]	95% Confidence Interval for Difference[b] Lower Bound	Upper Bound
1	2	-10.904	10.384	1.000	-42.769	20.961
	3	-31.771	10.883	.067	-65.168	1.625
	4	-32.433*	8.589	.012	-58.790	-6.075
2	1	10.904	10.384	1.000	-20.961	42.769
	3	-20.867*	5.494	.012	-37.728	-4.007
	4	-21.529*	4.564	.002	-35.535	-7.522
3	1	31.771	10.883	.067	-1.625	65.168
	2	20.867*	5.494	.012	4.007	37.728
	4	-.661	5.446	1.000	-17.374	16.051
4	1	32.433*	8.589	.012	6.075	58.790
	2	21.529*	4.564	.002	7.522	35.535
	3	.661	5.446	1.000	-16.051	17.374

Based on estimated marginal means

*. The mean difference is significant at the .05 level.

b. Adjustment for multiple comparisons: Bonferroni.

This table presents the results of the Bonferroni post hoc test, which allows to discover which specific means differed. It can be seen that there was a significant difference in $IR_{biofilm}$ between t_2 and t_3 ($p < 0.05$), in 1-Day biofilm group.

Table 3.7: Tests of Within-Subjects Effects Table - 2-Day Biofilm group

Tests of Within-Subjects Effects

Measure: MEASURE_1

Source		Type III Sum of Squares	df	Mean Square	F	Sig.	Partial Eta Squared
Time	Sphericity Assumed	9313.075	3	3104.358	11.129	.000	.443
	Greenhouse-Geisser	9313.075	2.087	4462.917	11.129	.000	.443
	Huynh-Feldt	9313.075	2.460	3786.451	11.129	.000	.443
	Lower-bound	9313.075	1.000	9313.075	11.129	.005	.443
Error(Time)	Sphericity Assumed	11715.781	42	278.947			
	Greenhouse-Geisser	11715.781	29.215	401.023			
	Huynh-Feldt	11715.781	34.434	340.238			
	Lower-bound	11715.781	14.000	836.841			

A repeated measures ANOVA with a Greenhouse-Geisser correction showed that the mean scores for $IR_{biofilm}$ was statistically significantly different ($F(2.087, 29.215) = 11.129$, $p < 0.05$) for 2-Day Biofilm group.

Table 3.8: Pairwise Comparisons Table – 2-Day Biofilm group

Pairwise Comparisons

Measure: MEASURE_1

(I) Time	(J) Time	Mean Difference (I-J)	Std. Error	Sig.[b]	95% Confidence Interval for Difference[b] Lower Bound	Upper Bound
1	2	-1.887	6.510	1.000	-21.865	18.092
	3	-24.135*	4.715	.001	-38.606	-9.665
	4	-27.311*	6.446	.005	-47.093	-7.530
2	1	1.887	6.510	1.000	-18.092	21.865
	3	-22.249*	5.839	.011	-40.166	-4.331
	4	-25.425*	8.164	.046	-50.479	-.371
3	1	24.135*	4.715	.001	9.665	38.606
	2	22.249*	5.839	.011	4.331	40.166
	4	-3.176	4.031	1.000	-15.545	9.193
4	1	27.311*	6.446	.005	7.530	47.093
	2	25.425*	8.164	.046	.371	50.479
	3	3.176	4.031	1.000	-9.193	15.545

Based on estimated marginal means

*. The mean difference is significant at the .05 level.

b. Adjustment for multiple comparisons: Bonferroni.

This table presents the results of the Bonferroni post hoc test, which allows to discover which specific means differed. It can be seen that there was a significant difference in $IR_{biofilm}$ between t_2 and t_3 ($p < 0.05$), in 2-Day biofilm group.

Table 3.9: Tests of Within-Subjects Effects Table - 3-Day Biofilm group

Tests of Within-Subjects Effects

Measure: MEASURE_1

Source		Type III Sum of Squares	df	Mean Square	F	Sig.	Partial Eta Squared
Time	Sphericity Assumed	20200.446	3	6733.482	18.603	.000	.571
	Greenhouse-Geisser	20200.446	1.209	16715.169	18.603	.000	.571
	Huynh-Feldt	20200.446	1.261	16021.792	18.603	.000	.571
	Lower-bound	20200.446	1.000	20200.446	18.603	.001	.571
Error(Time)	Sphericity Assumed	15202.161	42	361.956			
	Greenhouse-Geisser	15202.161	16.919	898.519			
	Huynh-Feldt	15202.161	17.651	861.246			
	Lower-bound	15202.161	14.000	1085.869			

A repeated measures ANOVA with a Greenhouse-Geisser correction showed that the mean scores for $IR_{biofilm}$ was statistically significantly different (F(1.209, 16.919) = 18.603, $p < 0.05$) for 3-Day Biofilm group.

Table 3.10: Pairwise Comparisons Table – 3-Day Biofilm group

Pairwise Comparisons

Measure: MEASURE_1

(I) Time	(J) Time	Mean Difference (I-J)	Std. Error	Sig.[b]	95% Confidence Interval for Difference[b] Lower Bound	Upper Bound
1	2	22.509	9.962	.242	-8.061	53.079
	3	-22.973	9.281	.160	-51.455	5.508
	4	-20.561	9.097	.242	-48.478	7.355
2	1	-22.509	9.962	.242	-53.079	8.061
	3	-45.483*	3.421	.000	-55.981	-34.984
	4	-43.071*	2.772	.000	-51.577	-34.564
3	1	22.973	9.281	.160	-5.508	51.455
	2	45.483*	3.421	.000	34.984	55.981
	4	2.412	1.433	.686	-1.984	6.808
4	1	20.561	9.097	.242	-7.355	48.478
	2	43.071*	2.772	.000	34.564	51.577
	3	-2.412	1.433	.686	-6.808	1.984

Based on estimated marginal means

*. The mean difference is significant at the .05 level.

b. Adjustment for multiple comparisons: Bonferroni.

This table presents the results of the Bonferroni post hoc test.. It can be seen that there was a significant difference in $IR_{biofilm}$ between t_2 and t_3 ($p < 0.05$), in 3-Day biofilm group.

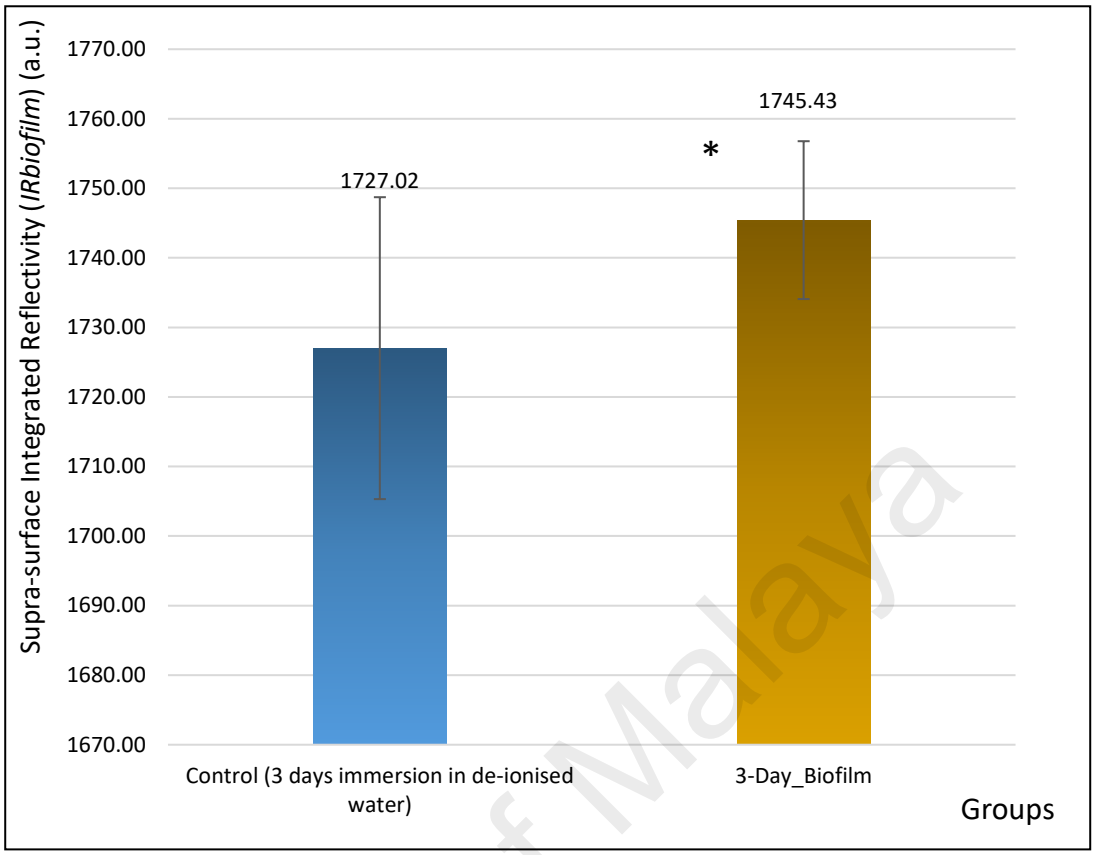

Figure 3.17: Data comparing $IR_{biofilm}$ of 3-Day biofilm group and control group at t_3. (* sig. difference at $p<0.05$)

Mean values of $IR_{biofilm}$ ± SD, for enamel specimens for two experimental groups (n=15) at t_3. One-way ANOVA showed statistically significant different between control and 3-Day Biofilm groups at t_3, $p < 0.05$.

Table 3.11: Descriptive Table - One-way ANOVA of $IR_{biofilm}$

Descriptives

IR_biofilm_t3

		N	Mean	Std. Deviation	Std. Error	95% Confidence Interval for Mean		Minimum	Maximum	Between-Component Variance
						Lower Bound	Upper Bound			
CONTROL		15	1727.0180	21.70296	5.60368	1714.9993	1739.0367	1692.89	1782.86	
1 DAY		15	1750.7767	15.31818	3.95514	1742.2937	1759.2596	1734.02	1780.91	
2 DAY		15	1738.0727	9.76586	2.52153	1732.6645	1743.4808	1717.44	1755.98	
3 DAY		15	1745.4280	11.34620	2.92958	1739.1447	1751.7113	1726.35	1766.57	
Total		60	1740.3238	17.35875	2.24100	1735.8396	1744.8081	1692.89	1782.86	
Model	Fixed Effects			15.24609	1.96826	1736.3809	1744.2667			
	Random Effects				5.14318	1723.9559	1756.6917			90.31284

Table 3.12: One-way ANOVA of $IR_{biofilm.}$

ANOVA

IR_biofilm_t3

	Sum of Squares	df	Mean Square	F	Sig.
Between Groups	4761.408	3	1587.136	6.828	.001
Within Groups	13016.829	56	232.443		
Total	17778.237	59			

This table presents the results of the one-way ANOVA of $IR_{biofilm}$ at t_3. There was a statistically significant different between groups, $F(3,56) = 6.828$, $p \leqslant 0.05$).

Table 3.13: Post Hoc Test for $IR_{biofilm}$ showing the p-values for four experimental groups (N=60, n=15).

Multiple Comparisons

Dependent Variable: IR_biofilm_t3

Tukey HSD

(I) Group	(J) Group	Mean Difference (I-J)	Std. Error	Sig.	95% Confidence Interval	
					Lower Bound	Upper Bound
CONTROL	1 DAY	-23.75867*	5.56709	.000	-38.4997	-9.0176
	2 DAY	-11.05467	5.56709	.206	-25.7957	3.6864
	3 DAY	-18.41000*	5.56709	.009	-33.1510	-3.6690
1 DAY	CONTROL	23.75867*	5.56709	.000	9.0176	38.4997
	2 DAY	12.70400	5.56709	.115	-2.0370	27.4450
	3 DAY	5.34867	5.56709	.772	-9.3924	20.0897
2 DAY	CONTROL	11.05467	5.56709	.206	-3.6864	25.7957
	1 DAY	-12.70400	5.56709	.115	-27.4450	2.0370
	3 DAY	-7.35533	5.56709	.554	-22.0964	7.3857
3 DAY	CONTROL	18.41000*	5.56709	.009	3.6690	33.1510
	1 DAY	-5.34867	5.56709	.772	-20.0897	9.3924
	2 DAY	7.35533	5.56709	.554	-7.3857	22.0964

*. The mean difference is significant at the 0.05 level.

This table presents the results of the Tukey post hoc analysis. Results revealed that there was a significant difference in $IR_{biofilm}$ between Control and 1-Day biofilm group, and between Control and 3-Day biofilm group ($p < 0.05$).

Table 3.14: Descriptive table - One-way ANOVA of Δ $IR_{biofilm.}$

Descriptives								
$\Delta IR_{biofilm}$								
Group	N	Mean	Std. Deviation	Std. Error	95% Confidence Interval for Mean		Minimum	Maximum
					Lower Bound	Upper Bound		
1_Day Biofilm	15	0.012	0.012	0.003	0.005	0.019	-0.019	0.034
2_Day Biofilm	15	0.013	0.013	0.003	0.006	0.020	-0.023	0.029
3_Day Biofilm	15	0.027	0.008	0.002	0.022	0.031	0.016	0.041
Total	60	0.016	0.013	0.002	0.013	0.019	-0.023	0.041

Table 3.15: One-way ANOVA of Δ $IR_{biofilm.}$

ANOVA					
$\Delta IR_{biofilm}$					
	Sum of Squares	df	Mean Square	F	Sig.
Between Groups	.002	3	.001	5.455	.002
Within Groups	.008	56	.000		
Total	.010	59			

Table 3.16: Post Hoc Test for $\Delta IR_{biofilm}$ showing the P-values for four experimental groups (N=60, n=15).

Post Hoc Tests **Multiple Comparisons** Tukey HSD							
Dependent Variable	(I) Group	(J) Group	Mean Difference (I-J)	Std. Error	Sig.	95% Confidence Interval	
						Lower Bound	Upper Bound
$\Delta IR_{biofilm}$	CONTROL	1_DAY	0.00	0.00	1.00	-0.01	0.01
		2_DAY	0.00	0.00	1.00	-0.01	0.01
		3_DAY	-.015*	0.00	0.007 *	-0.03	0.00
	1 DAY	2_DAY	0.00	0.00	1.00	-0.01	0.01
		3_DAY	-.015*	0.00	0.01 *	-0.03	0.00
	2 DAY	3_DAY	-.014*	0.00	0.01 *	-0.03	0.00

* The mean difference is significant at $p < 0.05$

3.4.3 The change of OCT scattering within the subsurface region.

3.4.3.1 OCT - IR_{sub}

Enamel surface demineralisation induced by an acid solution was displayed as the area of increased brightness due to increased backscatter signal intensity as seen on the OCT B-scan images (**Figure 3.18**). In the B-scan image, the reflectivity from lesion areas can be directly integrated to represent the severity of demineralisation. The increase of OCT backscattered signal after the acid challenge was additionally detected from the shift of $IR_{biofilm}$ values.

The mean values of IR_{sub} with and without biofilm for all three experimental groups are shown in **Table 3.19**. Repeated measures ANOVA showed that there was a statistically significant different in IR_{sub} ($p < 0.05$) in 2-Day and 3-Day biofilm groups (**Table 3.17** - **Table 3.22**).

Table 3.23 and **Table 3.24** show the output of one-way ANOVA to see whether there is a statistically significant difference between the group means. There was a statistically significant difference between groups as determined by one-way ANOVA ($F(3,56) = 4.510$, $p \leqslant 0.05$). A Tukey post hoc test revealed that the mean of IR_{sub} was statistically significantly between control & 3-Day biofilm groups; and between 2-day & 3-Day biofilm groups ($p < 0.05$) (**Table 3.25**).

Table 3.26 and **Table 3.27** show the output of one-way ANOVA to see whether there is a statistically significant difference between the group means. There was a statistically significant difference between groups as determined by one-way ANOVA $F(2,42) = 13.698$, $p \leqslant 0.05$. A Tukey post hoc test revealed that the mean of ΔIR_{sub} was statistically significantly different between 1-Day & 3-Day biofilm groups; and between 2-Day & 3-Day biofilm groups ($p < 0.05$) (**Table 3.28**).

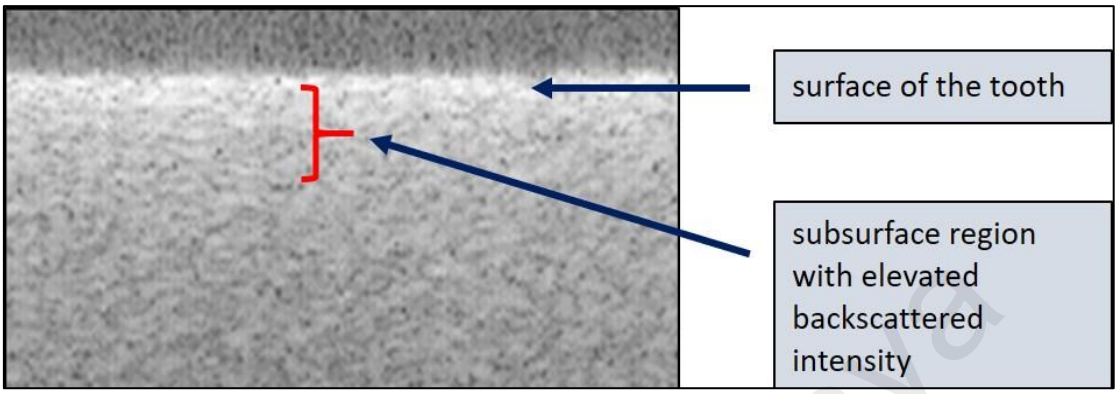

Figure 3.18: A representative B-scan of OCT image from a specimen after acid challenge (post-erosion, t_2)

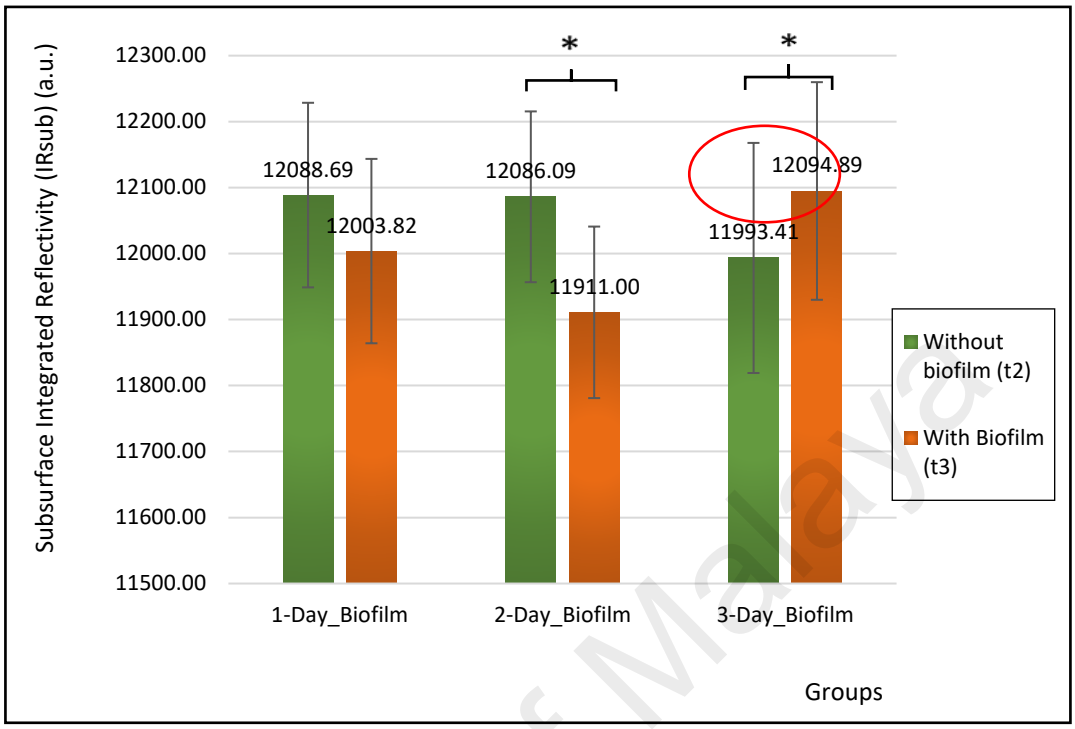

Figure 3.19: Mean IR_{sub} ± SD, without biofilm (t_2) and with biofilm (t_3) for three experimental groups. (* sig. difference at p<0.05)

= not following the expected trend

Mean values of IR_{sub} ± SD, for enamel specimens for three experimental groups (n=15) at t_2 and t_3. Repeated measures ANOVA showed statistically significant different between t_2 and t_3 in 2-Day and 3-Day Biofilm groups (**Table 3.17** - **Table 3.22**).

Table 3.17: Tests of Within-Subjects Effects Table - 1-Day Biofilm group

Tests of Within-Subjects Effects

Measure: MEASURE_1

Source		Type III Sum of Squares	df	Mean Square	F	Sig.	Partial Eta Squared
Time	Sphericity Assumed	194082.203	3	64694.068	3.628	.020	.206
	Greenhouse-Geisser	194082.203	1.991	97470.600	3.628	.040	.206
	Huynh-Feldt	194082.203	2.321	83634.026	3.628	.032	.206
	Lower-bound	194082.203	1.000	194082.203	3.628	.078	.206
Error(Time)	Sphericity Assumed	748996.564	42	17833.252			
	Greenhouse-Geisser	748996.564	27.877	26868.271			
	Huynh-Feldt	748996.564	32.489	23054.148			
	Lower-bound	748996.564	14.000	53499.755			

A repeated measures ANOVA with a Greenhouse-Geisser correction showed that the mean scores for IR_{sub} was statistically significantly different ($F(1.991, 27.877) = 3.628$, $p < 0.05$) for 1-Day Biofilm group.

Table 3.18: Pairwise Comparisons Table – 1-Day Biofilm group

Pairwise Comparisons

Measure: MEASURE_1

(I) Time	(J) Time	Mean Difference (I-J)	Std. Error	Sig.[a]	95% Confidence Interval for Difference[a] Lower Bound	Upper Bound
1	2	-97.650	49.972	.426	-251.003	55.703
	3	-12.784	53.703	1.000	-177.587	152.019
	4	-135.503	50.582	.108	-290.727	19.720
2	1	97.650	49.972	.426	-55.703	251.003
	3	84.866	51.847	.744	-74.242	243.974
	4	-37.853	13.716	.092	-79.945	4.238
3	1	12.784	53.703	1.000	-152.019	177.587
	2	-84.866	51.847	.744	-243.974	74.242
	4	-122.719	58.742	.333	-302.985	57.546
4	1	135.503	50.582	.108	-19.720	290.727
	2	37.853	13.716	.092	-4.238	79.945
	3	122.719	58.742	.333	-57.546	302.985

Based on estimated marginal means

a. Adjustment for multiple comparisons: Bonferroni.

This table presents the results of the Bonferroni post hoc test, which allows to discover which specific means differed. It can be seen that there was no significant difference in IR_{sub} between t_2 and t_3 ($p > 0.05$), in 1-Day biofilm group.

Table 3.19: Tests of Within-Subjects Effects Table - 2-Day Biofilm group

Tests of Within-Subjects Effects

Measure: MEASURE_1

Source		Type III Sum of Squares	df	Mean Square	F	Sig.	Partial Eta Squared
Time	Sphericity Assumed	272726.665	3	90908.888	10.670	.000	.433
	Greenhouse-Geisser	272726.665	1.986	137338.690	10.670	.000	.433
	Huynh-Feldt	272726.665	2.313	117918.459	10.670	.000	.433
	Lower-bound	272726.665	1.000	272726.665	10.670	.006	.433
Error(Time)	Sphericity Assumed	357846.644	42	8520.158			
	Greenhouse-Geisser	357846.644	27.801	12871.650			
	Huynh-Feldt	357846.644	32.380	11051.548			
	Lower-bound	357846.644	14.000	25560.475			

A repeated measures ANOVA with a Greenhouse-Geisser correction showed that the mean scores for IR_{sub} was statistically significantly different (F(1.986, 27.801) = 10.670, $p < 0.05$) for 2-Day Biofilm group.

Table 3.20: Pairwise Comparisons Table – 2-Day Biofilm group

Pairwise Comparisons

Measure: MEASURE_1

(I) Time	(J) Time	Mean Difference (I-J)	Std. Error	Sig.[b]	95% Confidence Interval for Difference[b] Lower Bound	Upper Bound
1	2	-23.438	36.153	1.000	-134.384	87.508
	3	151.657*	36.347	.006	40.116	263.197
	4	54.998	45.827	1.000	-85.635	195.631
2	1	23.438	36.153	1.000	-87.508	134.384
	3	175.095*	24.138	.000	101.020	249.170
	4	78.436	32.299	.175	-20.684	177.556
3	1	-151.657*	36.347	.006	-263.197	-40.116
	2	-175.095*	24.138	.000	-249.170	-101.020
	4	-96.659*	21.493	.003	-162.615	-30.702
4	1	-54.998	45.827	1.000	-195.631	85.635
	2	-78.436	32.299	.175	-177.556	20.684
	3	96.659*	21.493	.003	30.702	162.615

Based on estimated marginal means

*. The mean difference is significant at the .05 level.

b. Adjustment for multiple comparisons: Bonferroni.

This table presents the results of the Bonferroni post hoc test, which allows to discover which specific means differed. It can be seen that there was a significant difference in IR_{sub} between t_2 and t_3 ($p < 0.05$), in 2-Day biofilm group.

Table 3.21: Tests of Within-Subjects Effects Table - 3-Day Biofilm group

Tests of Within-Subjects Effects

Measure: MEASURE_1

Source		Type III Sum of Squares	df	Mean Square	F	Sig.	Partial Eta Squared
Time	Sphericity Assumed	262669.519	3	87556.506	7.183	.001	.339
	Greenhouse-Geisser	262669.519	1.666	157627.191	7.183	.005	.339
	Huynh-Feldt	262669.519	1.864	140879.601	7.183	.004	.339
	Lower-bound	262669.519	1.000	262669.519	7.183	.018	.339
Error(Time)	Sphericity Assumed	511981.122	42	12190.027			
	Greenhouse-Geisser	511981.122	23.330	21945.596			
	Huynh-Feldt	511981.122	26.103	19613.918			
	Lower-bound	511981.122	14.000	36570.080			

A repeated measures ANOVA with a Greenhouse-Geisser correction showed that the mean scores for IR_{sub} was statistically significantly different ($F(1.666, 23.330) = 7.183$, $p < 0.05$) for 3-Day Biofilm group.

Table 3.22: Pairwise Comparisons Table – 3-Day Biofilm group

Pairwise Comparisons

Measure: MEASURE_1

(I) Time	(J) Time	Mean Difference (I-J)	Std. Error	Sig.[b]	95% Confidence Interval for Difference[b] Lower Bound	Upper Bound
1	2	-35.587	46.635	1.000	-178.699	107.525
	3	-137.067	52.759	.126	-298.973	24.839
	4	-156.842*	50.824	.048	-312.810	-.874
2	1	35.587	46.635	1.000	-107.525	178.699
	3	-101.480*	32.847	.048	-202.280	-.680
	4	-121.255*	32.494	.013	-220.972	-21.538
3	1	137.067	52.759	.126	-24.839	298.973
	2	101.480*	32.847	.048	.680	202.280
	4	-19.775	8.707	.237	-46.496	6.946
4	1	156.842*	50.824	.048	.874	312.810
	2	121.255*	32.494	.013	21.538	220.972
	3	19.775	8.707	.237	-6.946	46.496

Based on estimated marginal means

*. The mean difference is significant at the .05 level.

b. Adjustment for multiple comparisons: Bonferroni.

This table presents the results of the Bonferroni post hoc test, which allows to discover which specific means differed. It can be seen that there was a significant difference in IR_{sub} between t_2 and t_3 ($p < 0.05$), in 3-Day biofilm group.

Table 3.23: Descriptive table - One-way ANOVA of IR_{sub}.

Descriptives

IR_sub_t3

		N	Mean	Std. Deviation	Std. Error	95% Confidence Interval for Mean		Minimum	Maximum	Between-Component Variance
						Lower Bound	Upper Bound			
CONTROL		15	11942.4773	153.82681	39.71791	11857.2909	12027.6638	11696.75	12223.36	
1 DAY		15	12003.8213	139.72985	36.07809	11926.4415	12081.2011	11798.47	12247.96	
2 DAY		15	11910.9960	129.97511	33.55943	11839.0182	11982.9738	11597.93	12085.62	
3 DAY		15	12094.8940	164.90963	42.57948	12003.5701	12186.2179	11805.10	12421.23	
Total		60	11988.0472	160.35131	20.70127	11946.6240	12029.4703	11597.93	12421.23	
Model	Fixed Effects			147.71242	19.06959	11949.8462	12026.2481			
	Random Effects				40.49543	11859.1726	12116.9217			5104.92351

Table 3.24: One-way ANOVA of IR_{sub}.

ANOVA

IR_sub_t3

	Sum of Squares	df	Mean Square	F	Sig.
Between Groups	295178.432	3	98392.811	4.510	.007
Within Groups	1221861.642	56	21818.958		
Total	1517040.074	59			

This table presents the results of the one-way ANOVA of IR_{sub} at t_3. There was a statistically significant different between groups, ($F(3,56) = 4.510$, $p < 0.05$).

Table 3.25: Tukey's HSD for IR_{sub} showing the p-values for four experimental groups (N=60, n=15).

Multiple Comparisons

Dependent Variable: IR_sub_t3

Tukey HSD

(I) Group	(J) Group	Mean Difference (I-J)	Std. Error	Sig.	95% Confidence Interval	
					Lower Bound	Upper Bound
CONTROL	1 DAY	-61.34400	53.93695	.668	-204.1630	81.4750
	2 DAY	31.48133	53.93695	.937	-111.3376	174.3003
	3 DAY	-152.41667*	53.93695	.032	-295.2356	-9.5977
1 DAY	CONTROL	61.34400	53.93695	.668	-81.4750	204.1630
	2 DAY	92.82533	53.93695	.323	-49.9936	235.6443
	3 DAY	-91.07267	53.93695	.339	-233.8916	51.7463
2 DAY	CONTROL	-31.48133	53.93695	.937	-174.3003	111.3376
	1 DAY	-92.82533	53.93695	.323	-235.6443	49.9936
	3 DAY	-183.89800*	53.93695	.006	-326.7170	-41.0790
3 DAY	CONTROL	152.41667*	53.93695	.032	9.5977	295.2356
	1 DAY	91.07267	53.93695	.339	-51.7463	233.8916
	2 DAY	183.89800*	53.93695	.006	41.0790	326.7170

*. The mean difference is significant at the 0.05 level.

This table presents the results of the Tukey post hoc analysis. Results revealed that there was a significant different in IR_{sub} between control & 3-Day biofilm groups; and between 2-day & 3-Day biofilm groups ($p < 0.05$).

Table 3.26: Descriptive Table - One-way ANOVA of ΔIR_{sub}.

Descriptives

d_IR_sub_t3

		N	Mean	Std. Deviation	Std. Error	95% Confidence Interval for Mean		Minimum	Maximum	Between-Component Variance
						Lower Bound	Upper Bound			
1 DAY		15	-.006897	.0166553	.0043004	-.016120	.002327	-.0282	.0297	
2 DAY		15	-.014462	.0077160	.0019923	-.018735	-.010189	-.0272	.0000	
3 DAY		15	.008538	.0106986	.0027624	.002613	.014462	-.0078	.0299	
Total		45	-.004274	.0154049	.0022964	-.008902	.000355	-.0282	.0299	
Model	Fixed Effects			.0122664	.0018286	-.007964	-.000583			
	Random Effects				.0067677	-.033393	.024846			.0001274

Table 3.27: One-way ANOVA of ΔIR_{sub}.

ANOVA

d_IR_sub_t3

	Sum of Squares	df	Mean Square	F	Sig.
Between Groups	.004	2	.002	13.698	.000
Within Groups	.006	42	.000		
Total	.010	44			

This table presents the results of the one-way ANOVA of ΔIR_{sub} at t_3. There was a statistically significant different between groups, ($F(2,42) = 13.698$, $p < 0.05$).

Table 3.28: Tukey's HSD for ΔIR_{sub} showing the p-values for three experimental groups (N=60, n=15).

Multiple Comparisons

Dependent Variable: d_IR_sub_t3

Tukey HSD

(I) Group	(J) Group	Mean Difference (I-J)	Std. Error	Sig.	95% Confidence Interval	
					Lower Bound	Upper Bound
1 DAY	2 DAY	.0075651	.0044791	.221	-.003317	.018447
	3 DAY	-.0154345*	.0044791	.004	-.026316	-.004553
2 DAY	1 DAY	-.0075651	.0044791	.221	-.018447	.003317
	3 DAY	-.0229995*	.0044791	.000	-.033881	-.012118
3 DAY	1 DAY	.0154345*	.0044791	.004	.004553	.026316
	2 DAY	.0229995*	.0044791	.000	.012118	.033881

*. The mean difference is significant at the 0.05 level.

This table presents the results of the Tukey post hoc analysis. Results revealed that there was a significant different in ΔIR_{sub} between 1-Day & 3-Day biofilm groups; and between 2-Day & 3-Day biofilm groups ($p < 0.05$).

3.5 Discussion

In the current study, laboratory-cultivated biofilm was created on to the enamel specimens using three types of bacteria that were identified in the literature as early colonisers. The three bacteria chosen as the representatives of bacteria that exist in the early dental biofilm were *Strep. Sanguinis, Strep. Mitis* and *Actinomyces.* A few studies had identified streptococci as the predominant colonizers of early enamel biofilms (J. Li et al., 2004; Nyvad & Kilian, 1987). Nyvad and Kilian (1987) characterized the cultivable bacteria colonizing enamel samples exposed to the oral cavity and found that, after 4 h and 8 h of plaque formation, Streptococci made up approximately 63% and 86% (mean value of samples from four individuals) of isolated bacteria, respectively.

3.5.1 Dental biofilm

For this study, natural occurring biofilm was not used due to the uniqueness of the plaque matrix biofilms where there may be more or less than 1000 different microbial species (Saini, Saini, & Sharma, 2011).

In this *in vitro* study, using the 'modified NAM model', the enamel surface was exposed to the whole saliva for two minutes to allow for the deposition of salivary components to its surface. As opposed to the original NAM model as reported by (Rahim et al., 2008), where glass surface was used to represent the hard surface of the tooth. The coating of the surfaces with saliva would simulate the pellicle-covered tooth surfaces in the oral cavity. This experimental pellicle that was formed on the enamel surface, like the acquired pellicle on tooth surfaces have a net negative charge due to its acidic protein components (Gibbins, Yakubov, Proctor, Wilson, & Carpenter, 2014). The presence of the artificial pellicle is important as it is a deposition of many salivary components which may act as receptors in the attachment of the early biofilm settlers to the surface.

Mechanical properties of biofilms are still one of the blind spots in biofilm research. A major reason is the lack of applicable methods for the determination of relevant parameters such as Young's modulus, shear modulus, adhesive or tensile strength (Billings, Birjiniuk, Samad, Doyle, & Ribbeck, 2015). The most important problem is that biofilm specimens cannot easily be transferred to the measuring device without altering or manipulating the desired properties. Biofilms are in some cases extremely thin, so that they cannot be transported to a measuring device at all. In general, the best way would be to measure the characteristics in place without disturbing the biofilm specimen (Wagner & Horn, 2017).

From an eco-systematic point of view, variations in oral biofilms can be detected only if a representative area of the biofilm is analysed. The automated microscopy-based system used in this study allows the minimally destructive investigation of intact biofilm across the complete surface of the enamel plate (Karygianni et al., 2012). However, despite the issues mentioned, *in vitro* studies should be treated as an artificial model that may not precisely simulate the complex process that occurs *in vivo*.

3.5.2 CLSM

In the present study, CLSM was used for qualitative analysis where image of biofilm was taken showing the presence of the laboratory-cultivated biofilm formed on the specimens. The CLSM has been applied for observation and analysis of bacterial biofilms. Some studies have applied CLSM for evaluating dental biofilm formed on enamel surface (Paschos et al., 2016; Pelka, Trautmann, Petschelt, & Lohbauer, 2010). However, in this study, identification of specific bacteria was not included. The identification of each type of bacteria used in this study was not carried out due to methodological limitations, and thus, could not eliminate possibility of bacterial

contamination. Therefore, further studies should clarify the percentage of each species of bacteria that exist on the specimen surfaces.

After three days, the amount green stains of biofilm were seen to be increasing compared to day 1 and 2 (**Figure 3.14**). Al-Ahmad et al. (2007) reported that the thickness of the oral biofilm increased significantly after 2 days, analysed under CLSM, which is in agreement with this study.

CLSM presents advantages for the study of biofilms without the necessity of a specific treatment applied to the sample, such as dehydration or sputter coating, which are usually necessary when a conventional scanning electron microscope (SEM) is used (Brunk, Collins, & Arro, 1981; Lawrence et al., 1991).

The choice of the vital fluorescence staining with Fluorescein Diacetate and Ethidium Bromide technique was due to the well-documented experience on the staining of dental plaque. Furthermore, the technique seems to be the proven and suitable method in biofilm research (Netuschil et al., 2014). However, a disadvantage of fluorescein is that it is not retained in the cells for a prolonged time. All measurements had to be performed within 15 min after the staining.

The simultaneous use of both confocal microscopy and vital fluorescence techniques made the examination of the three-dimensional architecture of dental biofilm possible. The vital fluorescence technique discriminates vital from dead cells, while CLSM allows the optical sectioning of undisturbed biofilms leaving the samples intact during analysis (Netuschil et al., 1998). Vital fluorescence staining with Fluorescein Diacetate and Ethidium Bromide seems to be the best proven and suitable method in biofilm research (Netuschil et al., 2014).

The main difficulty encountered with CLSM in this study was to get a good image showing the stained biofilm. Finding the areas with biofilm was time-consuming may be

due to uneven spread of biofilm on the specimens. Azeredo et al. (2017) reported limitations of biofilm analysis by CLSM include: (i) interference of local physico-chemical properties of the biofilm with fluorescence probes and (ii) natural auto-fluorescence of the sample hiding the signal of interest.

3.5.3 OCT

OCT has been widely used in assessment of demineralisation based on two main principles; increased light scattering in the porous demineralised tissue, and depolarization of the incident light by the demineralised tissue. The former phenomenon can be observed as increased signal intensity by both conventional and polarized sensitive OCT systems, however, the latter necessitates a polarization- sensitive OCT (PS-OCT) or cross-polarization OCT setup, (R. S. Jones, Darling, Featherstone, & Fried, 2006b; H. Kang et al., 2012). Image analysis techniques in correlative OCT studies have been mainly based on the increased signal intensity values to quantify parameters such as depth (as a cut-off point) and mineral loss (dB values integrated over depth) in demineralised lesions (Natsume et al., 2011).

OCT was used to quantify the effect of biofilm on the initially eroded enamel surface. Eroded enamel appeared a bright zone in B-scan images due to the backscattered light. The OCT image was able to indicate the presence of biofilm due to optical variation between air, biofilm and tooth structure, leading to increased brightness on the enamel surface. The presence of biofilm was confirmed by the CLSM images.

A previous study reported finding four phenomena that occur during interactions between a tooth and the amount of light. These include specular transmission of the light flux through the tooth, specular reflection at the surface, diffuse light reflection at the surface, and then absorption and scattering of the flux within the tooth (Karlsson, 2010).

The present study was undertaken to evaluate the effect of OCT intensity in the presence of biofilm. OCT provides additional information on the subsurface characteristics of the eroded enamel. It not only provides information regarding the degree of demineralisation from the backscattered intensity, it also provides information about lesion depth. As demineralisation progresses, the development of porosity continues from the enamel-air interface towards the deeper layers.

The attenuation coefficient in biological tissue is related to the intensity of light that is backscattered from the specimen and measured by the OCT system (G. T. Smith et al., 2015). OCT is a method based on measurements of the backscattered light intensity versus specimen depth using an interferometer set-up and a partly coherent source, the obtained signal being modulated by the optical parameters and homogenous properties of the investigated specimen, *i.e.*, the tooth (Sowa, Popescu, Friesen, Hewko, & Choo-Smith, 2011). OCT investigations for enamel surfaces were done at 1310 nm or 850 nm as the probing wavelength (Sowa et al., 2011). Longer wavelengths, like 1310 nm offered a greater potential for clinical optical imaging due to the weak scattering and absorption in sound dental hard tissues (Fried et al., 2011).

Expected trend for $IR_{biofilm}$ is an increase in mean $IR_{biofilm}$ in specimens with biofilm compared to without biofilm. The results showed significant increase in $IR_{biofilm}$, after presence of biofilm in all the groups as shown in **Figure 3.16**. **Figure 3.10** shows evidence of thick biofilm causing the light to backscatter which resulted in increased in intensity, thus increased in brightness as seen on the B-scan. Furthermore, a significant increase was also shown in $IR_{biofilm}$ in the 3-day biofilm group compared to control group where the specimens were kept in de-ionised water for 3 days (**Figure 3.17**). The increase in backscattered intensity was most probably due to the presence of thick 3-day biofilm.

Expected trend for IR_{sub} is a decrease in mean IR_{sub} in specimens with biofilm compared to without biofilm. This trend were shown in 1-day and 2-day biofilm groups

although the difference was not significant in 1-day biofilm, however, in 3-day biofilm, result was opposite the trend. The increase in IR_{sub} shown for 3-day biofilm could probably be due to uneven spread of biofilm during OCT scanning whereby in certain areas where the thickness of biofilm could be more compared to certain areas within the scope of scanning.

Amaechi et al. (2001) demonstrated that the loss of penetration depth in conventional OCT images correlated well with the mineral loss measured with microradiography for shallow artificial lesions on smooth surfaces. Although this approach provided good results for shallow lesions on flat surfaces, there are several issues with using the loss of light penetration as a measure of lesion severity. In order to utilize loss of OCT signal intensity one must arbitrarily choose a distance from the surface to serve as a cut-off point, based on an arbitrary intensity loss. This is feasible for smooth surfaces with uniform artificial lesions of known depth, but is not possible for highly convoluted surfaces, irregular lesion geometry or for lesions with significant structural characteristic of natural lesions. Moreover, OCT provides measurements of the reflectivity from each layer in the tissue. Since the reflectivity increases markedly with increases in light scattering, the lesion is most likely to cause an increase in signal rather than a loss in signal especially for natural lesions, and one cannot assume that the underlying enamel is sound.

Popescu et al. (2008) on the other hand concluded that increasing demineralisation in the lesion actually decreased the total scattering in the lesion, because the rate of decline of the A-scan intensity decreased in natural smooth surface lesions compared to sound enamel. The authors attributed this phenomenon to the different scattering behaviour of pores in the lesion, but this interpretation is not supported by any modelling or experimental measurements and it contradicts previous angularly resolved light scattering measurements in sound and demineralised enamel in the near-IR which shows

a 2–3 fold increase in light scattering with demineralisation (Darling, Huynh, & Fried, 2006).

In previous studies, caries lesions have been detected by OCT analysing the reduction in enamel reflectivity (Amaechi, Podoleanu, Higham, & Jackson, 2003), the mineral loss correlation with the increase in reflectivity (Chan et al., 2015; Douglas, Fried, & Darling, 2010; Le et al., 2010), by the refractive index alterations (Hariri et al., 2012), and by changes in the attenuation coefficient of the signal exponential decay (Mandurah et al., 2013; Popescu et al., 2008).

Projection images were formed over a depth of 500 μm, one hundred times the expected depth of the softened layer found in enamel smooth surface. The rationale for this is as follows. Erosive changes predominantly affect the enamel surface to a depth of 2-5 μm. When the initial surface is polished, as in this study, the initial change is from a specular reflection to a slightly diffuse scattering interaction. Thus, the intensity of light coupled back into the OCT collection optics immediately from the surface is reduced. Furthermore, the intensity of light transmitted into the specimen without interaction and backscattered from within the sample back through the diffuse surface is also modified. The net result of this change is a reduction in the B-Scan image intensity, this is visually apparent. Whilst it has been shown to be possible to detect erosive changes by concentrating on the intensity of only the surface reflection (Chan et al., 2013; Chew et al., 2014), these approaches ignore the integrated effect at depth that is more than simply a shadowing influence of the surface. When considering this effect, it is important to remember that OCT B-Scan images are typically rendered on a logarithmic scale. In linear units, the axial OCT signal corresponding to a homogeneous scattering medium is typically represented by a strong initial surface reflection peak followed by an exponential intensity attenuation. Thus, integrating the OCT signal over some axial depth is akin to performing an exponential weighted average, with preference for the surface signal.

Clinically, blot drying or gentle air drying of the surface would be necessary to remove excessive amounts of saliva or water over the area of interest (Mandurah et al., 2013). Also, cleaning the surface before imaging is essential as plaque and calculus could interfere with the light propagation through the lesion, thus, to avoid its effect on the OCT measurements. Likewise, a protective cover placed over the OCT intraoral imaging probe for infection control purposes may refract and attenuate nonuniformly, therefore an autoclavable dental OCT intraoral probe that requires no disposable cover is desirable. It is also noteworthy that the depth of field is restricted in the current OCT systems; therefore, controlling the object-probe distance is important to maintain the image focused and avoid signal loss.

3.5.4 Study design

In vitro models are extremely useful for evaluating dental erosion because the experiment can be conducted over a short period of time, require low operating cost and do not depend on volunteers' collaboration. These methods enable highly controllable experimental conditions, which is a good starting point for understanding these complex interactions and often a necessary step, as in situ observations can be infeasible due to high complexity of the system. However, they are not able to replicate the oral cavity with all the biological characteristics which is known to interfere on erosion development, such as saliva.

It is suggested that freshly extracted teeth are the most suitable substrate for *in vitro* evaluation of adhesive systems. However, to acquire the sufficient number of tooth specimens, freshly extracted teeth must be collected over time − which means that they must be stored after extraction. Storage solutions are thus used to prevent dehydration of teeth as well as cross-contamination between extracted teeth. Based on the results of this study, we recommended that care should be taken when selecting storage solutions for *in*

vitro studies. This is because the chemical nature of the storing agent may affect the tooth structure and material properties at the tested interface (Tosun, Sener, & Sengun, 2007).

3.6 Conclusions

1. CLMS images showed that the oral biofilm was cultivated after 1-day, 2-day and 3-day, respectively.

2. The laboratory-cultivated oral biofilm increased the attenuation of OCT intensity within the biofilm (i.e. above the surface of the tooth) for each group.

3. The OCT backscattered intensity decreased at the immediate tooth subsurface, with the presence of laboratory-cultivated oral biofilm.

CHAPTER 4: EFFECT OF DENTAL WATER JET ON SOFTENED ENAMEL AND ITS ABILITY IN REMOVING BIOFILM

4.1 Introduction

Ideally, all enamel surfaces should be clear from biofilm during OCT measurements, similar to the *in vitro* study. Therefore, a suitable method needs to be applied in order to get a clean surface prior to taking accurate measurement using OCT.

OCT technology has shown a steady progress during recent years with regards to its application on dental enamel. From the results obtained in Chapter 3, it was found that the presence of biofilm on enamel surface does affect the attenuation of the near infra-red light of OCT, to some extent. Thus, obscuring the OCT signal into the subsurface regions. Hence, ideally biofilm is to be removed prior to OCT scanning.

Dental erosion was earlier defined as an irreversible loss of dental structure due to a chemical process not involving bacteria (Imfeld, 1996). In the last decade, the terms to describe the effects of acids on the tooth surface were more precisely defined. Initially, the acid contact causes an erosive softening due to a demineralisation of the outermost enamel layer. Continuous acid contact leads to a measurable erosive enamel loss (Huysmans et al., 2011; Shellis et al., 2011). Dental erosion is a multifactorial and complex condition determined by chemical (type of acid), biological (saliva, acquired pellicle) and behaviour (frequency of acid exposure, brushing habits) factors (Lussi & Carvalho, 2014; Zero & Lussi, 2006). It is most likely that in real life, dental erosion alone is not the main reason for dental hard tissue loss, but it is a mixture of a chemical-mechanical processes involving erosion, abrasion and attrition (Aykut-Yetkiner, Wiegand, Bollhalder, Becker, & Attin, 2013).

The oral cavity is colonized with a complex and heterogeneous mixture of microorganisms. These microorganisms are embedded in an extracellular polymeric matrix, forming biofilms. Biofilms on natural teeth or implants are intimately responsible for caries formation or aetiology of periodontitis or peri-implantitis (Dhir, 2013).

There are two basic strategies of dental biofilm control: either inactivating the biofilm by antimicrobial agents or removing the biofilm with mechanical procedures. The chemical approach suffers from the limitation that the antimicrobial agents are hindered from penetrating the biofilm and can only reach the outer layers of the biofilm in antimicrobially effective concentration, and thus the biofilm can easily return to its original state after treatment (Donlan, 2001). The mechanical removal is the most effective treatment currently available for the control of dental plaque (Petersilka, Ehmke, & Flemmig, 2002). Examples of mechanical methods include toothbrushing, oral irrigation and flossing. However, in this study only water jet was chosen for biofilm removal method and its efficacy of doing so was evaluated. The concept of using water jet was based on the usage of oral irrigator which is widely used as an adjunct to tooth brushing for biofilm control. Furthermore, it was thought to be the simplest way to remove biofilm prior to OCT measurement.

Nevertheless, a problem may be the removal of acid-induced softened enamel beneath a biofilm when subjected to pressure exerted by the waterjet to remove the biofilm. The suitability of the water jet for biofilm removal during any *in vivo* initial erosion studies needs to be validated.

The dental water jet has been used for biofilm control as an adjunct device to tooth-brushing. Among the home care devices used for daily oral hygiene, dental water jets (also known as oral irrigators) have been reported to be effective in eliminating biofilm from tooth surfaces (Gorur, Lyle, Schaudinn, & Costerton, 2009). Nevertheless,

a question remains and that is whether dental water jet removes the already softened enamel layer if it is applied after the teeth have been exposed to acid challenge.

4.2 Literature Review

4.2.1 Initial erosion and enamel softening

The early stage of enamel dissolution is characterized by softening of the enamel surface (Addy & Shellis, 2006). This softening process happens when the enamel layer loses minerals from a layer extending between 0.2 μm and 5 μm below the tooth surface (Hemingway, Parker, Addy, & Barbour, 2006; Wiegand, Wegehaupt, Werner, & Attin, 2007). As softening progresses further into enamel, it may result in substantial loss of minerals in the most superficial layer where this layer is lost completely (Amaechi & Higham, 2001b). Further progressive loss will eventually lead to subsequent exposure of the underlying dentine, dentine sensitivity, loss of occlusal vertical height and aesthetic problems.

Enamel softening is however reversible, whereby salivary calcium and phosphate has been reported to remineralise the softened enamel (Attin, Buchalla, Gollner, & Hellwig, 2000). It was shown that the abrasion resistance of erosively altered enamel can be improved when exposed to artificial saliva *in vitro* (Attin et al., 2000) and to a smaller degree, to the oral environment (*in situ*) (Attin et al., 2000; Jaeggi & Lussi, 1999), which means that the enamel softening stage can be reversed and have the potential to re-harden (Gedalia, Ionat-Bendat, Ben-Mosheh, & Shapira, 1991). The clinical manifestation of erosion, therefore, may be the result of the removal of the softened surface before the remineralising action of saliva.

Intra-orally, erosion does not occur exclusively where the chemical dissolution occurs simultaneously with mechanical forces (Kelleher & Bishop, 1999; B. G. Smith &

Knight, 1984). As minerals are released during erosion, the mechanical and physical properties of this softened enamel is modified and is more susceptible than sound enamel to mechanical wear such as attrition and abrasion (Attin et al., 2000; Attin, Knofel, Buchalla, & Tutuncu, 2001). Attrition is the gradual loss of hard tooth substance from occlusal contacts with an opposing dentition or restorations (Hattab & Yassin, 2000), and this could be caused by extrinsic factors such as parafunctional habits of bruxism, traumatic occlusion in the partially edentulous dentition, and malocclusion (Litonjua, Andreana, Bush, & Cohen, 2003). Zhang, Arsecularatne, and Hoffman (2015) reported that in acidic environment, the softened enamel layer became relatively smooth following enamel-on-enamel (attrition) wear.

Softened enamel has also been reported to be prone to abrasion (Attin et al., 1997). Abrasion is the loss of tooth substance through mechanical means, other than tooth contact (Mair, 1992). The most common cause of dental abrasion is toothbrushing and the severity and distribution of toothbrushing abrasion wear may be related to brushing technique, time, frequency, bristle design and the abrasiveness of the dentifrice (Bishop et al., 1997; Hattab & Yassin, 2000). However without the presence of acid, neither toothbrushing alone nor toothbrushing with toothpaste had shown to cause wear of enamel (Hemingway et al., 2006). Thus, toothbrushing following the consumption of acidic beverages was recommended to be postponed to minimise or avoid enamel loss (Hemingway et al., 2006). This recommendation was based on the significant decrease in enamel loss observed when brushing was performed 60 min after the erosion attack (Attin et al., 2001).

Apart from toothbrushing, softened enamel may also be worn by abrasion from soft tissues including tongue (Gregg, Mace, West, & Addy, 2004) and buccal mucosa during mastication and swallowing (Amaechi, Higham, et al., 2003). The palatal surfaces of upper teeth are areas known to be constantly subjected to shear forces either from the

keratinized dorsum of the tongue during speech and swallowing or through food mastication (occlusal surfaces) (Amaechi, Higham, et al., 2003). Abrasive action from ultrasonication with water, in an ultrasonic bath with a power output of 100 W at a frequency of 38 kHz has also been reported to be able to remove the softened enamel surface, evaluated using profilometry measurements (Eisenburger et al., 2000). Wiegand et al. (2007) reported that enamel loss after 30-second ultrasonication with water seems to match abrasion after 20 brushing strokes with toothpaste slurry or 50 brushing strokes with distilled water.

4.2.2 Biofilm control

Colonization of bacteria on tooth surfaces, termed as dental plaque or oral biofilm is recognised as the key aetiological factor of dental caries, gingivitis, and periodontitis (Axelsson, Albandar, & Rams, 2002).] Thus, the removal of biofilm is important to maintain a healthy oral environment and also, as a prerequisite for a successful treatment of biofilm-associated diseases. Biofilm control is defined as biofilm removal on a routine daily basis and preventing its re-accumulation on tooth surfaces, and it can be achieved either mechanically or chemically as well as by the combination of two procedures (Mandal, Singh, Siddiqui, Das, & Dey, 2017).

Dental biofilm is mainly comprised of bacteria in salivary glycoprotein matrix and extracellular polysaccharides. One gram of the biofilm (wet weight) contains approximately 10^{11} bacteria (Socransky & Haffajee, 2002). Thus, use of mechanical tools is the most effective biofilm removal method (S. M. de Oliveira, Torres, Pereira, Mota, & Carlos, 2008). However, daily tooth brushing along with the use of other mechanical tools such as interdental floss and oral irrigation devices, are the most reliable method for maintaining oral hygiene (N. Claydon et al., 2000; S. M. de Oliveira et al., 2008).

4.2.3 Dental water jet

The dental water jet (also known as oral irrigators or water flosser) is designed to remove biofilm and soft debris through the mechanical action of a jet stream of water and has been used as an adjunct device to toothbrushing. It has been reported to be effective in eliminating biofilm from tooth surfaces and the reduction of subgingival pathogenic bacteria from pockets as deep as six mm with the use of water flossing (Cobb, Rodgers, & Killoy, 1988; Drisko, White, Killoy, & Mayberry, 1987; Gorur et al., 2009). With regards to its mechanism of action, the dental water jet works by directly applying a pulsated stream of water at the dental biofilm (Joyce, 2010). Research showed that the production of 1,200 to 1,400 pulsations per minute with a pressure range of medium to high or 50 psi to 90 psi produced the best results in biofilm removal (Bhaskar, Cutright, & Frisch, 1969). A study at the University of Southern California found that a 3 sec treatment of pulsating water (1,200 pulses per minute) at medium pressure (70 psi) removed 99.9% of biofilm from treated areas (Gorur et al., 2009). Furthermore, Kato, Tamura, and Nakagaki (2012) reported that approximately 85% of oral biofilms could be removed by being irrigated them vertically with water pressures exceeding 350 kPa, which is approximately equivalent to 50.8 psi. Therefore, it might be speculated that due to the amount of pressure exerted from the water jet on to the softened surface, certain amount of the demineralised layer might be removed.

Taking into account that to date, there is no report on whether water jet potentially removes acid-induced softened enamel. Thus, this led to the hypothesis that enamel specimens exposed to acid challenge *in vitro* is susceptible to surface loss if subjected to water jet after the challenge than if they received erosion alone. This study was designed to test this hypothesis. To date, it has not been investigated whether the effects of water jet are comparable to other abrasive forces such as toothbrushing, ultrasonication or action by buccal mucosa, which might influence the progression of erosive/abrasive lesions.

Furthermore, uncertainty remains regarding the susceptibility of briefly eroded enamel specimens to water jet and it might be speculated that due to the amount of pressure exerted from the water jet on to the softened surface, certain amount of the demineralised layer might be removed. Apart from that, the ability of the water jet in removing the biofilm that occur on the tooth surface, will also be investigated in this study.

4.2.4 Aim and objectives

Aim:

To evaluate the effect of dental water jet on acid-induced softened human enamel surfaces and on the removal of biofilm.

Objectives:

1. To determine the enamel thickness of acid-induced softened human enamel following the application of dental water jet.
2. To evaluate the ability of dental water jet in removing laboratory-cultivated biofilm on acid-induced softened human enamel surface.

Null hypothesis:

1. The application of dental water jet has no effect on the enamel thickness of acid-induced softened human enamel.
2. The dental water jet is unable to remove laboratory-cultivated biofilm on acid-induced softened human enamel surface.

4.3 Materials and Methods

4.3.1 Ethics and Specimens Collection

(Refer to section 3.3.1 pg. 85).

4.3.2 Preparation of enamel specimens

The specimens used in Chapter 3 were the same specimens used in Chapter 4. The detail preparation of the specimens was described in section 3.3.2 pg. 85.

4.3.3 Acid challenge

The acid challenge protocol was described in Chapter 3, section 3.3.3, pg. 86. Specimens were immersed in citric acid (150 ml, of 0.003 M, pH 3.2) for 30 min. Specimens were then removed from the citric acid, rinsed under running water and dried for 20 sec with compressed air at a fixed distance (10 mm) prior to measurement.

4.3.4 Allocation of specimens

After being subjected to acid challenge, the specimens were randomly divided into four groups, with twenty specimens in each group (n=20). Specimens from group 2, 3 and 4 were inoculated with early laboratory-cultivated biofilm for 1, 2 and 3 days, respectively (**Table 4.1**). Specimens from group 1 (control group) were stored in de-ionised water for three days after the acid challenge and were not inoculated with laboratory-cultivated biofilm. All specimens were then subjected to water jet (WJ) for 20 sec. Swept Source OCT (SS-OCT) (OCS1300SS, Thorlabs Ltd., UK) was used to scan the specimens at baseline (t_1), post-erosion (t_2), with biofilm (t_3) and post-water jet (t_4) time points. Surface Microhardness (SMH) was measured at all time points except at t_3 (**Table 4.2**).

Table 4.1: Experimental groups.

Groups		N=80	Description
1	Control Group (No biofilm)	n=20	Specimens not containing biofilm.
2	1-Day Biofilm Group	n=20	Specimens containing 1-day old biofilm.
3	2-Day Biofilm Group	n=20	Specimens containing 2-day old biofilm.
4	3-Day Biofilm Group	n=20	Specimens containing 3-day old biofilm.

Table 4.2: Measurement time points.

Time points		
Baseline	t_1	SMH_1 OCT_1
Post-erosion	t_2	SMH_2 OCT_2
Biofilm	t_3	OCT_3
Post-Water jet	t_4	OCT_4

4.3.5 Artificial Mouth Model

The protocol was described in Chapter 3, section 3.3.4, pg. 86.

4.3.6 Dental Water Jet

Using a triple syringe attached to a portable cutting unit (Forest Medical, USA) with oil-free compressed air, water jet was sprayed onto the enamel specimens by pressing both water and air buttons simultaneously (**Figure 4.1**) at a pressure of 70 psi for 20 sec (Sahni, Khashai, Forghany, Krasieva, & Wilder-Smith, 2016). The tip of the syringe was placed 10 mm perpendicular to the enamel surface. The water jet procedure was done prior to the measurements at t_4 (OCT_4).

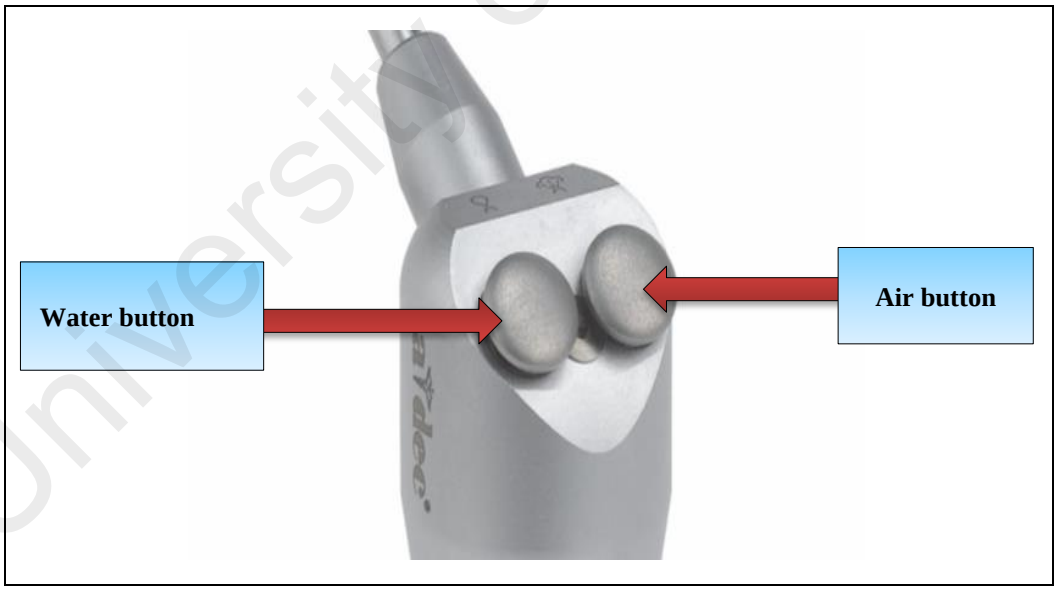

Figure 4.1: Water and air buttons on a triple syringe (for water jet spray, both buttons were pressed simultaneously).

4.3.7 Measurements of specimens

4.3.7.1 Surface Microhardness (SMH)

SMH measurement is a gold standard test for demineralisation. SMH measurements were performed using the microhardness indenter (HMV- 2000; Shimadzu Corporation, Tokyo, Japan) as a measure of enamel softening and demineralisation. The specimens were inserted into a customised jig (**Figure 4.2**) that was positioned parallel to the stage to minimize sliding of the indenter during loading. The jig was also used to obtain a reproducible position during all measurements at various time points. The enamel specimen was placed parallel to the stage prior to indentation and approximately 1 mm^2 of surface area was identified for indentation. Microindentations were made using a Knoop diamond indenter, under a static load of 50 g applied for five sec (de Fatima Carvalho Vasconcelos et al., 2017; Ferreira, Ramos-Jorge, Delbem, & Vieirac Rde, 2013) to obtain the Knoop Hardness Number (KHN). The apparatus was recalibrated before each use. Five indentations were made on each specimen approximately 100 μm apart at the identified area and the mean KHN was then calculated. The width of each indentation was measured and the KHN was generated from the HMV-2000 software, based on the width of each indentation.

4.3.7.2 OCT

A commercially available SS-OCT system (OCS1300SS, Thorlabs Ltd., UK) was used to capture cross-sectional images of the enamel specimens. The light beam was configured to scan an area of 2 mm x 4 mm window. The OCT data acquisition and data processing were described in detail in Chapter 3, section 3.3.7.1,sub-section i, and ii, pg 95 and 98, respectively.

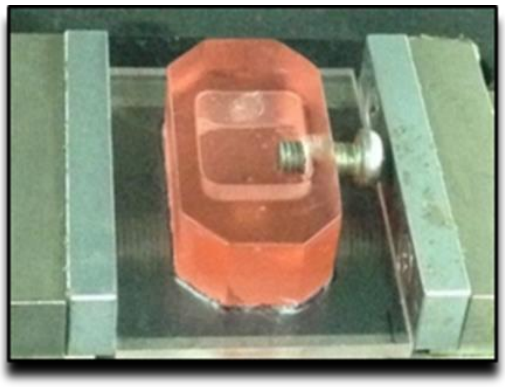

Figure 4.2: Jig for the placement of enamel specimens during microhardness measurement.

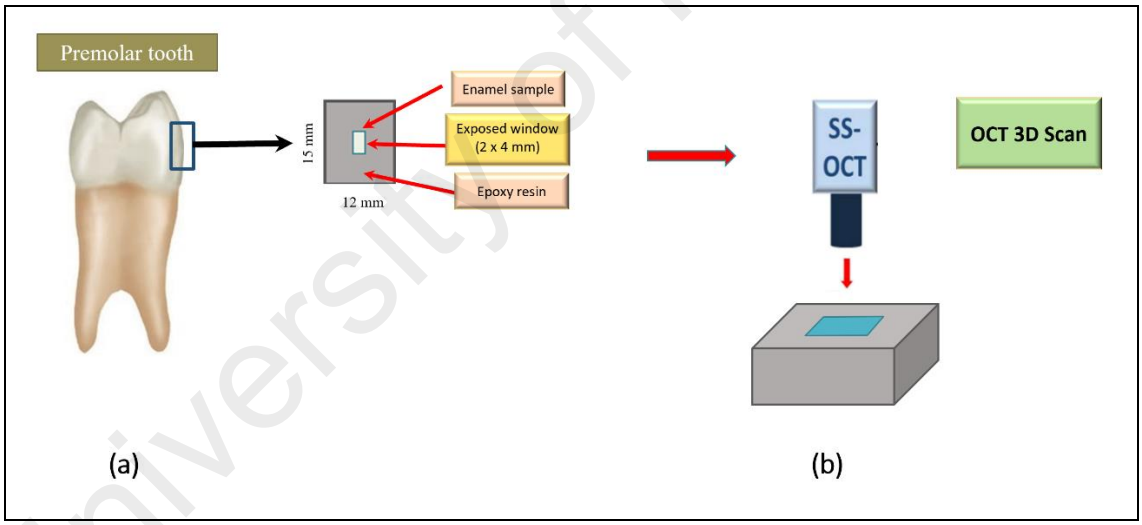

Figure 4.3: Schematic illustration of the experiment. (a) Preparation of enamel specimens, (b) Acquisition of OCT B-scans of enamel specimen.

i. **Enamel thickness**

The enamel thickness was measured using the mean A-scan generated from the ROIs. The first maximum intensity (I_1) observed in the mean A-scan, indicates the change in reflectivity between background and enamel and was used to represent the enamel-air interface. The intensity of the reflected light attenuates exponentially thereafter as the light transmits through enamel until dentine is reached, where another obvious increase in intensity (I_2) is observed. The location of I_2 for this study was defined as the highest intensity that immediately follows the lowest point of the attenuation from I_1 (**Figure 4.4**). The thickness of enamel (D) was then determined by the distance between I_1 and I_2 (Algarni, Kang, Fried, Eckert, & Hara, 2016). Three values of enamel thickness were calculated from each specimen and they were averaged to get the mean value.

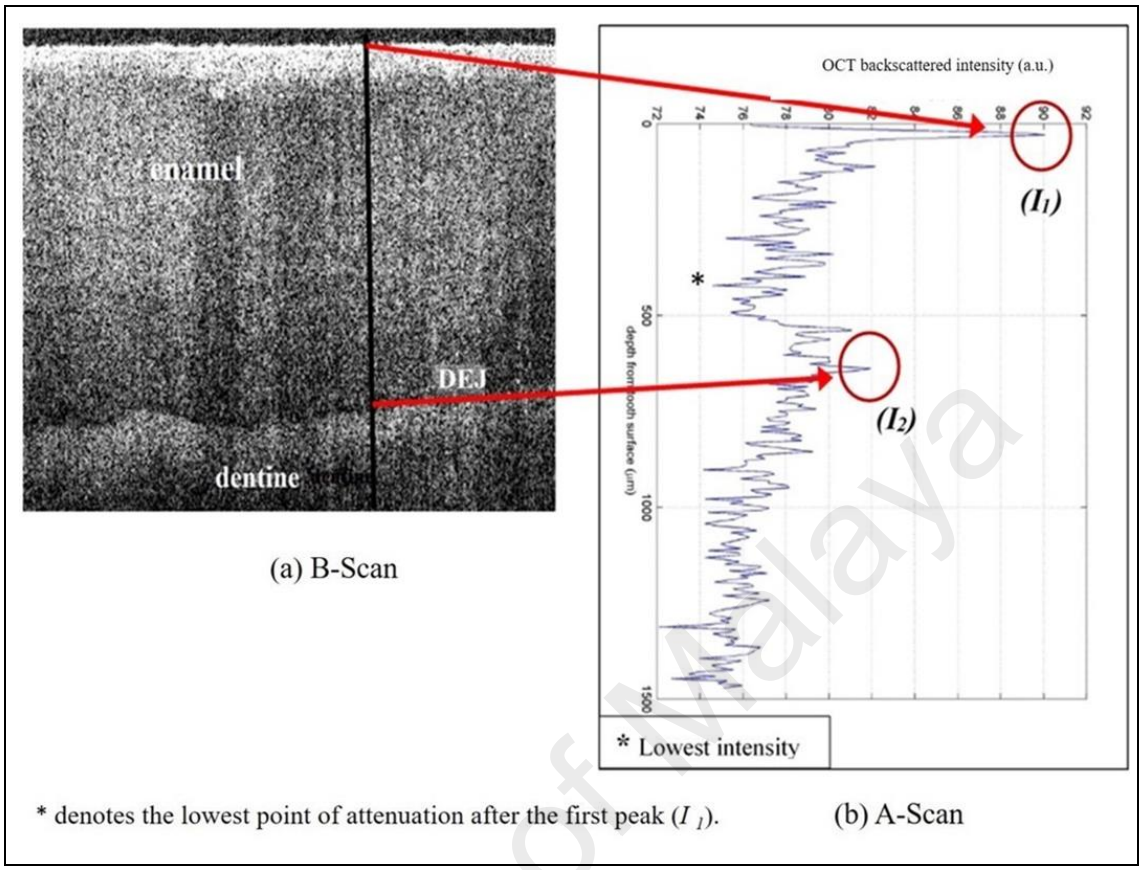

Figure 4.4: (a) A B-scan obtained from OCT and the vertical line represents the measurement position, and (b) the corresponding A-Scan. Arrows represent the position of the enamel-air interface (I_1) and dentine (I_2) peaks, by which their distance determines the enamel thickness.

ii. **Integrated Reflectivity (*IR*)**

Refer to section 3.3.7.1, sub-section iii , pg. 99. The chosen height on the surface for this study were Pixel-4 (biofilm-air interface) and Pixel-10 (biofilm-tooth interface). Assuming that the refractive index of biofilm is similar to that of water (refractive index of water = 1.33), these chosen levels translated to the physical depth of 17.6 μm and 44.1 μm below the biofilm-air interface, respectively, or in other words, this area with biofilm is expected to be approximately 26.5 μm between air and tooth surface. The intensity of the backscattered light at Pixel-10-50 is the intensity where in the A-scans had reached a plateau and were assumed not affected by the acid challenge. It was observed to be at the subsurface physical depth of 167.6 μm for this study.

Integrated Reflectivity (*IR*) between Pixel-4 and Pixel-10 is called Supra-Surface Integrated Reflectivity ($IR_{biofilm}$) (**Figure 3.11**). $IR_{biofilm}$ represented the area where the biofilm accumulated over the tooth surface. $IR_{biofilm}$ is proportional to the amount of backscattered intensity as it travels starting from the light source into the biofilm, prior to hitting the tooth surface (i.e. the total amount of biofilm accumulates on the tooth surface).

The removal capacity of biofilm by water jet was estimated from the $IR_{biofilm}$ which in this case represents the biofilm accumulation over the tooth surface, which was calculated from the differences of backscattered intensity of the same specimens before and after water jet application.

4.3.8 Outcome measures

The outcome measure used for SMH was the fractional change of the surface microhardness (*ΔSMC*). *ΔSMC* was calculated using the formula shown below:

$$\Delta SMC\ (t_2) = \left[\frac{KHN\ (t_2) - KHN\ (t_1)}{KHN\ (t_1)}\right]$$

$KHN\ (t_1)$ = KHN at Baseline

$$\Delta SMC\ (t_4) = \left[\frac{KHN\ (t_4) - KHN\ (t_2)}{KHN\ (t_2)}\right]$$

$KHN\ (t_2)$ = KHN Post-Erosion

The outcome measure used for thickness of enamel (*D*) was the fractional change of the enamel thickness (Δ*D*). Δ*D* (*t*) for each measurement time point was calculated using the formula shown below:

$$\Delta D\ (t_2) = \left[\frac{D\ (t_2) - D\ (t_1)}{D\ (t_1)}\right]$$

$D\ (t_1)$ = *D* at Baseline

$$\Delta D\ (t_4) = \left[\frac{D\ (t_4) - D\ (t_2)}{D\ (t_2)}\right]$$

$D\ (t_2)$ = *D* at Post-Erosion

The outcome measure used for the integrated reflectivity of OCT was the fractional change of the integrated reflectivity (Δ*IR*), which is the difference of backscattered intensity of the same specimen, before and after water jet application. This value should provide a value that corrects for any compositional variations and therefore produce comparable results. 'Before water jet' time point was actually the same as 'With Biofilm time point (t_3). The value was calculated for all the specimens using the formula below:

$$\Delta\ IR = \left[\frac{IR\ (t_4) - IR\ (t_3)}{IR\ (t_3)}\right]$$

$IR\ (t_3)$ = *IR* (with biofilm)

Table 4.3: Description of outcome measures used in the study.

Outcome measures	***Description***
Fractional change of the surface microhardness (*ΔSMC*).	The mean difference of SMH of the same specimen, before and after acid challenge.
Fractional change of the enamel thickness (Δ *D*)	The mean difference of D value of the same specimen, before and after acid challenge.
Fractional change of the integrated reflectivity (Δ *IR*).	The mean difference of integrated reflectivity of the same specimen, before and after water jet application.

4.3.9 Statistical Analysis

The data from surface microhardness, enamel thickness and integrated reflectivity (*IR*) were subjected to statistical analysis using the statistic package for social study (SPSS) version 25.0 (SPSS Inc., Chicago, USA). Data from integrated reflectivity (*IR*) presented normal distribution. The data were subjected to repeated measures analysis of variance (ANOVA) and Bonferroni post-hoc tests were performed to detect any significant different after each consecutive time points (baseline, post-erosion and post-water jet). One-way ANOVA was used to assess the differences in *IR* and fractional change of *IR* among the three experimental groups (1-Day Biofilm, 2-Day Biofilm and 3-Day Biofilm),–Tukey's post hoc test was applied, when necessary, in cases where ANOVA revealed significant differences. The level of significance was set at $p < 0.05$.

The summary of the study flowchart is shown in **Figure 4.5**.

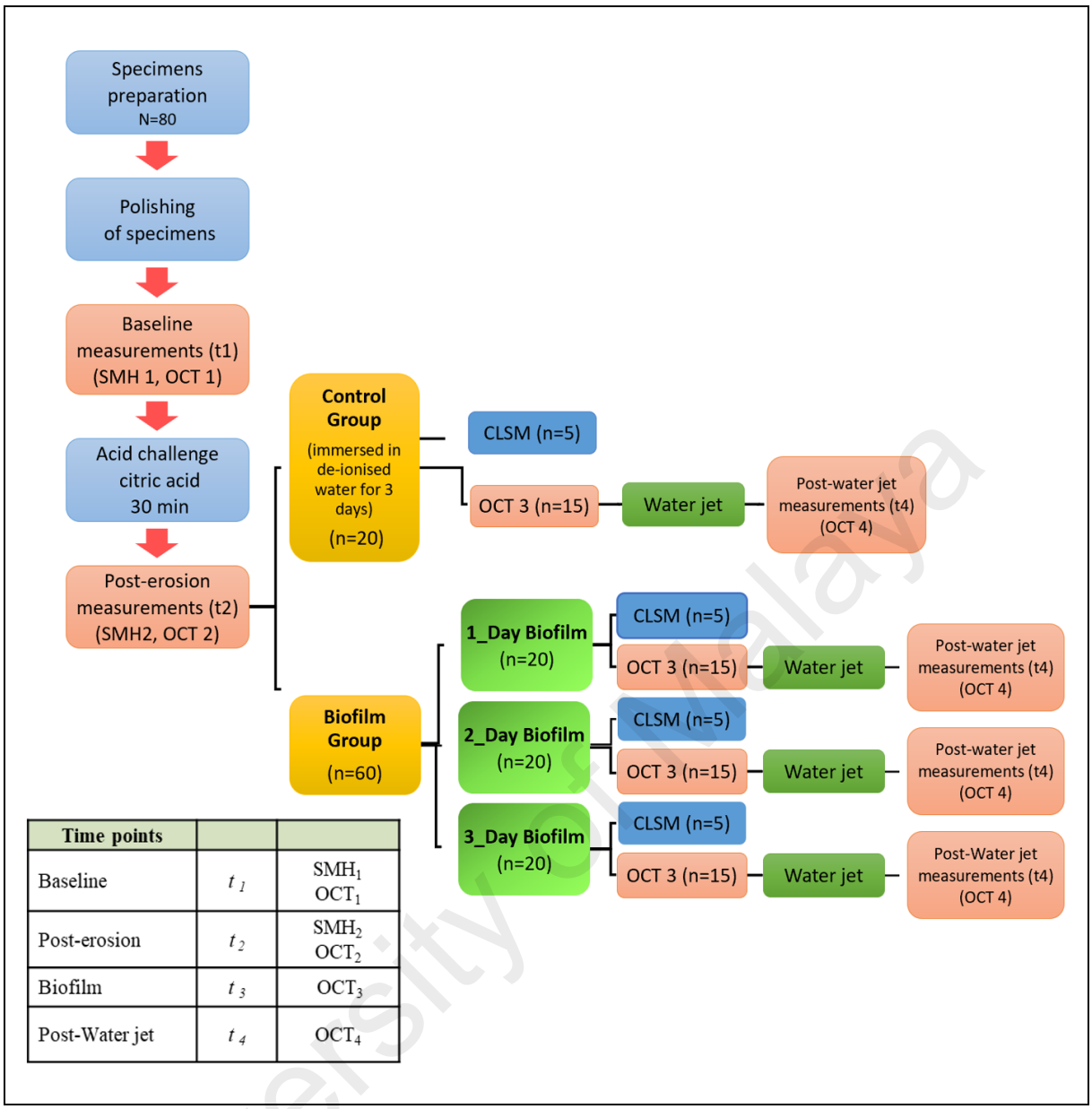

Time points		
Baseline	t_1	SMH_1 OCT_1
Post-erosion	t_2	SMH_2 OCT_2
Biofilm	t_3	OCT_3
Post-Water jet	t_4	OCT_4

Figure 4.5: Flowchart of the study design.

4.4 Results

4.4.1 Softening of enamel surface using citric acid

After the acid challenge, the mean reduction in SMH was 137.6 ± 19.03 KHN (**Table 4.4)** which amounts to a mean fractional change of -0.49 ± 0.16 of Δ*SMC* (t_2) (**Table 4.5**). Repeated measures ANOVA showed that there was a statistically significant difference in the mean surface microhardness ($p < 0.05$) after acid challenge in citric acid, as shown in **Table 4.4** and **Figure 4.6**. Thus, the protocol used was able to induce softening of enamel surface as there was a significant reduction in SMH ($p < 0.05$).

Table 4.4: Results of repeated measures ANOVA for SMH, showing the p-values between time points (n=15).

		Pairwise Comparisons		
		Surface Microhardness (KHN)		
Time points		Mean Difference	Std. Error	P-value
Baseline (t_1)	Post-erosion (t_2)	-137.60	19.03	< 0.001
Post-erosion (t_2)	Post-water jet (t_4)	11.78	9.32	0.68

Table 4.5: Mean values of fractional changes (*ΔSMC* ± SD) and (Δ*D* ± SD) for enamel specimens (control group) at each time point (t_2 and t_4).

		Post-erosion (t_2)	**Post-Water jet** (t_4)
Fractional Change	*ΔSMC* ± SD	-0.49 ± 0.16	0.14 ± 0.35
	ΔD ± SD	-0.08 ± 0.33	0.05 ± 0.19

Table 4.6: Results of repeated measures ANOVA for enamel thickness, showing the P-values between time points (n=15).

		Pairwise Comparisons		
		Enamel Thickness (*μm*)		
Time points		Mean Difference	Std. Error	P-value
Baseline (t_1)	Post-erosion (t_2)	-55.14	24.80	0.13
Post-erosion (t_2)	Post-water jet (t_4)	10.29	15.08	1.00

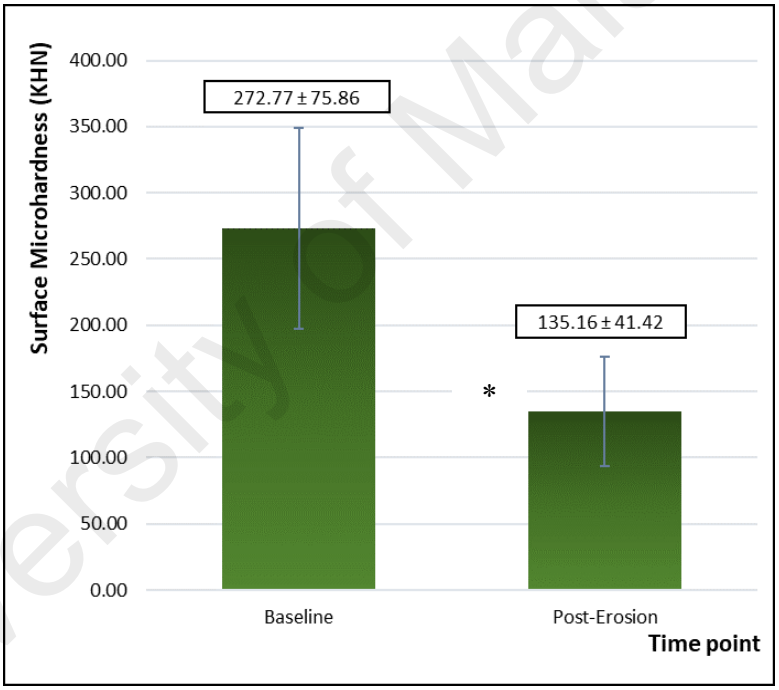

Figure 4.6: Surface microhardness of enamel before and after acid challenge.

Mean SMH (KHN) ± SD, for enamel specimens in the control group (n=15) at baseline and post-erosion. Repeated measures ANOVA showed significant difference in the SMH of enamel before and after acid challenge (* significant difference at $p < 0.05$).

Table 4.7: Tests of Within-Subjects Effects Table – control group

Tests of Within-Subjects Effects

Measure: MEASURE_1

Source		Type III Sum of Squares	df	Mean Square	F	Sig.	Partial Eta Squared
Time	Sphericity Assumed	174525.781	2	87262.890	43.889	.000	.758
	Greenhouse-Geisser	174525.781	1.376	126792.835	43.889	.000	.758
	Huynh-Feldt	174525.781	1.477	118149.680	43.889	.000	.758
	Lower-bound	174525.781	1.000	174525.781	43.889	.000	.758
Error(Time)	Sphericity Assumed	55670.960	28	1988.249			
	Greenhouse-Geisser	55670.960	19.270	2888.922			
	Huynh-Feldt	55670.960	20.680	2691.991			
	Lower-bound	55670.960	14.000	3976.497			

A repeated measures ANOVA with a Greenhouse-Geisser correction showed that the mean values for SMH was statistically significantly different ($F(1.376, 19.270) = 43.889$, $p < 0.05$) for control group (n=15).

Table 4.8: Pairwise Comparisons Table – Control group

Pairwise Comparisons

Measure: MEASURE_1

(I) Time	(J) Time	Mean Difference (I-J)	Std. Error	Sig.[b]	95% Confidence Interval for Difference[b] Lower Bound	Upper Bound
1	2	137.604*	19.026	.000	85.895	189.313
	3	125.823*	18.612	.000	75.242	176.405
2	1	-137.604*	19.026	.000	-189.313	-85.895
	3	-11.781	9.322	.681	-37.116	13.555
3	1	-125.823*	18.612	.000	-176.405	-75.242
	2	11.781	9.322	.681	-13.555	37.116

Based on estimated marginal means

*. The mean difference is significant at the .05 level.

b. Adjustment for multiple comparisons: Bonferroni.

This table presents the results of the Bonferroni post hoc test, which allows to discover which specific means differed. It can be seen that there was a significant difference in SMH between t_1 and t_2 ($p < 0.05$), in control group (n=15).

4.4.2 Enamel thickness following the application of dental water jet

After the acid challenge, the mean reduction in enamel thickness was 55.14 ± 24.80 μm (Table 4.6), which amounts to a mean fractional change of -0.08 ± 0.33 of ΔD (t_2) (**Table 4.5**). After the applications of dental water jet, the mean difference in enamel thickness obtained from the OCT A-scans was 10.29 ± 15.08 μm (**Table 4.6)**, which amounts to a mean fractional change of enamel thickness ΔD (t_4), was 0.05 ± 0.19, (Table 4.5). However, repeated measures ANOVA showed that the difference in the mean enamel thickness was not statistically significant ($p > 0.05$) between all groups (**Table 4.6** and **Figure 4.7**).

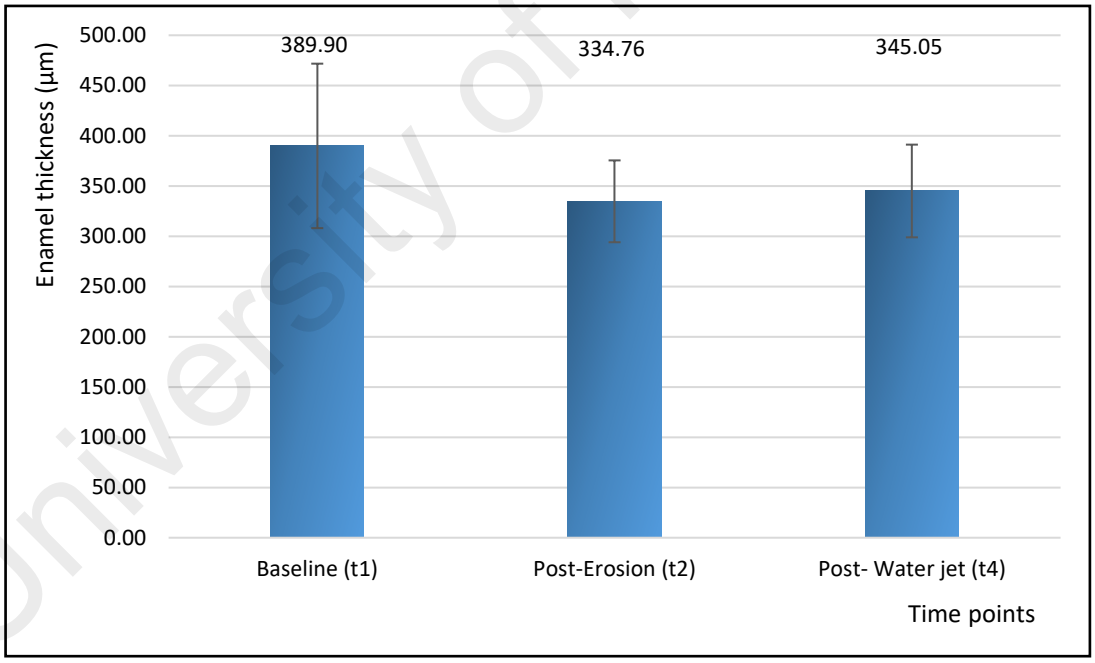

Figure 4.7: Enamel thickness at baseline, post-erosion, and post-water jet time points.

Mean values of enamel thickness (μm) ± SD, for enamel specimens in the control group (n=15) at baseline(t_1), post-erosion (t_2) and post-water jet (t_4). Repeated measures ANOVA showed no significant difference of the enamel thickness at three consecutive time points ($p > 0.05$).

4.4.3 The ability of dental water jet in removing laboratory-cultivated biofilm on acid-induced softened human enamel surface.

4.4.3.1 OCT - $IR_{biofilm}$

The mean values of $IR_{biofilm}$ before (t_3) and after water jet application (post-water jet, t_4) for all 4 groups are shown in **Figure 4.8**. Repeated measures ANOVA revealed that the $IR_{biofilm}$ mean values showed no significant different at t_3 compared to t_4 ($p > 0.05$) in all the groups **Table 4.9**, **Table 4.10** and **Table 4.11**.

A one-way ANOVA was conducted to compare the mean value of $IR_{biofilm}$ and the fractional changes of $IR_{biofilm}$ ($\Delta IR_{biofilm}$) between groups, after water jet application (t_4). The result showed that there was no statistically significant difference between groups at the $p > 0.05$ level; ($F(3,56) = 0.385$, $p = 0.764$) (**Table 4.13**).

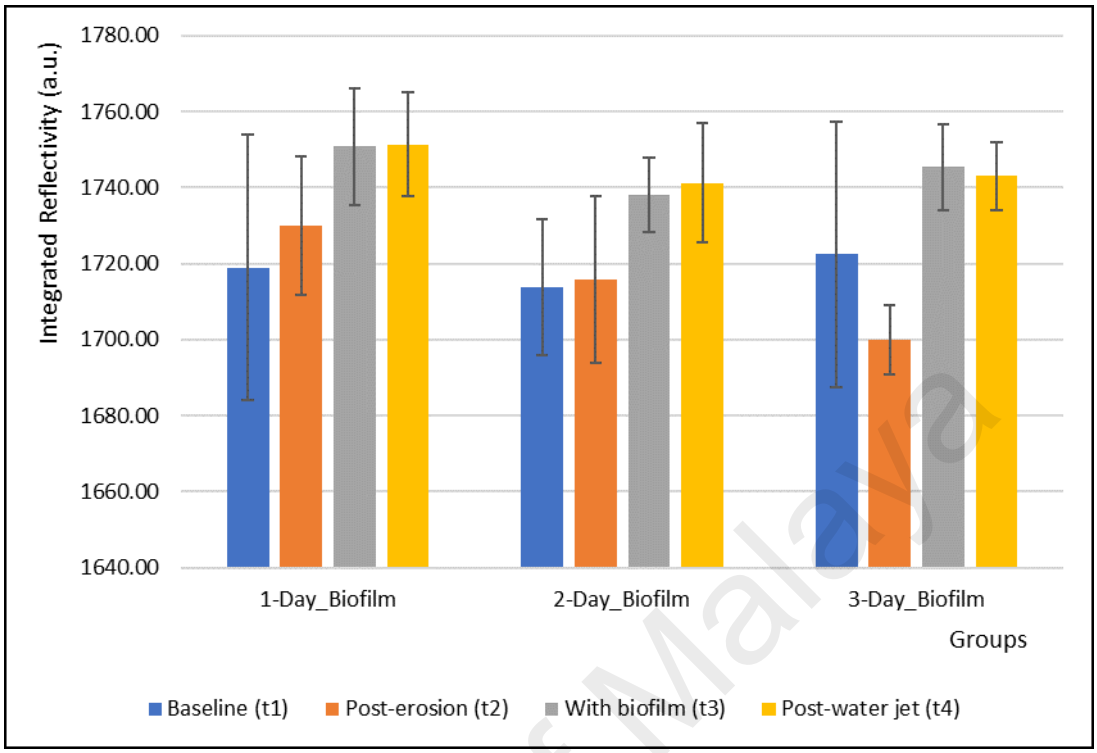

Figure 4.8: Integrated reflectivity of enamel at baseline, post-erosion, with biofilm and post-water jet

Mean $IR_{biofilm}$ ± SD at consecutive time points, from baseline until post-water jet following application of water jet (t_4) on acid-induced softened human enamel with 1, 2 and 3-day biofilm groups. Repeated measures ANOVA showed no significant difference in the $IR_{biofilm}$ of enamel before (t_3) and after the application of dental water jet (t_4) for all experimental groups.

Table 4.9: Pairwise Comparisons Table – 1-Day Biofilm group

Pairwise Comparisons

Measure: MEASURE_1

(I) Time	(J) Time	Mean Difference (I-J)	Std. Error	Sig.[b]	95% Confidence Interval for Difference[b] Lower Bound	Upper Bound
1	2	-10.904	10.384	1.000	-42.769	20.961
	3	-31.771	10.883	.067	-65.168	1.625
	4	-32.433*	8.589	.012	-58.790	-6.075
2	1	10.904	10.384	1.000	-20.961	42.769
	3	-20.867*	5.494	.012	-37.728	-4.007
	4	-21.529*	4.564	.002	-35.535	-7.522
3	1	31.771	10.883	.067	-1.625	65.168
	2	20.867*	5.494	.012	4.007	37.728
	4	-.661	5.446	1.000	-17.374	16.051
4	1	32.433*	8.589	.012	6.075	58.790
	2	21.529*	4.564	.002	7.522	35.535
	3	.661	5.446	1.000	-16.051	17.374

Based on estimated marginal means

*. The mean difference is significant at the .05 level.

b. Adjustment for multiple comparisons: Bonferroni.

This table presents the results of the Bonferroni post hoc test, which allows to discover which specific means differed. It can be seen that there was no significant difference in $IR_{biofilm}$ between t_3 and t_4 ($p > 0.05$), in 1-Day biofilm group.

Table 4.10: Pairwise Comparisons Table – 2-Day Biofilm group

Pairwise Comparisons

Measure: MEASURE_1

(I) Time	(J) Time	Mean Difference (I-J)	Std. Error	Sig.[b]	95% Confidence Interval for Difference[b] Lower Bound	Upper Bound
1	2	-1.887	6.510	1.000	-21.865	18.092
	3	-24.135*	4.715	.001	-38.606	-9.665
	4	-27.311*	6.446	.005	-47.093	-7.530
2	1	1.887	6.510	1.000	-18.092	21.865
	3	-22.249*	5.839	.011	-40.166	-4.331
	4	-25.425*	8.164	.046	-50.479	-.371
3	1	24.135*	4.715	.001	9.665	38.606
	2	22.249*	5.839	.011	4.331	40.166
	4	-3.176	4.031	1.000	-15.545	9.193
4	1	27.311*	6.446	.005	7.530	47.093
	2	25.425*	8.164	.046	.371	50.479
	3	3.176	4.031	1.000	-9.193	15.545

Based on estimated marginal means

*. The mean difference is significant at the .05 level.

b. Adjustment for multiple comparisons: Bonferroni.

This table presents the results of the Bonferroni post hoc test, which allows to discover which specific means differed. It can be seen that there was no significant difference in $IR_{biofilm}$ between t_2 and t_3 ($p > 0.05$), in 2-Day biofilm group.

Table 4.11: Pairwise Comparisons Table – 3-Day Biofilm group

Pairwise Comparisons

Measure: MEASURE_1

(I) Time	(J) Time	Mean Difference (I-J)	Std. Error	Sig.[b]	95% Confidence Interval for Difference[b]	
					Lower Bound	Upper Bound
1	2	22.509	9.962	.242	-8.061	53.079
	3	-22.973	9.281	.160	-51.455	5.508
	4	-20.561	9.097	.242	-48.478	7.355
2	1	-22.509	9.962	.242	-53.079	8.061
	3	-45.483*	3.421	.000	-55.981	-34.984
	4	-43.071*	2.772	.000	-51.577	-34.564
3	1	22.973	9.281	.160	-5.508	51.455
	2	45.483*	3.421	.000	34.984	55.981
	4	2.412	1.433	.686	-1.984	6.808
4	1	20.561	9.097	.242	-7.355	48.478
	2	43.071*	2.772	.000	34.564	51.577
	3	-2.412	1.433	.686	-6.808	1.984

Based on estimated marginal means

*. The mean difference is significant at the .05 level.

b. Adjustment for multiple comparisons: Bonferroni.

This table presents the results of the Bonferroni post hoc test, which allows to discover which specific means differed. It can be seen that there was no significant different in $IR_{biofilm}$ between t_3 and t_4 ($p > 0.05$), in 3-Day biofilm group.

Table 4.12: Descriptive Table - One-way ANOVA of Δ $IR_{biofilm}$.

Descriptives

d_IR_biofilm_t4

	N	Mean	Std. Deviation	Std. Error	95% Confidence Interval for Mean		Minimum	Maximum
					Lower Bound	Upper Bound		
CONTROL	15	.000618	.0063280	.0016339	-.002887	.004122	-.0199	.0083
1 DAY	15	.000448	.0119740	.0030917	-.006183	.007079	-.0241	.0179
2 DAY	15	.001843	.0089592	.0023133	-.003119	.006804	-.0137	.0215
3 DAY	15	-.001372	.0031706	.0008186	-.003128	.000384	-.0068	.0040
Total	60	.000384	.0081422	.0010512	-.001719	.002488	-.0241	.0215

Table 4.13: One-way ANOVA of Δ $IR_{biofilm.}$

ANOVA

d_IR_biofilm_t4

	Sum of Squares	df	Mean Square	F	Sig.
Between Groups	.000	3	.000	.385	.764
Within Groups	.004	56	.000		
Total	.004	59			

This table presents the results of the one-way ANOVA of IR_{sub} at t_3. There was no statistically significant different between groups, ($F(3,56) = 0.385$, $p > 0.05$).

4.5 Discussion

4.5.1 Preparation of enamel surface

This section discusses the rationale of methods used in the experiments and significant results observed from research objectives. The current study model was designed to simulate the clinical stages of initial enamel erosion where the degree of demineralisation incurred in the present study was small, only involving surface-softening with no evidence of surface loss or step change of more than 10 μm as observed in the B-Scans of OCT at the end of the erosion interval.

Many studies have examined the erosive potential of foodstuffs and beverages, but different protocols have been used (Gonzalez-Aragon Pineda, Borges-Yanez, Irigoyen-Camacho, & Lussi, 2019; E. Santos et al., 2019).Various *in vitro* studies have immersed teeth in different types of acidic challenges and using different time durations (usually a prolonged period of time). Although these *in vitro* studies provided information on the erosive potential of these drinks, it exaggerated the erosive effect due to the absence of modifying influence of saliva.

In this study, the enamel surface was ground and polished, removing the outermost enamel layer. The outermost layer of enamel is hyper-mineralised by fluoride and saliva during the de- and remineralisation processes (Cardoso, Magalhaes, Rios, & Lima, 2009). The removal of the outer enamel reduces the variation among the specimens (Ganss et al., 2000).

4.5.1 Acid challenge

It is known that acid softened enamel has an increased risk of being abraded and attrited. An *in-situ* study reported that, softened bovine enamel surface was easily removed when subjected to mechanical abrasive forces from toothbrushing (Rios,

Honorio, Magalhaes, Buzalaf, et al., 2006) whilst another *in situ* study showed that the mean surface loss of softened human enamel specimens could reach 0.258 μm after abrasion (Jaeggi & Lussi, 1999) However, no one to date have reported on the effect of water jet on softened enamel surface.

Oliveira et al. (2017) justified that in the process of the initial lesion, corresponding to the phase of enamel softening, the hardness decreased because of the loss of tooth minerals. The subsequent prolonged challenge results in substance loss, with the remaining superficial enamel becoming softened (Brevik, Lussi, & Rakhmatullina, 2013). By continuing with the acid challenge, this softened layer reaches balance and does not progress, but enamel structure is still lost (Shellis et al., 2013).

A 30-min acid exposure was chosen for this study, in order to make sure that signals will be picked up in OCT, although it has been reported that changes could already be seen after 10 min of acid challenge (Chew, 2013; Chew et al., 2014).

4.5.2 Surface Microhardness

This study showed that there was a slight increase in the mean surface microhardness value of the softened enamel. This may be suggestive that there had been some surface loss of the softened surface layer and the hardness measurement was that of the underlying layer which is less demineralised. However, the increase was not statistically significant. This finding is supported by the result of enamel thickness whereby the mean values were not significantly different before and after water jet application.

Studies have shown that the hardness test is an adequate method to evaluate the initial softening of enamel surface (Hara & Zero, 2008; Stenhagen, Hove, Holme, Taxt-Lamolle, & Tveit, 2010). Thus, in this study, the initial stage of enamel erosion was established based on SMH measurement. Softening, i.e. loss of hardness is measured by

the resistance of a substrate to the penetration of an indenter. Indentation techniques have been used extensively to investigate enamel erosion by measuring the hardness of the enamel surface. Microhardness is measured with either a Knoop or a Vickers diamond indenter, which are rhomboidal and tetra-pyramidal, respectively. The Knoop or Vickers hardness numbers are calculated from the length of the indentation and the applied load.

The Knoop diamond penetrates sound enamel by about 1.5 μm, while that of Vickers would penetrate about 5 μm given the usual loads (Featherstone, 1992) of 50 g and 200 g, respectively. Therefore, it can be speculated that Knoop hardness is more sensitive to changes in the most superficial layer of an erosive lesion (Schlueter et al., 2011).

The erosive effect was confirmed by a softening of the enamel surface, which presented a decrease in KHN mean value, resultant from the mineral loss caused by acid challenge. The measurement of the softened enamel surface was assessed by SMH rather than profilometry (Attin, 2006). The latter measures material loss, and is most suitable for erosion at more advanced stages (Barbour & Rees, 2004).

SMH was chosen as the established assessment technique for initial erosion because it has been shown that SMH is sensitive in detecting the initial stages of erosions with softening of the enamel surface although it has limitations in the analysis of advanced lesions with substance loss (Hara & Zero, 2008; Jaeggi & Lussi, 1999). Therefore, SMH was chosen as the established assessment technique for initial erosion.

In early stages of erosion, calcium dissolution typically results in enamel surface softening (Attin, Meyer, Hellwig, Buchalla, & Lennon, 2003; Barbour, Parker, & Jandt, 2003) and this can be measured through the substrate resistance to the pressure exerted by a Knoop and Vickers indenter. Meredith, Sherriff, Setchell, and Swanson (1996), reported that the Knoop has been the most popular method. Knoop indentation is longer

and shallower compared to Vickers indentation, so a load impression can be applied to brittle materials without the risk of cracking. Furthermore, the longer diagonal is easier to read than the short diagonal of the Vickers. The Knoop indenter is also more sensitive to changes in the superficial layer of the erosive lesion (Schlueter et al., 2011) and for this reason, the Knoop indenter was used in this study.

It is therefore assumed that the susceptibility of enamel to erosive subsurface softening may depend on the hardness of the particular enamel specimen. In order to minimize the influence of different enamel hardness values on the outcome of an erosion experiment, Attin et al. (1997) recommended following the advice of Lussi et al. (1995) who suggested a procedure for evenly distributing enamel specimens with respect to hardness among various experimental groups.

Sahyoun (2016), found that changes in OCT signal were correlated with microhardness changes. However, the strength of this correlation was not strong. The hardness value of enamel has been reported in the range of 314 to 361 KHN (Jennett et al., 1994)or 322 to 353 VHN (Lupi-Pegurier, Muller, Leforestier, Bertrand, & Bolla, 2003). However, in this study, lower mean values of microhardness at baseline, were obtained. This broad variation of microhardness values may be due to factors such as specimen preparation, diagonal length reading error (Gutiérrez-Salazar & Reyes-Gasga, 2003), variation in chemical composition (Braly, Darnell, Mann, Teaford, & Weihs, 2007), age and the enamel surface location within the tooth (Park, Wang, Zhang, Romberg, & Arola, 2008). Hence, no attempt was made to correlate the hardness values to OCT findings.

In this study, it was shown that the application of dental water jet has no effect on the surface microhardness of softened enamel surface which means that the mean value of microhardness of eroded enamel did not changed significantly and remained almost the same although in terms of its actual mean value, it had slightly increased. This may

suggest that the softened surface layer may had been partially lost and the measurement of the hardness was being made on the underlying layer (de Alencar et al., 2014). Furthermore, if there was a significant increase in the microhardness value, the indentation may have been made in an underlying layer or on a 'fresh' enamel layer where all softened enamel layer had been totally removed, similar to the condition at baseline. However, this is not the case in this study whereby the enamel thickness result would justify this finding. When the microhardness value remained similar, it can be hypothesized that the condition of existing softened enamel after acid challenge had not changed after the application of water jet. Furthermore, the pressure induced by water jet may not be as high as toothbrushing (Addy, 2005) which may explain the non-significant loss of softened enamel layer.

4.5.3 OCT

4.5.3.1 Enamel thickness

Several studies have used OCT to measure enamel thickness (Algarni et al., 2016; Chan et al., 2013; C. H. Wilder-Smith et al., 2009) either by visually assessing the cross-sectional images (B-scans) or by using the depth-resolved intensity profile (A-scans). C. H. Wilder-Smith et al. (2009) monitored over 3 weeks the erosive wear of patients having Gastroesophageal Reflux Disease (GERD) *in vivo,* by measuring the distance of the enamel surface to the DEJ on OCT B-Scans generated by a swept-source OCT. They found that the imaging depth was more than adequate to measure the full enamel thickness and the DEJ served well as accurate baseline reference. However, Chan et al. (2013) when attempting to measure enamel thickness of eroded enamel *in vitro* with PS-OCT, by comparing the heights of the demineralised windows and laser-irradiated regions to the surface protected ends of the sample on the B-scans, found that the increase in scattering

due to subsurface demineralisation or surface roughness limited the ability to resolve the DEJ. This particular problem was not encountered in this study as the DEJ was clearly noted with difference in intensity. The contradictory findings between C. H. Wilder-Smith et al. (2009) and Chan et al. (2013) were most likely due to the difference in severity of subsurface demineralisation in these two studies. The level of demineralisation *in vivo* is known to be lower than that induced *in vitro* due to the remineralisation effect of saliva. In addition to that, Chan et al. (2013) exposed their specimens to acid for 12 hours which would have resulted in severe demineralisation which in turn would have caused high scattering at the immediate subsurface.

Recently, Algarni et al. (2016) measured enamel thickness with OCT A-scans by measuring the distance between the coordinates of the first peak and that of the second peak, where the first peak represents the enamel surface and the second peak represents the most evident change in reflectivity between enamel and dentine, near the DEJ area. They validated it against micro-computed tomography and histology and found good agreement between the measurements made with the three equipment. However, they noted that there was some degree of subjectivity in the protocol of determining the second peak. In order to reduce this subjectivity, an additional criterion was added in this study where the second peak (I_2) is established as the peak that immediately follows the lowest point of attenuation after the first peak (I_1) (**Figure 4.4**).

It was verified that stronger optical attenuation for demineralised specimens, was due to the increase of inter-crystalline spaces in the enamel structure and the disorganization of the prismatic structures, both promoted by the demineralisation process (Cara, Zezell, Ana, Maldonado, & Freitas, 2014).

4.5.3.2 Integrated Reflectivity

The capacity of water jet to remove biofilm by was estimated from the $IR_{biofilm}$ which in this case represents the biofilm accumulation over the tooth surface (supra), before and after water jet application. The results showed no significant difference in $IR_{biofilm}$, before and after water jet application in all the groups. The concept of water jet used in this study was based on the usage of oral irrigator as an adjunct to tooth brushing for biofilm control. The adjunctive aid of the oral irrigator is designed to remove biofilm and soft debris through the mechanical action of a jet stream of water of a set pressure. The pressure exerted from the unit varies between the water jet devices, ranging from 10 - 120 psi (Macpherson, 2012). Kato et al. (2012) evaluated plaque biofilm removing capacity of the dental water jet using a new method, electron-probe microanalyzer (EPMA) to measure biofilm thickness. They reported that approximately 85% of biofilm biofilms could be removed by vertical irrigation with water pressures exceeding 50.8 psi. In this study, it was shown that there was no significant difference in $IR_{biofilm}$ after water jet application. However, this result was purely based on $IR_{biofilm}$ quantifiable value. It would probably be more justifiable and worthwhile to investigate further the thickness of the biofilms using CLSM, in order to justify the application of the device successfully as an adjunct for biofilm control and relate it with OCT $IR_{biofilm}$ values. Nonetheless, the insignificant removal could be due to the number of dental water jet applications itself, where in this study, it was applied only once prior to OCT scanning. An oral irrigator device has demonstrated its effectiveness in decreasing the dental plaque, when used on a daily basis rather than a one-off application (Al-Mubarak et al., 2002). Furthermore, Barnes, Russell, Reinhardt, Payne, and Lyle (2005) reported that a dental water jet paired with either manual or sonic toothbrushing showed a greater reduction in biofilm removal compared with manual toothbrushing or flossing alone.

4.6 Conclusions

1. The application of dental water jet did not significantly cause enamel surface loss of acid-induced softened human enamel; thus, the null hypothesis was accepted.

2. The dental water jet could not significantly remove laboratory-cultivated biofilm on acid-induced softened human enamel; thus, the null hypothesis was accepted.

CHAPTER 5: *IN VIVO* EVALUATION OF INITIAL ENAMEL EROSION USING OPTICAL COHERENCE TOMOGRAPHY (OCT)

5.1 Introduction

This chapter aimed to use the findings from the previous *in vitro* studies to design and conduct a clinical investigation on the detection of initial enamel erosion. It has been a clinical concern that very early signs of erosive tooth wear could not be detected. To date, there is no clinically accepted technique in detecting and measuring initial enamel erosion *in vivo*.

Dental erosion is defined as a chemical process that involves the dissolution of enamel and dentine by acid not derived from bacteria (M. J. Larsen, 1990). Its initial stage involves the softening of enamel due to the increase in porosity of the tooth surface, and if the condition occurs in combination with other mechanical factors such as abrasion and attrition, it will result in pathological wear of the tooth. Although the terms dental erosion and dental erosive wear are often considered synonymous, in this thesis/chapter the term 'erosive wear' will be referred to the erosion-facilitated wear while, erosion will be confined to the chemical process as defined above.

It is well understood that in the clinical condition, erosive tooth wear is known to have a multifactorial aetiology (Young et al., 2008). In addition to the limitations in the clinical detection of signs of 'purely' erosive wear, this suggests that types of wear are not mutually exclusive, but rather reflect overlapping zones in a broader aetiological range.

New methods are needed for the non-destructive measurement of tooth demineralisation and remineralisation in order to monitor the progression of enamel erosion for effective non-surgical intervention and to evaluate the performance of anti-

erosive treatments. A non-destructive, quantitative method of monitoring initial erosion *in vivo* with high sensitivity would be invaluable for use in short-term clinical trials for various anti-erosive agents such as fluoride dentifrices.

Initial erosion causes a change in the optical scattering properties of enamel/dentine and attempts have been made to quantify these changes with OCT. OCT is uniquely capable of this task since it provides a measure of the reflectivity from each layer of the lesion and is able to resolve the formation of remineralised zones of increased mineral density and reduced light scattering. Furthermore, OCT is not only valuable as a non-destructive tool for the assessment of anti-erosive agents *in vivo* but is also valuable for *in vitro* studies as well since it does not require thin sectioning of the tooth, and it can be carried out rapidly. OCT typically produces vast volumes of data and methods are needed for analysis and quantifications.

OCT performs cross-sectional imaging by measuring the magnitude and echo time delay of backscattered light from a tissue. It enables non-invasive 'optical biopsies' to be taken from a tissue by illuminating it with a broadband light source. The intensity of the reflected light can then be measured from the resulting A-scans and also recorded for image processing by generating the B-scans.

5.1.1 Clinical relevance

The rate and severity of erosive wear depends on the amount of interactions between several chemical, biological and behavioural factors. Although some of these factors may be modelled *in vitro* or *in situ* to some degree, all factors actually interact and contribute to the clinical manifestation of erosive wear, *in vivo*. Therefore, for the final validation of the results of *in vitro* and *in situ* study designs, clinical studies using the natural dentition of appropriate study populations are necessary and are more relevant in terms of understanding the true process occurring in the oral cavity.

At the present time, dental practitioners normally estimate tooth wear by comparing sequential study casts taken over long period of time (Pretty et al., 2004). This method may satisfy most clinical demands in making decision whether the patient requires restoration or prevention counselling. However, more accurate methods may be useful in the detection of initial signs of tooth erosion, so that preventive treatment can begin immediately.

Quantitative methods such as ultrasound, profilometry, and quantitative light-induced fluorescence (QLF) have been suggested by different researchers as potential tools for diagnosing dental erosion more accurately (Moazzez, Bartlett, & Anggiansah, 2004). However, most of these methods have not yet been tested clinically or *in vivo*. Further research will determine whether they are suitable for measurement of tooth wear *in vivo* and thus, whether they should be recommended for use in a clinical trials or settings.

OCT has been reported to have a significant potential in detecting the earliest signs of enamel erosion (Huysmans et al., 2011), such as mineral loss (Chew et al., 2014) or changes in surface texture (Austin, Giusca, Macaulay, Moazzez, & Bartlett, 2016) prior to further loss of tissue. Although, there have been significant *in vitro* developments for the detection of early erosion using OCT (Chew et al., 2014), early erosive wear remains a very challenging clinical condition to be detected *in vivo*. As a result, if OCT becomes available in clinical practice, it can help clinicians to differentiate between sound and eroded tissues. Furthermore, since OCT is well suited for measuring small dimensional changes on tooth surfaces it has great potential for monitoring the progression of tooth erosion.

There is currently no clinical tool that could objectively measure and monitor initial enamel erosion *in vivo* which could be useful in the assessment for erosion in a clinical trial. Therefore, the possibilities for the quantitative *in vivo* diagnosis of initial

enamel erosion and monitoring of the treatment efficiencies *in vivo* are very attractive long-term goals in dentistry. However, exposing natural dentition to acid attack would be an ethical issue, thus, strong evidence showing that the whole process is reversible and insignificant amount of enamel layer is removed during the erosive process, is important to support the *in vivo* part of this study. In order to receive an ethical approval for the next *in vivo* study, the data has to strongly support that the initial softening effect after acid exposure is clinically insignificant and could be reversed or remineralised either with an oral health care product or by exposure to saliva. Data supporting that initial softening of enamel surface after acid exposure is clinically insignificant and could be reversed or remineralised either with an oral health care product or by exposure to saliva is crucial to gain the ethical approval for the *in vivo* study.

5.2 Literature Review

5.2.1 Acid challenge

In vitro and *in situ* studies of initial erosion have used acidic challenges consisting of either plain citric acid, various acidic beverages such as soft drinks (Coca Cola or Sprite: pH 2.3–3.2), juices (orange, grapefruit, lemon or blackcurrant: pH 3–4), wines (pH 2.9– 4.2), acidic candies (pH 2.3–3.1) or sprays (pH 1.9–2.3) (Brand, Gambon, et al., 2009; Davis, Marshall, Qian, Warren, & Wefel, 2007) (Gambon, Brand, & Nieuw Amerongen, 2009). Hydrochloric acid (0.01 M HCl at pH 2.2) has been used in many studies of erosion caused by reflux or by vomiting which are often associated with eating disturbances (L. Hove, Holme, Ogaard, Willumsen, & Tveit, 2006; L. H. Hove, Holme, Young, & Tveit, 2007, 2008; L. H. Hove, Young, & Tveit, 2007).

Despite the many types of acid used in initial erosion studies, exposure variables such as time, volume, flow rate of solutions and consumption habits are probably the main source of variation among *in vitro* and *in situ* models evaluating initial erosion. In order to simulate the clinical situation as closely as possible, prolonged erosive exposure should be avoided, since the resulting eroded surface would irreversible and no longer retain the same susceptibilities to remineralisation or abrasion (Cheng et al., 2009; Field et al., 2010). On the other hand, the exposure time and acid challenge have to produce a change so that it can be measured by any chosen method.

In the mouth, the time span where the pH remains low is usually less than 2 min (Millward, Shaw, Harrington, & Smith, 1997) and similar exposure times should be followed by *in vitro* and *in situ* models to better simulate conditions *in vivo*, unless specific conditions are to be modelled, such as low salivary flow rates or extensive periods of exposure to acids. Some *in vitro* studies have indeed shown how the prolonged

exposure to acids modifies the eroded surface (Cheng et al., 2009), perhaps to an unrealistic condition, where a restoration need to be placed.

Some *in situ* studies have avoided the ethical problem of exposing test subjects to acids by performing the acidic challenge *ex vivo* whereby specimens were attached to removable intra-oral appliances and acid challenges were introduced outside the mouth. This approach has been commonly used in cyclic challenge studies resulting in tooth surface loss rather than just initial erosion. *In situ* studies on initial erosion generally involve short acid exposure times ranging from a single 15 s exposure and repeated consumption of acidic beverages to a period of up to 1 h. Furthermore, in many *in situ* study models, the test exposure is equivalent to a common acidic consumption in the population, and as such can be argued to be ethically unproblematic. Using an ex vivo design for the acidic challenge requires care in maintaining a clinically relevant acidic challenge. Ex vivo salivary pellicle formation is considered inappropriate as a relevant model in *in situ* studies.

In studies on the erosive potential of sucking acidic candies or lollipops, although the exposure time is much greater than that associated with drinking acidic beverages, higher salivary flow rates were reported, at least initially, with candies (Brand, Tjoe Fat, et al., 2009; Jensdottir, Nauntofte, Buchwald, & Bardow, 2005). Salivary clearance rate and the concentrations of buffers would be affected when there are changes in salivary flow rates.

5.2.2 Methods of acid exposure

In situ models involving specimens mounted in appliances have used either extra-oral or *in situ* acid challenge. The first type was presumably in most studies designed to avoid unnecessary acid exposure of the teeth of the test subjects. In these studies, the acid was often gently agitated during the exposure, but this was not always specified.

In order to study the detection of initial erosion *in vivo*, teeth have to be exposed to acidic environment. Activity such as swishing, sipping, rinsing of beverages, or either actively sucked or passively retained candies in the mouth may have to be employed in the study.

From clinical studies it can be estimated that enamel loss may reach values of 0.07–0.15 mm per year in patients with erosion (Bartlett, Blunt, & Smith, 1997; Milosevic, Young, & Lennon, 1994).

A method for clinical monitoring of dental erosion must fulfil several requirements. Firstly, it must allow the quantification of dental substance loss. As the amount of loss to be measured clinically is usually relatively small, the method must also be sensitive to avoid extended observation periods. Furthermore, it must be simple to perform and acceptable for patients; the equipment must be available in several centres and the procedure must be cost effective (Schlueter et al., 2005).

5.2.3 Methods of assessing erosion

To date, there is no *in vivo* dental tool available that can aid dental clinicians in diagnosing and monitoring the progression (or stabilization) of the erosive process reproducibly and quantitatively (Amaechi & Higham, 2005). The currently used methods for monitoring erosive tooth surface loss are sequential study casts (Wickens, 1999), silicone putty index (Shaw & Smith, 1999), photographs and erosive tooth surface loss indices (Bartlett et al., 2008; Eccles, 1979; I. B. Larsen et al., 2000; Linkosalo & Markkanen, 1985; O'Sullivan & Curzon, 2000a), which are subjective and are not reproducible and do not measure enamel at a submillimetre level. Laboratory based methods, such as profilometry (Bartlett, Bureau, & Anggiansah, 2003), are costly and cannot be used in the dental surgery. Profilometry also requires an impression of the teeth

from which replicas are made, but it has been found that impressions can lead to inaccurate measurements (Rodriguez & Bartlett, 2011).

A method for clinical assessment or monitoring of tooth erosion must fulfil several requirements. Firstly, it must allow the quantification of dental substance loss. As the amount of loss to be measured clinically is usually relatively small, the method must also be sensitive to avoid extended observation periods. Furthermore, it must be simple to perform and acceptable for patients; the equipment must be available in several centres and the procedure must be cost effective (Schlueter et al., 2005).

The complexity of the chemical, biological and behavioural modulating factors for dental erosion, makes the predictive validity of *in vivo* when assessing interventions. Studies under natural oral conditions, on real people using their natural teeth, would be the most ideal, however, such studies are challenging, and difficult to perform especially in terms of standardisations of study specimens.

At present, the clinical trials involving dental erosion are of the '*in situ'* design where subjects had to wear appliances with embedded enamel or dentine. The '*in situ*' design has added cost, is uncomfortable to the subject and affects the salivary flow rate of the subjects due to the presence of an appliance in the mouth.

When erosion is induced intra-orally, the dentition of the subjects is also exposed to the acidic challenge and hence is also being eroded. This is not ethically permissible especially if the expected degree of erosion is high. Studies that had adopted this study design either chose to monitor the net bulk loss of the specimens and drop subjects that demonstrated more than 200 μm of surface loss from the study and remineralisation intervention put in place (S. Hooper et al., 2004) or to use a detection method that is sensitive to the very early stages of erosion when surface loss has not occurred and remineralisation of the eroded teeth was possible. Austin et al. (2017) reported an *in vivo*

study, no oral appliances were used, and all acid challenges and measurements were done intra-orally on natural teeth.

For assessing erosion in isolation from erosive wear, two approaches might be employed: measurement of the amount of calcium released by an acid challenge, or quantification of changes in the optical characteristics, roughness or hardness of the partially demineralised surface (Huysmans et al., 2011).

5.2.3.1 Dissolved or mobilised mineral

Interventions that modulate the effects of acid dissolution by modifying the tooth surface, e.g. through incorporation of fluoride or other ions, buffering acid or protecting the tooth surface, might be assessed by chemical analysis of enamel dissolution.

Calcium analysis of the run-off solution provides a direct measure of the amount of enamel dissolution as reported by Young, Thrane, Saxegaard, Jonski, and Rolla (2006), where labial surfaces of anterior teeth of healthy subjects were exposed to short, mild acid challenges (5 ml of 0.01 mol/l citric acid was dripped onto the tooth surface for about 50 s). Although the study may be a true clinical model, several key factors in clinical erosion and erosive wear were not taken into account. Most importantly, the acid challenge was unnatural, where the natural mouth physiology of saliva and soft tissue were excluded.

5.2.3.2 Optical detection of surface demineralisation

Developing instruments that can quantify subtle surface changes, such as early demineralisation and erosive softening *in vivo*, are extremely challenging. Such instruments need to be able to assess the natural enamel surface with its intrinsic curvature and the natural dentine surface with its persistent demineralised organic matrix. In addition, when small amounts of mineral loss are to be monitored, the tooth surface

should be placed in as reproducible a position as possible for measurement, because surfaces are often inhomogeneous (Huysmans et al., 2011).

In general, possible methods of qualitatively assessing early stage of erosion are based on the optical properties of enamel or dentine. The principle of these methods is that after erosion the tooth surface is roughened and porous, and thus will scatter more light and transmit less compared to sound tissue. Methods such as laser light backscattering, previously investigated for the detection and measurement of early caries lesions, might also be applicable to dental erosion (Angmar-Mansson & ten Bosch, 1987). However, currently, the two most promising methods of assessing the surface characteristics of enamel *in vivo* are quantitative light-induced fluorescence (QLF) and optical coherence tomography (OCT).

i. **Quantitative Light-Induced Fluorescence (QLF)**

QLF is a non-invasive optical technique initially developed for *in vivo* measurement of early caries (E. de Josselin de Jong et al., 1995) and since then, it was used extensively for caries investigation and to a lesser extent fluorosis (Pretty et al., 2006). In order for the method to be used to measure erosion, an area with little or no surface scattering needs to be employed as a reference area to calculate relative loss of fluorescence (ΔF) in the test area. In practice, this might be achieved by either protecting part of the surface prior to erosion or alternatively it might be possible to use a fluid, e.g. water, which will reduce scattering in the reference area.

Pretty et al. (2004) demonstrated the ability of QLF to detect and longitudinally monitor erosion on unpolished enamel surfaces subjected to 30-min intervals of erosion for up to 15 h. Elton et al. (2009) concluded that QLF is reliable for shallow erosive lesions but becomes less consistent as erosion advances. QLF may have the potential to measure early erosion *in vivo*, particularly in its earlier stages prior to surface loss.

ii. **Optical Coherence Tomography (OCT)**

Optical coherence tomography (OCT) is an imaging modality that is analogous to ultrasound imaging but uses light instead of sound. Cross-sectional images are generated by measuring the echo time delay and intensity of light that is reflected or backscattered from internal structures in tissue (J. G. Fujimoto, 2003; D. Huang et al., 1991). Optical coherence tomography improves localization of the returned signal origin due to the much shorter wavelength of the imaging light when compared with ultrasound; hence, OCT offers significantly improved resolution. As the speed of light does not allow direct measurement of the echo time delay, interferometric techniques have been developed to analyse the reflected light signal.

OCT has been developed rapidly in recent years in terms of resolution, data acquisition speed, tissue penetration, contrast enhancement and delivery systems for clinical application. The method provides cross-sectional imaging by measuring the magnitude and echo time delay of backscattered light. The increased porosity of demineralised enamel, compared to sound enamel, results in a change in optical property, and hence a difference in intensity of the reflected light can also be quantified and analysed (Amaechi, Podoleanu, et al., 2003; Popescu et al., 2008).

For dental erosion, the method is based upon quantitative measurements of the backscattered light intensity at the surface, which indicates surface porosity and also depth of penetration of the region of interest, which is reduced when surface scattering occurs. Using this approach, the increased porosity of demineralised enamel compared to sound enamel can be estimated. Recently, OCT was used to quantify demineralisation in an *in vivo* study of the effectiveness of a treatment for GERD (C. H. Wilder-Smith et al., 2009). A significantly reduced intensity of backscattered light was observed in the treatment group compared to the placebo group.

OCT provides real-time imaging and does not require specimen processing. It is non-invasive and can potentially measure both surface characteristics and quantitative loss of tooth structure. Ideally, as with other techniques of this type, accurate repositioning of the probe is required, so that the same area is measured at different time points. An area of no change may also be required for reference.

5.2.3.3 Evaluation of erosion and erosive wear

Depending on whether the aim is to study erosion (chemical process) or erosive wear (the multifactorial clinical condition), in general, two approaches in conducting clinical studies might be taken. Ideally, it would be desirable to test interventions on erosive wear, but this requires either complicated study design that takes into account multiple factors, or actual clinical trials with associated time consuming and high cost. As erosion precedes erosive wear and is assumed to be the overriding factor in erosive wear, studying erosion may be expected to contribute significantly to the knowledge and prevention of erosive wear.

5.2.4 Saliva

The biological factor that is well recognised as the most important in determining the rate of erosion is saliva. Studies have shown that erosion is strongly associated with low salivary flow and low buffering capacity (Jarvinen et al., 1991; Rytomaa et al., 1998). Saliva reduces the rate of erosion by clearing away the acid, buffering the causative acid and by promoting remineralisation of any demineralisation that might have occurred due to previous erosive attack or is currently occurring (Hara, Lussi, & Zero, 2006). Salivary calcium, phosphate, and fluoride ions can stop demineralisation and help hard dental tissue remineralisation (Filipi, Halackova, & Filipi, 2011). Therefore, the stimulation of salivary flow rate, for example, by chewing sugar-free chewing gum, can enhance this

salivary remineralising effect by an increase in bicarbonate buffer and salivary mineral content, which can facilitate mineral re-deposition onto the enamel surface, decreasing enamel loss (Dawes, 1969). In contrast, reduced salivary flow rate is a risk factor for erosive tooth wear. Flow rate can be reduced by, for instance high levels of exercise, systemic disease (e.g., Sjögren's syndrome), and certain medications (e.g., antihypertensives, antidepressants) (Carvalho et al., 2015).

In vivo, tooth surfaces are covered with an acquired salivary pellicle which helps to protect enamel from tooth erosion (Siqueira, Custodio, & McDonald, 2012). The pellicle acts as a diffusion barrier aiding the protection against demineralisation (Siqueira, Margolis, Helmerhorst, Mendes, & Oppenheim, 2010). The protective effect of the pellicle will largely depend on the strength and duration of the acidic challenge and, when evaluated *in vitro* or *in situ*, will be affected by the study design. For example, prolonged immersion in acid solutions may reduce the power of the study to detect a significant effect of the pellicle (Young & Tenuta, 2011). The salivary factors associated dental erosion is shown in **Figure 5.1**.

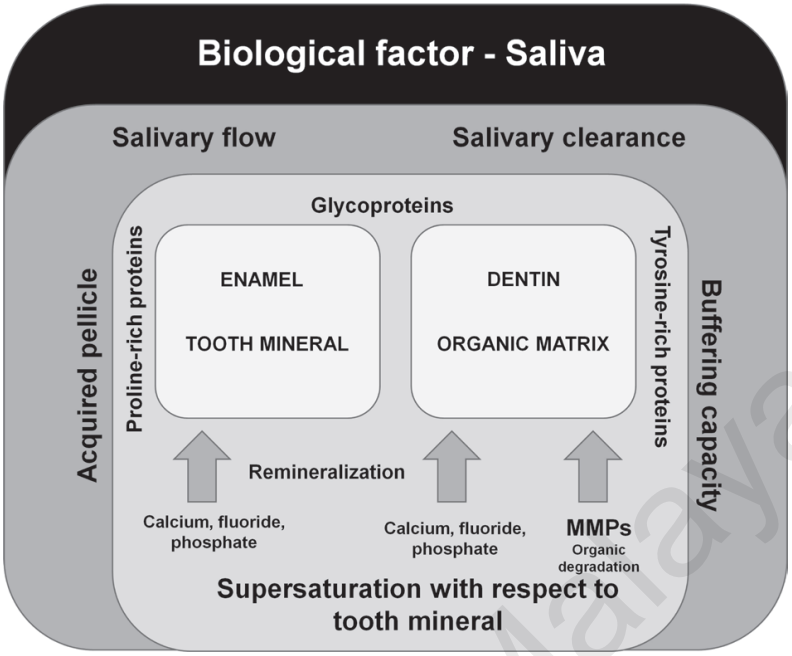

Figure 5.1: Salivary factors associated with the control of dental erosion in enamel and dentine (Adapted from (Buzalaf et al., 2012)).

5.2.5 Chewing gum in promoting remineralisation

Sugar-free chewing gum is known to be a useful adjunct to common oral hygiene because of the stimulation of salivary flow rate. Rios, Honorio, Magalhaes, Delbem, et al. (2006) showed that saliva stimulation by the use of sugar-free chewing gum promoted a remineralising action in the events of enamel erosion and abrasion. Furthermore, it has been shown to promote the remineralisation of enamel subsurface lesions *in situ* (Leach, Lee, & Edgar, 1989).

Stimulated saliva has an increased concentration of bicarbonates that result in elevated biofilm pH and enhanced acid buffering capacity (Imfeld, 1999; Kitasako et al., 2005). The stimulated saliva is also in a state of mineral supersaturation that promotes enamel remineralisation (Aiuchi et al., 2008; Ly, Milgrom, & Rothen, 2008). Moreover, the use of the sugar-free chewing gum as an adjunct to tooth brushing is beneficial for oral hygiene including clearance of food debris and biofilm control (Keukenmeester, Slot, Putt, & Van der Weijden, 2014).

Sugar-free chewing gum is also a well-known and effective strategy for preventing caries (Kandelman & Gagnon, 1990) and acts primarily by inhibiting *Strep. mutans* activity in the biofilm (Shinga-Ishihara et al., 2012). A number of clinical controlled trials, both randomized and non-randomized, have compared sugar-free gum with various controls, and there is a growing body of evidence which supports the caries-preventive nature of chewing sugar-free gum (Cochrane et al., 2012; Morgan et al., 2008; Shen, Cai, Nowicki, Vincent, & Reynolds, 2001).

5.2.6 Study design

5.2.6.1 *In situ* vs *in vivo*

In situ studies are being widely have been carried out in dental research as they simulate the natural oral processes better than animal or *in vitro* studies without being as time consuming or costly as *in vivo* studies. Furthermore, *in situ* studies allow for better control of the study subjects and better compliance than *in vivo* studies as the latter last longer (Zero, 1995). Intra-oral models involve less subjects and use *in vitro* measurement techniques which are very sensitive resulting in observation of the desired effect in much less time than when conducting an *in vivo* study. However, an *in situ* study can only be considered as an intermediate step between *in vitro* or animal and *in vivo* studies and should not be overestimated against *in vivo* studies and results are carefully extrapolated (Manning & Edgar, 1992).

Various *in situ* designs have been implemented depending on the specific parameters which are to be evaluated. Cross-over designs have been commonly used in intra-oral models as they have the advantage of using the same subject as its own control and therefore facilitating the process of subject selection and decreasing the number of volunteers required. However, these study designs last longer and consequently compliance might be compromised as the same subject participates for a longer period in the study. In addition, a carry-over effect from the treatment of the first leg might be a disadvantage of a cross-over study. A one-week wash-out period was included in the design of this study.

5.2.7 Quantitative assessment

Quantitative methods such as ultrasound, profilometry, and quantitative light-induced fluorescence have been suggested by different researchers as potential tools for diagnosing dental erosion more accurately (Moazzez et al., 2004). However, most of these methods have not yet been tested clinically. Further research will determine the suitability for measurement of tooth wear *in vivo* and thus whether they should be recommended for use in a clinical setting.

Within the oral cavity, demineralisation and remineralisation of tooth surfaces (enamel, dentine) are in a state of equilibrium. Even without the participation of bacteria (caries) in a multifactorial process, a shift in the balance can occur towards demineralisation, which is caused by different patient-related and nutritional factors, e.g., eating/drinking habits, oral hygiene, medication and saliva conditions. The destructive effect of acid-induced tissue loss of tooth surface and subsurface regions is known as dental erosion (erosive tooth wear) (Lussi, 2006).

Clinical diagnosis indices for recording the erosive wear include morphological as well as quantitative criteria, particularly the Basic Erosive Wear Examination (BEWE) (Ganss & Lussi, 2014). However, the validity of diagnostic criteria and grading/scoring are unsatisfactory or unclear. Thus, there is a need to develop practicable and preferably chairside diagnostic tools (Ganss & Lussi, 2014). Different assessment methods have been applied for *in vitro* and *in vivo* studies to evaluate erosive tooth wear, e.g., profilometry, measuring microscopy techniques, TMR, SEM, atomic force microscopy, nanohardness and microhardness tests, iodide permeability test, as well as methods which chemically analyse minerals dissolves from dental hard tissue (Attin & Wegehaupt, 2014). In this context, OCT has been described as a suitable tool for the investigations of initial erosion (Attin & Wegehaupt, 2014).

OCT allows the assessment of the mineralization degree of enamel or dentine and the visualization of very early demineralisations, and thus permits early erosive lesions to be characterized (Attin & Wegehaupt, 2014). Until now, erosion could only be assessed clinically through long-term observations of the loss of hard tooth tissue over months to years, well after the erosion has been initiated. With OCT, initial erosion without loss of enamel height could be recognized and a therapeutic remineralisation process could be monitored and assessed (Mandurah et al., 2013).

5.2.8 Aim and Objectives

Aim: To explore the utility of OCT to detect initial enamel erosion, *in vivo*.

Objectives:

1. To induce initial enamel erosion *in vivo* without causing enamel surface loss.
2. To assess the ability of OCT in the detection of initial enamel erosion following acid challenge at different time intervals.
3. To evaluate the ability of OCT to detect the change in enamel backscattering after gum chewing.

Null hypothesis:

1. Initial enamel erosion *in vivo* will not result in enamel surface loss.
2. OCT is not able to detect initial enamel erosion following acid challenge.
3. OCT is unable to detect the change in enamel backscattering after gum chewing.

5.3 PILOT STUDY

Prior to the *in vivo* study, application for the medical ethics approval was done. In spite of the literatures provided, the committee was concerned if the acid challenge protocol outlined could cause significant amount of enamel erosion. A conditional approval was given; a pilot study involving a small group of subjects was suggested before the ethics approval could be granted.

5.3.1 Objective

To induce initial enamel erosion *in vivo* without causing enamel surface loss.

5.3.2 Materials and methods

5.3.2.1 Subjects recruitment - inclusion and exclusion criteria

A pilot study was carried out among the researchers within the research group. The subjects consisted of four females with a mean age of 34.5 years (range 30 - 42 years). All subjects fulfilled the inclusion and exclusion criteria (**Table 5.1**).

Table 5.1: Sample inclusion and exclusion criteria.

Inclusion Criteria	Exclusion Criteria
Good oral hygiene with all sound anterior teeth (11 or 21) without any evidence of fluorosis, dental erosion, restorations or caries.	Presence of underlying disease that can interfere with the study such as Gastro-esophageal reflux disease (GERD).
Able to agree to sign the consent form.	Presence of gingival/periodontal disease.
Unstimulated salivary flow rate of more than 0.2 ml / minute.	Smoking.
18 to 30 years old (reasonably similar age if possible).	Known medical illness that reduces salivary flow.
In good health.	Pregnant or lactating.
Agree to return for scheduled visits.	Tetracycline stained teeth/fluorosis..

Subjects were advised to use soft bristled toothbrush with fluoridated toothpaste and throughout the study. Subjects were allowed to perform their usual oral hygiene regimen, such as brushing teeth twice a day with fluoridated tooth paste, before or after each daily study period (0900 to 1700 h). However, they were instructed to abstain from tooth brushing at least one hour before attending the experiment sessions. They were also prevented from taking any acidic food during the day of challenge with the orange juice.

5.3.2.2 Clinical Procedure

The commercially packed orange juice was administered at the study site every acid challenge day. Subjects were instructed to use a soft bristled toothbrush with fluoridated toothpaste in the morning and night throughout the pilot study period. Visit timings were monitored and recorded and subjects were reminded when they should attend for their next visit. Cartons of commercially available orange juice (Peel fresh, Malaysia Milk Sdn Bhd) were purchased from the same batch to standardise the acidic conditions. The pH was recorded as 3.4 before the start of the study. In order to ensure standardisation of effect, a staff was allocated to supervise each acid challenge session. Acid challenge day procedures followed a predefined order as summarised in **Figure 5.2**. A total of 250 ml of orange juice was swished at each time point, three times per day resulting in the teeth being exposed to 750 ml of juice each day. At each time point, subjects swished 25 ml of orange juice for one min before expectoration. This procedure was performed 10 times over a 10-minute period without any water rinses between swishes in order to obtain a steady, controlled flow of acidic challenge over the tooth specimens for all subjects throughout the study and to minimise variation. Ten minutes of acid challenges was used because it had been suggested that this time period represents a reasonable time for consumption of a juice beverage or soft drink (S. Hooper et al., 2007; S. M. Hooper et al., 2007)**.** Then subjects were asked to rinse their mouth with tap water for one minute to remove all residue of orange juice.

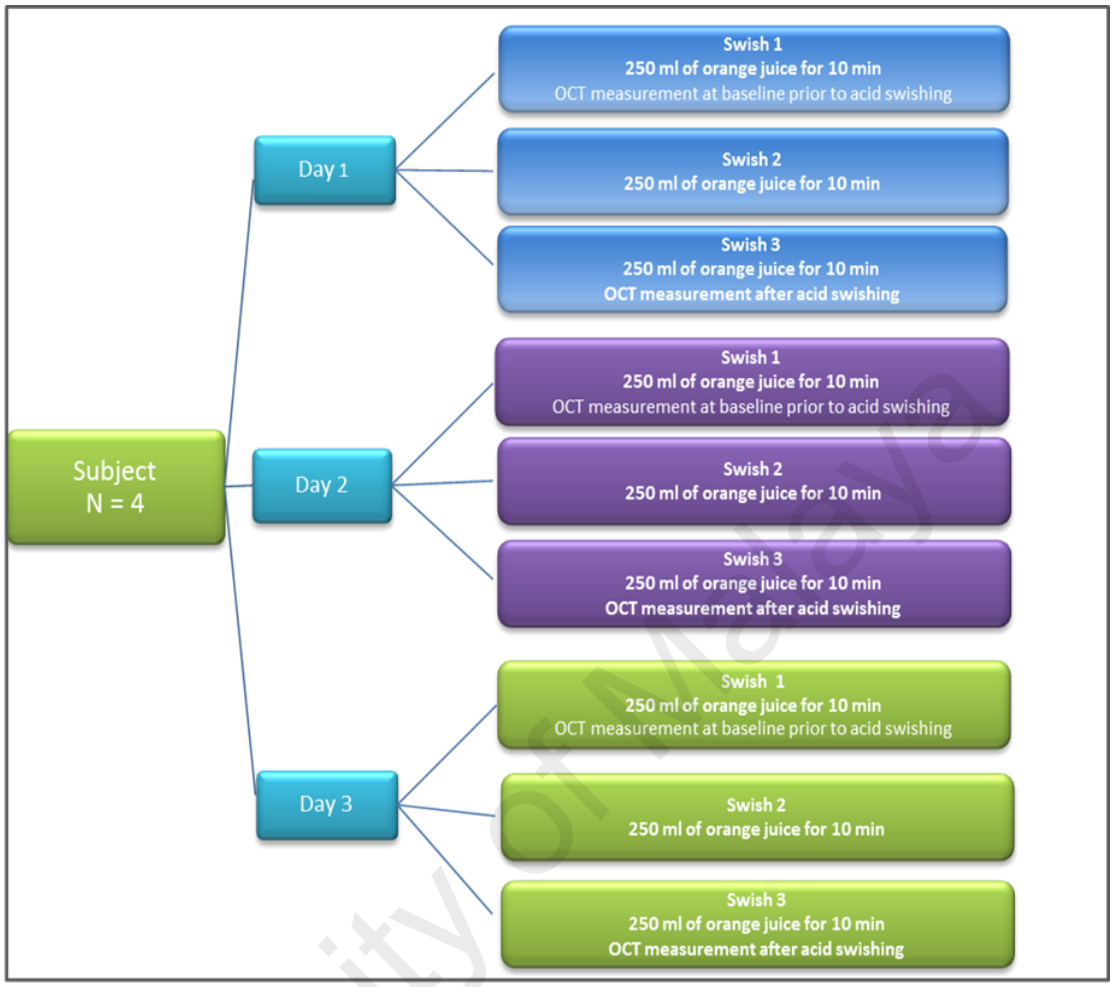

Figure 5.2: Illustration of 3-day study design for each subject and number of swishes per day with the amount of orange juice used throughout the pilot study.

5.3.2.3 OCT measurement

OCT scans were performed using the commercially available OCT THORLABS 1300SS OCS, and its imaging probe. For acquisition of OCT images, the subjects used an acrylic stent to indicate the position for image capture and a cotton roll was inserted into the upper anterior sulcus to retract the upper front lip for better expose the central incisors. They remained seated, with the head resting on a specific positioner (**Figure 5.3**a), perpendicular to the focus of the laser guide light emitter. The light beam was configured to scan an area of 10 mm x 2 mm window in the X-Y direction and at a depth of 3 mm in air, corresponding to an axial physical depth of 1.85 mm (Z-axis) in enamel (refractive index = 1.62), with a resolution of 1024, 512 and 512 pixels at the X, Y and Z axis, respectively. OCT images were acquired, and backscattered light intensity as a function of depth was analysed for each time point. Teeth were dried with compressed air using a dental three-way syringe at 29 psi, from a standardised distance of 3 ± 1 cm, for 10 sec (Shimamura et al., 2011) prior to OCT scanning. In order to gain stability and for repositioning purposes, subjects were asked to rest their chin on a 'Imaging Module Patient Positioning System' (Kevork Instruments) during scanning and bite on a piece of acrylic cylinder where a horizontal slot was created on the upper surface to position the selected incisal edges of the central incisors. The OCT scanning beam was directed perpendicular to the labial surface of the upper left central incisors. For each subject, the middle third of the labial surface of upper left central incisor (tooth 11) was scanned (**Figure 5.3**b). After each measurement, the acrylic cylinder was cleaned/disinfected with antiseptic wipes.

The enamel thickness was measured through visual assessment of the entire B-scan. The following criteria were used to ensure that subsequent images at different time points were at the same scanning level or area: (1) Visible evidence of incisal edge of the central incisors using OCT images prior to initial scanning (Todea et al., 2010). (2) For

the subsequent OCT measurements, the most identical frame to the baseline images was closely identified, in order to ensure standardization. Monitoring of possible tooth surface loss was done at the end of each day by comparing the enamel thickness to that of baseline using the Thorlabs OCS1300SS Software. Two horizontal straight line was drawn on the surface of the enamel and on the highest point of the DEJ, and the distance between the two lines was recoded (**Figure 5.4**). All enamel thickness measurements were repeated three times on the same B-scan image of each subject at different time of the day without referring to the previous measurements. The display settings, such as brightness and contrast, were the same for all the B-scan images. The three values were then averaged to provide the mean values. The differences between the baseline and the readings taken after the third acid challenge at the end of each day were calculated for each subject.

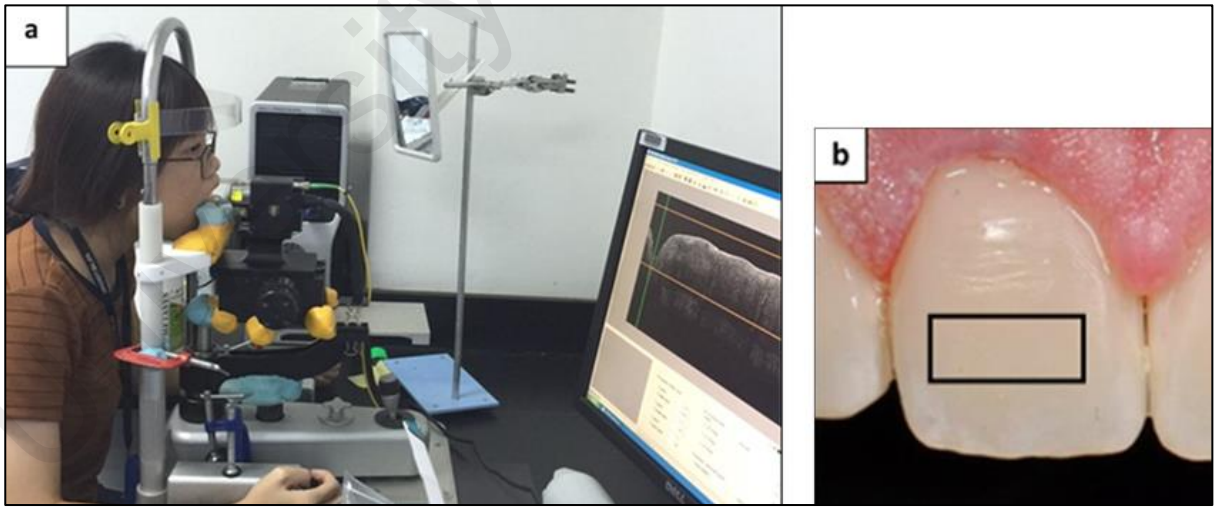

Figure 5.3: (a) Position of the subject for image acquisition and measurement using OCT. Illustration. (b) Region to be studied (labial).

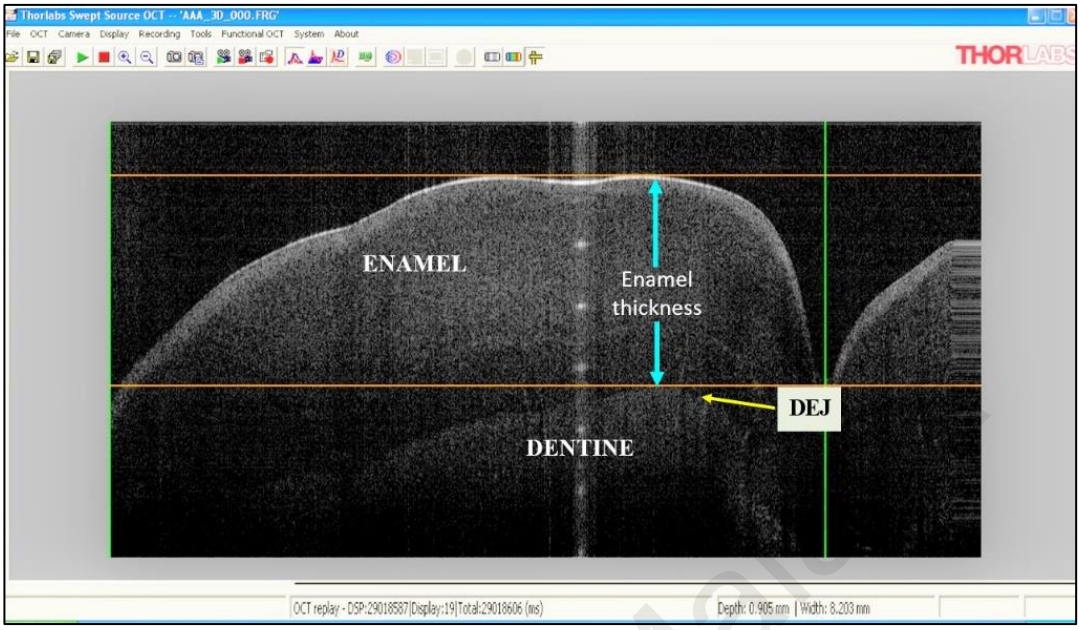

Figure 5.4: Enamel thickness measurement with Thorlabs OCS1300ss Software. OCT B-scan of an incisor used for enamel thickness measurement (distance from enamel surface to DEJ).

5.3.2.4 Statistical Analysis

The mean daily changes of enamel thickness were analysed using paired t-test. For intra-examiner consistency evaluation, the three repeated measurements on the same B-scan of each subject at one time point were assessed using the Intraclass Correlation Coefficient (ICC). The statistical analysis was performed using the statistical software package SPSS version 25.0 (SPSS Inc., Chicago, USA). All levels of significance were set at $p < 0.05$.

5.3.3 Results

All subjects completed the study and no adverse events were observed or reported. The 20 μm enamel loss safety margin incorporated into the protocol was not approached/met by any subject. **Figure 5.5** and **Figure 5.6** show representatives OCT B-scans from the labial enamel of the same area of the same tooth before (left image, t_1) and after swishing with orange juice (right image, t_2).

All intraclass correlation coefficients (ICC) were 0.93 or higher, which indicates good agreement in the measurements of enamel thickness **Table 5.2** and **Table 5.3.**

Table 5.4 shows paired t-test results comparing the enamel thickness from Day-1, Day-2 and Day-3. It can be seen that there were no statistically significant difference in the enamel thickness between Day-1 and Day-2 ($p = 0.095$); and between Day-2 and Day-3 ($p = 0.696$).

The mean daily changes of enamel thickness, expressed in microns, after third acid challenge is shown in **Table 5.5**. The results showed no significant progressive changes in enamel thickness with time throughout the study. **Table 5.5** shows the changes in enamel thickness for each subject throughout the three days and shows the mean enamel thickness for all subjects at their consecutive time points.

Time points / Day	t_1	t_2
1	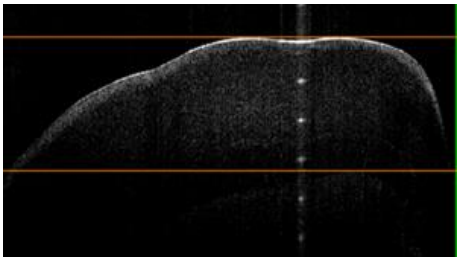	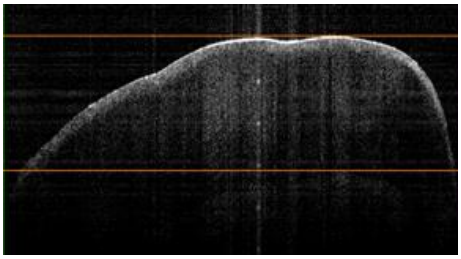
2	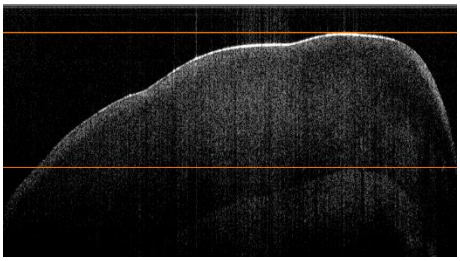	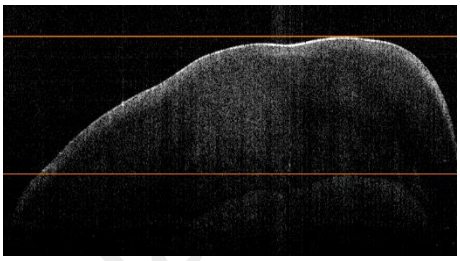
3	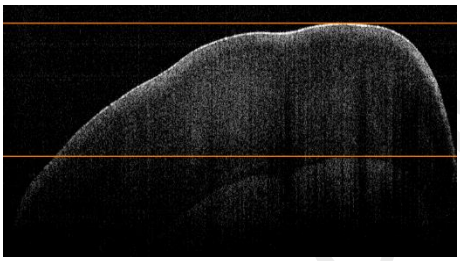	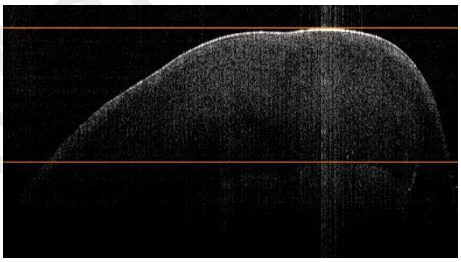

Figure 5.5: OCT B-scans of a subject's enamel surface taken at two time points (t_1 and t_2) at day 1, day 2 and day 3.

The backscattered intensity at after three swishing with orange juice of 10 mins each appeared with higher intensities (t_2) when compared to baseline (t_1).

Time points / Day	t_1	t_2
1	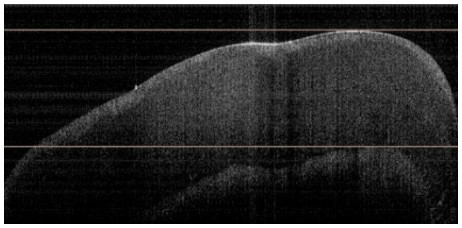	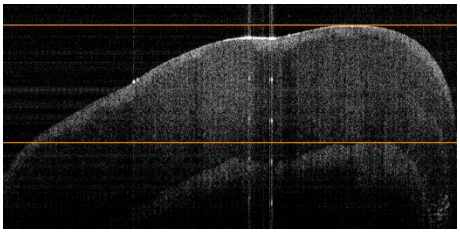
2	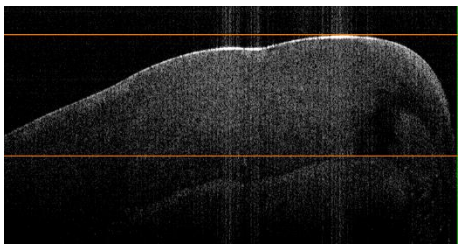	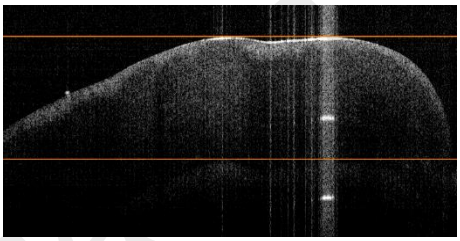
3	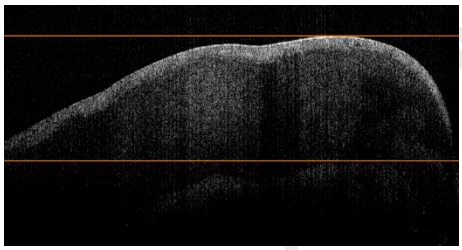	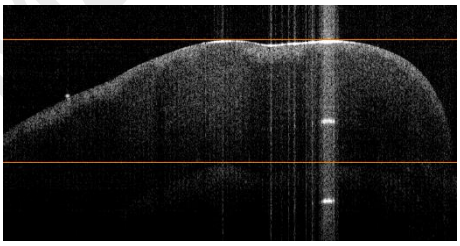

Figure 5.6: OCT B-scans of a subject's enamel surface taken at two time points (t_1 and t_2) at day 1, day 2 and day 3.

The backscattered intensity at after three swishing with orange juice of 10 mins each a appeared with higher intensities (t_2) when compared to baseline (t_1).

Table 5.2: Intraclass correlation coefficient (ICC) table.

Intraclass Correlation Coefficient

	Intraclass Correlation[b]	95% Confidence Interval		F Test with True Value 0			
		Lower Bound	Upper Bound	Value	df1	df2	Sig
Single Measures	.993[a]	.481	1.000	1249.865	3	3	.000
Average Measures	.996[c]	.649	1.000	1249.865	3	3	.000

Two-way mixed effects model where people effects are random and measures effects are fixed.

a. The estimator is the same, whether the interaction effect is present or not.

b. Type A intraclass correlation coefficients using an absolute agreement definition.

c. This estimate is computed assuming the interaction effect is absent, because it is not estimable otherwise.

Table 5.2 shows the ICC and 95% confidence intervals for pre acid challenge measurements of enamel thickness. ICC value of 0.993, indicates good agreement among the measurements made by a single examiner.

Table 5.3: Intraclass correlation coefficient (ICC) table.

Intraclass Correlation Coefficient

	Intraclass Correlation[b]	95% Confidence Interval		F Test with True Value 0			
		Lower Bound	Upper Bound	Value	df1	df2	Sig
Single Measures	.996[a]	.948	1.000	404.622	3	3	.000
Average Measures	.998[c]	.973	1.000	404.622	3	3	.000

Two-way mixed effects model where people effects are random and measures effects are fixed.

a. The estimator is the same, whether the interaction effect is present or not.

b. Type A intraclass correlation coefficients using an absolute agreement definition.

c. This estimate is computed assuming the interaction effect is absent, because it is not estimable otherwise.

Table 5.3 shows ICC and 95% confidence intervals for post acid challenge measurements of enamel thickness. ICC value of 0.996, indicates good agreement among the measurements made by a single examiner.

Table 5.4: Paired t-test comparing enamel thickness between two consecutive days.

Paired Specimens Test									
		Paired Differences					t	df	Sig. (2-tailed)
		Mean	Std. Deviation	Std. Error Mean	95% Confidence Interval of the Difference				
					Lower	Upper			
Pair 1	**Day_1 - Day_2**	0.014	0.01184	0.00592	-0.0046	0.0331	2.407	3	0.095
Pair 2	**Day_2 - Day_3**	0.002	0.00931	0.00465	-0.0128	0.01681	0.43	3	0.696

Mean enamel thickness ± SD of the labial enamel of maxillary incisor (N=4) at day 1 and 2. Paired t-test showed no statistically significant different between day 1 and 2. And between day 2 and 3. ($p > 0.05$).

Table 5.5: Mean differences values of enamel thickness (μm) compared to baseline at Day-1, Day-2 and Day-3.

	Differences in enamel thickness from baseline (μm)		
	Day 1	**Day 2**	**Day 3**
Subject 1	0.002	-0.006	-0.011
Subject 2	0.012	0.003	0.012
Subject 3	0.01	0.003	0.004
Subject 4	0.017	-0.015	-0.028
Mean	0.01	-0.004	-0.006
SD	0.006	0.008	0.018

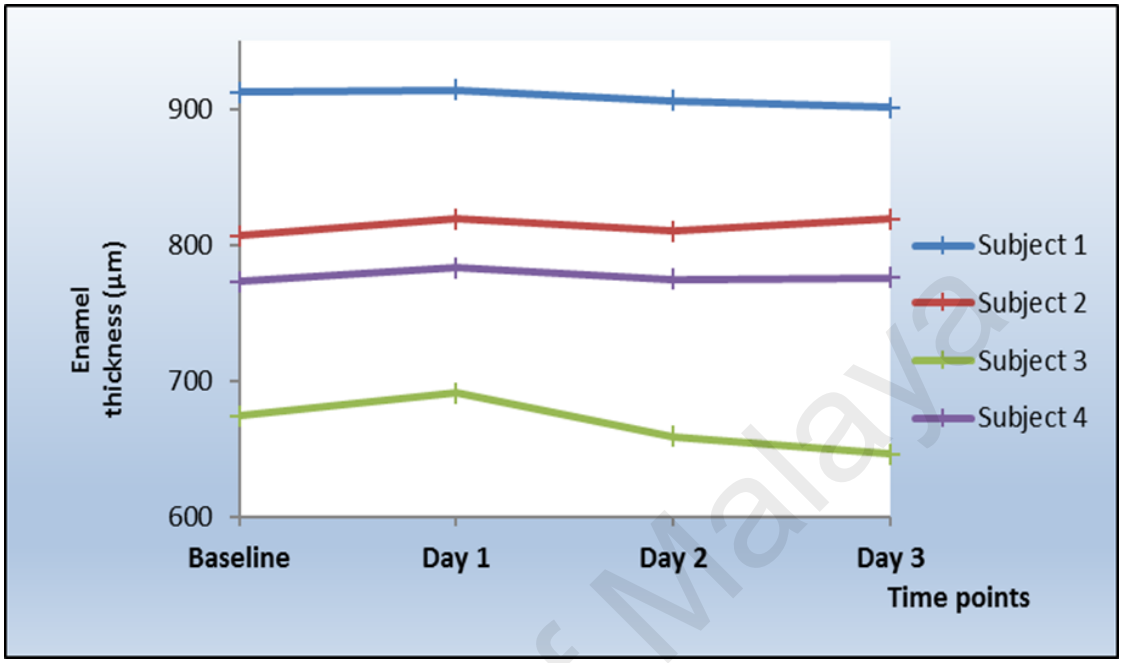

Figure 5.7: Graph showing the mean enamel thickness (μm) and their consecutive time points for each subject.

5.3.4 Discussion

The objective of the pilot study was to evaluate the effect of acid challenge on enamel thickness using OCT. Measuring the remaining enamel thickness can also be used as an indicator of erosion. Demineralisation was quantified from representative images of B-scans (**Figure 5.5** and **Figure 5.6**).

Studies had used OCT to monitor the remaining enamel thickness by using the dentino-enamel junction (DEJ) as reference (Chan et al., 2013; C. H. Wilder-Smith et al., 2009). C. H. Wilder-Smith et al. (2009) carried out an *in vivo* study of erosion caused by Gastro-Esophageal Reflux Disease (GERD) and they were able to measure very small rates of erosion. However, there were challenges in accurately measuring the remaining enamel thickness using this method. For example, the DEJ is scalloped and does not present a sharp boundary. If erosion is accompanied by subsurface demineralisation or roughening of the surface, the strong increase in light scattering interferes with the ability to accurately resolve the DEJ, thus measurement of enamel thickness may not be as accurate (Chan et al., 2013).

5.3.5 Conclusion

Higher intensities observed from the B-scans following acid challenges indicated that OCT could detect initial enamel erosion. The findings from this pilot study showed that, quantitatively, there were no significant difference in enamel thickness after acid challenges in three days of multiple swishing with orange juice compared to baseline. Therefore, the suggested protocol would not cause enamel surface loss and it was safe for the subjects involved in the study.

5.4 MAIN STUDY

This section aimed to use the experience gained from the previous *in vitro* and the pilot studies to design and conduct a clinical investigation on initial erosion. A new study protocol for the actual *in vivo* study was designed, with few modifications made to the previous pilot study protocol.

5.4.1 Materials and methods

5.4.1.1 Subjects recruitment

Using *in vitro* data, a sample size of 22 was estimated, based on the assumption that SS-OCT would detect a 5% change in backscattered OCT signal intensity (D) after 30 min of orange juice rinsing (SD 5%) assuming a power of 95%, and $p < 0.05$ being regarded as statistically significant. G Power software was used to estimate the sample size.

Twenty-two healthy adults (11 males and 11 females), age 23-33 participated in the study. Subjects were enrolled in the clinical study if all the inclusion and exclusion criteria were met (**Table 5.1**). Prior to receiving any study procedures, subjects were given Subject Information Sheet and an informed consent to be obtained. Sample size calculation was based on a previous *in situ* study, on the assumption that OCT would detect a 5% change in backscattered OCT signal intensity (D) after 30 min of orange juice rinsing (SD 5%) assuming, $p < 0.05$ being regarded as statistically significant.

All subjects were asked to provide unstimulated saliva specimens for 5 min prior to the start of the experiment to ensure that each subject's saliva flow rate is within the normal salivary flow rates (unstimulated flow > 0.2 ml/min). Unstimulated saliva was collected by the draining method where subjects were instructed to swallow to begin a

collection trial, and were then told to allow saliva to drain out between parted lips into the test tube (Navazesh & Christensen, 1982). The whole volume collected for 5 min was then measured. The salivary flow rate (ml/min) was estimated by dividing the volume of the saliva specimens (1 g of saliva equals 1 ml) by collection time (min) (Navazesh & Christensen, 1982). Subject with an unstimulated salivary flow rate of less than 0.1 mL/min is at five-times-greater risk of erosion than those with higher flow rates (Jarvinen et al., 1991).

Each subject was given a toothpaste (Colgate® Maximum Cavity Protection Plus Sugar Acid Neutraliser) and adult soft bristle toothbrush (Colgate®-Palmolive, New York, NY, USA) which to be used for two min, twice a day at least a minimum of two days prior to the commencement of the study and throughout the duration of the study.

5.4.1.2 Study design

This was an *in vivo* experimental study of two phases with each phase being three days and a wash out period of two days in between the two phases. This study protocol was reviewed and approved by the Medical Ethics Committee, Faculty of Dentistry, University of Malaya (DF RD1617/0054(P)) (Appendix 2) and was in accordance with the ethical guidelines for research involving human subjects. The study was conducted at the Faculty of Dentistry, University of Malaya.

5.4.1.3 Study protocol

This study consisted of two phases:

i. **Phase-A** (acid challenge without chewing gum)

The commercially packed orange juice was administered at the study site every acid challenge day. Visit timings were monitored and recorded and subjects were

reminded when they should attend for their next visit. Cartons of commercially available orange juice (Peel fresh, Malaysia Milk Sdn Bhd) were purchased from the same batch to standardise the acidic conditions. The pH was recorded as 3.4 before the start of the study. In order to ensure standardisation of effect, a staff was allocated to supervise each acid challenge session. For each day in Phase-A, subjects were asked to swish 25 ml of orange juice for 30 sec, expectorate, then rest for 30 sec, in a 10 min period (acidic challenge) for three times with a three-hour interval. A total of 250 ml orange juice was swished around their mouth for the 10-min period.

ii. **Phase-B** (acid challenge followed by 15 min of chewing gum)

In Phase-B, they had to continue with chewing gum (Wrigley's Extra® Sugar free Chewing Gum, Peppermint flavour) for 15 min after each swishing. For both phases, the same protocol was repeated for three consecutive days. Each phase was separated by a 2-day washout period. The summary of the study design is shown in **Figure 5.8** and **Figure 5.9**.

5.4.1.4 OCT imaging

All OCT scans were performed by a single operator using the commercially available OCT (OCS1300SS Thorlabs Ltd., USA) and its imaging probe. Subjects were asked to rest their chin on a 'Patient Positioning Imaging Module System' for the purpose of repositioning during repeated measurements (**Figure 5.3**a), with the subjects remained seated. A cotton roll was inserted into the upper anterior sulcus to retract the upper front lip for better expose the central incisors and the scanning beam was positioned perpendicular to the tooth surface.

The light beam was configured to scan an area of 10 mm x 2 mm in the X-Y direction and at a depth of 3 mm in air, corresponding to an axial physical depth of 1.85 mm (Z-axis) in enamel (refractive index = 1.62), with a resolution of 1024, 512 and 512

pixels at the X, Y and Z axis, respectively (**Table 5.6)**. OCT images were acquired, and backscattered light intensity as a function of depth was analysed for each time point.

Teeth were dried with compressed air from a dental three-way syringe, from a distance of 3 ± 1 cm, for 20 sec prior to OCT scanning. The subjects were asked to bite on a piece of acrylic cylinder where a horizontal slot was created on the upper surface to position the selected incisal edges of the central incisors. For each subject, the middle third of the labial surface of upper left central incisor (tooth 11) was scanned (**Figure 5.3**b). After the measurement of each subject, the acrylic cylinder was disinfected with antiseptic wipes.

During both phases, baseline OCT scans were taken at the beginning of each treatment day prior to the first acid challenge. The second OCT measurement was taken after each acid challenge, totalling of three orange juice acid challenges and six OCT measurements per day ($t_1 - t_6$).

Table 5.6: OCT scans configuration

Dimension	Image resolution	Scanning length (physical length)
X-width	1024 pixels	10 mm
Y-length	512 pixels	2 mm
Z-depth	512 pixels	1.85 mm

5.4.1.5 OCT data processing

The primary outcome was expressed as the change in backscattered OCT signal intensity, at the level of the incisor teeth pairs. For this study, the protocols of OCT data processing and method used to quantify the OCT backscattered intensity by calculating the Integrated Reflectivity, *IR* as described in Chapter 3, section 3.3.7.1, (ii), pg. 98 and section 3.3.7.1, (iii) pg. 99, respectively.

From the *in vitro* study, it was found that biofilm or plaque needed to be removed prior to OCT scanning in order to minimise the effect of this particular confounding factor on the OCT reading. The outcome measure IR_{sub} was used for analysis rather than $IR_{biofilm}$ as biofilm was removed prior to each measurement.

5.4.1.6 Statistical analysis

Data were normally distributed, and parametric tests were applied. Data was managed based on the study objectives. The data for integrated reflectivity (*IR*) were subjected to statistical analysis using the statistic package for social study (SPSS) version 25.0 (SPSS Inc., Chicago, USA). Repeated Measures ANOVA were applied. The paired sample t-test was used to compare the difference between related time points between Phase-A and B. The level of significance was set at $p<0.05$.

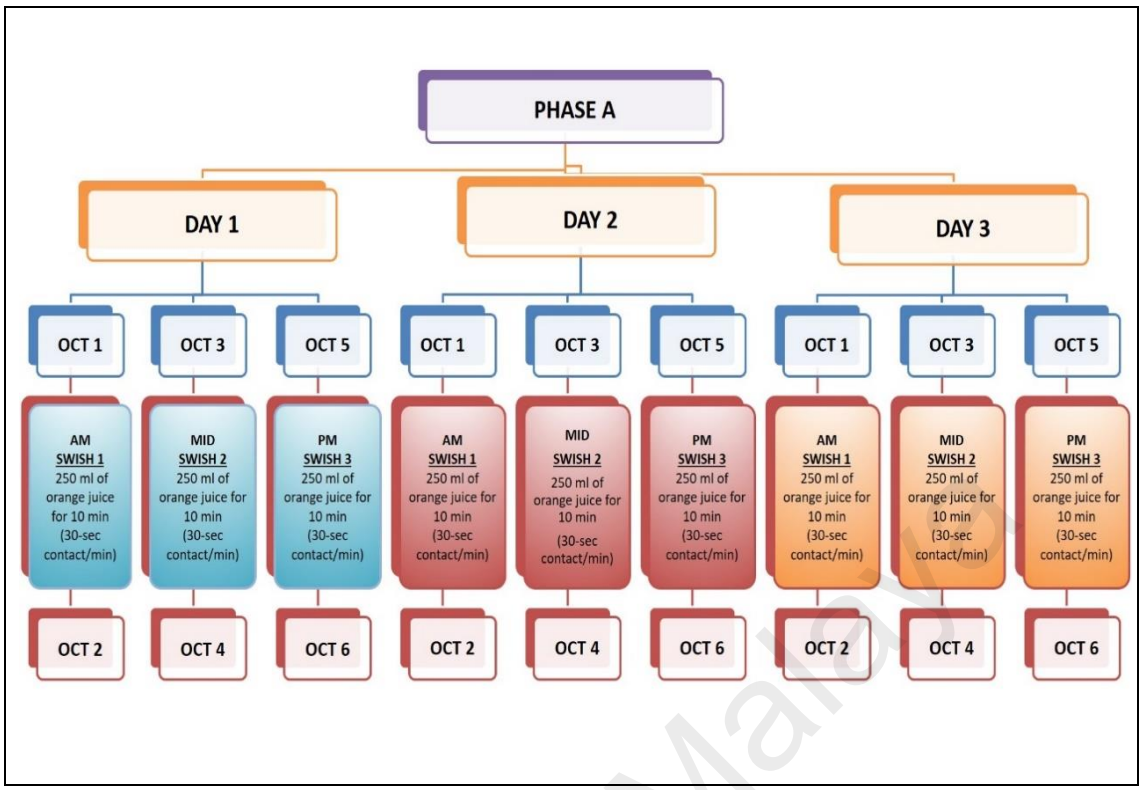

Figure 5.8: Flow chart of study design of Phase-A (N=22).

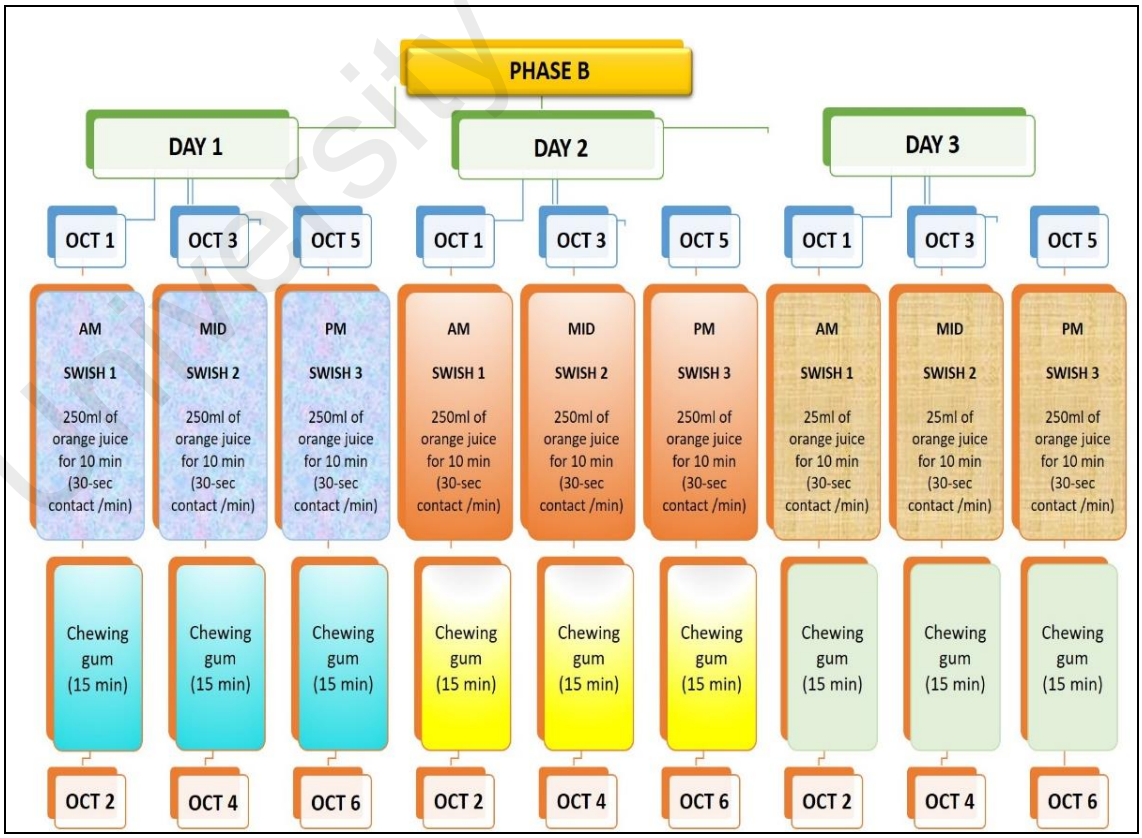

Figure 5.9: Flow chart of study design of Phase-B (N=22).

5.4.2 Results

5.4.2.1 The ability of OCT in the detection of initial enamel erosion following acid challenge at different intervals.

All 22 subjects who met the eligibility criteria consented to take part in and completed the study. Data was analysed based on the study objectives. The following images are representative examples of data clinically obtained using the OCT. Visual comparison of the B-scan images showed increased backscattered intensities when the enamel surface was exposed to repeated acid challenge.

Figure 5.10 to **Figure 5.23** show representative OCT B-scans from the labial enamel of the same area of the same tooth before (left image) and after swishing with orange juice (right image) of Phase-A and B, at day 1, 2 and 3. All images displayed a high-resolution air/enamel interface with differing rates of decay of backscattered OCT signal.

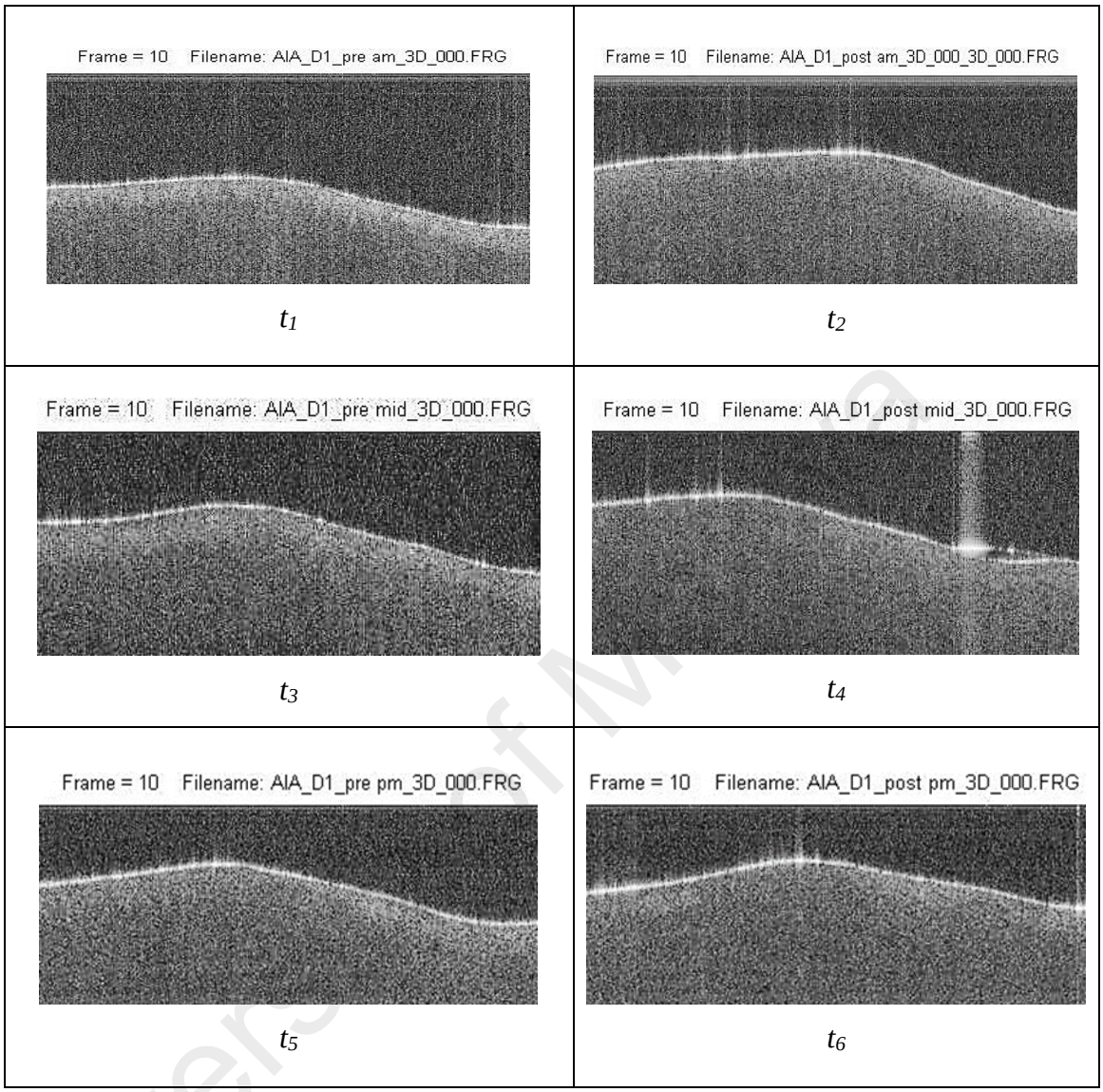

t_1 t_2 t_3 t_4 t_5 t_6

Figure 5.10: OCT B-scans of a subject's enamel surface taken at each time point, t_1 –t_6 at day 1 in Phase-A (subject 1).

The backscattered intensity at baseline (t_1) already showed evidence of erosion, however visual observation showed that the backscattering intensities appeared higher after swishing with orange juice for 10 mins at time points, t_2, t_4, t_6 when compared to the measurements before swishing, t_1, t_3, t_5.

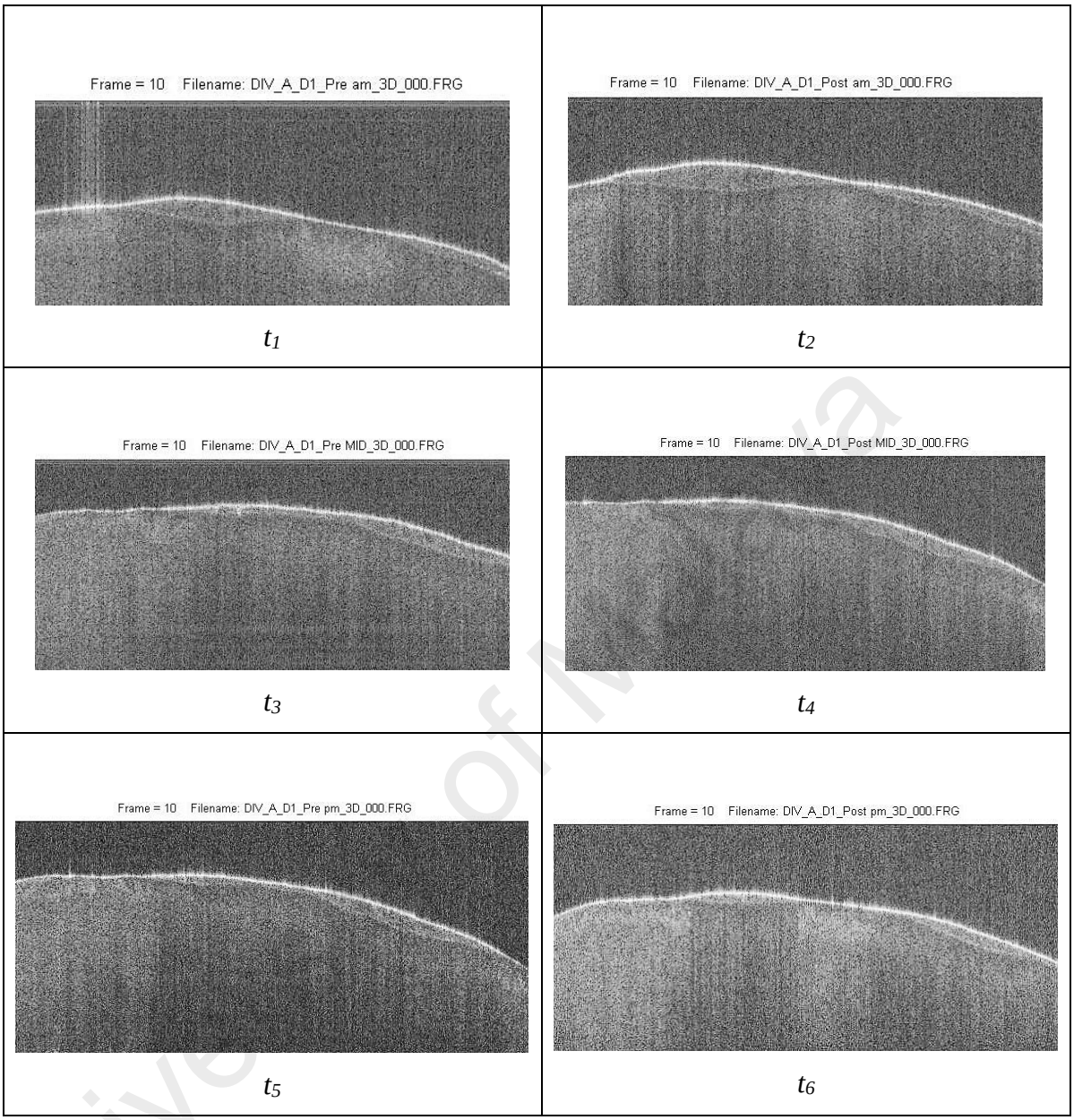

Figure 5.11: OCT B-scans of a subject's enamel surface taken at each time point, $t_1 - t_6$ at day 1 in Phase-A (subject 2).

The backscattered intensity at baseline (t_1) already showed evidence of erosion, however visual observation showed that the backscattering intensities appeared higher after swishing with orange juice for 10 mins at time points, t_2, t_4, t_6 when compared to the measurements before swishing, t_1, t_3, t_5.

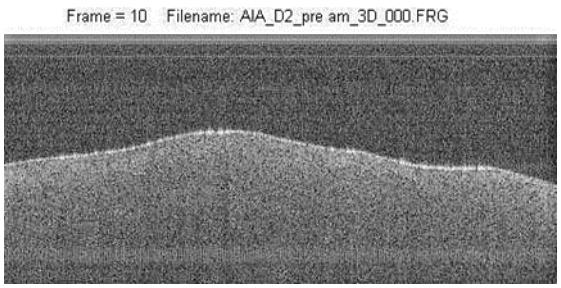

t_1

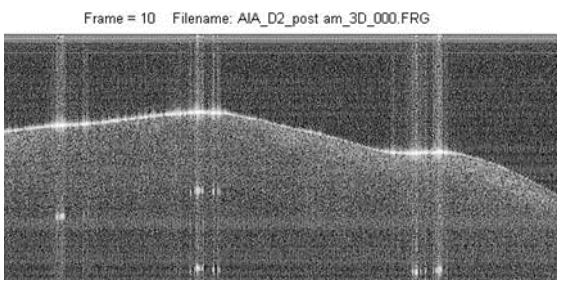

t_2

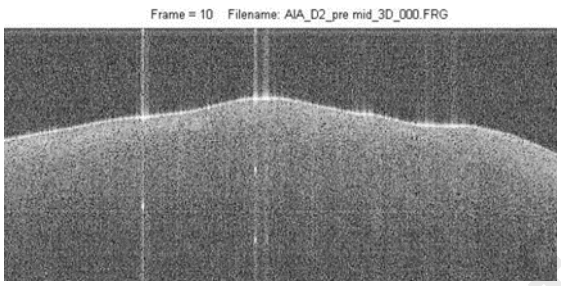

t_3

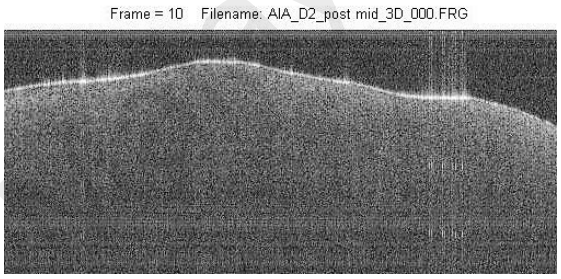

t_4

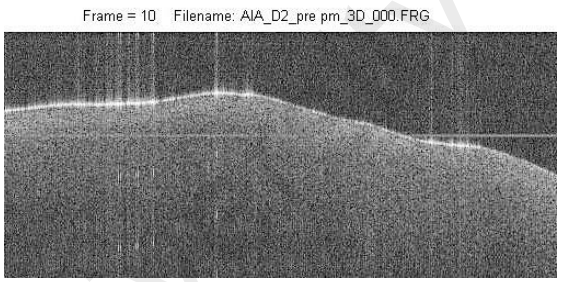

t_5

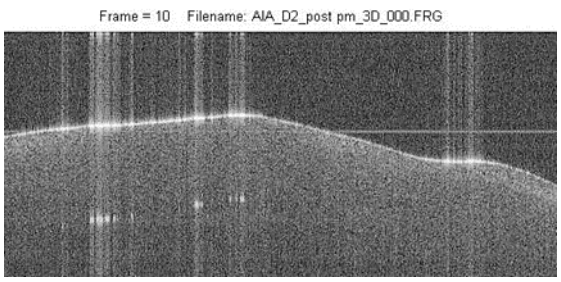

t_6

Figure 5.12: OCT B-scans of a subject's enamel surface taken at each time point, $t_1 - t_6$ at day 2 in Phase-A (subject 1).

The backscattered intensity at baseline (t_1) already showed evidence of erosion, however visual observation showed that the backscattering intensities appeared higher after swishing with orange juice for 10 mins at time points, t_2, t_4, t_6 when compared to the measurements before swishing, t_1, t_3, t_5.

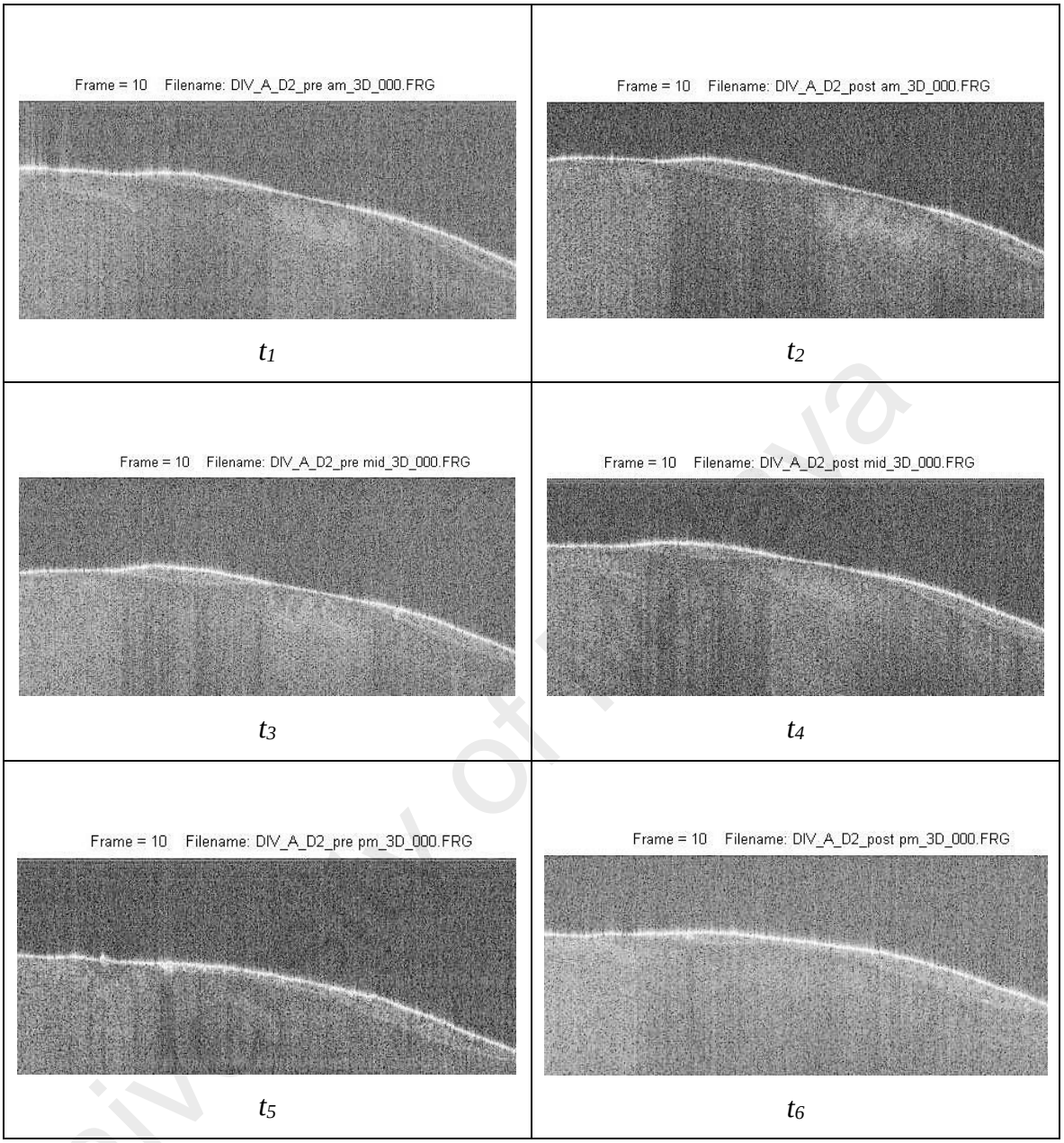

Figure 5.13: OCT B-scans of a subject's enamel surface taken at each time point, $t_1 - t_6$ at day 2 in Phase-A (subject 2).

The backscattered intensity at baseline (t_1) already showed evidence of erosion, however visual observation showed that the backscattering intensities appeared higher after swishing with orange juice for 10 mins at time points, t_2, t_4, t_6 when compared to the measurements before swishing, t_1, t_3, t_5.

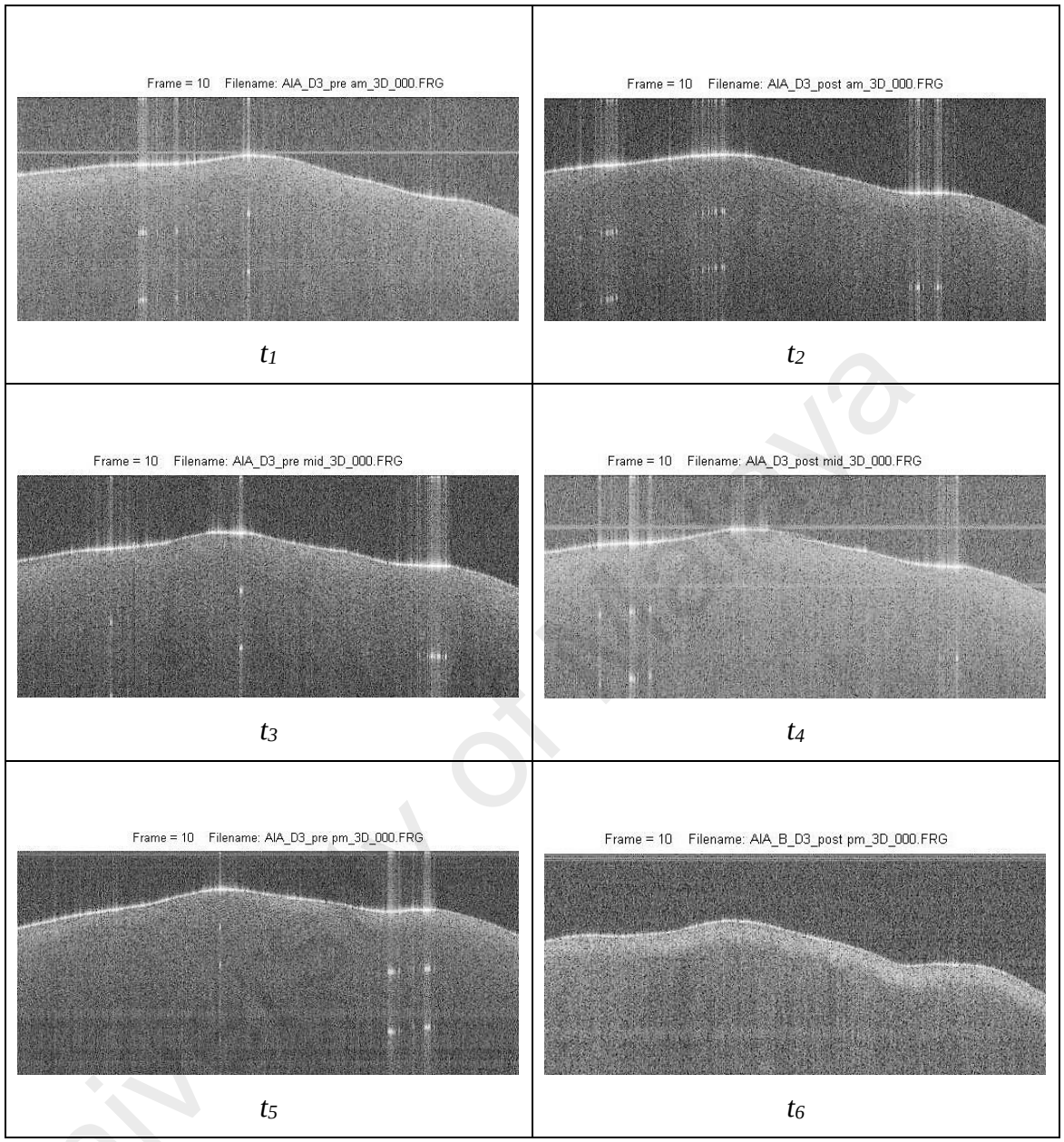

Figure 5.14: OCT B-scans of a subject's enamel surface taken at each time point, $t_1 - t_6$ at day 3 in Phase-A (subject 1).

The backscattered intensity at baseline (t_1) already showed evidence of erosion, however visual observation showed that the backscattering intensities appeared higher after swishing with orange juice for 10 mins at time points, t_2, t_4, t_6 when compared to the measurements before swishing, t_1, t_3, t_5.

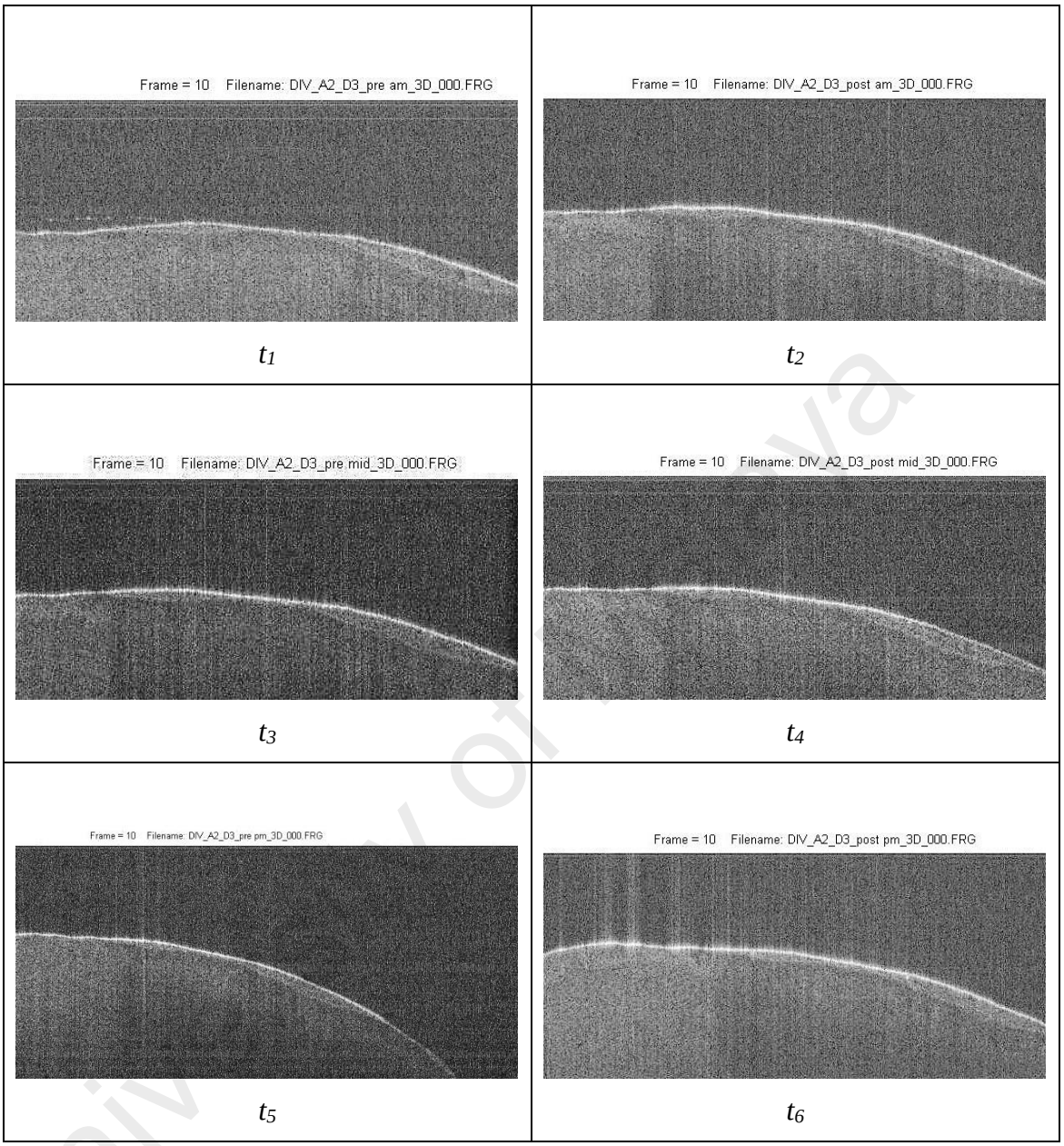

Figure 5.15: OCT B-scans of a subject's enamel surface taken at each time point, $t_1 - t_6$ at day 3 in Phase-A (subject 2).

The backscattered intensity at baseline (t_1) already showed evidence of erosion, however visual observation showed that the backscattering intensities appeared higher after swishing with orange juice for 10 mins at time points, t_2, t_4, t_6 when compared to the measurements before swishing, t_1, t_3, t_5.

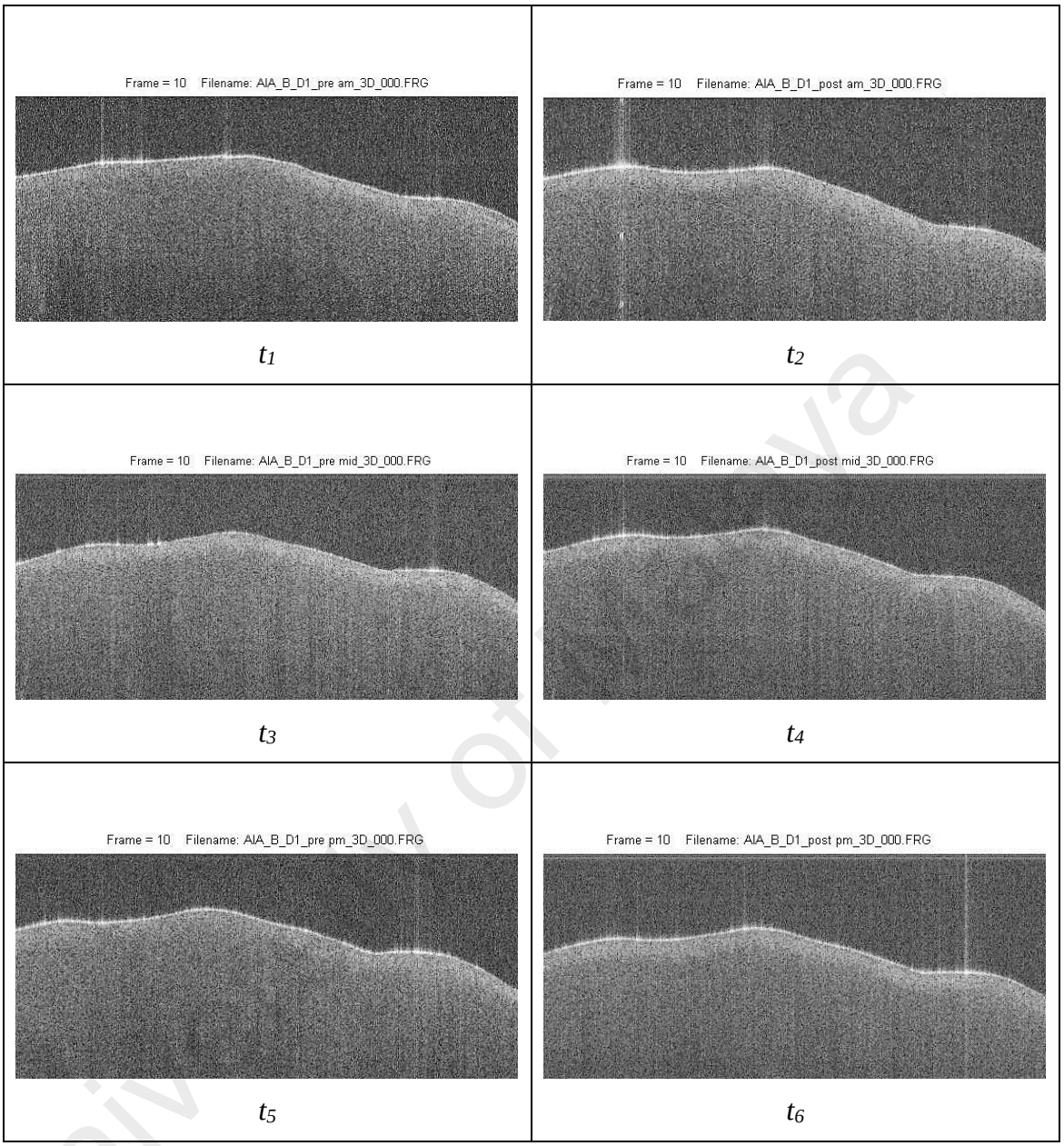

Figure 5.16: OCT B-scans of a subject's enamel surface taken at each time point, $t_1 - t_6$ at day 1 in Phase-B (subject 1).

The backscattered intensity at baseline (t_1) already showed evidence of erosion, however visual observation showed that the backscattering intensities appeared higher after swishing with orange juice for 10 mins at time points, t_2, t_4, t_6 when compared to the measurements before swishing, t_1, t_3, t_5.

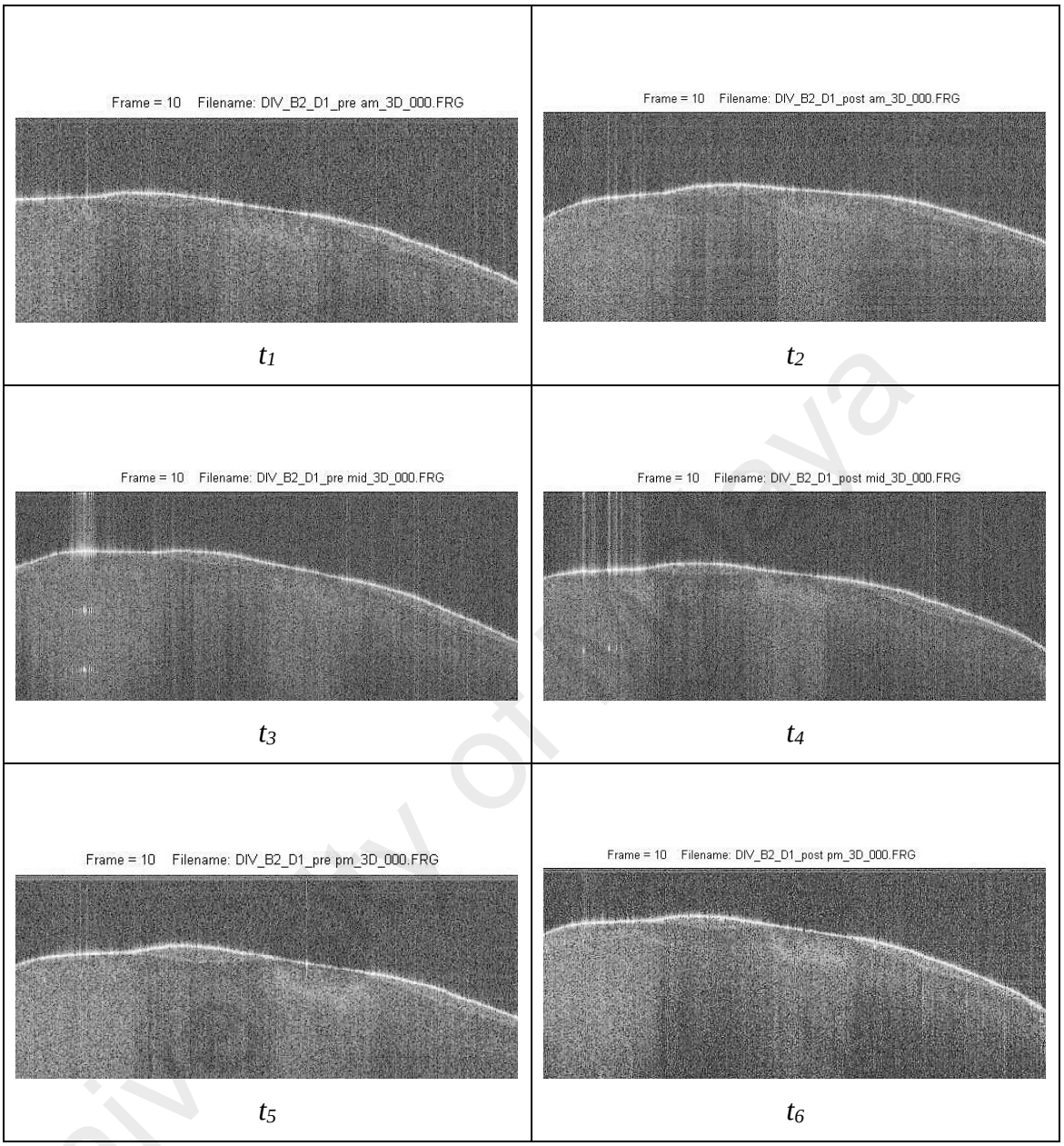

Figure 5.17: OCT B-scans of a subject's enamel surface taken at each time point, $t_1 - t_6$ at day 1 in Phase-B (subject 2).

The backscattered intensity at baseline (t_1) already showed evidence of erosion, however visual observation showed that the backscattering intensities appeared higher after swishing with orange juice for 10 mins at time points, t_2, t_4, t_6 when compared to the measurements before swishing, t_1, t_3, t_5.

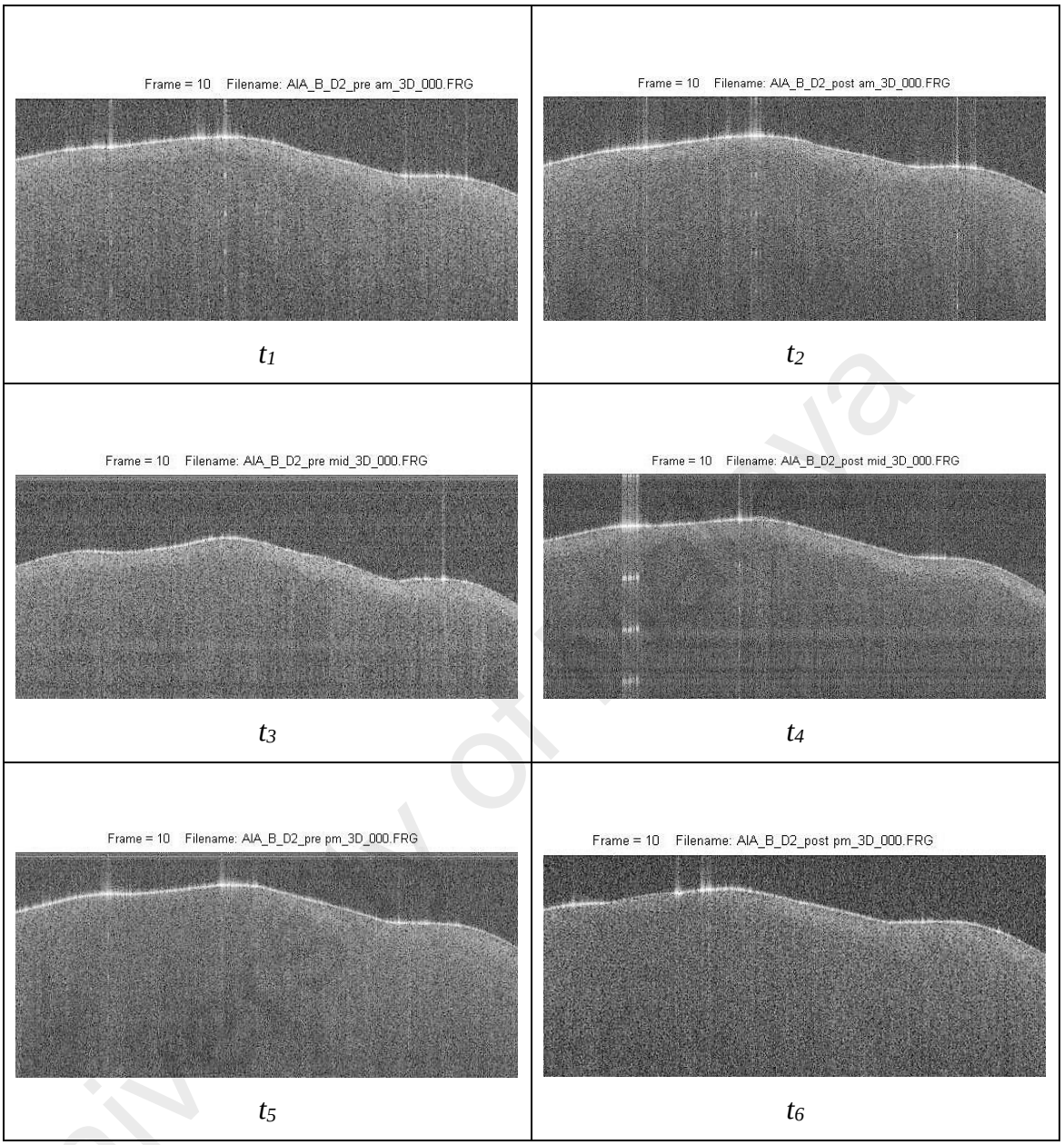

Figure 5.18: OCT B-scans of a subject's enamel surface taken at each time point, $t_1 - t_6$ at day 2 in Phase-B (subject 1).

The backscattered intensity at baseline (t_1) already showed evidence of erosion, however visual observation showed that the backscattering intensities appeared higher after swishing with orange juice for 10 mins at time points, t_2, t_4, t_6 when compared to the measurements before swishing, t_1, t_3, t_5.

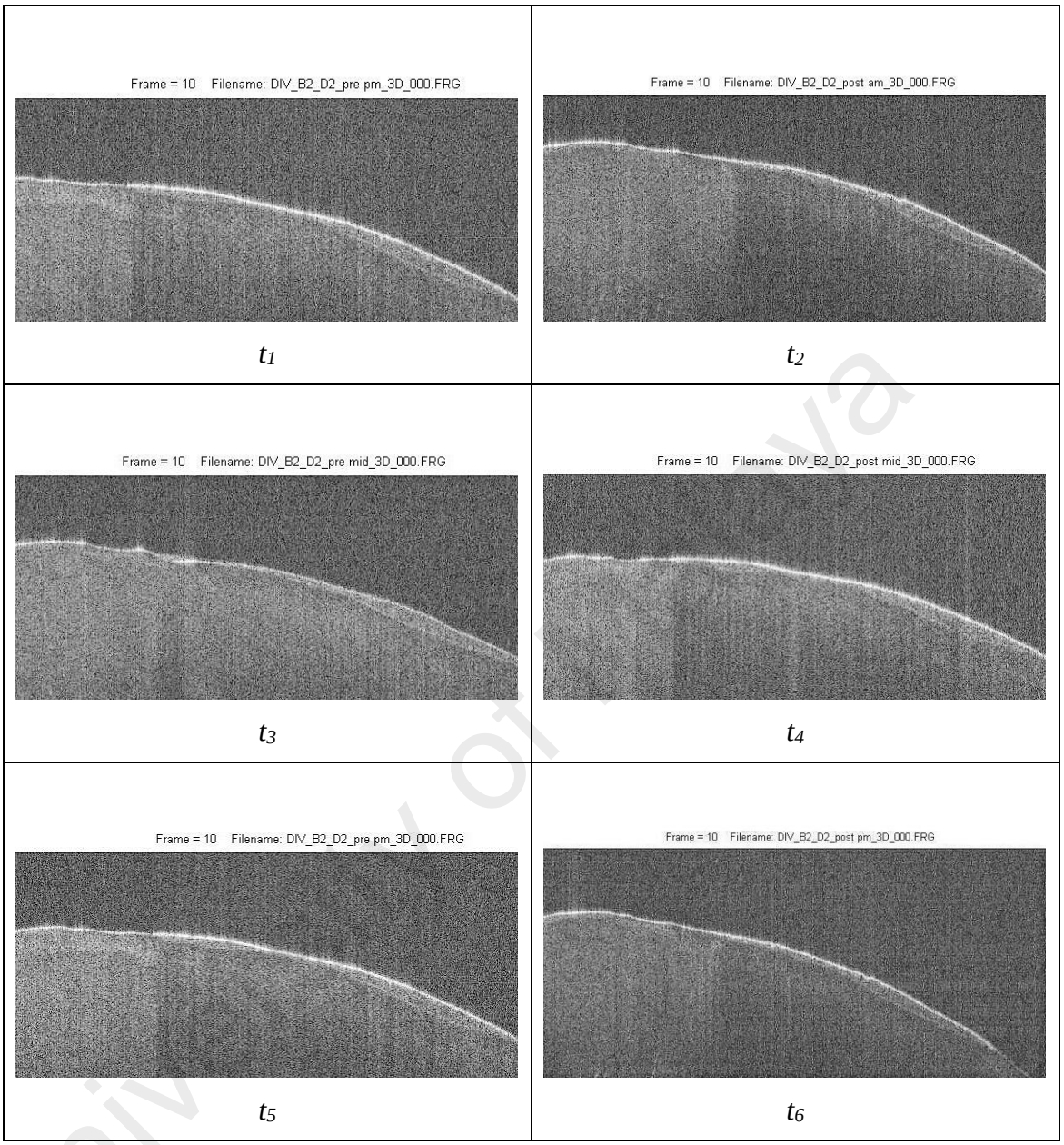

Figure 5.19: OCT B-scans of a subject's enamel surface taken at each time point, $t_1 - t_6$ at day 2 in Phase-B (subject 2).

The backscattered intensity at baseline (t_1) already showed evidence of erosion, however visual observation showed that the backscattering intensities appeared higher after swishing with orange juice for 10 mins at time points, t_2, t_4, t_6 when compared to the measurements before swishing, t_1, t_3, t_5.

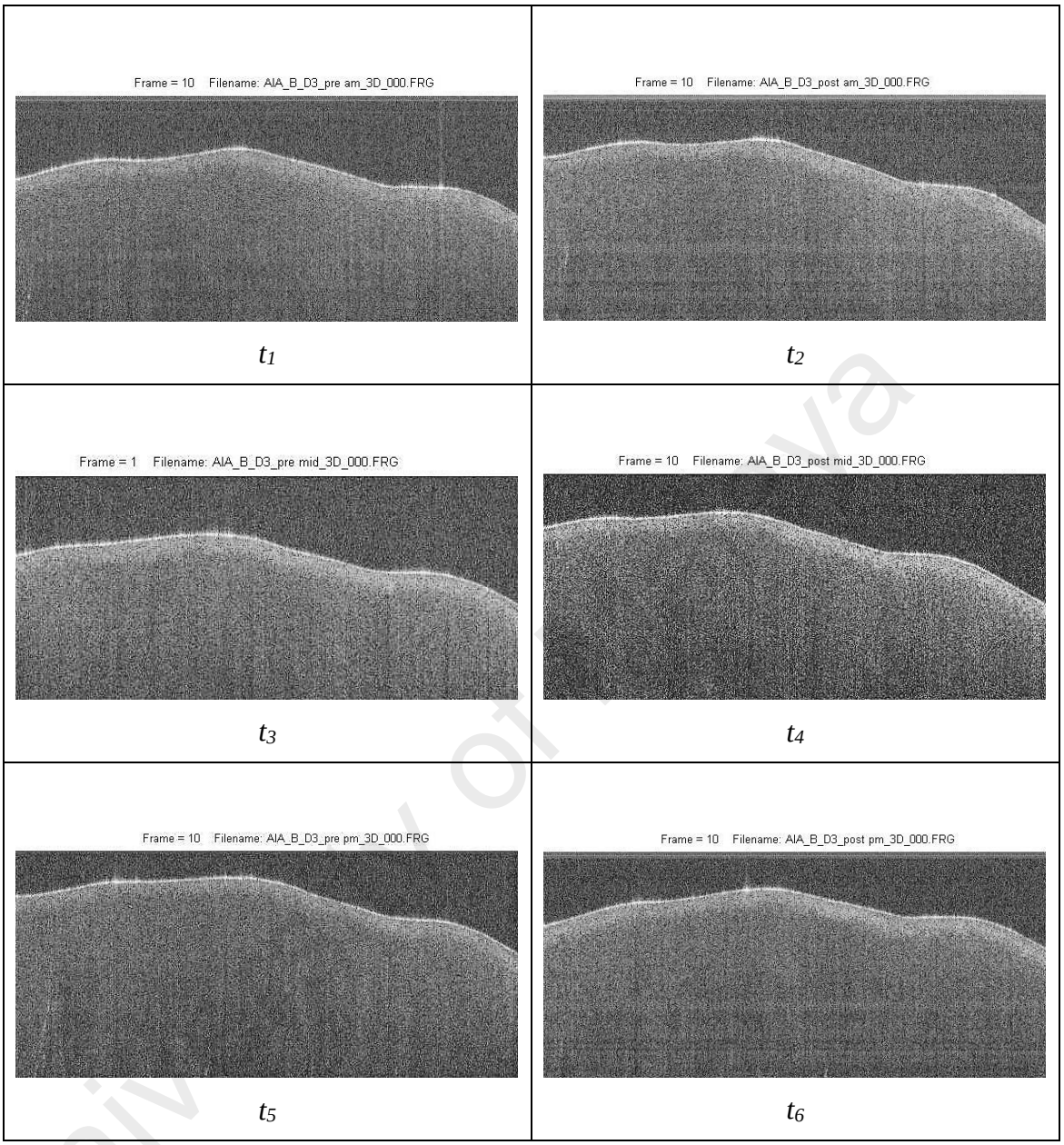

Figure 5.20: OCT B-scans of a subject's enamel surface taken at each time point, $t_1 - t_6$ at day 3 in Phase-B (subject 1).

The backscattered intensity at baseline (t_1) already showed evidence of erosion, however visual observation showed that the backscattering intensities appeared higher after swishing with orange juice for 10 mins at time points, t_2, t_4, t_6 when compared to the measurements before swishing, t_1, t_3, t_5.

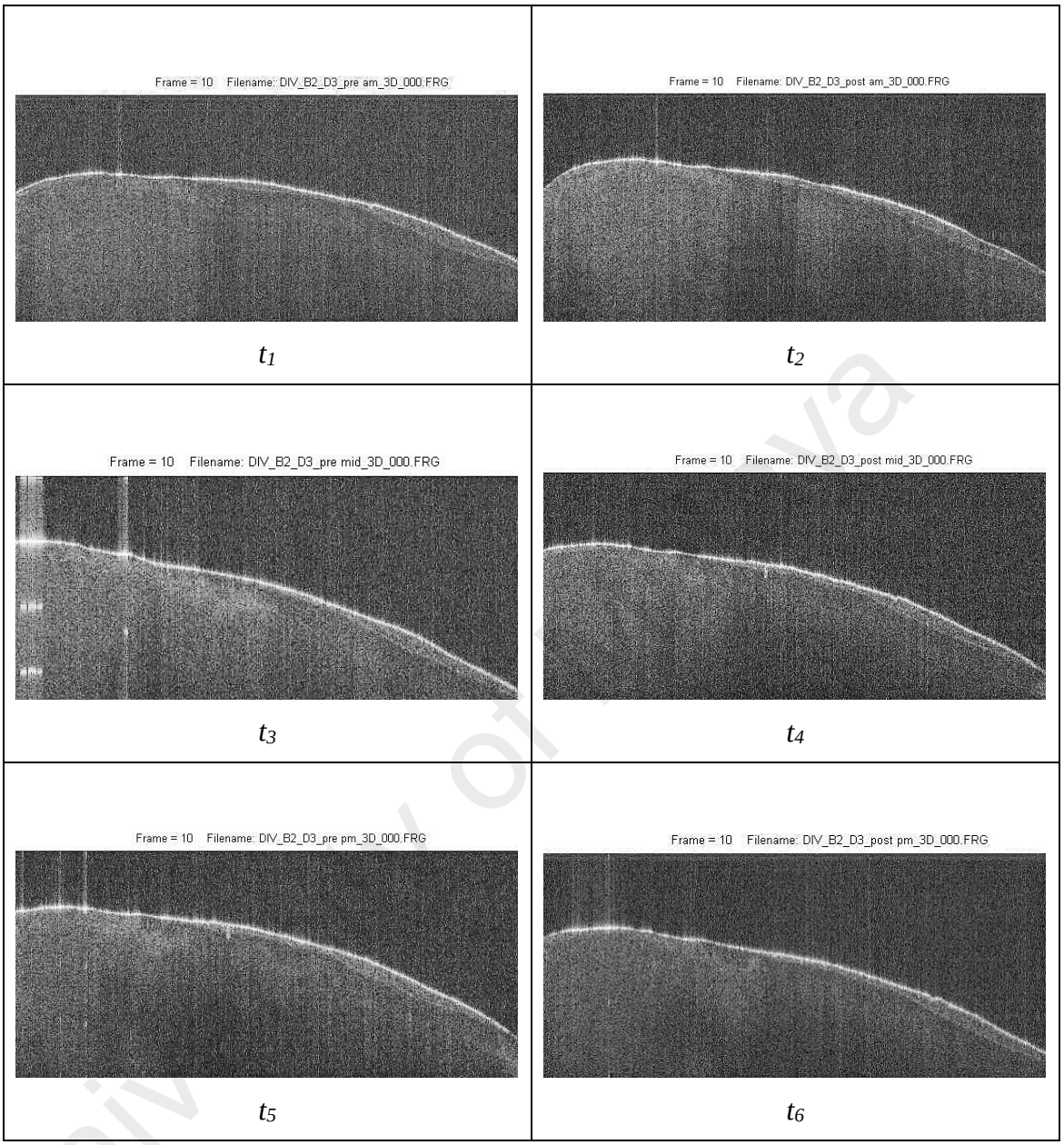

Figure 5.21: OCT B-scans of a subject's enamel surface taken at each time point, $t_1 - t_6$ at day 3 in Phase-B (subject 2).

The backscattered intensity at baseline (t_1) already showed evidence of erosion, however visual observation showed that the backscattering intensities appeared higher after swishing with orange juice for 10 mins at time points, t_2, t_4, t_6 when compared to the measurements before swishing, t_1, t_3, t_5.

Time point / Day	t_1	t_6
1	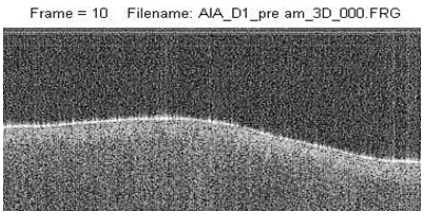	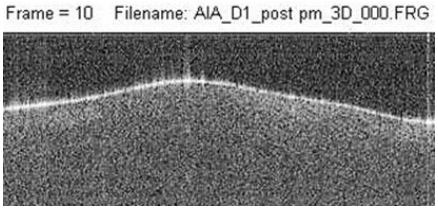
2	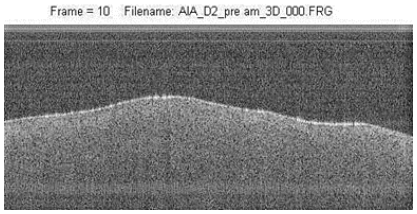	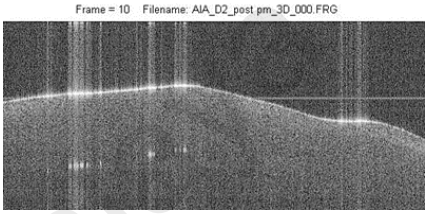
3	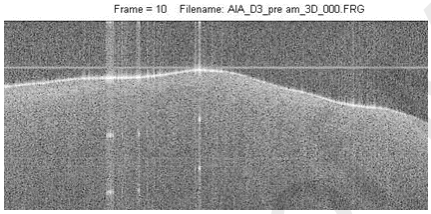	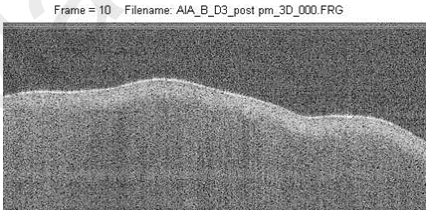

Figure 5.22: OCT B-scans of a subject's enamel surface taken at two time points (t_1 and t_6) at day 1, day 2 and day 3 in Phase-A.

The backscattered intensity at baseline (t_1) shows evidence of erosion, however visual observation showed that the backscattering intensities appeared higher after swishing with orange juice for 10 mins at time point, t_6 when compared to the first measurement of each day, t_1.

Time point / Day	t_1	t_6
1	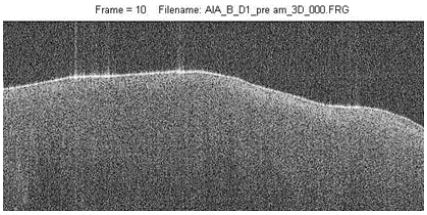	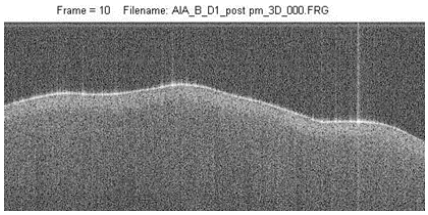
2	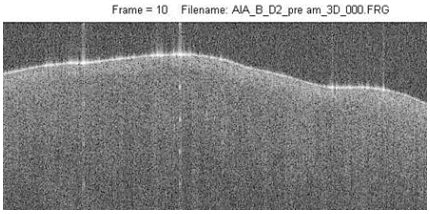	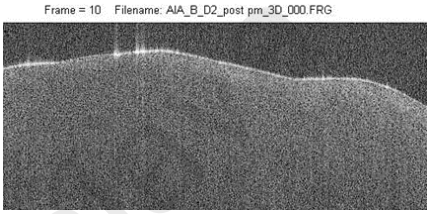
3	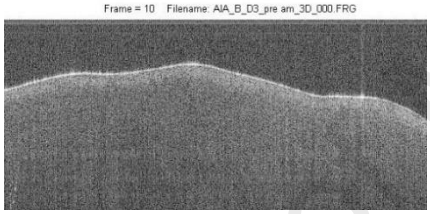	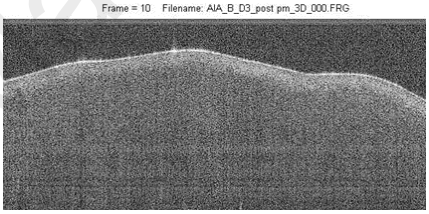

Figure 5.23: OCT B-scans of a subject's enamel surface taken at two time points (t_1 and t_6) at day 1, day 2 and day 3 in Phase-B.

The backscattered intensity at baseline (t_1) shows evidence of erosion, however visual observation showed that the backscattering intensities appeared higher after swishing with orange juice for 10 mins at time point, t_6, when compared to the first measurement of each day, t_1.

Figure 5.24 shows the graph of the IR_{sub} mean values at six consecutive time points from t_1 to t_6 for day 1, 2 and 3, of Phase-A.

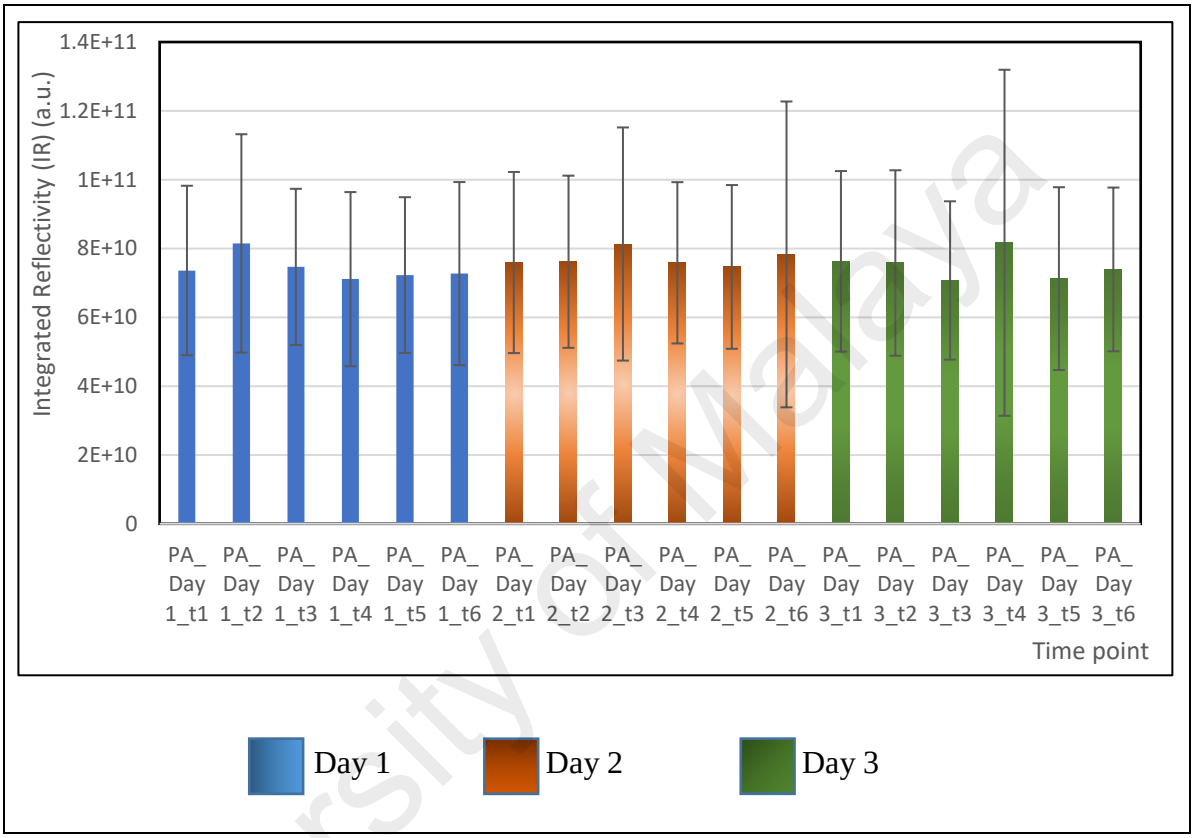

Figure 5.24: Integrated reflectivity of the enamel of maxillary incisor at all consecutive time points, $t_1 - t_6$ of Phase-A at day 1, 2 and 3.

Mean IR_{sub} ± SD of the labial enamel of maxillary incisor (N=22) at six consecutive time points, $t_1 - t_6$ of Phase-A at day 1, 2 and 3. Repeated measures ANOVA showed no statistically significant difference in the IR_{sub} at all consecutive time points in Phase-A ($p > 0.05$)

Table 5.7, **Table 5.8** and **Table 5.9** show the results of repeated measures ANOVA of Phase-A.

Table 5.7: Tests of Within-Subjects Effects Table -Phase-A - day 1, $t_1 - t_6$.

Tests of Within-Subjects Effects

Measure: MEASURE_1

Source		Type III Sum of Squares	df	Mean Square	F	Sig.	Partial Eta Squared
Time	Sphericity Assumed	1.520E+21	5	3.040E+20	1.133	.348	.051
	Greenhouse-Geisser	1.520E+21	3.430	4.432E+20	1.133	.345	.051
	Huynh-Feldt	1.520E+21	4.181	3.636E+20	1.133	.347	.051
	Lower-bound	1.520E+21	1.000	1.520E+21	1.133	.299	.051
Error(Time)	Sphericity Assumed	2.818E+22	105	2.684E+20			
	Greenhouse-Geisser	2.818E+22	72.034	3.912E+20			
	Huynh-Feldt	2.818E+22	87.807	3.209E+20			
	Lower-bound	2.818E+22	21.000	1.342E+21			

A repeated measures ANOVA with a Greenhouse-Geisser correction showed that the mean scores for IR_{sub} was not statistically significant (F(3.430, 72.034) = 1.133, p > 0.05) in Phase-A at day 1.

Table 5.8: Tests of Within-Subjects Effects Table -Phase-A - day 2, $t_1 - t_6$.

Tests of Within-Subjects Effects

Measure: MEASURE_1

Source		Type III Sum of Squares	df	Mean Square	F	Sig.	Partial Eta Squared
Time	Sphericity Assumed	6.360E+20	5	1.272E+20	.284	.921	.013
	Greenhouse-Geisser	6.360E+20	2.545	2.499E+20	.284	.805	.013
	Huynh-Feldt	6.360E+20	2.926	2.174E+20	.284	.832	.013
	Lower-bound	6.360E+20	1.000	6.360E+20	.284	.600	.013
Error(Time)	Sphericity Assumed	4.707E+22	105	4.483E+20			
	Greenhouse-Geisser	4.707E+22	53.450	8.806E+20			
	Huynh-Feldt	4.707E+22	61.442	7.661E+20			
	Lower-bound	4.707E+22	21.000	2.241E+21			

A repeated measures ANOVA with a Greenhouse-Geisser correction showed that the mean scores for IR_{sub} was not statistically significant (F(2.545, 53.450) = 0.284, p > 0.05) in Phase-A at day 2.

Table 5.9: Tests of Within-Subjects Effects Table -Phase-A - day 3, $t_1 - t_6$.

Tests of Within-Subjects Effects

Measure: MEASURE_1

Source		Type III Sum of Squares	df	Mean Square	F	Sig.	Partial Eta Squared
Time	Sphericity Assumed	1.765E+21	5	3.531E+20	1.002	.420	.046
	Greenhouse-Geisser	1.765E+21	2.805	6.295E+20	1.002	.395	.046
	Huynh-Feldt	1.765E+21	3.281	5.381E+20	1.002	.402	.046
	Lower-bound	1.765E+21	1.000	1.765E+21	1.002	.328	.046
Error(Time)	Sphericity Assumed	3.701E+22	105	3.524E+20			
	Greenhouse-Geisser	3.701E+22	58.895	6.283E+20			
	Huynh-Feldt	3.701E+22	68.901	5.371E+20			
	Lower-bound	3.701E+22	21.000	1.762E+21			

A repeated measures ANOVA with a Greenhouse-Geisser correction showed that the mean scores for IR_{sub} was not statistically significant ($F(2.805, 58.895) = 1.002$, $p > 0.05$) in Phase-A at day 3.

Figure 5.25 shows the graph of the IR_{sub} mean values at all consecutive time points from t_1 to t_6 for day 1, 2 and 3, of Phase-B.

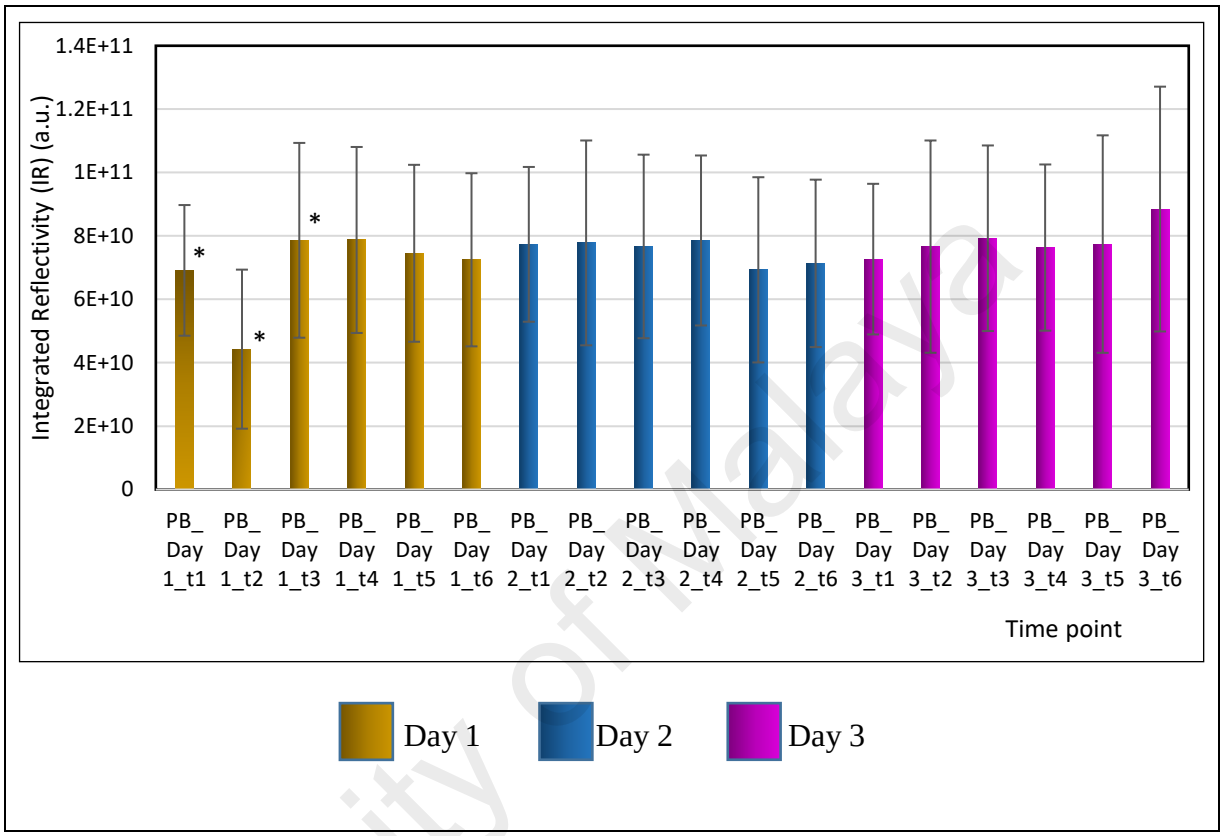

Figure 5.25: Integrated reflectivity of the enamel of maxillary incisor at all consecutive time points, $t_1 - t_6$ of Phase-B at day 1, 2 and 3

* indicates significant difference at $p < 0.05$

Mean IR_{sub} ± SD of the labial enamel of maxillary incisor (N=22) at all consecutive time points, $t_1 - t_6$ of Phase-B at day 1, 2 and 3. Repeated measures ANOVA showed statistically significant difference in the IR_{sub} between t_1 - t_2, and t_2 - t_3. ($p < 0.05$) at day 1.

Table 5.10 to **Table 5.14** show the results of repeated measures ANOVA of Phase-B.

Table 5.10: Descriptive Statistics Table for Phase-B at day 1.

Descriptive Statistics			
Phase-B – Day 1	Mean	Std. Deviation	N
t_1	6.91E+10	2.06E+10	22
t_2	4.43E+10	2.51E+10	22
t_3	7.86E+10	3.07E+10	22
t_4	7.87E+10	2.93E+10	22
t_5	7.45E+10	2.79E+10	22
t_6	7.25E+10	2.73E+10	22

Table 5.11: Tests of Within-Subjects Effects Table – Phase-B - day 1, $t_1 - t_6$.

Tests of Within-Subjects Effects

Measure: MEASURE_1

Source		Type III Sum of Squares	df	Mean Square	F	Sig.	Partial Eta Squared
Time	Sphericity Assumed	1.845E+22	5	3.690E+21	20.640	.000	.496
	Greenhouse-Geisser	1.845E+22	3.580	5.154E+21	20.640	.000	.496
	Huynh-Feldt	1.845E+22	4.406	4.187E+21	20.640	.000	.496
	Lower-bound	1.845E+22	1.000	1.845E+22	20.640	.000	.496
Error(Time)	Sphericity Assumed	1.877E+22	105	1.788E+20			
	Greenhouse-Geisser	1.877E+22	75.171	2.497E+20			
	Huynh-Feldt	1.877E+22	92.522	2.029E+20			
	Lower-bound	1.877E+22	21.000	8.938E+20			

A repeated measures ANOVA with a Greenhouse-Geisser correction showed that the mean scores for IR_{sub} was statistically significantly different ($F(3.580, 75.171) = 20.640$, $p < 0.05$) in Phase-B at day 1.

Table 5.12: Pairwise Comparisons Table Phase-B - day 1, $t_1 - t_6$

Pairwise Comparisons

Measure: MEASURE_1

(I) Time	(J) Time	Mean Difference (I-J)	Std. Error	Sig.[b]	95% Confidence Interval for Difference[b]	
					Lower Bound	Upper Bound
1	2	2.485E+10*	3639934736	.000	1.280E+10	3.690E+10
	3	-9487301914	4273403530	.563	-2.363E+10	4656447178
	4	-9593654806	5157610863	1.000	-2.666E+10	7476568832
	5	-5398809077	3899488839	1.000	-1.831E+10	7507388836
	6	-3345481140	4138780289	1.000	-1.704E+10	1.035E+10
2	1	-2.485E+10*	3639934736	.000	-3.690E+10	-1.280E+10
	3	-3.434E+10*	4570403069	.000	-4.947E+10	-1.921E+10
	4	-3.445E+10*	4911759577	.000	-5.070E+10	-1.819E+10
	5	-3.025E+10*	4215390530	.000	-4.420E+10	-1.630E+10
	6	-2.820E+10*	4331636652	.000	-4.253E+10	-1.386E+10
3	1	9487301914	4273403530	.563	-4656447178	2.363E+10
	2	3.434E+10*	4570403069	.000	1.921E+10	4.947E+10
	4	-106352892	3390756525	1.000	-1.133E+10	1.112E+10
	5	4088492837	3043673891	1.000	-5985201239	1.416E+10
	6	6141820774	4049073330	1.000	-7259459219	1.954E+10
4	1	9593654806	5157610863	1.000	-7476568832	2.666E+10
	2	3.445E+10*	4911759577	.000	1.819E+10	5.070E+10
	3	106352891.9	3390756525	1.000	-1.112E+10	1.133E+10
	5	4194845728	3576905520	1.000	-7643693236	1.603E+10
	6	6248173666	3974382310	1.000	-6905900315	1.940E+10
5	1	5398809077	3899488839	1.000	-7507388836	1.831E+10
	2	3.025E+10*	4215390530	.000	1.630E+10	4.420E+10
	3	-4088492837	3043673891	1.000	-1.416E+10	5985201239
	4	-4194845728	3576905520	1.000	-1.603E+10	7643693236
	6	2053327938	2453133107	1.000	-6065844266	1.017E+10
6	1	3345481140	4138780289	1.000	-1.035E+10	1.704E+10
	2	2.820E+10*	4331636652	.000	1.386E+10	4.253E+10
	3	-6141820774	4049073330	1.000	-1.954E+10	7259459219
	4	-6248173666	3974382310	1.000	-1.940E+10	6905900315
	5	-2053327938	2453133107	1.000	-1.017E+10	6065844266

Based on estimated marginal means

*. The mean difference is significant at the .05 level.

b. Adjustment for multiple comparisons: Bonferroni.

This table presents the results of the Bonferroni post hoc test, which allows to discover which specific means differed. It can be seen that there was a significant difference in IR_{sub} between t_1 and t_2 ($p < 0.05$), and between t_2 and t_3 ($p < 0.05$), but no significant differences between subsequent time points ($p > 0.05$) in Phase-B at day 1.

Table 5.13: Tests of Within-Subjects Effects Table -Phase-B at day 2, $t_1 - t_6$.

Tests of Within-Subjects Effects

Measure: MEASURE_1

Source		Type III Sum of Squares	df	Mean Square	F	Sig.	Partial Eta Squared
Time	Sphericity Assumed	1.638E+21	5	3.277E+20	1.282	.277	.058
	Greenhouse-Geisser	1.638E+21	2.811	5.828E+20	1.282	.289	.058
	Huynh-Feldt	1.638E+21	3.291	4.979E+20	1.282	.287	.058
	Lower-bound	1.638E+21	1.000	1.638E+21	1.282	.270	.058
Error(Time)	Sphericity Assumed	2.684E+22	105	2.556E+20			
	Greenhouse-Geisser	2.684E+22	59.039	4.545E+20			
	Huynh-Feldt	2.684E+22	69.101	3.883E+20			
	Lower-bound	2.684E+22	21.000	1.278E+21			

A repeated measures ANOVA with a Greenhouse-Geisser correction showed that the mean scores for IR_{sub} was not statistically significantly different (F(2.811, 59.039) = 1.282, p > 0.05) in Phase-B at day 2.

Table 5.14: Tests of Within-Subjects Effects Table -Phase-B at day 3, $t_1 - t_6$.

Tests of Within-Subjects Effects

Measure: MEASURE_1

Source		Type III Sum of Squares	df	Mean Square	F	Sig.	Partial Eta Squared
Time	Sphericity Assumed	3.155E+21	5	6.309E+20	2.511	.034	.107
	Greenhouse-Geisser	3.155E+21	3.044	1.036E+21	2.511	.066	.107
	Huynh-Feldt	3.155E+21	3.618	8.719E+20	2.511	.054	.107
	Lower-bound	3.155E+21	1.000	3.155E+21	2.511	.128	.107
Error(Time)	Sphericity Assumed	2.638E+22	105	2.513E+20			
	Greenhouse-Geisser	2.638E+22	63.924	4.127E+20			
	Huynh-Feldt	2.638E+22	75.981	3.472E+20			
	Lower-bound	2.638E+22	21.000	1.256E+21			

A repeated measures ANOVA with a Greenhouse-Geisser correction showed that the mean scores for IR_{sub} was not statistically significantly different (F(3.044, 63.924) = 2.511, p > 0.05) in Phase-B at day 3.

In Phase-A, repeated measures ANOVA with a Greenhouse-Geisser correction revealed no statistically significant difference between all time points in Day 1, 2 and 3 (**Table 5.7**, **Table 5.8** and **Table 5.9**). On the other hand, in Day 1 of Phase-B, repeated measures ANOVA with a Greenhouse-Geisser correction showed that mean IR_{sub} were statistically significant difference between time points ($p < 0.05$) (**Table 5.11**). Post hoc tests using the Bonferroni correction revealed that there was a statistically signficant reduction in *IR* from t_1 to t_2, and a statistically significant increased in IR_{sub} from t_2 to t_3 (6.91E+10 ± 2.06E+10, 4.43E+10 ± 2.51E+10, 7.86E+10 ± 3.07E+10, respectively) ($p < 0.05$) (**Table 5.10** and **Table 5.12**). However, there was no statistically significant difference at subsequent time points, from t_3 to t_6 ($p > 0.05$) in both day 2 and 3 of Phase-B (**Table 5.13** and **Table 5.14**).

5.4.2.2 The effect of chewing gum as an adjunct for remineralisation of initial enamel erosion at different time intervals.

For this objective, IR_{sub} was compared with the corresponding time points for both Phase-A and B (**Figure 5.26** and **Table 5.15**). A paired-samples t-test was used to determine whether there was any statistically significant mean difference between the two phases with similar time points. As shown in **Table 5.15**, there were significant difference between both Phase-A and B in Day 1 and Day 3 at t_2 and t_6, respectively, $p < 0.05$. For Day 1, results showed significant decrease in IR_{sub} whereas for Day 3, results showed significant increase in IR_{sub}.

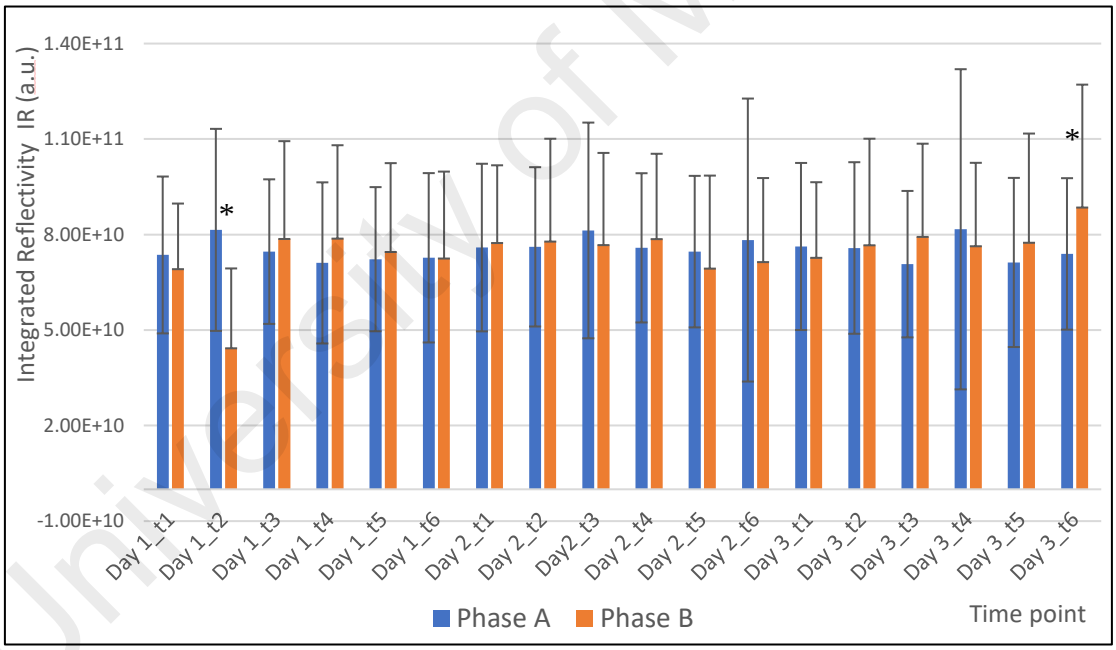

Figure 5.26: Integrated reflectivity of the labial enamel of maxillary incisor at consecutive time points, $t_1 - t_6$ for Phase-A and B at day 1, 2 and 3.

* indicates significant difference at $p < 0.05$

Mean IR_{sub} ± SD of the labial enamel of maxillary incisor (N=22) at six consecutive time points, $t_1 - t_6$ of Phase-A and Phase-B at day 1, 2 and 3. Paired t-test showed statistically significant difference in the IR_{sub} between Day 1 of Phase-A and Day 1 of Phase-B at t_1; and between Day 3 of Phase-A and Day 3 of Phase-B at t_6 ($p < 0.05$).

Table 5.15: Paired t-test between Phase-A and Phase-B at day 1, 2 and 3.

Paired Samples Test

		Paired Differences					t	df	Sig. (2-tailed)
		Mean	Std. Deviation	Std. Error Mean	95% Confidence Interval of the Difference Lower	Upper			
Pair 1	PA_Day1_t1 - PB_Day1_t1	4467587832	1.90476E+10	4060970994	-3977663671	1.29128E+10	1.100	21	.284
Pair 2	PA_Day1_t2 - PB_Day1_t2	3.72023E+10	3.22160E+10	6868471901	2.29185E+10	5.14860E+10	5.416	21	.000
Pair 3	PA_Day1_t3 - PB_Day1_t3	-3970359552	2.79621E+10	5961530249	-1.6368E+10	8427321288	-.666	21	.513
Pair 4	PA_Day1_t4 - PB_Day1_t4	-7626240010	3.55281E+10	7574615927	-2.3379E+10	8126036140	-1.007	21	.325
Pair 5	PA_Day1_t6 - PB_Day1_t5	-1821308157	2.46178E+10	5248534480	-1.2736E+10	9093616813	-.347	21	.732
Pair 6	PA_Day1_t6 - PB_Day1_t6	232019780.5	2.31382E+10	4933088885	-1.0027E+10	1.04909E+10	.047	21	.963
Pair 7	PA_Day2_t1 - PB_Day2_t1	-1421056305	2.66464E+10	5681026807	-1.3235E+10	1.03933E+10	-.250	21	.805
Pair 8	PA_Day2_t2 - PB_Day2_t2	-1648454493	2.65862E+10	5668187018	-1.3436E+10	1.01392E+10	-.291	21	.774
Pair 9	PA_Day2_t3 - PB_Day2_t3	4610581495	3.68746E+10	7861697535	-1.1739E+10	2.09599E+10	.586	21	.564
Pair 10	PA_Day2_t4 - PB_Day2_t4	-2731684413	2.29649E+10	4896138029	-1.2914E+10	7450392018	-.558	21	.583
Pair 11	PA_Day2_t5 - PB_Day2_t5	5337306815	3.65388E+10	7790096554	-1.0863E+10	2.15377E+10	.685	21	.501
Pair 12	PA_Day2_t6 - PB_Day2_t6	6932316326	3.41815E+10	7287522141	-8222915612	2.20875E+10	.951	21	.352
Pair 13	PA_Day3_t1 - PB_Day3_t1	3570498110	2.28279E+10	4866931068	-6550839120	1.36918E+10	.734	21	.471
Pair 14	PA_Day3_t2 - PB_Day3_t2	-841520988	3.38280E+10	7212156349	-1.5840E+10	1.41570E+10	-.117	21	.908
Pair 15	PA_Day3_t3 - PB_Day3_t3	-8559539228	2.07262E+10	4418841669	-1.7749E+10	629945084.1	-1.937	21	.066
Pair 16	PA_Day3_t4 - PB_Day3_t4	5331440378	3.73301E+10	7958795584	-1.1220E+10	2.18827E+10	.670	21	.510
Pair 17	PA_Day3_t5 - PB_Day3_t5	-6189338689	3.07509E+10	6556118058	-1.9824E+10	7444855191	-.944	21	.356
Pair 18	PA_Day3_t6 - PB_Day3_t6	-1.4560E+10	2.69981E+10	5756009465	-2.6530E+10	-2589709955	-2.530	21	.019

Red circles indicate significant difference at $p < 0.05$

PA = Phase-A
PB = Phase-B

5.4.3 Discussion

Given the nature of this experimental *in vivo* study, the identification of early alterations in enamel surface after exposure to acidic drinks is still a great challenge. It is suggested that large individual physiological differences in the tooth enamel of the test subjects, and/or differences in the dietary and oral hygiene routines of these individuals will affect the results, but this will also be the case in 'real life'.

The second objective of this study was to assess the ability of OCT in the detection of initial enamel erosion following acid challenge at different time intervals. From the B-scans, visual observation indicated that there was increased intensity after acid challenge. However, quantitatively, the result in Phase-A did not reveal any statistically significant changes after acid challenge (**Figure 5.24**).

However, in Phase-B, quantitative results showed statistically significant increase in IR_{sub} after the third acid challenge in day 3 of Phase-B compared to the same amount of exposure in day 3 of Phase-A (**Figure 5.26**). Specifically, the results suggested that even with chewing gum or increased salivary flow and buffering capacity, repeated exposure to acidic environment can increase demineralisation. Increased scattering resulted from an increased porosity in demineralised tissue.

OCT is a method based on measurements of the light backscattered intensity *versus* specimen depth using an interferometer set-up and a partly coherent source, the obtained signal being modulated by the optical parameters and homogenous properties of the investigated specimen, *i.e.*, the tooth (Sowa et al., 2011). OCT investigations for enamel surfaces were done at 1310 nm or 850 nm as the probing wavelength (Sowa et al., 2011). Longer wavelengths, like 1310 nm offered a greater potential for clinical optical imaging due to the weak scattering and absorption in sound dental hard tissues (Fried et al., 2011). Previous studies have also found that demineralization results in an increased

scattering of the near-infrared OCT signal in the enamel (Hariri et al., 2013; Huynh, Darling, & Fried, 2004). Austin et al. (2017) reported the first *in vivo* study to pick up these optical changes i.e. increased in scattering, during initial erosion.

When the tooth surfaces subjected to orange juice rinsing, the intensity of the backscattered OCT signal in the subsurface enamel appears slightly increased after erosion, which suggests that erosion has occurred, whereas in the *in vitro* study, the erosion was confirmed via SMH testing. Previous authors have postulated that enamel demineralization causes surface texture changes and increased subsurface enamel porosity, which can be quantitatively measured as a change in the backscattered OCT signal intensity of the OCT signal in the deep subsurface layers (Huysmans et al., 2011).

An optical diagnostic method for enamel erosion, should ideally be able to detect the earliest pathological signs such as the quantitative optical changes induced by enamel mineral loss (Amaechi, Podoleanu, et al., 2003; Chew et al., 2014; Popescu et al., 2008) or changes in surface characteristics (Austin, Mullen, & Bartlett, 2015; Huysmans et al., 2011; Rakhmatullina et al., 2011; Young & Tenuta, 2011), prior to irreversible bulk tissue loss (Wilder-Smith, Materna, Martig, & Lussi, 2015). In this way, therefore, early prevention can be initiated to prevent further loss in enamel structure.

The third objective of this study was to evaluate the effect of chewing gum as an adjunct for remineralisation of initial enamel erosion at different time intervals. At day 1 of both phases (at t_2), results of this study showed significant decreased in IR_{sub} ($p < 0.05$) which could be due to increase in salivary flow as an effect of gum chewing (**Figure 5.26**). The efficacy of sugar-free chewing gum to remineralise enamel subsurface lesions has been demonstrated in clinical trials (de Alencar et al., 2014; Prestes et al., 2013; Rios, Honorio, Magalhaes, Delbem, et al., 2006). Stimulated saliva is known to promote remineralisation of early caries lesions due to its mineral supersaturation with respect to dental hard tissue.

Several studies have shown that the chewing of sugar-substituted gum after meals and snacks promoted in situ remineralisation of experimental caries-like lesions in human and bovine enamel specimens which were mounted in the oral cavities of volunteers (Creanor et al., 1992; Leach et al., 1989; Manning, Edgar, & Agalamanyi, 1992).

In day 3 of Phase-B (at t_6) , there was a significant increase in the IR_{sub} ($p < 0.05$) after repeated swishing with orange juice compared to t_6 of Phase-A (**Figure 5.26**). If there was an increased in salivary flow (chewing gum), there should be an increase in remineralisation resulting in a reduction of backscattered intensity. However, in this study, this was not the case, at day 3. Lussi, Bossen, et al. (2012) reported that the increased in *IR* values indicated smoothing of the enamel surfaces by the soft deposited salivary pellicle layer, whereby the salivary proteins adhere to the eroded enamel surface and fill the early eroded enamel, thus, reducing the overall surface roughness. Furthermore, the optical measurements addressed the overall surface roughness, thus, the received signal corresponded to the roughness of the pellicle layer rather than the actual eroded enamel tissue underneath, resulting in the measurement artefact (Lussi, Bossen, et al., 2012).

The main biological parameters that protect the oral environment are saliva and the acquired pellicle. Saliva maintains a constant pH, and the acquired pellicle, which is rich in mucins, proteins, and free from pathogenic bacteria, forms a protective pellicle in both teeth and the mucosa (Lussi, Hellwig, Zero, & Jaeggi, 2006). The acquired pellicle works as a mediator that diminishes the direct contact of acids with the enamel surface (Hannig & Hannig, 2014). Studies have shown that pellicles formed within two hours or less offer maximum protection against erosive demineralisation, without any increase in enamel erosion prevention with longer periods of maturation (Hannig, Hess, Hoth-Hannig, & De Vrese, 2003; Wetton, Hughes, West, & Addy, 2006).

It is well established that salivary factors, such as the buffering capacity, can protect the tooth surface against oral environmental pH changes (Barbour, Lussi, & Shellis, 2011). In addition, the stimulation of salivary flow rate by chewing gum can enhance this salivary effect by an increase in bicarbonate buffer and salivary mineral content, which can facilitate mineral deposition onto the enamel surface, promoting remineralisation of the demineralised tissue at the base of the eroded surface as well as decreasing enamel loss (Gudmundsson, Kristleifsson, Theodors, & Holbrook, 1995; Nongonierma & Fitzgerald, 2012). Thus, this explanation may be applied in this study whereby, no significant changes of OCT backscattered intensity, before and after gum chewing throughout Phase-B, except for between t_1 and t_2 of day 1; and between t_5 and t_6 of day 3.

Salivary flow stimulation can yield an increase in bicarbonate buffer and in salivary mineral content, which can facilitate calcium and phosphate redeposition onto the enamel and dentine surface and reduction of dental tissue loss (Dawes, 1969). Rios, Honorio, Magalhaes, Delbem, et al. (2006) showed that saliva stimulated by the use of sugar-free chewing gum promoted a remineralising action in the erosive/abrasive phenomena.

In this study, subjects were asked to use the given fluoridated toothpaste and toothbrush prior to the start of the study, but to abstain from tooth brushing at least one hour before attending the experiment sessions. Thus, it was not assumed that the utilization of fluoridated dentifrice more than an hour before the study might promote a residual effect of fluoride and this could mask the effect of fluoride mouth rinse (Bruun, Lambrou, Larsen, Fejerskov, & Thylstrup, 1982). In addition to that, the subjects were also drinking fluoridated water, which may also give an effect. However, Bruun, Givskov, and Thylstrup (1984) reported that there was residual fluoride in saliva for more than one hour after toothbrushing with fluoridated dentifrice, compared to saliva of the placebo

dentifrice. Thus, future studies should ideally evaluate certain factors such as, the fluoride in saliva prior to onset of the *in vivo* study, increase the washout period of dentifrice, or employ non-fluoridated dentifrice.

Hara, Gonzalez-Cabezas, Creeth, and Zero (2008) reported that softened (demineralised) enamel showed less surface loss when treated with artificial saliva compared to human saliva treatment. *In situ* studies have shown the beneficial effects of saliva exposure and could be clearly seen after one hour (Attin et al., 2001; Jaeggi & Lussi, 1999).

Exposure of enamel to acid leads to a softening of the tissue and subsequent abrasion causes surface loss. Various techniques have been used to investigate these two aspects of erosive wear. Clinically, early enamel erosion is created leading to very small loss of mineral with erosive craters in a nanometre scale being formed (Attin & Wegehaupt, 2014). It is therefore reasonable to assume that the structural changes occurring under clinical conditions are much less pronounced than those observed in laboratory reports (Ganss et al., 2014) . The ability to detect such small alterations in the enamel surface would enable researchers to examine the effects after a brief acid challenge instead of the long or repeated procedures used for laboratory or *in situ* experiments that possibly do not replicate the true condition (Attin & Wegehaupt, 2014). However, it should be noted that compared to artificial saliva, an *in situ* model with fresh saliva is expected to have a different potential for remineralisation, since it contains various proteins that are thought to inhibit mineral deposition on the tooth surface (Lussi & Carvalho, 2014).

Subjects in upright position tend to cause motion or movement during measurement. It would be suggested that for future study, patients may be placed in supine position with the OCT probe placed above the subjects with a stable positioning.

This may reduce the movement of the subject during OCT measuring. However, with the use of an intra oral probe, this problem may be reduced.

Some difficulties were found during the data collection, similar to a study reported by de Barros Correia Kyotoku (2011). The main challenge was to control the production of saliva and subsequent patient movement, which tended to produce image artefacts. The problem was minimized by careful explanation to the patient and the use of the stabilization bar where subjects were asked to hold on to the metal bars during OCT imaging. However, when considering *in vivo* models, the main advantage is the exposure of the enamel specimens to the oral cavity allowing the contact with saliva, which is the most important biological factor on the aetiology of erosion.

In this study, orange juice was considered a suitable representative of citric juices for dental erosion studies and some studies have reported its erosive potential. Among those cited acids, special attention has been given to the citric acid, since it is commonly found in citric fruits and juices (Voronets & Lussi, 2010). Due to its worldwide popularity, orange juice has been considered a suitable representative of citric juices for dental erosion studies and some studies have reported its erosive potential (West, Hughes, Parker, Newcombe, & Addy, 1999; West et al., 1998).

Erosive substance loss is a dynamic process involving alternating acid demineralisation and saliva remineralisation. At early stages, softening of enamel results from partial demineralisation of tooth surface, a stage at which remineralisation of the lesion is still possible (Schlueter et al., 2011), since the remaining tissue may act as a scaffold for replacement of the lost minerals (Voronets & Lussi, 2010). Furthermore, enamel erosion occurs at a pH of approximately 5.5, depending on the concentration of calcium and phosphate in the saliva (Gudmundsson et al., 1995). In the oral environment, saliva is recognized as the most important biological factor associated with protection

against tooth erosion (Buzalaf et al., 2012), minimizing enamel wears in erosive/ abrasive attack (Amaechi & Higham, 2001a).

Of major importance for the prevention of dental erosion is the reduction of the acid exposure. The frequency and duration of acid contact might be important variables for the development of erosive lesions (Eisenburger & Addy, 2001; West, Hughes, & Addy, 2000). Moreover, the adhesiveness and displacement of liquids might influence the erosive process, as an increased adherence of an acidic substance is associated with a longer contact time on the tooth. The ability of beverages to adhere on enamel is based on their thermodynamic properties (Ireland, McGuinness, & Sherriff, 1995).

5.4.4 Conclusions

Within the limitation of this study, the following conclusions can be drawn.

1. Higher intensities observed from the B-scans following acid challenges indicated that OCT could detect initial enamel erosion, however quantitatively there was no significant difference.
2. OCT did not detect the change in enamel backscattering after gum chewing.

CHAPTER 6: SUMMARY

OCT is a non-invasive, cross-sectional imaging system that can visualize the internal structures non-destructively. It was developed on the concept of low-coherence interferometry where the light is projected over a sample, and the backscattered signal intensity from the scattering medium reveals depth-resolved information about the scattering and reflection of the light in the sample. It generates cross-sectional images by performing multiple axial measurements of echo time delay (axial scans or A-scans) and scanning the incident optical beam transversely. A two-dimensional data set, which represents the optical backscattering in a cross-sectional plane through the tissue, is produced. Images or B-scans can be displayed in a false colour or grey scale to visualize tissue changes. A definitive goal of the studies embraced and depicted in this thesis was to look for a suitable device that could be utilized in clinical trials to assess the efficacy of interventions intended to lessen the rate of dental erosion.

The key beneficial features of OCT are that it provides live subsurface images at near-microscopic resolution, instant and direct imaging of tissue morphology and it employs nonionizing radiation. However, the main disadvantage of OCT is that the acquisition of the device requires relatively high cost. Therefore, cost effectiveness needs to be considered before using this technology for clinical studies and eventual routine clinical use.

In this thesis, OCT was investigated for quantitative assessment of initial enamel erosion in *in vitro* and *in vivo* studies. The *in vitro* study established a preliminary relationship between non-destructive OCT measurement and a current (destructive) gold-standard of microhardness testing; this allowed for confident conclusions regarding demineralisation responses. Together, these *in vitro* and *in vivo* research efforts suggested that OCT imaging may be an effective tool for longitudinal monitoring of hard tissue

conditions in the human oral cavity, that can be used in a clinical trial. Furthermore, the OCT technique is promising for detecting, diagnosing and monitoring erosive enamel lesion; however, further *in vitro* and *in vivo* research is needed to improve its use.

OCT signal patterns may be important for clinical diagnosis of initial erosion and measurement of structural depth for operative purposes using this technology. The higher backscattered intensity indicates more loss of enamel content due to acid exposure. However, in this study, the backscattered intensity has not been correlated to the amount of tooth substance lost.

The difficulties confronting clinical trials that evaluate early erosion are altogether different from clinical trials that set out to assess the viability of anti-caries agents. To date, one fundamental difficulty is the elusiveness of a definite description of the clinical presentation of erosive wear. At the point when a cavitated carious lesion is distinguished, one is sure that the injury is in actuality brought on by caries and not by some other means.

6.1 Overall conclusion

As a conclusion, results of this study further suggest that OCT has the potential for the non-invasive *in vivo* detection of early surface events occurring during dietary erosion. In addition, this study has generated information regarding the potential of OCT in the detection of initial enamel erosion *in vivo.* Higher intensities observed from the B-scans following acid challenges indicated that OCT could detect initial enamel erosion, however, quantitatively, no significant difference was observed.

Therefore, with regards to the overarching goal of this study, it is hoped that this will contribute to the availability of an objective tool to be used in clinical trials as well as in oral health surveys. Furthermore, it can be one of the methods developed to measure

the efficacy of interventions to prevent or reduce tooth erosion—an important step towards extending the life of teeth to match the increasing human lifespan.

6.2 Limitations of the study

In vivo studies allow analyses to be carried out under more realistic conditions, because they are conducted in an attempt to reproduce the process under the influence of biological factors in the oral cavity, such as saliva temperature, enzymes, and microorganisms. In the current study, the intra-oral model allowed the action of saliva and this may have been crucial for the findings observed. OCT unit used in this study was more suitable for an *in vitro* or *in situ* study. Thus, the scanning probe was modified in such a way to be used in an *in vivo* study where subjects were not sitting on a dental chair during OCT scanning. If this machine/instrument/equipment is to be recommended for clinical use, it is more appropriate to use the intra-oral probe. However, reproducible position of the probe is very crucial when designing the clinical study.

Within the limitation of these *in vitro* and *in vivo* studies, it is hoped that OCT can be a suitable diagnostic instrument for monitoring initial enamel erosion *in vivo* for a clinical trial. The employment of an appropriate intra-oral hand-piece compatible with the oral cavity, accompanied with a faster software image acquisition and possibly better penetration depths is certainly the way to bring this device to a clinical environment. Thus, this technology will potentially expand to clinical practice and improve prevention and diagnostics pertaining to dental erosion for long-term benefit to dental professionals and the patients. Furthermore, patients can be empowered with the knowledge that erosion are reversible and can be managed by improved dietary habits, risk management and preventive regimes.

6.3 Recommendation for future studies

Suggestions for future studies are as following:

1. Future studies are required, to elucidate, quantify, characterize the exact nature of surface events occurring *in vivo* during enamel erosion, and how these events result in changes in the optical properties of the enamel.

2. Further research is needed to evaluate the influence of possible preventive measures against abrasion for patients suffering from erosion. Rinsing with water or fluoride solutions in order to neutralize and to dilute acids as well as chewing gum to stimulate the secretion of saliva, with or without neutralizing mineral content, may be possible supplementary precautions to minimize the risk for lesions by toothbrush abrasion after erosive attacks. Such measures might make it possible to reduce the above-recommended intraoral exposure interval between an erosive attack and toothbrushing. Also, further work will be needed to show the risk of toothbrush abrasion and its prevention for special population groups with active erosive lesions such as patients suffering from anorexia nervosa and bulimia nervosa.

3. Future *in vivo* OCT studies may employ a robust standardisation of the relative levels of tooth hydration, in order to prevent confounding of possible changes in the enamel OCT signal from an acid challenge.

REFERENCES

Ablal, M. A., Milosevic, A., Preston, A. J., & Higham, S. M. (2017). A novel approach to study in situ enamel erosion and abrasion lesions. *J Dent, 59*, 78-85.

Addy, M. (2005). Tooth brushing, tooth wear and dentine hypersensitivity--are they associated? *Int Dent J, 55*(4 Suppl 1), 261-267.

Addy, M., & Shellis, R. P. (2006). Interaction between attrition,abrasion and erosion in tooth wear. *Monogr Oral Sci, 20*, 17-31.

Adhi, M., & Duker, J. S. (2013). Optical coherence tomography--current and future applications. *Curr Opin Ophthalmol, 24*(3), 213-221.

Aggarwal, A., Panat, S., Agarwal, N., Sowmya, G., Alok, A., & Kishore, M. (2013). Optical coherence tomography: an emerging perspective. *J Dent Sci Oral Rehabil*, 4-7.

Aiuchi, H., Kitasako, Y., Fukuda, Y., Nakashima, S., Burrow, M. F., & Tagami, J. (2008). Relationship between quantitative assessments of salivary buffering capacity and ion activity product for hydroxyapatite in relation to cariogenic potential. *Aust Dent J, 53*(2), 167-171.

Al-Ahmad, A., Wunder, A., Auschill, T. M., Follo, M., Braun, G., Hellwig, E., & Arweiler, N. B. (2007). The in vivo dynamics of Streptococcus spp., Actinomyces naeslundii, Fusobacterium nucleatum and Veillonella spp. in dental plaque biofilm as analysed by five-colour multiplex fluorescence in situ hybridization. *J Med Microbiol, 56*(Pt 5), 681-687.

Al-Dlaigan, Y. H., Shaw, L., & Smith, A. (2001). Dental erosion in a group of British 14-year-old school children. Part II: Influence of dietary intake. *Br Dent J, 190*(5), 258-261.

Al-Malik, M. I., Holt, R. D., & Bedi, R. (2001). Clinical and photographic assessment of erosion in 2-5-year-old children in Saudi Arabia. *Community Dent Health, 18*(4), 232-235.

Al-Malik, M. I., Holt, R. D., & Bedi, R. (2002). Erosion, caries and rampant caries in preschool children in Jeddah, Saudi Arabia. *Community Dent Oral Epidemiol, 30*(1), 16-23.

Al-Malik, M. I., Holt, R. D., Bedi, R., & Speight, P. M. (2001). Investigation of an index to measure tooth wear in primary teeth. *J Dent, 29*(2), 103-107.

Al-Mubarak, S., Ciancio, S., Aljada, A., Mohanty, P., Ross, C., & Dandona, P. (2002). Comparative evaluation of adjunctive oral irrigation in diabetics. *J Clin Periodontol, 29*(4), 295-300.

Al-Salihi, K., & Tarmidzi, N. (2009). Preliminary study of In vivo formed dental plaque using confocal microscopy and scanning electron microscopy. *Journal of Dentistry of Tehran University of Medical Sciences, 6*(4), 159-167.

Algarni, A., Kang, H., Fried, D., Eckert, G. J., & Hara, A. T. (2016). Enamel Thickness Determination by Optical Coherence Tomography: In vitro Validation. *Caries Res, 50*(4), 400-406.

Amaechi, B. T., & Higham, S. M. (2001a). Eroded enamel lesion remineralization by saliva as a possible factor in the site-specificity of human dental erosion. *Arch Oral Biol, 46*(8), 697-703.

Amaechi, B. T., & Higham, S. M. (2001b). In vitro remineralisation of eroded enamel lesions by saliva. *J Dent, 29*(5), 371-376.

Amaechi, B. T., & Higham, S. M. (2005). Dental erosion: possible approaches to prevention and control. *J Dent, 33*(3), 243-252.

Amaechi, B. T., Higham, S. M., & Edgar, W. M. (2003). Influence of abrasion in clinical manifestation of human dental erosion. *J Oral Rehabil, 30*(4), 407-413.

Amaechi, B. T., Higham, S. M., Edgar, W. M., & Milosevic, A. (1999). Thickness of acquired salivary pellicle as a determinant of the sites of dental erosion. *J Dent Res, 78*(12), 1821-1828.

Amaechi, B. T., Higham, S. M., Podoleanu, A. G., Rogers, J. A., & Jackson, D. A. (2001). Use of optical coherence tomography for assessment of dental caries: quantitative procedure. *J Oral Rehabil, 28*(12), 1092-1093.

Amaechi, B. T., Podoleanu, A., Higham, S. M., & Jackson, D. A. (2003). Correlation of quantitative light-induced fluorescence and optical coherence tomography applied for detection and quantification of early dental caries. *J Biomed Opt, 8*(4), 642-647.

Anderson, P., & Elliott, J. C. (2000). Rates of mineral loss in human enamel during in vitro demineralization perpendicular and parallel to the natural surface. *Caries Res, 34*(1), 33-40.

Anderson, P., Levinkind, M., & Elliot, J. C. (1998). Scanning microradiographic studies of rates of in vitro demineralization in human and bovine dental enamel. *Arch Oral Biol, 43*(8), 649-656.

Ando, M., Hall, A. F., Eckert, G. J., Schemehorn, B. R., Analoui, M., & Stookey, G. K. (1997). Relative ability of laser fluorescence techniques to quantitate early mineral loss in vitro. *Caries Res, 31*(2), 125-131.

Angmar-Mansson, B., & ten Bosch, J. J. (1987). Optical methods for the detection and quantification of caries. *Adv Dent Res, 1*(1), 14-20.

Angmar-Mansson, B., & ten Bosch, J. J. (2001). Quantitative light-induced fluorescence (QLF): a method for assessment of incipient caries lesions. *Dentomaxillofac Radiol, 30*(6), 298-307.

Arends, J., Ruben, J. L., & Inaba, D. (1997). Major topics in quantitative microradiography of enamel and dentin: R parameter, mineral distribution visualization, and hyper-remineralization. *Adv Dent Res, 11*(4), 403-414.

Arends, J., & ten Bosch, J. J. (1992). Demineralization and remineralization evaluation techniques. *J Dent Res, 71 Spec No*, 924-928.

Arnadottir, I. B., Saemundsson, S. R., & Holbrook, W. P. (2003). Dental erosion in Icelandic teenagers in relation to dietary and lifestyle factors. *Acta Odontol Scand, 61*(1), 25-28.

Arweiler, N. B., Netuschil, L., Beier, D., Grunert, S., Heumann, C., Altenburger, M. J., . . . Auschill, T. M. (2014). Action of food preservatives on 14-days dental biofilm formation, biofilm vitality and biofilm-derived enamel demineralisation in situ. *Clin Oral Investig, 18*(3), 829-838.

Attin, T. (2006). Methods for assessment of dental erosion. *Monogr Oral Sci, 20*, 152-172.

Attin, T., Buchalla, W., Gollner, M., & Hellwig, E. (2000). Use of variable remineralization periods to improve the abrasion resistance of previously eroded enamel. *Caries Res, 34*(1), 48-52.

Attin, T., Knofel, S., Buchalla, W., & Tutuncu, R. (2001). In situ evaluation of different remineralization periods to decrease brushing abrasion of demineralized enamel. *Caries Res, 35*(3), 216-222.

Attin, T., Koidl, U., Buchalla, W., Schaller, H. G., Kielbassa, A. M., & Hellwig, E. (1997). Correlation of microhardness and wear in differently eroded bovine dental enamel. *Arch Oral Biol, 42*(3), 243-250.

Attin, T., Meyer, K., Hellwig, E., Buchalla, W., & Lennon, A. M. (2003). Effect of mineral supplements to citric acid on enamel erosion. *Arch Oral Biol, 48*(11), 753-759.

Attin, T., & Wegehaupt, F. J. (2014). Methods for assessment of dental erosion. *Monogr Oral Sci, 25*, 123-142.

Auschill, T. M., Arweiler, N. B., Brecx, M., Reich, E., Sculean, A., & Netuschil, L. (2002). The effect of dental restorative materials on dental biofilm. *Eur J Oral Sci, 110*(1), 48-53.

Auschill, T. M., Hein, N., Hellwig, E., Follo, M., Sculean, A., & Arweiler, N. B. (2005). Effect of two antimicrobial agents on early in situ biofilm formation. *J Clin Periodontol, 32*(2), 147-152.

Austin, R. S., Giusca, C. L., Macaulay, G., Moazzez, R., & Bartlett, D. W. (2016). Confocal laser scanning microscopy and area-scale analysis used to quantify enamel surface textural changes from citric acid demineralization and salivary remineralization in vitro. *Dent Mater, 32*(2), 278-284.

Austin, R. S., Haji Taha, M., Festy, F., Cook, R., Andiappan, M., Gomez, J., . . . Moazzez, R. (2017). Quantitative Swept-Source Optical Coherence Tomography of Early Enamel Erosion in vivo. *Caries Res, 51*(4), 410-418.

Austin, R. S., Mullen, F., & Bartlett, D. W. (2015). Surface texture measurement for dental wear applications. *Surface Topography: Metrology and Properties, 3*(2), 023002.

Avanaki, M. R., Bradu, A., Trifanov, I., Ribeiro, A. B. L., Hojjatoleslami, A., & Podoleanu, A. G. (2013). Algorithm for excitation optimization of Fabry–Pérot filters used in swept sources. *Ieee Photonics Technology Letters, 25*(5), 472-475.

Axelsson, P., Albandar, J. M., & Rams, T. E. (2002). Prevention and control of periodontal diseases in developing and industrialized nations. *Periodontol 2000, 29*, 235-246.

Aykut-Yetkiner, A., Wiegand, A., Bollhalder, A., Becker, K., & Attin, T. (2013). Effect of acidic solution viscosity on enamel erosion. *J Dent Res, 92*(3), 289-294.

Azeredo, J., Azevedo, N. F., Briandet, R., Cerca, N., Coenye, T., Costa, A. R., . . . Sternberg, C. (2017). Critical review on biofilm methods. *Crit Rev Microbiol, 43*(3), 313-351.

Azzopardi, A., Bartlett, D. W., Watson, T. F., & Sherriff, M. (2004). The surface effects of erosion and abrasion on dentine with and without a protective layer. *Br Dent J, 196*(6), 351-354; discussion 339.

Azzopardi, A., Bartlett, D. W., Watson, T. F., & Smith, B. G. (2000). A literature review of the techniques to measure tooth wear and erosion. *Eur J Prosthodont Restor Dent, 8*(3), 93-97.

Bakhsh, T. A., Sadr, A., Shimada, Y., Tagami, J., & Sumi, Y. (2011). Non-invasive quantification of resin-dentin interfacial gaps using optical coherence tomography: validation against confocal microscopy. *Dent Mater, 27*(9), 915-925.

Bakke, R., Kommedal, R., & Kalvenes, S. (2001). Quantification of biofilm accumulation by an optical approach. *J Microbiol Methods, 44*(1), 13-26.

Bakry, A. S., Marghalani, H. Y., Amin, O. A., & Tagami, J. (2014). The effect of a bioglass paste on enamel exposed to erosive challenge. *J Dent, 42*(11), 1458-1463.

Balas, C. (2009). Review of biomedical optical imaging—a powerful, non-invasive, non-ionizing technology for improving in vivo diagnosis. *Measurement Science and Technology, 20*(10), 104020.

Barbour, M. E., Finke, M., Parker, D. M., Hughes, J. A., Allen, G. C., & Addy, M. (2006). The relationship between enamel softening and erosion caused by soft drinks at a range of temperatures. *J Dent, 34*(3), 207-213.

Barbour, M. E., Lussi, A., & Shellis, R. P. (2011). Screening and prediction of erosive potential. *Caries Res, 45 Suppl 1*, 24-32.

Barbour, M. E., Parker, D. M., Allen, G. C., & Jandt, K. D. (2003a). Enamel dissolution in citric acid as a function of calcium and phosphate concentrations and degree of saturation with respect to hydroxyapatite. *Eur J Oral Sci, 111*(5), 428-433.

Barbour, M. E., Parker, D. M., Allen, G. C., & Jandt, K. D. (2003b). Human enamel dissolution in citric acid as a function of pH in the range 2.30< or =pH< or =6.30--a nanoindentation study. *Eur J Oral Sci, 111*(3), 258-262.

Barbour, M. E., Parker, D. M., Allen, G. C., & Jandt, K. D. (2005). Human enamel erosion in constant composition citric acid solutions as a function of degree of saturation with respect to hydroxyapatite. *J Oral Rehabil, 32*(1), 16-21.

Barbour, M. E., Parker, D. M., & Jandt, K. D. (2003). Enamel dissolution as a function of solution degree of saturation with respect to hydroxyapatite: a nanoindentation study. *J Colloid Interface Sci, 265*(1), 9-14.

Barbour, M. E., & Rees, J. S. (2004). The laboratory assessment of enamel erosion: a review. *J Dent, 32*(8), 591-602.

Bardolia, P., Burnside, G., Ashcroft, A., Milosevic, A., Goodfellow, S. A., Rolfe, E. A., & Pine, C. M. (2010). Prevalence and risk indicators of erosion in thirteen- to fourteen-year-olds on the Isle of Man. *Caries Res, 44*(2), 165-168.

Barlow, A. P., Sufi, F., & Mason, S. C. (2009). Evaluation of different fluoridated dentifrice formulations using an in situ erosion remineralization model. *J Clin Dent, 20*(6), 192-198.

Barnes, C. M., Russell, C. M., Reinhardt, R. A., Payne, J. B., & Lyle, D. M. (2005). Comparison of irrigation to floss as an adjunct to tooth brushing: effect on bleeding, gingivitis, and supragingival plaque. *J Clin Dent, 16*(3), 71-77.

Barron, R. P., Carmichael, R. P., Marcon, M. A., & Sandor, G. K. (2003). Dental erosion in gastroesophageal reflux disease. *J Can Dent Assoc, 69*(2), 84-89.

Bartlett, D. W., Blunt, L., & Smith, B. G. (1997). Measurement of tooth wear in patients with palatal erosion. *Br Dent J, 182*(5), 179-184.

Bartlett, D. W., Bureau, G. P., & Anggiansah, A. (2003). Evaluation of the pH of a new carbonated soft drink beverage: an in vivo investigation. *J Prosthodont, 12*(1), 21-25.

Bartlett, D. W., Ganss, C., & Lussi, A. (2008). Basic Erosive Wear Examination (BEWE): a new scoring system for scientific and clinical needs. *Clin Oral Investig, 12 Suppl 1*, S65-68.

Bartlett, D. W., Lussi, A., West, N. X., Bouchard, P., Sanz, M., & Bourgeois, D. (2013). Prevalence of tooth wear on buccal and lingual surfaces and possible risk factors in young European adults. *J Dent, 41*(11), 1007-1013.

Baumgartner, A., Dichtl, S., Hitzenberger, C. K., Sattmann, H., Robl, B., Moritz, A., . . . Sperr, W. (2000). Polarization-sensitive optical coherence tomography of dental structures. *Caries Res, 34*(1), 59-69.

Bernardi, G., Giro, M. G., & Gaillard, C. (1972). Chromatography of polypeptides and proteins on hydroxyapatite columns: some new developments. *Biochim Biophys Acta, 278*(3), 409-420.

Bhaskar, S. N., Cutright, D. E., & Frisch, J. (1969). Effect of high pressure water jet on oral mucosa of varied density. *J Periodontol, 40*(10), 593-598.

Billings, N., Birjiniuk, A., Samad, T. S., Doyle, P. S., & Ribbeck, K. (2015). Material properties of biofilms-a review of methods for understanding permeability and mechanics. *Rep Prog Phys, 78*(3), 036601.

Bishop, K., Kelleher, M., Briggs, P., & Joshi, R. (1997). Wear now? An update on the etiology of tooth wear. *Quintessence Int, 28*(5), 305-313.

Blauert, F., Horn, H., & Wagner, M. (2015). Time-resolved biofilm deformation measurements using optical coherence tomography. *Biotechnol Bioeng, 112*(9), 1893-1905.

Braly, A., Darnell, L. A., Mann, A. B., Teaford, M. F., & Weihs, T. P. (2007). The effect of prism orientation on the indentation testing of human molar enamel. *Arch Oral Biol, 52*(9), 856-860.

Brand, H. S., Gambon, D. L., Paap, A., Bulthuis, M. S., Veerman, E. C., & Amerongen, A. V. (2009). The erosive potential of lollipops. *Int Dent J, 59*(6), 358-362.

Brand, H. S., Tjoe Fat, G. M., & Veerman, E. C. (2009). The effects of saliva on the erosive potential of three different wines. *Aust Dent J, 54*(3), 228-232.

Brauer, D. S., Karpukhina, N., Law, R. V., & Hill, R. G. (2009). Structure of fluoride-containing bioactive glasses. *Journal of Materials Chemistry, 19*(31), 5629-5636.

Brauer, D. S., Karpukhina, N., O'Donnell, M. D., Law, R. V., & Hill, R. G. (2010). Fluoride-containing bioactive glasses: effect of glass design and structure on degradation, pH and apatite formation in simulated body fluid. *Acta Biomater, 6*(8), 3275-3282.

Brevik, S. C., Lussi, A., & Rakhmatullina, E. (2013). A new optical detection method to assess the erosion inhibition by in vitro salivary pellicle layer. *J Dent, 41*(5), 428-435.

Brunk, U., Collins, V. P., & Arro, E. (1981). The fixation, dehydration, drying and coating of cultured cells of SEM. *J Microsc, 123*(Pt 2), 121-131.

Bruun, C., Givskov, H., & Thylstrup, A. (1984). Whole saliva fluoride after toothbrushing with NaF and MFP dentifrices with different F concentrations. *Caries Res, 18*(3), 282-288.

Bruun, C., Lambrou, D., Larsen, M. J., Fejerskov, O., & Thylstrup, A. (1982). Fluoride in mixed human saliva after different topical fluoride treatments and possible relation to caries inhibition. *Community Dent Oral Epidemiol, 10*(3), 124-129.

Buczkowska-Radlinska, J., Lagocka, R., Kaczmarek, W., Gorski, M., & Nowicka, A. (2013). Prevalence of dental erosion in adolescent competitive swimmers exposed to gas-chlorinated swimming pool water. *Clin Oral Investig, 17*(2), 579-583.

Bunting, R. (1928). Studies of the relation of Bacillus acidophilus to dental caries. *JD Res, 8*, 222.

Buzalaf, M. A., Hannas, A. R., & Kato, M. T. (2012). Saliva and dental erosion. *J Appl Oral Sci, 20*(5), 493-502.

Cara, A. C., Zezell, D. M., Ana, P. A., Maldonado, E. P., & Freitas, A. Z. (2014). Evaluation of two quantitative analysis methods of optical coherence tomography for detection of enamel demineralization and comparison with microhardness. *Lasers Surg Med, 46*(9), 666-671.

Cardoso, C. A., Magalhaes, A. C., Rios, D., & Lima, J. E. (2009). Cross-sectional hardness of enamel from human teeth at different posteruptive ages. *Caries Res, 43*(6), 491-494.

Carvalho, T. S., Colon, P., Ganss, C., Huysmans, M. C., Lussi, A., Schlueter, N., . . . Wiegand, A. (2016). Consensus Report of the European Federation of Conservative Dentistry: Erosive tooth wear diagnosis and management. *Swiss Dent J, 126*(4), 342-346.

Carvalho, T. S., Colon, P., Ganss, C., Huysmans, M. C., Lussi, A., Schlueter, N., . . . Wiegand, A. (2015). Consensus report of the European Federation of Conservative Dentistry: erosive tooth wear--diagnosis and management. *Clin Oral Investig, 19*(7), 1557-1561.

Cassimiro-Silva, P. F., Maia, A. M. A., Monteiro, G. Q. d. M., & Gomes, A. S. L. (2016). *Mitigation of enamel erosion using commercial toothpastes evaluated with optical coherence tomography.* Paper presented at the Sixth International Conference on Lasers in Medicine.

Ceci, M., Mirando, M., Beltrami, R., Chiesa, M., Colombo, M., & Poggio, C. (2016). Effect of self-assembling peptide P11 -4 on enamel erosion: AFM and SEM studies. *Scanning, 38*(4), 344-351.

Chan, K. H., Chan, A. C., Darling, C. L., & Fried, D. (2013). Methods for Monitoring Erosion Using Optical Coherence Tomography. *Proc SPIE Int Soc Opt Eng, 8566*, 856606.

Chan, K. H., Chan, A. C., Fried, W. A., Simon, J. C., Darling, C. L., & Fried, D. (2015). Use of 2D images of depth and integrated reflectivity to represent the severity of demineralization in cross-polarization optical coherence tomography. *J Biophotonics, 8*(1-2), 36-45.

Chapple, I. L., & Gilbert, A. D. (2002). *Understanding periodontal diseases: Assessment and diagnostic procedures in practice.* (6th ed.): London: Quintessence Pub. Co.

Chehal, H. K., Pate, D. H., Cohen, D. M., & Bhattacharyya, I. (2009). Dental erosion due to excessive wine consumption. *Gen Dent, 57*(5), 519-523.

Chen, Y., Otis, L., Piao, D., & Zhu, Q. (2005). Characterization of dentin, enamel, and carious lesions by a polarization-sensitive optical coherence tomography system. *Appl Opt, 44*(11), 2041-2048.

Cheng, Z. J., Wang, X. M., Cui, F. Z., Ge, J., & Yan, J. X. (2009). The enamel softening and loss during early erosion studied by AFM, SEM and nanoindentation. *Biomed Mater, 4*(1), 015020.

Chetrus, V., & Ion, I. R. (2013). Dental plaque–classification, formation and identification. *Int J Med Dent, 3*(2), 139-143.

Chew, H. P. (2013). *Novel Assessments of Early Enamel Erosion.* University of Manchester.

Chew, H. P., Zakian, C. M., Pretty, I. A., & Ellwood, R. P. (2014). Measuring initial enamel erosion with quantitative light-induced fluorescence and optical coherence tomography: an in vitro validation study. *Caries Res, 48*(3), 254-262.

Chiego, D. J. (2018). *Essentials of Oral Histology and Embryology E-Book: A Clinical Approach*: Elsevier Health Sciences.

Choma, M., Sarunic, M., Yang, C., & Izatt, J. (2003). Sensitivity advantage of swept source and Fourier domain optical coherence tomography. *Opt Express, 11*(18), 2183-2189.

Choo-Smith, L. P., Dong, C. C., Cleghorn, B., & Hewko, M. (2008). Shedding new light on early caries detection. *J Can Dent Assoc, 74*(10), 913-918.

Claydon, N., Leech, K., Addy, M., Newcombe, R. G., Ley, F., & Scratcher, C. (2000). Comparison of a double-textured prototype manual toothbrush with 3 branded products. A professional brushing study. *J Clin Periodontol, 27*(10), 744-748.

Claydon, N. C. (2008). Current concepts in toothbrushing and interdental cleaning. *Periodontol 2000, 48*, 10-22.

Cobb, C. M., Rodgers, R. L., & Killoy, W. J. (1988). Ultrastructural examination of human periodontal pockets following the use of an oral irrigation device in vivo. *J Periodontol, 59*(3), 155-163.

Cochrane, N. J., Cai, F., Huq, N. L., Burrow, M. F., & Reynolds, E. C. (2010). New approaches to enhanced remineralization of tooth enamel. *J Dent Res, 89*(11), 1187-1197.

Cochrane, N. J., Shen, P., Byrne, S. J., Walker, G. D., Adams, G. G., Yuan, Y., . . . Reynolds, E. C. (2012). Remineralisation by chewing sugar-free gums in a randomised, controlled in situ trial including dietary intake and gauze to promote plaque formation. *Caries Res, 46*(2), 147-155.

Colston, B., Sathyam, U., Dasilva, L., Everett, M., Stroeve, P., & Otis, L. (1998). Dental OCT. *Opt Express, 3*(6), 230-238.

Colston, B. W., Jr., Everett, M. J., Da Silva, L. B., Otis, L. L., Stroeve, P., & Nathel, H. (1998). Imaging of hard- and soft-tissue structure in the oral cavity by optical coherence tomography. *Appl Opt, 37*(16), 3582-3585.

Coombes, J. S. (2005). Sports drinks and dental erosion. *Am J Dent, 18*(2), 101-104.

Cury, J. A., & Tenuta, L. M. (2008). How to maintain a cariostatic fluoride concentration in the oral environment. *Adv Dent Res, 20*(1), 13-16.

Dahl, B. L., Oilo, G., Andersen, A., & Bruaset, O. (1989). The suitability of a new index for the evaluation of dental wear. *Acta Odontol Scand, 47*(4), 205-210.

Darby, M. L., & Walsh, M. (2014). *Dental hygiene: theory and practice*: Elsevier Health Sciences.

Darling, C. L., Huynh, G. D., & Fried, D. (2006). Light scattering properties of natural and artificially demineralized dental enamel at 1310 nm. *J Biomed Opt, 11*(3), 34023.

Davis, R. E., Marshall, T. A., Qian, F., Warren, J. J., & Wefel, J. S. (2007). In vitro protection against dental erosion afforded by commercially available, calcium-fortified 100 percent juices. *J Am Dent Assoc, 138*(12), 1593-1598; quiz 1615.

Dawes, C. (1969). The effects of flow rate and duration of stimulation on the condentrations of protein and the main electrolytes in human parotid saliva. *Arch Oral Biol, 14*(3), 277-294.

de Alencar, C. R., Magalhaes, A. C., de Andrade Moreira Machado, M. A., de Oliveira, T. M., Honorio, H. M., & Rios, D. (2014). In situ effect of a commercial CPP-ACP chewing gum on the human enamel initial erosion. *J Dent, 42*(11), 1502-1507.

de Barros Correia Kyotoku, B. (2011). *Applications of optical coherence tomography and advances into a photonic integrated device.*

de Boer, J. F., Cense, B., Park, B. H., Pierce, M. C., Tearney, G. J., & Bouma, B. E. (2003). Improved signal-to-noise ratio in spectral-domain compared with time-domain optical coherence tomography. *Opt Lett, 28*(21), 2067-2069.

de Fatima Carvalho Vasconcelos, M., Fonseca-Goncalves, A., de Franca, A. K. A., de Medeiros, U. V., Maia, L. C., & Queiroz, C. S. (2017). An In Vitro Evaluation of Human Enamel Surfaces Subjected to Erosive Challenge After Bleaching. *J Esthet Restor Dent, 29*(2), 128-136.

De Jong, E. D. J., van der Linden, A., & Ten Bosch, J. (1987). Longitudinal microradiography: a non-destructive automated quantitative method to follow mineral changes in mineralised tissue slices. *Phys Med Biol, 32*(10), 1209.

De Jong, M. H., & Van der Hoeven, J. S. (1987). The growth of oral bacteria on saliva. *J Dent Res, 66*(2), 498-505.

de Josselin de Jong, E., Higham, S. M., Smith, P. W., van Daelen, C. J., & van der Veen, M. H. (2009). Quantified light-induced fluorescence, review of a diagnostic tool in prevention of oral disease. *Journal of Applied Physics, 105*(10), 102031.

de Josselin de Jong, E., Sundstrom, F., Westerling, H., Tranaeus, S., ten Bosch, J. J., & Angmar-Mansson, B. (1995). A new method for in vivo quantification of changes in initial enamel caries with laser fluorescence. *Caries Res, 29*(1), 2-7.

De Josselin De Jong, E., Van Der Linden, A., Borsboom, P., & Ten Bosch, J. (1988). Determination of mineral changes in human dental enamel by longitudinal microradiography and scanning optical monitoring and their correlation with chemical analysis. *Caries Res, 22*(3), 153-159.

de Oliveira, A. F., de Oliveira Diniz, L. V., Forte, F. D., Sampaio, F. C., Ccahuana-Vasquez, R. A., & Tochukwu Amaechi, B. (2017). In situ effect of a CPP-ACP chewing gum on enamel erosion associated or not with abrasion. *Clin Oral Investig, 21*(1), 339-346.

de Oliveira Mota, C. C., Gueiros, L. A., Maia, A. M., Santos-Silva, A. R., Gomes, A. S., Alves Fde, A., . . . Lopes, M. A. (2013). Optical coherence tomography as an auxiliary tool for the screening of radiation-related caries. *Photomed Laser Surg, 31*(7), 301-306.

de Oliveira, S. M., Torres, T. C., Pereira, S. L., Mota, O. M., & Carlos, M. X. (2008). Effect of a dentifrice containing Aloe vera on plaque and gingivitis control. A double-blind clinical study in humans. *J Appl Oral Sci, 16*(4), 293-296.

Deng, M., Wen, H. L., Dong, X. L., Li, F., Xu, X., Li, H., . . . Zhou, X. D. (2013). Effects of 45S5 bioglass on surface properties of dental enamel subjected to 35% hydrogen peroxide. *Int J Oral Sci, 5*(2), 103-110.

Devlin, H., Bassiouny, M. A., & Boston, D. (2006). Hardness of enamel exposed to Coca-Cola and artificial saliva. *J Oral Rehabil, 33*(1), 26-30.

Dhir, S. (2013). Biofilm and dental implant: The microbial link. *J Indian Soc Periodontol, 17*(1), 5-11.

Donlan, R. M. (2001). Biofilm formation: a clinically relevant microbiological process. *Clin Infect Dis, 33*(8), 1387-1392.

Douglas, S. M., Fried, D., & Darling, C. L. (2010). Imaging Natural Occlusal Caries Lesions with Optical Coherence Tomography. *Proc SPIE Int Soc Opt Eng, 7549*, 75490N.

Drisko, C. L., White, C. L., Killoy, W. J., & Mayberry, W. E. (1987). Comparison of dark-field microscopy and a flagella stain for monitoring the effect of a Water Pik on bacterial motility. *J Periodontol, 58*(6), 381-386.

Eccles, J. D. (1978). The treatment of dental erosion. *J Dent, 6*(3), 217-221.

Eccles, J. D. (1979). Dental erosion of nonindustrial origin. A clinical survey and classification. *J Prosthet Dent, 42*(6), 649-653.

Edgar, W., O'Mullane, D., & Dawes, C. (2004). *Saliva and oral health*: British Dental Association London.

Eisenburger, M., & Addy, M. (2001). Evaluation of pH and erosion time on demineralisation. *Clin Oral Investig, 5*(2), 108-111.

Eisenburger, M., & Addy, M. (2003). Influence of liquid temperature and flow rate on enamel erosion and surface softening. *J Oral Rehabil, 30*(11), 1076-1080.

Eisenburger, M., Hughes, J., West, N. X., Jandt, K. D., & Addy, M. (2000). Ultrasonication as a method to study enamel demineralisation during acid erosion. *Caries Res, 34*(4), 289-294.

Eisenburger, M., Hughes, J., West, N. X., Shellis, R. P., & Addy, M. (2001). The use of ultrasonication to study remineralisation of eroded enamel. *Caries Res, 35*(1), 61-66.

El Aidi, H., Bronkhorst, E. M., Huysmans, M. C., & Truin, G. J. (2011). Multifactorial analysis of factors associated with the incidence and progression of erosive tooth wear. *Caries Res, 45*(3), 303-312.

El Aidi, H., Bronkhorst, E. M., & Truin, G. J. (2008). A longitudinal study of tooth erosion in adolescents. *J Dent Res, 87*(8), 731-735.

Elton, V., Cooper, L., Higham, S. M., & Pender, N. (2009). Validation of enamel erosion in vitro. *J Dent, 37*(5), 336-341.

Evans, J. A., Poneros, J. M., Bouma, B. E., Bressner, J., Halpern, E. F., Shishkov, M., . . . Tearney, G. J. (2006). Optical coherence tomography to identify intramucosal carcinoma and high-grade dysplasia in Barrett's esophagus. *Clin Gastroenterol Hepatol, 4*(1), 38-43.

Faller, R. V., & Noble, W. H. (2018). Protection From Dental Erosion: All Fluorides are Not Equal. *Compend Contin Educ Dent, 39*(3), e13-e17.

Fareed, K., Johansson, A., & Omar, R. (1990). Prevalence and severity of occlusal tooth wear in a young Saudi population. *Acta Odontol Scand, 48*(4), 279-285.

Featherstone, J. D. (1992). Consensus conference on intra-oral models: evaluation techniques. *J Dent Res, 71 Spec No*, 955-956.

Featherstone, J. D. (2000). The science and practice of caries prevention. *J Am Dent Assoc, 131*(7), 887-899.

Featherstone, J. D. (2008). Dental caries: a dynamic disease process. *Aust Dent J, 53*(3), 286-291.

Fejerskov, O., & Kidd, E. (2009). *Dental caries: the disease and its clinical management*: John Wiley & Sons.

Fercher, A. F., Hitzenberger, C. K., Drexler, W., Kamp, G., & Sattmann, H. (1993). In vivo optical coherence tomography. *Am J Ophthalmol, 116*(1), 113-114.

Fercher, A. F., Mengedoht, K., & Werner, W. (1988). Eye-length measurement by interferometry with partially coherent light. *Opt Lett, 13*(3), 186-188.

Ferreira, M. C., Ramos-Jorge, M. L., Delbem, A. C., & Vieirac Rde, S. (2013). Effect of Toothpastes with Different Abrasives on Eroded Human Enamel: An in situ/ex vivo Study. *Open Dent J, 7*, 132-139.

Field, J., Waterhouse, P., & German, M. (2010). Quantifying and qualifying surface changes on dental hard tissues in vitro. *J Dent, 38*(3), 182-190.

Filipi, K., Halackova, Z., & Filipi, V. (2011). Oral health status, salivary factors and microbial analysis in patients with active gastro-oesophageal reflux disease. *Int Dent J, 61*(4), 231-237.

Filoche, S. K., Coleman, M. J., Angker, L., & Sissons, C. H. (2007). A fluorescence assay to determine the viable biomass of microcosm dental plaque biofilms. *J Microbiol Methods, 69*(3), 489-496.

Finke, M. (2001). Mechanical properties of in situ demineralised human enamel measured by AFM nanoindentation. *Surface Science, 491*(3), 456-467.

Fowler, C., Willson, R., & Rees, G. D. (2006). In vitro microhardness studies on a new anti-erosion desensitizing toothpaste. *J Clin Dent, 17*(4), 100-105.

Fried, D., Staninec, M., Darling, C. L., Chan, K. H., & Pelzner, R. B. (2013). Clinical Monitoring of Early Caries Lesions using Cross Polarization Optical Coherence Tomography. *Proc SPIE Int Soc Opt Eng, 8566*.

Fried, D., Staninec, M., Darling, C. L., Lee, C., Kang, H., & Chan, K. H. (2011). In vivo Near-IR Imaging of Occlusal Lesions at 1310-nm. *Proc SPIE Int Soc Opt Eng, 7884*(78840B).

Fried, D., Xie, J., Shafi, S., Featherstone, J. D., Breunig, T. M., & Le, C. (2002). Imaging caries lesions and lesion progression with polarization sensitive optical coherence tomography. *J Biomed Opt, 7*(4), 618-627.

Fujimoto, J., & Drexler, W. (2008). Introduction to optical coherence tomography *Optical coherence tomography* (pp. 1-45): Springer.

Fujimoto, J. G. (2003). Optical coherence tomography for ultrahigh resolution in vivo imaging. *Nat Biotechnol, 21*(11), 1361-1367.

Fujimoto, J. G., Brezinski, M. E., Tearney, G. J., Boppart, S. A., Bouma, B., Hee, M. R., . . . Swanson, E. A. (1995). Optical biopsy and imaging using optical coherence tomography. *Nat Med, 1*(9), 970-972.

Gambon, D. L., Brand, H. S., & Nieuw Amerongen, A. V. (2009). The erosive potential of candy sprays. *Br Dent J, 206*(10), E20; discussion 530-531.

Ganss, C., Klimek, J., & Borkowski, N. (2002). Characteristics of tooth wear in relation to different nutritional patterns including contemporary and medieval subjects. *Eur J Oral Sci, 110*(1), 54-60.

Ganss, C., Klimek, J., Schaffer, U., & Spall, T. (2001). Effectiveness of two fluoridation measures on erosion progression in human enamel and dentine in vitro. *Caries Res, 35*(5), 325-330.

Ganss, C., Klimek, J., & Schwarz, N. (2000). A comparative profilometric in vitro study of the susceptibility of polished and natural human enamel and dentine surfaces to erosive demineralization. *Arch Oral Biol, 45*(10), 897-902.

Ganss, C., & Lussi, A. (2014). Diagnosis of erosive tooth wear. *Monogr Oral Sci, 25*, 22-31.

Ganss, C., Lussi, A., & Schlueter, N. (2014). The histological features and physical properties of eroded dental hard tissues. *Monogr Oral Sci, 25*, 99-107.

Garcia-Godoy, F., & Hicks, M. J. (2008). Maintaining the integrity of the enamel surface: the role of dental biofilm, saliva and preventive agents in enamel demineralization and remineralization. *J Am Dent Assoc, 139 Suppl*, 25S-34S.

Gedalia, I., Dakuar, A., Shapira, L., Lewinstein, I., Goultschin, J., & Rahamim, E. (1991). Enamel softening with Coca-Cola and rehardening with milk or saliva. *Am J Dent, 4*(3), 120-122.

Gedalia, I., Ionat-Bendat, D., Ben-Mosheh, S., & Shapira, L. (1991). Tooth enamel softening with a cola type drink and rehardening with hard cheese or stimulated saliva in situ. *J Oral Rehabil, 18*(6), 501-506.

George, R., Chell, A., Chen, B., Undery, R., & Ahmed, H. (2014). Dental erosion and dentinal sensitivity amongst professional wine tasters in South East Queensland, Australia. *ScientificWorldJournal, 2014*, 516975.

Gibbins, H. L., Yakubov, G. E., Proctor, G. B., Wilson, S., & Carpenter, G. H. (2014). What interactions drive the salivary mucosal pellicle formation? *Colloids Surf B Biointerfaces, 120*, 184-192.

Gimbel, C. (2008). Optical coherence tomography diagnostic imaging. *Gen Dent, 56*(7), 750-757; quiz 758-759, 768.

Gjorgievska, E., & Nicholson, J. W. (2011). Prevention of enamel demineralization after tooth bleaching by bioactive glass incorporated into toothpaste. *Aust Dent J, 56*(2), 193-200.

Gjorgievska, E. S., & Nicholson, J. W. (2010). A preliminary study of enamel remineralization by dentifrices based on Recalden (CPP-ACP) and Novamin (calcium-sodium-phosphosilicate). *Acta Odontol Latinoam, 23*(3), 234-239.

Godara, P., Dubis, A. M., Roorda, A., Duncan, J. L., & Carroll, J. (2010). Adaptive optics retinal imaging: emerging clinical applications. *Optom Vis Sci, 87*(12), 930-941.

Gonzalez-Aragon Pineda, A. E., Borges-Yanez, S. A., Irigoyen-Camacho, M. E., & Lussi, A. (2019). Relationship between erosive tooth wear and beverage consumption among a group of schoolchildren in Mexico City. *Clin Oral Investig, 23*(2), 715-723.

Gorur, A., Lyle, D. M., Schaudinn, C., & Costerton, J. W. (2009). Biofilm removal with a dental water jet. *Compend Contin Educ Dent, 30 Spec No 1*, 1-6.

Gracia, L. H., Rees, G. D., Brown, A., & Fowler, C. E. (2010). An in vitro evaluation of a novel high fluoride daily mouthrinse using a combination of microindentation, 3D profilometry and DSIMS. *J Dent, 38 Suppl 3*, S12-20.

Gravelle, B. L., Hagen, T. W., II, Mayhew, S. L., Crumpton, B., Sanders, T., & Horne, V. (2015). Soft drinks and in vitro dental erosion. *Gen Dent, 63*(4), 33-38.

Gregg, T., Mace, S., West, N. X., & Addy, M. (2004). A study in vitro of the abrasive effect of the tongue on enamel and dentine softened by acid erosion. *Caries Res, 38*(6), 557-560.

Grenby, T. H. (1996). Methods of assessing erosion and erosive potential. *Eur J Oral Sci, 104*(2 (Pt 2)), 207-214.

Grippo, J. O. (1991). Abfractions: a new classification of hard tissue lesions of teeth. *J Esthet Dent, 3*(1), 14-19.

Gudmundsson, K., Kristleifsson, G., Theodors, A., & Holbrook, W. P. (1995). Tooth erosion, gastroesophageal reflux, and salivary buffer capacity. *Oral Surg Oral Med Oral Pathol Oral Radiol Endod, 79*(2), 185-189.

Guidoni, G. M., Swain, M. V., & Jäger, I. (2009). Wear behaviour of dental enamel at the nanoscale with a sharp and blunt indenter tip. *Wear, 266*(1-2), 60-68.

Gurenlian, J. R. (2007). The role of dental plaque biofilm in oral health. *American Dental Hygienists Association, 81*(suppl 1), 116-116.

Gutiérrez-Salazar, M., & Reyes-Gasga, J. (2003). Microhardness and chemical composition of human tooth. *Materials Research-Ibero-American Journal of Materials, 6*(3), 367-373.

Habelitz, S., Marshall, G. W., Jr., Balooch, M., & Marshall, S. J. (2002). Nanoindentation and storage of teeth. *J Biomech, 35*(7), 995-998.

Hall, A. F., Sadler, J. P., Strang, R., de Josselin de Jong, E., Foye, R. H., & Creanor, S. L. (1997). Application of transverse microradiography for measurement of mineral loss by acid erosion. *Adv Dent Res, 11*(4), 420-425.

Hangai, M., Ojima, Y., Gotoh, N., Inoue, R., Yasuno, Y., Makita, S., . . . Yoshimura, N. (2007). Three-dimensional imaging of macular holes with high-speed optical coherence tomography. *Ophthalmology, 114*(4), 763-773.

Hannig, M., & Hannig, C. (2014). The pellicle and erosion. *Monogr Oral Sci, 25*, 206-214.

Hannig, M., Hess, N. J., Hoth-Hannig, W., & De Vrese, M. (2003). Influence of salivary pellicle formation time on enamel demineralization--an in situ pilot study. *Clin Oral Investig, 7*(3), 158-161.

Hara, A. T., Gonzalez-Cabezas, C., Creeth, J., & Zero, D. T. (2008). The effect of human saliva substitutes in an erosion-abrasion cycling model. *Eur J Oral Sci, 116*(6), 552-556.

Hara, A. T., Lussi, A., & Zero, D. T. (2006). Biological factors. *Monogr Oral Sci, 20*, 88-99.

Hara, A. T., & Zero, D. T. (2008). Analysis of the erosive potential of calcium-containing acidic beverages. *Eur J Oral Sci, 116*(1), 60-65.

Harding, M. A., Whelton, H., O'Mullane, D. M., & Cronin, M. (2003). Dental erosion in 5-year-old Irish school children and associated factors: a pilot study. *Community Dent Health, 20*(3), 165-170.

Hariri, I., Sadr, A., Nakashima, S., Shimada, Y., Tagami, J., & Sumi, Y. (2013). Estimation of the enamel and dentin mineral content from the refractive index. *Caries Res, 47*(1), 18-26.

Hariri, I., Sadr, A., Shimada, Y., Tagami, J., & Sumi, Y. (2012). Effects of structural orientation of enamel and dentine on light attenuation and local refractive index: an optical coherence tomography study. *J Dent, 40*(5), 387-396.

Hasselkvist, A., Johansson, A., & Johansson, A. K. (2016). A 4 year prospective longitudinal study of progression of dental erosion associated to lifestyle in 13-14 year-old Swedish adolescents. *J Dent, 47*, 55-62.

Hattab, F. N., & Yassin, O. M. (2000). Etiology and diagnosis of tooth wear: a literature review and presentation of selected cases. *Int J Prosthodont, 13*(2), 101-107.

Hayashi, O., Chiba, T., Shimoda, S., & Momoi, Y. (2016). Demineralization and Remineralization Phenomena of Human Enamel in Acid Erosion Model. *Journal of Hard Tissue Biology, 25*(1), 27-34.

Hede, B. (1996). Determinants of oral health in a group of Danish alcoholics. *Eur J Oral Sci, 104*(4 (Pt 1)), 403-408.

Hee, M. R., Swanson, E. A., Fujimoto, J. G., & Huang, D. (1992). Polarization-sensitive low-coherence reflectometer for birefringence characterization and ranging. *Journal of the Optical Society of America B, 9*(6), 903-908.

Hellwig, E., & Lennon, A. M. (2004). Systemic versus topical fluoride. *Caries Res, 38*(3), 258-262.

Hemingway, C. A., Parker, D. M., Addy, M., & Barbour, M. E. (2006). Erosion of enamel by non-carbonated soft drinks with and without toothbrushing abrasion. *Br Dent J, 201*(7), 447-450; discussion 439; quiz 466.

Hench, L. L. (1991). Bioceramics: from concept to clinic. *J Am Ceram Soc, 74*(7), 1487-1510.

Hendargo, H. C., McNabb, R. P., Dhalla, A. H., Shepherd, N., & Izatt, J. A. (2011). Doppler velocity detection limitations in spectrometer-based versus swept-source optical coherence tomography. *Biomed Opt Express, 2*(8), 2175-2188.

Heurich, E., Beyer, M., Jandt, K. D., Reichert, J., Herold, V., Schnabelrauch, M., & Sigusch, B. W. (2010). Quantification of dental erosion—a comparison of stylus profilometry and confocal laser scanning microscopy (CLSM). *Dental Materials, 26*(4), 326-336.

Hicks, J., Garcia-Godoy, F., & Flaitz, C. (2004). Biological factors in dental caries enamel structure and the caries process in the dynamic process of demineralization and remineralization (part 2). *Journal of Clinical Pediatric Dentistry, 28*(2), 119-124.

Honorio, H. M., Rios, D., Santos, C. F., Magalhaes, A. C., Buzalaf, M. A., & Machado, M. A. (2008). Effects of erosive, cariogenic or combined erosive/cariogenic challenges on human enamel: an in situ/ex vivo study. *Caries Res, 42*(6), 454-459.

Hooper, S., Hughes, J., Parker, D., Finke, M., Newcombe, R. G., Addy, M., & West, N. (2007). A clinical study in situ to assess the effect of a food approved polymer on the erosion potential of drinks. *J Dent, 35*(6), 541-546.

Hooper, S., West, N. X., Sharif, N., Smith, S., North, M., De'Ath, J., . . . Addy, M. (2004). A comparison of enamel erosion by a new sports drink compared to two proprietary products: a controlled, crossover study in situ. *J Dent, 32*(7), 541-545.

Hooper, S. M., Hughes, J. A., Newcombe, R. G., Addy, M., & West, N. X. (2005). A methodology for testing the erosive potential of sports drinks. *J Dent, 33*(4), 343-348.

Hooper, S. M., Newcombe, R. G., Faller, R., Eversole, S., Addy, M., & West, N. X. (2007). The protective effects of toothpaste against erosion by orange juice: studies in situ and in vitro. *J Dent, 35*(6), 476-481.

Hove, L., Holme, B., Ogaard, B., Willumsen, T., & Tveit, A. B. (2006). The protective effect of TiF4, SnF2 and NaF on erosion of enamel by hydrochloric acid in vitro measured by white light interferometry. *Caries Res, 40*(5), 440-443.

Hove, L. H., Holme, B., Young, A., & Tveit, A. B. (2007). The erosion-inhibiting effect of TiF4, SnF2, and NaF solutions on pellicle-covered enamel in vitro. *Acta Odontol Scand, 65*(5), 259-264.

Hove, L. H., Holme, B., Young, A., & Tveit, A. B. (2008). The protective effect of TiF4, SnF2 and NaF against erosion-like lesions in situ. *Caries Res, 42*(1), 68-72.

Hove, L. H., Young, A., & Tveit, A. B. (2007). An in vitro study on the effect of TiF(4) treatment against erosion by hydrochloric acid on pellicle-covered enamel. *Caries Res, 41*(1), 80-84.

Howlin, R. P., Fabbri, S., Offin, D. G., Symonds, N., Kiang, K. S., Knee, R. J., . . . Stoodley, P. (2015). Removal of Dental Biofilms with an Ultrasonically Activated Water Stream. *J Dent Res, 94*(9), 1303-1309.

Huang, D., Swanson, E. A., Lin, C. P., Schuman, J. S., Stinson, W. G., Chang, W., . . . et al. (1991). Optical coherence tomography. *Science, 254*(5035), 1178-1181.

Huang, R., Li, M., & Gregory, R. L. (2011). Bacterial interactions in dental biofilm. *Virulence, 2*(5), 435-444.

Hughes, J. A., Jandt, K. D., Baker, N., Parker, D., Newcombe, R. G., Eisenburger, M., & Addy, M. (2002). Further modification to soft drinks to minimise erosion. A study in situ. *Caries Res, 36*(1), 70-74.

Huynh, G. D., Darling, C. L., & Fried, D. (2004). *Changes in the optical properties of dental enamel at 1310-nm after demineralization.* Paper presented at the Proc. of SPIE Vol.

Huysmans, M. C., Chew, H. P., & Ellwood, R. P. (2011). Clinical studies of dental erosion and erosive wear. *Caries Res, 45 Suppl 1*, 60-68.

Huysmans, M. C., & Thijssen, J. M. (2000). Ultrasonic measurement of enamel thickness: a tool for monitoring dental erosion? *J Dent, 28*(3), 187-191.

Huysmans, M. C., Young, A., & Ganss, C. (2014). The role of fluoride in erosion therapy. *Monogr Oral Sci, 25*, 230-243.

Ibusuki, T., Kitasako, Y., Sadr, A., Shimada, Y., Sumi, Y., & Tagami, J. (2015). Observation of white spot lesions using swept source optical coherence tomography (SS-OCT): in vitro and in vivo study. *Dent Mater J, 34*(4), 545-552.

Imai, K., Shimada, Y., Sadr, A., Sumi, Y., & Tagami, J. (2012). Noninvasive cross-sectional visualization of enamel cracks by optical coherence tomography in vitro. *J Endod, 38*(9), 1269-1274.

Imfeld, T. (1996). Dental erosion. Definition, classification and links. *Eur J Oral Sci, 104*(2 (Pt 2)), 151-155.

Imfeld, T. (1999). Chewing gum--facts and fiction: a review of gum-chewing and oral health. *Crit Rev Oral Biol Med, 10*(3), 405-419.

Ireland, A. J., McGuinness, N., & Sherriff, M. (1995). An investigation into the ability of soft drinks to adhere to enamel. *Caries Res, 29*(6), 470-476.

Jaeggi, T., & Lussi, A. (1999). Toothbrush abrasion of erosively altered enamel after intraoral exposure to saliva: an in situ study. *Caries Res, 33*(6), 455-461.

Jaeggi, T., & Lussi, A. (2006). Prevalence, incidence and distribution of erosion. *Monogr Oral Sci, 20*, 44-65.

Jaeggi, T., & Lussi, A. (2014). Prevalence, incidence and distribution of erosion. *Monogr Oral Sci, 25*, 55-73.

Jandt, K. D. (2006). Probing the future in functional soft drinks on the nanometre scale—towards tooth friendly soft drinks. *Trends in food science & technology, 17*(5), 263-271.

Jarvinen, V. K., Rytomaa, II, & Heinonen, O. P. (1991). Risk factors in dental erosion. *J Dent Res, 70*(6), 942-947.

Jeng, Y. R., Lin, T. T., & Shieh, D. B. (2009). Nanotribological characterization of tooth enamel rod affected by surface treatment. *J Biomech, 42*(14), 2249-2254.

Jeng, Y. R., Lin, T. T., Wong, T. Y., Chang, H. J., & Shieh, D. B. (2008). Nano-mechanical properties of fluoride-treated enamel surfaces. *J Dent Res, 87*(4), 381-385.

Jennett, E., Motamedi, M., Rastegar, S., Frederickson, C., Arcoria, C., & Powers, J. M. (1994). Dye-enhanced ablation of enamel by pulsed lasers. *J Dent Res, 73*(12), 1841-1847.

Jensdottir, T., Nauntofte, B., Buchwald, C., & Bardow, A. (2005). Effects of sucking acidic candy on whole-mouth saliva composition. *Caries Res, 39*(6), 468-474.

Joiner, A., Schafer, F., Naeeni, M. M., Gupta, A. K., & Zero, D. T. (2014). Remineralisation effect of a dual-phase calcium silicate/phosphate gel combined with calcium silicate/phosphate toothpaste on acid-challenged enamel in situ. *J Dent, 42 Suppl 1*, S53-59.

Jones, R., Aparicio, C., Chityala, R., Chen, R., Fok, A., & Rudney, J. (2012). Assessing ex vivo dental biofilms and in vivo composite restorations using cross-polarization optical coherence tomography. *Lasers in Dentistry Xviii, 8208*.

Jones, R. S., Darling, C. L., Featherstone, J. D., & Fried, D. (2006a). Imaging artificial caries on the occlusal surfaces with polarization-sensitive optical coherence tomography. *Caries Res, 40*(2), 81-89.

Jones, R. S., Darling, C. L., Featherstone, J. D., & Fried, D. (2006b). Remineralization of in vitro dental caries assessed with polarization-sensitive optical coherence tomography. *J Biomed Opt, 11*(1), 014016.

Jones, R. S., & Fried, D. (2006). Remineralization of enamel caries can decrease optical reflectivity. *J Dent Res, 85*(9), 804-808.

Jones, R. S., Huynh, G. D., Jones, G. C., & Fried, D. (2003). Near-infrared transillumination at 1310-nm for the imaging of early dental decay. *Opt Express, 11*(18), 2259-2265.

Jones, S. B., Davies, M., Chapman, N., Willson, R., Hornby, K., Joiner, A., & West, N. X. (2014). Introduction of an interproximal mineralisation model to measure remineralisation caused by novel formulations containing calcium silicate, sodium phosphate salts and fluoride. *J Dent, 42 Suppl 1*, S46-52.

Joshi, M., Joshi, N., Kathariya, R., Angadi, P., & Raikar, S. (2016). Techniques to Evaluate Dental Erosion: A Systematic Review of Literature. *J Clin Diagn Res, 10*(10), ZE01-ZE07.

Joyce, M. (2010). Effectiveness of dental water jets as part of an oral health regime. *Dental Nursing, 6*(7), 380.

Jun, M. K., Ku, H. M., Kim, E., Kim, H. E., Kwon, H. K., & Kim, B. I. (2016). Detection and Analysis of Enamel Cracks by Quantitative Light-induced Fluorescence Technology. *J Endod, 42*(3), 500-504.

Kaidonis, J. A., Richards, L. C., Townsend, G. C., & Tansley, G. D. (1998). Wear of human enamel: a quantitative in vitro assessment. *J Dent Res, 77*(12), 1983-1990.

Kandelman, D., & Gagnon, G. (1990). A 24-month clinical study of the incidence and progression of dental caries in relation to consumption of chewing gum containing xylitol in school preventive programs. *J Dent Res, 69*(11), 1771-1775.

Kang, H., Chan, K., Darling, C. L., & Fried, D. (2013). *Monitoring the remineralization of early simulated lesions using a pH cycling model with CP-OCT*. Paper presented at the Lasers in Dentistry XIX.

Kang, H., Darling, C. L., & Fried, D. (2012). Nondestructive monitoring of the repair of enamel artificial lesions by an acidic remineralization model using polarization-sensitive optical coherence tomography. *Dent Mater, 28*(5), 488-494.

Karlsson, L. (2010). Caries Detection Methods Based on Changes in Optical Properties between Healthy and Carious Tissue. *Int J Dent, 2010*, 270729.

Karygianni, L., Follo, M., Hellwig, E., Burghardt, D., Wolkewitz, M., Anderson, A., & Al-Ahmad, A. (2012). Microscope-based imaging platform for large-scale analysis of oral biofilms. *Appl Environ Microbiol, 78*(24), 8703-8711.

Kato, K., Tamura, K., & Nakagaki, H. (2012). Quantitative evaluation of the oral biofilm-removing capacity of a dental water jet using an electron-probe microanalyzer. *Arch Oral Biol, 57*(1), 30-35.

Kelleher, M., & Bishop, K. (1999). Tooth surface loss: an overview. *Br Dent J, 186*(2), 61-66.

Keukenmeester, R. S., Slot, D. E., Putt, M. S., & Van der Weijden, G. A. (2014). The effect of medicated, sugar-free chewing gum on plaque and clinical parameters of gingival inflammation: a systematic review. *Int J Dent Hyg, 12*(1), 2-16.

Kilpatrick, N., & Mahoney, E. K. (2004). Dental erosion: part 2. The management of dental erosion. *N Z Dent J, 100*(2), 42-47.

Kitasako, Y., Moritsuka, M., Foxton, R. M., Ikeda, M., Tagami, J., & Nomura, S. (2005). Simplified and quantitative saliva buffer capacity test using a hand-held pH meter. *Am J Dent, 18*(3), 147-150.

Kitchens, M., & Owens, B. M. (2007). Effect of carbonated beverages, coffee, sports and high energy drinks, and bottled water on the in vitro erosion characteristics of dental enamel. *Journal of Clinical Pediatric Dentistry, 31*(3), 153-159.

Knoop, F., Peters, C. G., & Emerson, W. B. (1939). A sensitive pyramidal-diamond tool for indentation measurements. *Journal of Research of the National Bureau of standards, 23*(1), 39-61.

Kolenbrander, P. E. (2000). Oral microbial communities: biofilms, interactions, and genetic systems. *Annu Rev Microbiol, 54*, 413-437.

Kolenbrander, P. E., Palmer, R. J., Jr., Periasamy, S., & Jakubovics, N. S. (2010). Oral multispecies biofilm development and the key role of cell-cell distance. *Nat Rev Microbiol, 8*(7), 471-480.

Koshoji, N. H., Bussadori, S. K., Bortoletto, C. C., Prates, R. A., Oliveira, M. T., & Deana, A. M. (2015). Laser speckle imaging: a novel method for detecting dental erosion. *PLoS One, 10*(2), e0118429.

Koulourides, T., & Volker, J. F. (1964). Changes of Enamel Microhardness in the Human Mouth. *Ala J Med Sci, 1*, 435-437.

Kreth, J., Merritt, J., & Qi, F. (2009). Bacterial and host interactions of oral streptococci. *DNA Cell Biol, 28*(8), 397-403.

Kreulen, C. M., Van 't Spijker, A., Rodriguez, J. M., Bronkhorst, E. M., Creugers, N. H., & Bartlett, D. W. (2010). Systematic review of the prevalence of tooth wear in children and adolescents. *Caries Res, 44*(2), 151-159.

Lagerweij, M. D., Buchalla, W., Kohnke, S., Becker, K., Lennon, A. M., & Attin, T. (2006). Prevention of erosion and abrasion by a high fluoride concentration gel applied at high frequencies. *Caries Res, 40*(2), 148-153.

Larsen, I. B., Westergaard, J., Stoltze, K., Larsen, A. I., Gyntelberg, F., & Holmstrup, P. (2000). A clinical index for evaluating and monitoring dental erosion. *Community Dent Oral Epidemiol, 28*(3), 211-217.

Larsen, M. J. (1990). Chemical events during tooth dissolution. *J Dent Res, 69 Spec No*, 575-580; discussion 634-576.

Larsen, M. J., & Richards, A. (2002). Fluoride is unable to reduce dental erosion from soft drinks. *Caries Res, 36*(1), 75-80.

Lawrence, J. R., Korber, D. R., Hoyle, B. D., Costerton, J. W., & Caldwell, D. E. (1991). Optical sectioning of microbial biofilms. *J Bacteriol, 173*(20), 6558-6567.

Lawrence, J. R., & Neu, T. R. (1999). Confocal laser scanning microscopy for analysis of microbial biofilms. *Methods Enzymol, 310*, 131-144.

Lawrence, J. R., Swerhone, G. D., Leppard, G. G., Araki, T., Zhang, X., West, M. M., & Hitchcock, A. P. (2003). Scanning transmission X-ray, laser scanning, and transmission electron microscopy mapping of the exopolymeric matrix of microbial biofilms. *Appl Environ Microbiol, 69*(9), 5543-5554.

Le, M. H., Darling, C. L., & Fried, D. (2010). Automated analysis of lesion depth and integrated reflectivity in PS-OCT scans of tooth demineralization. *Lasers Surg Med, 42*(1), 62-68.

Leach, S. A., Lee, G. T., & Edgar, W. M. (1989). Remineralization of artificial caries-like lesions in human enamel in situ by chewing sorbitol gum. *J Dent Res, 68*(6), 1064-1068.

Lee, J. W., Lee, E. S., & Kim, B. I. (2018). Optical diagnosis of dentin caries lesions using quantitative light-induced fluorescence technology. *Photodiagnosis Photodyn Ther, 23*, 68-70.

Leitgeb, R., Hitzenberger, C., & Fercher, A. (2003). Performance of fourier domain vs. time domain optical coherence tomography. *Opt Express, 11*(8), 889-894.

Lenton, P., Rudney, J., Chen, R., Fok, A., Aparicio, C., & Jones, R. S. (2012). Imaging in vivo secondary caries and ex vivo dental biofilms using cross-polarization optical coherence tomography. *Dent Mater, 28*(7), 792-800.

Li, J., Helmerhorst, E. J., Leone, C. W., Troxler, R. F., Yaskell, T., Haffajee, A. D., . . . Oppenheim, F. G. (2004). Identification of early microbial colonizers in human dental biofilm. *J Appl Microbiol, 97*(6), 1311-1318.

Li, X., Wang, J., Joiner, A., & Chang, J. (2014). The remineralisation of enamel: a review of the literature. *J Dent, 42 Suppl 1*, S12-20.

Li, Y. H., Tang, N., Aspiras, M. B., Lau, P. C. Y., Lee, J. H., Ellen, R. P., & Cvitkovitch, D. G. (2002). A Quorum-Sensing Signaling System Essential for Genetic Competence in Streptococcus mutans Is Involved in Biofilm Formation. *J Bacteriol, 184*(10), 2699-2708.

Linkosalo, E., & Markkanen, H. (1985). Dental erosions in relation to lactovegetarian diet. *Scand J Dent Res, 93*(5), 436-441.

Lippert, F., Parker, D. M., & Jandt, K. D. (2004). Toothbrush abrasion of surface softened enamel studied with tapping mode AFM and AFM nanoindentation. *Caries Res, 38*(5), 464-472.

Listgarten, M. A. (1994). The structure of dental plaque. *Periodontol 2000, 5*, 52-65.

Litkowski, L. J., Hack, G. D., Sheaffer, H. B., & Greenspan, D. C. (1997). Occlusion of dentin tubules by 45S5 Bioglass®. *Bioceramics, 10*(411), 411.

Litonjua, L. A., Andreana, S., Bush, P. J., & Cohen, R. E. (2003). Tooth wear: attrition, erosion, and abrasion. *Quintessence Int, 34*(6), 435-446.

Louwerse, C., Kjaeldgaard, M., & Huysmans, M. C. (2004). The reproducibility of ultrasonic enamel thickness measurements: an in vitro study. *J Dent, 32*(1), 83-89.

Lupi-Pegurier, L., Muller, M., Leforestier, E., Bertrand, M. F., & Bolla, M. (2003). In vitro action of Bordeaux red wine on the microhardness of human dental enamel. *Arch Oral Biol, 48*(2), 141-145.

Lussi, A. (1996). Dental erosion clinical diagnosis and case history taking. *Eur J Oral Sci, 104*(2 (Pt 2)), 191-198.

Lussi, A. (2006). Erosive tooth wear - a multifactorial condition of growing concern and increasing knowledge. *Monogr Oral Sci, 20*, 1-8.

Lussi, A., Bossen, A., Hoschele, C., Beyeler, B., Megert, B., Meier, C., & Rakhmatullina, E. (2012). Effects of enamel abrasion, salivary pellicle, and measurement angle on the optical assessment of dental erosion. *J Biomed Opt, 17*(9), 97009-97001.

Lussi, A., & Carvalho, T. S. (2014). Erosive tooth wear: a multifactorial condition of growing concern and increasing knowledge. *Monogr Oral Sci, 25*, 1-15.

Lussi, A., Hellwig, E., Zero, D., & Jaeggi, T. (2006). Erosive tooth wear: diagnosis, risk factors and prevention. *Am J Dent, 19*(6), 319-325.

Lussi, A., & Jaeggi, T. (2008). Erosion--diagnosis and risk factors. *Clin Oral Investig, 12 Suppl 1*, S5-13.

Lussi, A., Jaeggi, T., & Jaeggi-Scharer, S. (1995). Prediction of the erosive potential of some beverages. *Caries Res, 29*(5), 349-354.

Lussi, A., Schaffner, M., Hotz, P., & Suter, P. (1991). Dental erosion in a population of Swiss adults. *Community Dent Oral Epidemiol, 19*(5), 286-290.

Lussi, A., Schlueter, N., Rakhmatullina, E., & Ganss, C. (2011). Dental erosion--an overview with emphasis on chemical and histopathological aspects. *Caries Res, 45 Suppl 1*, 2-12.

Lussi, A., von Salis-Marincek, M., Ganss, C., Hellwig, E., Cheaib, Z., & Jaeggi, T. (2012). Clinical study monitoring the pH on tooth surfaces in patients with and without erosion. *Caries Res, 46*(6), 507-512.

Ly, K. A., Milgrom, P., & Rothen, M. (2008). The potential of dental-protective chewing gum in oral health interventions. *J Am Dent Assoc, 139*(5), 553-563.

Machado, C., Lacefield, W., & Catledge, A. (2008). Human enamel nanohardness, elastic modulus and surface integrity after beverage contact. *Braz Dent J, 19*(1), 68-72.

Machado, F. C., Cesar, D. E., Assis, A. V., Diniz, C. G., & Ribeiro, R. A. (2012). Detection and enumeration of periodontopathogenic bacteria in subgingival biofilm of pregnant women. *Braz Oral Res, 26*(5), 443-449.

Machoy, M., Seeliger, J., Szyszka-Sommerfeld, L., Koprowski, R., Gedrange, T., & Woźniak, K. (2017). The Use of Optical Coherence Tomography in Dental Diagnostics. A State-Of-the-Art Review. *Journal of Healthcare Engineering*.

Macpherson, P. (2012). The benefits of dental water jets and air flossers. *Dental Nursing, 8*(10), 636.

Madan, N., Madan, N., Sharma, V., Pardal, D., & Madan, N. (2011). Tooth remineralization using bio-active glass-A novel approach. *J Acad Adv Dent Res, 2*, 45-49.

Magalhaes, A. C., Wiegand, A., Rios, D., Buzalaf, M. A., & Lussi, A. (2011). Fluoride in dental erosion. *Monogr Oral Sci, 22*, 158-170.

Mahoney, E., Beattie, J., Swain, M., & Kilpatrick, N. (2003). Preliminary in vitro assessment of erosive potential using the ultra-micro-indentation system. *Caries Res, 37*(3), 218-224.

Maia, A. M., de Freitas, A. Z., de, L. C. S., Gomes, A. S., & Karlsson, L. (2016). Evaluation of dental enamel caries assessment using Quantitative Light Induced Fluorescence and Optical Coherence Tomography. *J Biophotonics, 9*(6), 596-602.

Mair, L. (1992). Wear in dentistry—current terminology. *J Dent (Shiraz), 20*(3), 140-144.

Makishi, P., Shimada, Y., Sadr, A., Tagami, J., & Sumi, Y. (2011). Non-destructive 3D imaging of composite restorations using optical coherence tomography: marginal adaptation of self-etch adhesives. *J Dent, 39*(4), 316-325.

Malterud, M. I. (2006). Minimally invasive restorative dentistry: a biomimetic approach. *Pract Proced Aesthet Dent, 18*(7), 409-414.

Mandal, A., Singh, D. K., Siddiqui, H., Das, D., & Dey, A. K. (2017). New dimensions in mechanical plaque control: An overview. *Indian Journal of Dental Sciences, 9*(2), 133.

Mandel, L. (2005). Dental erosion due to wine consumption. *J Am Dent Assoc, 136*(1), 71-75.

Mandurah, M. M., Sadr, A., Shimada, Y., Kitasako, Y., Nakashima, S., Bakhsh, T. A., . . . Sumi, Y. (2013). Monitoring remineralization of enamel subsurface lesions by optical coherence tomography. *J Biomed Opt, 18*(4), 046006.

Manesh, S. K., Darling, C. L., & Fried, D. (2009). Polarization-sensitive optical coherence tomography for the nondestructive assessment of the remineralization of dentin. *J Biomed Opt, 14*(4), 044002.

Manning, R. H., & Edgar, W. M. (1992). Salivary stimulation by chewing gum and its role in the remineralization of caries-like lesions in human enamel in situ. *J Clin Dent, 3*(3), 71-74.

Manz, B., Volke, F., Goll, D., & Horn, H. (2005). Investigation of biofilm structure, flow patterns and detachment with magnetic resonance imaging. *Water science and technology, 52*(7), 1-6.

Marsh, P. D. (2004). Dental plaque as a microbial biofilm. *Caries Res, 38*(3), 204-211.

Marsh, P. D., & Bradshaw, D. J. (1995). Dental plaque as a biofilm. *J Ind Microbiol, 15*(3), 169-175.

Maupome, G., Diez-de-Bonilla, J., Torres-Villasenor, G., Andrade-Delgado, L. C., & Castano, V. M. (1998). In vitro quantitative assessment of enamel microhardness after exposure to eroding immersion in a cola drink. *Caries Res, 32*(2), 148-153.

Maupome, G., & Ray, J. M. (2000). Structured review of enamel erosion literature (1980-1998): a critical appraisal of experimental, clinical and review publications. *Oral Dis, 6*(4), 197-207.

Meredith, Sherriff, M., Setchell, D. J., & Swanson, S. A. V. (1996). Measurement of the microhardness and young's modulus of human enamel and dentine using an indentation technique. *Arch Oral Biol, 41*(6), 539-545.

Miller, C. H., & Palenik, C. J. (2014). *Infection Control and Management of Hazardous Materials for the Dental Team5: Infection Control and Management of Hazardous Materials for the Dental Team*: Elsevier Health Sciences.

Miller, W. R., & Rose, G. S. (2009). Toward a theory of motivational interviewing. *Am Psychol, 64*(6), 527-537.

Millward, A., Shaw, L., Harrington, E., & Smith, A. J. (1997). Continuous monitoring of salivary flow rate and pH at the surface of the dentition following consumption of acidic beverages. *Caries Res, 31*(1), 44-49.

Milosevic, A. (1997). Sports drinks hazard to teeth. *Br J Sports Med, 31*(1), 28-30.

Milosevic, A., & Lo, M. S. (1996). Tooth wear in three ethnic groups in Sabah (northern Borneo). *Int Dent J, 46*(6), 572-578.

Milosevic, A., Young, P. J., & Lennon, M. A. (1994). The prevalence of tooth wear in 14-year-old school children in Liverpool. *Community Dent Health, 11*(2), 83-86.

Moazzez, R., Bartlett, D., & Anggiansah, A. (2004). Dental erosion, gastro-oesophageal reflux disease and saliva: how are they related? *J Dent, 32*(6), 489-494.

Moazzez, R., Smith, B. G., & Bartlett, D. W. (2000). Oral pH and drinking habit during ingestion of a carbonated drink in a group of adolescents with dental erosion. *J Dent, 28*(6), 395-397.

Morgan, M. V., Adams, G. G., Bailey, D. L., Tsao, C. E., Fischman, S. L., & Reynolds, E. C. (2008). The anticariogenic effect of sugar-free gum containing CPP-ACP nanocomplexes on approximal caries determined using digital bitewing radiography. *Caries Res, 42*(3), 171-184.

Mueller, L. N., de Brouwer, J. F., Almeida, J. S., Stal, L. J., & Xavier, J. B. (2006). Analysis of a marine phototrophic biofilm by confocal laser scanning microscopy using the new image quantification software PHLIP. *BMC Ecol, 6*, 1.

Mulic, A., Skudutyte-Rysstad, R., Tveit, A. B., & Skaare, A. B. (2012). Risk indicators for dental erosive wear among 18-yr-old subjects in Oslo, Norway. *Eur J Oral Sci, 120*(6), 531-538.

Muller-Bolla, M., Courson, F., Smail-Faugeron, V., Bernardin, T., & Lupi-Pegurier, L. (2015). Dental erosion in French adolescents. *BMC Oral Health, 15*(1), 147.

Murdoch-Kinch, C. A., & McLean, M. E. (2003). Minimally invasive dentistry. *J Am Dent Assoc, 134*(1), 87-95.

Nakagawa, H., Sadr, A., Shimada, Y., Tagami, J., & Sumi, Y. (2013). Validation of swept source optical coherence tomography (SS-OCT) for the diagnosis of smooth surface caries in vitro. *J Dent, 41*(1), 80-89.

Nakajima, Y., Shimada, Y., Sadr, A., Wada, I., Miyashin, M., Takagi, Y., . . . Sumi, Y. (2014). Detection of occlusal caries in primary teeth using swept source optical coherence tomography. *J Biomed Opt, 19*(1), 16020.

Natsume, Y., Nakashima, S., Sadr, A., Shimada, Y., Tagami, J., & Sumi, Y. (2011). Estimation of lesion progress in artificial root caries by swept source optical coherence tomography in comparison to transverse microradiography. *J Biomed Opt, 16*(7), 071408.

Navazesh, M., & Christensen, C. M. (1982). A comparison of whole mouth resting and stimulated salivary measurement procedures. *J Dent Res, 61*(10), 1158-1162.

Nazari, A., Sadr, A., Campillo-Funollet, M., Nakashima, S., Shimada, Y., Tagami, J., & Sumi, Y. (2013). Effect of hydration on assessment of early enamel lesion using swept-source optical coherence tomography. *J Biophotonics, 6*(2), 171-177.

Nee, A., Chan, K., Kang, H., Staninec, M., Darling, C. L., & Fried, D. (2014). Longitudinal monitoring of demineralization peripheral to orthodontic brackets using cross polarization optical coherence tomography. *J Dent, 42*(5), 547-555.

Netuschil, L., Auschill, T. M., Sculean, A., & Arweiler, N. B. (2014). Confusion over live/dead stainings for the detection of vital microorganisms in oral biofilms--which stain is suitable? *BMC Oral Health, 14*, 2.

Netuschil, L., Reich, E., Unteregger, G., Sculean, A., & Brecx, M. (1998). A pilot study of confocal laser scanning microscopy for the assessment of undisturbed dental plaque vitality and topography. *Arch Oral Biol, 43*(4), 277-285.

Netuschil, L., Weiger, R., Preisler, R., & Brecx, M. (1995). Plaque bacteria counts and vitality during chlorhexidine, meridol and listerine mouthrinses. *Eur J Oral Sci, 103*(6), 355-361.

Nield-Gehrig, J. S. (2005). Dental plaque biofilms. *Journal of Practical Hygiene, 14*(16), 1-6.

Nongonierma, A. B., & Fitzgerald, R. J. (2012). Biofunctional properties of caseinophosphopeptides in the oral cavity. *Caries Res, 46*(3), 234-267.

Nygaard Östby, B., Mörch, T., & Hals, E. (1958). A method for caries production on selected tooth surfaces in vivo. *Acta Odontol Scand, 15*(4), 357-363.

Nyvad, B., & Kilian, M. (1987). Microbiology of the early colonization of human enamel and root surfaces in vivo. *Scand J Dent Res, 95*(5), 369-380.

Nyvad, B., & Kilian, M. (1990). Comparison of the initial streptococcal microflora on dental enamel in caries-active and in caries-inactive individuals. *Caries Res, 24*(4), 267-272.

O'Sullivan, E. A. (2000). A new index for the measurement of erosion in children. *Eur J Paediatr Dent, 2*(1), 69-74.

O'Sullivan, E. A., & Curzon, M. E. (2000a). A comparison of acidic dietary factors in children with and without dental erosion. *ASDC J Dent Child, 67*(3), 186-192, 160.

O'Sullivan, E. A., & Curzon, M. E. (2000b). Salivary factors affecting dental erosion in children. *Caries Res, 34*(1), 82-87.

Oilo, G., Dahl, B. L., Hatle, G., & Gad, A. L. (1987). An index for evaluating wear of teeth. *Acta Odontol Scand, 45*(5), 361-365.

Oliveira, G. C., Tereza, G. P. G., Boteon, A. P., Ferrairo, B. M., Goncalves, P. S. P., Silva, T. C. D., . . . Rios, D. (2017). Susceptibility of bovine dental enamel with initial erosion lesion to new erosive challenges. *PLoS One, 12*(8), e0182347.

Olsen, J., Themstrup, L., & Jemec, G. B. (2015). Optical coherence tomography in dermatology. *G Ital Dermatol Venereol, 150*(5), 603-615.

Onisei, D., Onisei, D., Feier, I., Rusu, D., & Stratul, S. (2008). The Biofilm: Formation and Removal. *Timisoara Medical Journal.(serie en Internet)*, 1-2.

Otis, L. L., Colston, B. W., Jr., Everett, M. J., & Nathel, H. (2000). Dental optical coherence tomography: a comparison of two in vitro systems. *Dentomaxillofac Radiol, 29*(2), 85-89.

Paice, E. M., Vowles, R. W., West, N. X., & Hooper, S. M. (2011). The erosive effects of saliva following chewing gum on enamel and dentine: an ex vivo study. *Br Dent J, 210*(3), E3.

Panich, M., & Poolthong, S. (2009). The effect of casein phosphopeptide-amorphous calcium phosphate and a cola soft drink on in vitro enamel hardness. *J Am Dent Assoc, 140*(4), 455-460.

Pantanella, F., Valenti, P., Natalizi, T., Passeri, D., & Berlutti, F. (2013). Analytical techniques to study microbial biofilm on abiotic surfaces: pros and cons of the main techniques currently in use. *Ann Ig, 25*(1), 31-42.

Park, S., Wang, D. H., Zhang, D., Romberg, E., & Arola, D. (2008). Mechanical properties of human enamel as a function of age and location in the tooth. *J Mater Sci Mater Med, 19*(6), 2317-2324.

Parker, A. S., Patel, A. N., Al Botros, R., Snowden, M. E., McKelvey, K., Unwin, P. R., . . . Peruffo, M. (2014). Measurement of the efficacy of calcium silicate for the protection and repair of dental enamel. *J Dent, 42 Suppl 1*, S21-29.

Paschos, E., Geiger, F. J., Malyk, Y., Rudzki, I., Wichelhaus, A., & Ilie, N. (2016). Efficacy of four preventive measures against enamel demineralization at the bracket periphery-comparison of microhardness and confocal laser microscopy analysis. *Clin Oral Investig, 20*(6), 1355-1366.

Pelka, M., Trautmann, S., Petschelt, A., & Lohbauer, U. (2010). Influence of air-polishing devices and abrasives on root dentin-an in vitro confocal laser scanning microscope study. *Quintessence Int, 41*(7), e141-148.

Petersilka, G. J., Ehmke, B., & Flemmig, T. F. (2002). Antimicrobial effects of mechanical debridement. *Periodontol 2000, 28*, 56-71.

Piangprach, T., Hengtrakool, C., Kukiattrakoon, B., & Kedjarune-Leggat, U. (2009). The effect of salivary factors on dental erosion in various age groups and tooth surfaces. *J Am Dent Assoc, 140*(9), 1137-1143.

Picos, A., Chisnoiu, A., & Dumitrasc, D. L. (2013). Dental erosion in patients with gastroesophageal reflux disease. *Advances in Clinical and Experimental Medicine, 22*(3), 303-307.

Piekarz, C., Ranjitkar, S., Hunt, D., & McIntyre, J. (2008). An in vitro assessment of the role of Tooth Mousse in preventing wine erosion. *Aust Dent J, 53*(1), 22-25.

Pierce, M. C., Strasswimmer, J., Park, H., Cense, B., & de Boer, J. F. (2004). Birefringence measurements in human skin using polarization-sensitive optical coherence tomography. *Journal of Biomedical Optics, 9*(2), 287-292.

Pigman, W., Elliott, H. C., Jr., & Laffre, R. O. (1952). An artificial mouth for caries research. *J Dent Res, 31*(5), 627-633.

Pigman, W., & Newbrun, E. (1962). Evaluation of anticaries agents by the use of the artificial mouth. *J Dent Res, 41*(6), 1304-1311.

Pizzo, G., Piscopo, M. R., Pizzo, I., & Giuliana, G. (2007). Community water fluoridation and caries prevention: a critical review. *Clin Oral Investig, 11*(3), 189-193.

Poggio, C., Lombardini, M., Dagna, A., Chiesa, M., & Bianchi, S. (2009). Protective effect on enamel demineralization of a CPP-ACP paste: an AFM in vitro study. *J Dent, 37*(12), 949-954.

Poggio, C., Lombardini, M., Vigorelli, P., & Ceci, M. (2013). Analysis of dentin/enamel remineralization by a CPP-ACP paste: AFM and SEM study. *Scanning, 35*(6), 366-374.

Poneros, J. M., Brand, S., Bouma, B. E., Tearney, G. J., Compton, C. C., & Nishioka, N. S. (2001). Diagnosis of specialized intestinal metaplasia by optical coherence tomography. *Gastroenterology, 120*(1), 7-12.

Popescu, D. P., Sowa, M. G., Hewko, M. D., & Choo-Smith, L. P. (2008). Assessment of early demineralization in teeth using the signal attenuation in optical coherence tomography images. *J Biomed Opt, 13*(5), 054053.

Potsaid, B., Baumann, B., Huang, D., Barry, S., Cable, A. E., Schuman, J. S., . . . Fujimoto, J. G. (2010). Ultrahigh speed 1050nm swept source/Fourier domain OCT retinal and anterior segment imaging at 100,000 to 400,000 axial scans per second. *Opt Express, 18*(19), 20029-20048.

Potsaid, B., Gorczynska, I., Srinivasan, V. J., Chen, Y., Jiang, J., Cable, A., & Fujimoto, J. G. (2008). Ultrahigh speed spectral/Fourier domain OCT ophthalmic imaging at 70,000 to 312,500 axial scans per second. *Opt Express, 16*(19), 15149-15169.

Prestes, L., Souza, B. M., Comar, L. P., Salomao, P. A., Rios, D., & Magalhaes, A. C. (2013). In situ effect of chewing gum containing CPP-ACP on the mineral precipitation of eroded bovine enamel-a surface hardness analysis. *J Dent, 41*(8), 747-751.

Pretty, I. A., Edgar, W. M., & Higham, S. M. (2004). The validation of quantitative light-induced fluorescence to quantify acid erosion of human enamel. *Arch Oral Biol, 49*(4), 285-294.

Pretty, I. A., Tavener, J. A., Browne, D., Brettle, D. S., Whelton, H., & Ellwood, R. P. (2006). Quantification of dental fluorosis using fluorescence imaging. *Caries Res, 40*(5), 426-434.

Rahim, Z. H. A., Fathilah, A. R., Irwan, S., & Wan Nordini Hasnor, W. I. (2008). An Artificial mouth system (NAM Model) for oral biofilm research. *Research Journal of Microbiology, 3*(6), 466 - 473.

Rakhmatullina, E., Bossen, A., Hoschele, C., Wang, X., Beyeler, B., Meier, C., & Lussi, A. (2011). Application of the specular and diffuse reflection analysis for in vitro diagnostics of dental erosion: correlation with enamel softening, roughness, and calcium release. *J Biomed Opt, 16*(10), 107002.

Ramos-Oliveira, T. M., Silva, C. V., Nunes, P. M., Turssi, C. P., Rechmann, P., & Freitas, P. M. (2017). AmF/NaF/SnCl2 solution reduces in situ enamel erosion -

profilometry and cross-sectional nanoindentation analysis. *Braz Oral Res, 31*(0), e20.

Ranjitkar, S., Kaidonis, J. A., Townsend, G. C., Vu, A. M., & Richards, L. C. (2008). An in vitro assessment of the effect of load and pH on wear between opposing enamel and dentine surfaces. *Arch Oral Biol, 53*(11), 1011-1016.

Ranjitkar, S., Rodriguez, J. M., Kaidonis, J. A., Richards, L. C., Townsend, G. C., & Bartlett, D. W. (2009). The effect of casein phosphopeptide-amorphous calcium phosphate on erosive enamel and dentine wear by toothbrush abrasion. *J Dent, 37*(4), 250-254.

Ratheesh Kumar, M., Murukeshan, V. M., Seah, L. K., & Shearwood, C. (2015). *Quantification of biofilm thickness using a swept source based optical coherence tomography system.* Paper presented at the The International Society for Optical Engineering · April 2015.

Razak, F. A., & Rahim, Z. H. (2003). The anti-adherence effect of Piper betle and Psidium guajava extracts on the adhesion of early settlers in dental plaque to saliva-coated glass surfaces. *J Oral Sci, 45*(4), 201-206.

Rees, J., Hughes, J., & Innes, C. (2002). An in vitro assessment of the erosive potential of some white wines. *Eur J Prosthodont Restor Dent, 10*(1), 37-42.

Rees, J., Loyn, T., & McAndrew, R. (2005). The acidic and erosive potential of five sports drinks. *Eur J Prosthodont Restor Dent, 13*(4), 186-190.

Rehder Neto, F. C., Maeda, F. A., Turssi, C. P., & Serra, M. C. (2009). Potential agents to control enamel caries-like lesions. *J Dent, 37*(10), 786-790.

Ren, Y. F., Amin, A., & Malmstrom, H. (2009). Effects of tooth whitening and orange juice on surface properties of dental enamel. *J Dent, 37*(6), 424-431.

Ren, Y. F., Zhao, Q., Malmstrom, H., Barnes, V., & Xu, T. (2009). Assessing fluoride treatment and resistance of dental enamel to soft drink erosion in vitro: applications of focus variation 3D scanning microscopy and stylus profilometry. *J Dent, 37*(3), 167-176.

Rimayanti, U., Kiuchi, Y., & Maulidia, R. (2014). The Development and Applications of Optical Coherence Tomography. *Austin J Clin Ophthalmol. 2014;1(7): 1032., 1*(7), 1032.

Rios, D., Honorio, H. M., Magalhaes, A. C., Buzalaf, M. A., Palma-Dibb, R. G., Machado, M. A., & da Silva, S. M. (2006). Influence of toothbrushing on enamel softening and abrasive wear of eroded bovine enamel: an in situ study. *Braz Oral Res, 20*(2), 148-154.

Rios, D., Honorio, H. M., Magalhaes, A. C., Delbem, A. C., Machado, M. A., Silva, S. M., & Buzalaf, M. A. (2006). Effect of salivary stimulation on erosion of human and bovine enamel subjected or not to subsequent abrasion: an in situ/ex vivo study. *Caries Res, 40*(3), 218-223.

Roberson, T., Heymann, H. O., & Swift Jr, E. J. (2006). *Sturdevant's Art and Science of Operative Dentistry*: Elsevier Health Sciences.

Robinson, C., Connell, S., Kirkham, J., Brookes, S. J., Shore, R. C., & Smith, A. M. (2004). The effect of fluoride on the developing tooth. *Caries Res, 38*(3), 268-276.

Rodriguez, J. M., & Bartlett, D. W. (2011). The dimensional stability of impression materials and its effect on in vitro tooth wear studies. *Dent Mater, 27*(3), 253-258.

Rosten, A., & Newton, T. (2017). The impact of bulimia nervosa on oral health: A review of the literature. *Br Dent J, 223*(7), 533-539.

Russell, C., & Coulter, W. A. (1975). Continuous monitoring of pH and Eh in bacterial plaque grown on a tooth in an artificial mouth. *Appl Microbiol, 29*(2), 141-144.

Ryge, G., & Snyder, M. (1973). Evaluating the clinical quality of restorations. *J Am Dent Assoc, 87*(2), 369-377.

Rytomaa, I., Jarvinen, V., Kanerva, R., & Heinonen, O. P. (1998). Bulimia and tooth erosion. *Acta Odontol Scand, 56*(1), 36-40.

Sadr, A., Mandurah, M., Nakashima, S., Shimada, Y., Kitasako, Y., Tagami, J., & Sumi, Y. (2013). *Monitoring of enamel lesion remineralization by optical coherence tomography: an alternative approach towards signal analysis.* Paper presented at the Lasers in Dentistry XIX.

Saerah, N. B., Ismail NM, L, N., & AR, I. (2006). Prevalence of tooth wear among 16-year-old secondary school children in Kota Bharu. *Arch Orofac Sci, 1*, 21-28.

Sahni, K., Khashai, F., Forghany, A., Krasieva, T., & Wilder-Smith, P. (2016). Exploring Mechanisms of Biofilm Removal. *Dentistry (Sunnyvale), 6*(4).

Sahyoun, C. C. (2016). *Optical coherence tomography for early detection of dental diseases: in vitro and in vivo feasibility studies.* Rutgers University-Graduate School-New Brunswick.

Saini, R., Saini, S., & Sharma, S. (2011). Biofilm: A dental microbial infection. *J Nat Sci Biol Med, 2*(1), 71-75.

Santos, E., Meira, I. A., Sousa, E. T., Amaechi, B. T., Sampaio, F. C., & Oliveira, A. F. B. (2019). Erosive potential of soy-based beverages on dental enamel. *Acta Odontol Scand*, 1-7.

Santos, N. C., & Castanho, M. A. (2004). An overview of the biophysical applications of atomic force microscopy. *Biophys Chem, 107*(2), 133-149.

Savas, S., Kavrik, F., & Kucukyilmaz, E. (2016). Evaluation of the remineralization capacity of CPP-ACP containing fluoride varnish by different quantitative methods. *J Appl Oral Sci, 24*(3), 198-203.

Schemehorn, B. R., Orban, J. C., Wood, G. D., Fischer, G. M., & Winston, A. E. (1999). Remineralization by fluoride enhanced with calcium and phosphate ingredients. *J Clin Dent, 10*(1 Spec No), 13-16.

Schlueter, N., Ganss, C., De Sanctis, S., & Klimek, J. (2005). Evaluation of a profilometrical method for monitoring erosive tooth wear. *Eur J Oral Sci, 113*(6), 505-511.

Schlueter, N., Hara, A., Shellis, R. P., & Ganss, C. (2011). Methods for the measurement and characterization of erosion in enamel and dentine. *Caries Res, 45 Suppl 1*, 13-23.

Schmitt, J. M., Xiang, S. H., & Yung, K. M. (1999). Speckle in optical coherence tomography. *J Biomed Opt, 4*(1), 95-105.

Schuman, J. S. (2008). Spectral domain optical coherence tomography for glaucoma (an AOS thesis). *Trans Am Ophthalmol Soc, 106*, 426-458.

Scolaro, L., McLaughlin, R. A., Klyen, B. R., Wood, B. A., Robbins, P. D., Saunders, C. M., . . . Sampson, D. D. (2012). Parametric imaging of the local attenuation coefficient in human axillary lymph nodes assessed using optical coherence tomography. *Biomed Opt Express, 3*(2), 366-379.

Selwitz, R. H., Ismail, A. I., & Pitts, N. B. (2007). Dental caries. *Lancet, 369*(9555), 51-59.

Shaw, L., & Smith, A. J. (1999). Dental erosion--the problem and some practical solutions. *Br Dent J, 186*(3), 115-118.

Shellis, R. P., & Addy, M. (2014). The interactions between attrition, abrasion and erosion in tooth wear. *Monogr Oral Sci, 25*, 32-45.

Shellis, R. P., Barbour, M. E., Jesani, A., & Lussi, A. (2013). Effects of buffering properties and undissociated acid concentration on dissolution of dental enamel in relation to pH and acid type. *Caries Res, 47*(6), 601-611.

Shellis, R. P., Ganss, C., Ren, Y., Zero, D. T., & Lussi, A. (2011). Methodology and models in erosion research: discussion and conclusions. *Caries Res, 45 Suppl 1*, 69-77.

Shellis, R. P., Wahab, F. K., & Heywood, B. R. (1993). The hydroxyapatite ion activity product in acid solutions equilibrated with human enamel at 37 degrees C. *Caries Res, 27*(5), 365-372.

Shen, P., Cai, F., Nowicki, A., Vincent, J., & Reynolds, E. C. (2001). Remineralization of enamel subsurface lesions by sugar-free chewing gum containing casein phosphopeptide-amorphous calcium phosphate. *J Dent Res, 80*(12), 2066-2070.

Shimada, Y., Nakagawa, H., Sadr, A., Wada, I., Nakajima, M., Nikaido, T., . . . Sumi, Y. (2014). Noninvasive cross-sectional imaging of proximal caries using swept-source optical coherence tomography (SS-OCT) in vivo. *J Biophotonics, 7*(7), 506-513.

Shimada, Y., Sadr, A., Burrow, M. F., Tagami, J., Ozawa, N., & Sumi, Y. (2010). Validation of swept-source optical coherence tomography (SS-OCT) for the diagnosis of occlusal caries. *J Dent, 38*(8), 655-665.

Shimada, Y., Sadr, A., Sumi, Y., & Tagami, J. (2015). Application of Optical Coherence Tomography (OCT) for Diagnosis of Caries, Cracks, and Defects of Restorations. *Curr Oral Health Rep, 2*(2), 73-80.

Shimamura, Y., Murayama, R., Kurokawa, H., Miyazaki, M., Mihata, Y., & Kmaguchi, S. (2011). Influence of tooth-surface hydration conditions on optical coherence-tomography imaging. *J Dent, 39*(8), 572-577.

Shinga-Ishihara, C., Nakai, Y., Milgrom, P., Soderling, E., Tolvanen, M., & Murakami, K. (2012). Xylitol carryover effects on salivary mutans streptococci after 13 months of chewing xylitol gum. *Caries Res, 46*(6), 519-522.

Shu, M., Wong, L., Miller, J. H., & Sissons, C. H. (2000). Development of multi-species consortia biofilms of oral bacteria as an enamel and root caries model system. *Arch Oral Biol, 45*(1), 27-40.

Silverstone, L. M., & Poole, D. F. (1969). Histologic and ultrastructural features of remineralized carious enamel. *J Dent Res, 48*(5), 766-770.

Singh, M., Singh, S., Nagpal, A., & Laller, S. (2015). Optical coherence tomography-a imaging modality in dentistry beyond x rays. *Int J Oral Maxillofac Res, 1*, 22-25.

Siqueira, W. L., Custodio, W., & McDonald, E. E. (2012). New insights into the composition and functions of the acquired enamel pellicle. *J Dent Res, 91*(12), 1110-1118.

Siqueira, W. L., Margolis, H. C., Helmerhorst, E. J., Mendes, F. M., & Oppenheim, F. G. (2010). Evidence of intact histatins in the in vivo acquired enamel pellicle. *J Dent Res, 89*(6), 626-630.

Sissons, C. H. (1997). Artificial dental plaque biofilm model systems. *Adv Dent Res, 11*(1), 110-126.

Sissons, C. H., Cutress, T. W., Hoffman, M. P., & Wakefield, J. S. (1991). A multi-station dental plaque microcosm (artificial mouth) for the study of plaque growth, metabolism, pH, and mineralization. *J Dent Res, 70*(11), 1409-1416.

Smith, B. G., & Knight, J. K. (1984). An index for measuring the wear of teeth. *Br Dent J, 156*(12), 435-438.

Smith, B. G., & Robb, N. D. (1989). Dental erosion in patients with chronic alcoholism. *J Dent, 17*(5), 219-221.

Smith, G. T., Dwork, N., O'Connor, D., Sikora, U., Lurie, K. L., Pauly, J. M., & Ellerbee, A. K. (2015). Automated, Depth-Resolved Estimation of the Attenuation Coefficient From Optical Coherence Tomography Data. *IEEE Trans Med Imaging, 34*(12), 2592-2602.

Soares, G. G., Magalhaes, P. A., Fonseca, A. B. M., Tostes, M. A., Silva, E. M. D., & Coutinho, T. C. L. (2017). Preventive Effect of CPP-ACPF Paste and Fluoride Toothpastes Against Erosion and Erosion Plus Abrasion In Vitro - A 3D Profilometric Analysis. *Oral Health Prev Dent, 15*(3), 269-277.

Socransky, S. S., & Haffajee, A. D. (2002). Dental biofilms: difficult therapeutic targets. *Periodontol 2000, 28*, 12-55.

Sowa, M. G., Popescu, D. P., Friesen, J. R., Hewko, M. D., & Choo-Smith, L. P. (2011). A comparison of methods using optical coherence tomography to detect demineralized regions in teeth. *J Biophotonics, 4*(11-12), 814-823.

Stenhagen, K. R., Hove, L. H., Holme, B., Taxt-Lamolle, S., & Tveit, A. B. (2010). Comparing different methods to assess erosive lesion depths and progression in vitro. *Caries Res, 44*(6), 555-561.

Stenhagen, K. R., Hove, L. H., Holme, B., & Tveit, A. B. (2013). The effect of daily fluoride mouth rinsing on enamel erosive/abrasive wear in situ. *Caries Res, 47*(1), 2-8.

Stocks, S. M. (2004). Mechanism and use of the commercially available viability stain, BacLight. *Cytometry A, 61*(2), 189-195.

Sudo, S. Z. (1977). Continuous culture of mixed oral flora on hydroxyapatite-coated glass beads. *Appl Environ Microbiol, 33*(2), 450-458.

Tang, G., Yip, H. K., Cutress, T. W., & Samaranayake, L. P. (2003). Artificial mouth model systems and their contribution to caries research: a review. *J Dent, 31*(3), 161-171.

Tantbirojn, D., Huang, A., Ericson, M. D., & Poolthong, S. (2008). Change in surface hardness of enamel by a cola drink and a CPP-ACP paste. *J Dent, 36*(1), 74-79.

Tezuka, H., Shimada, Y., Matin, K., Ikeda, M., Sadr, A., Sumi, Y., & Tagami, J. (2016). Assessment of cervical demineralization induced by Streptococcus mutans using swept-source optical coherence tomography. *J Med Imaging (Bellingham), 3*(1), 014504.

Thomas, M. S., Vivekananda Pai, A. R., & Yadav, A. (2015). Medication-related dental erosion: a review. *Compend Contin Educ Dent, 36*(9), 662-666; quiz 668.

Thurnheer, T., Gmur, R., & Guggenheim, B. (2004). Multiplex FISH analysis of a six-species bacterial biofilm. *J Microbiol Methods, 56*(1), 37-47.

Thurnheer, T., Rohrer, E., Belibasakis, G. N., Attin, T., & Schmidlin, P. R. (2014). Static biofilm removal around ultrasonic tips in vitro. *Clin Oral Investig, 18*(7), 1779-1784.

Todea, C., Negrutiu, M. L., Balabuc, C., Sinescu, C., Topala, F. I., Marcauteanu, C., . . . Podoleanu, A. G. (2010). Optical Coherence Tomography Applications in Dentistry. *TMJ, 60*(1), 5-17.

Tosun, G., Sener, Y., & Sengun, A. (2007). Effect of storage duration/solution on microshear bond strength of composite to enamel. *Dent Mater J, 26*(1), 116-121.

Turssi, C. P., Maeda, F. A., Messias, D. C., Neto, F. C., Serra, M. C., & Galafassi, D. (2011). Effect of potential remineralizing agents on acid softened enamel. *Am J Dent, 24*(3), 165-168.

Twetman, S. (2015). The evidence base for professional and self-care prevention--caries, erosion and sensitivity. *BMC Oral Health, 15 Suppl 1*, S4.

van der Meer, F. J., Faber, D. J., Baraznji Sassoon, D. M., Aalders, M. C., Pasterkamp, G., & van Leeuwen, T. G. (2005). Localized measurement of optical attenuation coefficients of atherosclerotic plaque constituents by quantitative optical coherence tomography. *IEEE Trans Med Imaging, 24*(10), 1369-1376.

Van der Veen, M., & de Jong, E. d. J. (2000). Application of quantitative light-induced fluorescence for assessing early caries lesions *Assessment of Oral Health* (Vol. 17, pp. 144-162): Karger Publishers.

van Rijkom, H. M., Truin, G. J., Frencken, J. E., Konig, K. G., van 't Hof, M. A., Bronkhorst, E. M., & Roeters, F. J. (2002). Prevalence, distribution and background variables of smooth-bordered tooth wear in teenagers in the hague, the Netherlands. *Caries Res, 36*(2), 147-154.

Vanichvatana, S., & Auychai, P. (2013). Efficacy of two calcium phosphate pastes on the remineralization of artificial caries: a randomized controlled double-blind in situ study. *Int J Oral Sci, 5*(4), 224-228.

Volgenant, C. M., van der Veen, M. H., de Soet, J. J., & ten Cate, J. M. (2013). Effect of metalloporphyrins on red autofluorescence from oral bacteria. *Eur J Oral Sci, 121*(3 Pt 1), 156-161.

Voronets, J., Jaeggi, T., Buergin, W., & Lussi, A. (2008). Controlled toothbrush abrasion of softened human enamel. *Caries Res, 42*(4), 286-290.

Voronets, J., & Lussi, A. (2010). Thickness of softened human enamel removed by toothbrush abrasion: an in vitro study. *Clin Oral Investig, 14*(3), 251-256.

Wagner, M., & Horn, H. (2017). Optical coherence tomography in biofilm research: A comprehensive review. *Biotechnol Bioeng, 114*(7), 1386-1402.

Wang, C. P., Huang, S. B., Liu, Y., Li, J. Y., & Yu, H. Y. (2014). The CPP-ACP relieved enamel erosion from a carbonated soft beverage: an in vitro AFM and XRD study. *Arch Oral Biol, 59*(3), 277-282.

Wang, X., Klocke, A., Mihailova, B., Tosheva, L., & Bismayer, U. (2008). New insights into structural alteration of enamel apatite induced by citric acid and sodium fluoride solutions. *Journal of Physical Chemistry B, 112*(29), 8840-8848.

Wang, X., Megert, B., Hellwig, E., Neuhaus, K. W., & Lussi, A. (2011). Preventing erosion with novel agents. *J Dent, 39*(2), 163-170.

Wang, X. J., Milner, T. E., de Boer, J. F., Zhang, Y., Pashley, D. H., & Nelson, J. S. (1999). Characterization of dentin and enamel by use of optical coherence tomography. *Appl Opt, 38*(10), 2092-2096.

Wang, Y., Bower, B. A., Izatt, J. A., Tan, O., & Huang, D. (2008). Retinal blood flow measurement by circumpapillary Fourier domain Doppler optical coherence tomography. *J Biomed Opt, 13*(6), 064003.

West, N. X., Hughes, J. A., & Addy, M. (2000). Erosion of dentine and enamel in vitro by dietary acids: the effect of temperature, acid character, concentration and exposure time. *J Oral Rehabil, 27*(10), 875-880.

West, N. X., Hughes, J. A., Parker, D. M., Newcombe, R. G., & Addy, M. (1999). Development and evaluation of a low erosive blackcurrant juice drink. 2. Comparison with a conventional blackcurrant juice drink and orange juice. *J Dent, 27*(5), 341-344.

West, N. X., Maxwell, A., Hughes, J. A., Parker, D. M., Newcombe, R. G., & Addy, M. (1998). A method to measure clinical erosion: the effect of orange juice consumption on erosion of enamel. *J Dent, 26*(4), 329-335.

West, N. X., Seong, J., Hellin, N., Eynon, H., Barker, M. L., & He, T. (2017). A clinical study to measure anti-erosion properties of a stabilized stannous fluoride dentifrice relative to a sodium fluoride/triclosan dentifrice. *Int J Dent Hyg, 15*(2), 113-119.

Wetton, S., Hughes, J., West, N., & Addy, M. (2006). Exposure time of enamel and dentine to saliva for protection against erosion: a study in vitro. *Caries Res, 40*(3), 213-217.

White, A. J., Yorath, C., ten Hengel, V., Leary, S. D., Huysmans, M. C., & Barbour, M. E. (2010). Human and bovine enamel erosion under 'single-drink' conditions. *Eur J Oral Sci, 118*(6), 604-609.

White, D. J., & Featherstone, J. D. (1987). A longitudinal microhardness analysis of fluoride dentifrice effects on lesion progression in vitro. *Caries Res, 21*(6), 502-512.

Wickens, J. L. (1999). Tooth surface loss. 6. Prevention and maintenance. *Br Dent J, 186*(8), 371-376.

Wiegand, A., & Attin, T. (2007). Occupational dental erosion from exposure to acids: a review. *Occup Med (Lond), 57*(3), 169-176.

Wiegand, A., Bichsel, D., Magalhaes, A. C., Becker, K., & Attin, T. (2009). Effect of sodium, amine and stannous fluoride at the same concentration and different pH on in vitro erosion. *J Dent, 37*(8), 591-595.

Wiegand, A., Wegehaupt, F., Werner, C., & Attin, T. (2007). Susceptibility of acid-softened enamel to mechanical wear--ultrasonication versus toothbrushing abrasion. *Caries Res, 41*(1), 56-60.

Wilder-Smith, C. H., Materna, A., Martig, L., & Lussi, A. (2015). Gastro-oesophageal reflux is common in oligosymptomatic patients with dental erosion: A pH-impedance and endoscopic study. *United European Gastroenterol J, 3*(2), 174-181.

Wilder-Smith, C. H., Materna, A., Martig, L., & Lussi, A. (2017). Longitudinal study of gastroesophageal reflux and erosive tooth wear. *BMC Gastroenterol, 17*(1), 113.

Wilder-Smith, C. H., Wilder-Smith, P., Kawakami-Wong, H., Voronets, J., Osann, K., & Lussi, A. (2009). Quantification of dental erosions in patients with GERD using optical coherence tomography before and after double-blind, randomized treatment with esomeprazole or placebo. *American Journal of Gastroenterology, 104*(11), 2788-2795.

Wilder-Smith, P., Lee, K., Guo, S., Zhang, J., Osann, K., Chen, Z., & Messadi, D. (2009). In vivo diagnosis of oral dysplasia and malignancy using optical coherence tomography: preliminary studies in 50 patients. *Lasers Surg Med, 41*(5), 353-357.

Willershausen, B., Callaway, A., Azrak, B., & Duschner, H. (2008). Influence of apple juice on human enamel surfaces of the first and second dentition-an in vitro study. *Eur J Med Res, 13*(7), 349-354.

Wong, I. Y., Koizumi, H., & Lai, W. W. (2011). Enhanced depth imaging optical coherence tomography. *Ophthalmic Surg Lasers Imaging, 42 Suppl*(4), S75-84.

Xie, H., Cook, G. S., Costerton, J. W., Bruce, G., Rose, T. M., & Lamont, R. J. (2000). Intergeneric communication in dental plaque biofilms. *J Bacteriol, 182*(24), 7067-7069.

Xu, H. H., Smith, D. T., Jahanmir, S., Romberg, E., Kelly, J. R., Thompson, V. P., & Rekow, E. D. (1998). Indentation damage and mechanical properties of human enamel and dentin. *J Dent Res, 77*(3), 472-480.

Yamanari, M., Lim, Y., Makita, S., & Yasuno, Y. (2009). Visualization of phase retardation of deep posterior eye by polarization-sensitive swept-source optical coherence tomography with 1-microm probe. *Opt Express, 17*(15), 12385-12396.

Yan-Fang, & Ren. (2011). Dental erosion: etiology, diagnosis and prevention. *31*(8).

Yaqoob, Z., Wu, J., & Yang, C. (2005). Spectral domain optical coherence tomography: a better OCT imaging strategy. *Biotechniques, 39*(6 Suppl), S6-13.

Yasuno, Y., Hong, Y., Makita, S., Yamanari, M., Akiba, M., Miura, M., & Yatagai, T. (2007). In vivo high-contrast imaging of deep posterior eye by 1-μm swept source optical coherence tomography and scattering optical coherence angiography. *Opt Express, 15*(10), 6121-6139.

Yip, H. K., Smales, R. J., & Kaidonis, J. A. (2002). Management of tooth tissue loss from erosion. *Quintessence Int, 33*(7), 516-520.

Young, A., Amaechi, B. T., Dugmore, C., Holbrook, P., Nunn, J., Schiffner, U., . . . Ganss, C. (2008). Current erosion indices--flawed or valid? Summary. *Clin Oral Investig, 12 Suppl 1*, S59-63.

Young, A., & Tenuta, L. M. (2011). Initial erosion models. *Caries Res, 45 Suppl 1*, 33-42.

Young, A., Thrane, P. S., Saxegaard, E., Jonski, G., & Rolla, G. (2006). Effect of stannous fluoride toothpaste on erosion-like lesions: an in vivo study. *Eur J Oral Sci, 114*(3), 180-183.

Yun, S., Tearney, G., de Boer, J., Iftimia, N., & Bouma, B. (2003). High-speed optical frequency-domain imaging. *Opt Express, 11*(22), 2953-2963.

Yun, S. H., Tearney, G., de Boer, J., & Bouma, B. (2004). Motion artifacts in optical coherence tomography with frequency-domain ranging. *Opt Express, 12*(13), 2977-2998.

Zaura-Arite, E., van Marle, J., & ten Cate, J. M. (2001). Conofocal microscopy study of undisturbed and chlorhexidine-treated dental biofilm. *J Dent Res, 80*(5), 1436-1440.

Zero, D. T. (1995). In situ caries models. *Adv Dent Res, 9*(3), 214-230; discussion 231-214.

Zero, D. T. (1996). Etiology of dental erosion--extrinsic factors. *Eur J Oral Sci, 104*(2 (Pt 2)), 162-177.

Zero, D. T., & Lussi, A. (2005). Erosion--chemical and biological factors of importance to the dental practitioner. *Int Dent J, 55*(4 Suppl 1), 285-290.

Zero, D. T., & Lussi, A. (2006). Behavioral factors. *Monogr Oral Sci, 20*, 100-105.

Zhang, Y., Arsecularatne, J. A., & Hoffman, M. (2015). The effects of three different food acids on the attrition-corrosion wear of human dental enamel. *Journal of Physics D: Applied Physics, 48*(28), 285401.

Zheng, J., Huang, H., Shi, M. Y., Zheng, L., Qian, L. M., & Zhou, Z. R. (2011). In vitro study on the wear behaviour of human tooth enamel in citric acid solution. *Wear, 271*(9-10), 2313-2321.

Zhou, S. L., Zhou, J., Watanabe, S., Watanabe, K., Wen, L. Y., & Xuan, K. (2012). In vitro study of the effects of fluoride-releasing dental materials on remineralization in an enamel erosion model. *J Dent, 40*(3), 255-263.

Zhou, X., & Li, Y. (2015). *Atlas of Oral Microbiology: From Healthy Microflora to Disease*: Academic Press.

Zijnge, V., van Leeuwen, M. B., Degener, J. E., Abbas, F., Thurnheer, T., Gmur, R., & Harmsen, H. J. (2010). Oral biofilm architecture on natural teeth. *PLoS One, 5*(2), e9321.

Zou, L., Cherukara, G., Hao, P., Seymour, K., & Samarawickrama, D. (2009). Geometrics of tooth wear. *Wear, 266*(5), 605-608.

LIST OF PUBLICATIONS AND PAPERS PRESENTED

1. Abdul Aziz, A., Zakian, C. M., Chew, H.P. The effect of water jet application on softened human enamel surfaces – an *in vitro* study. (Submitted)

2. Abdul Aziz, A., Gonzalez, M. A. G., Zakian, C. M., Chew, H.P., Yap, A. U. J. Impact of early biofilm on *in-vitro* measurement of initial enamel erosion using optical coherence tomography. (ongoing)

3. Abdul Aziz, A., Zakian, C. M., Chew, H.P. *In vivo* evaluation of initial enamel erosion using Optical Coherence Tomography. (ongoing)

Proceedings:

1. Abdul Aziz, A., Zakian, C. M., Chew, H. P. (August 2015). The effect of dental water jet application on softened human enamel surfaces – An *in vitro* study. Paper (poster) presented at the Hong Kong International Dental Expo and Symposium (HKIDEAS), Hong Kong.

2. Abdul Aziz, A., Chew, H. P. (July 2018). *In vivo* evaluation of initial enamel erosion using Optical Coherence Tomography (OCT). Paper (oral) presented at the 11th Postgraduate Conference 2018, Faculty of Dentistry, University of Malaya.

3. Abdul Aziz, A., Gonzalez, M. A. G, Chew, H. P. (September 2018). Effect of dental water jet on softened enamel and its efficacy in biofilm removal. Paper (poster) presented at the SEA-IADR 2018/32nd Annual Meeting Southeast Asian Division (IADR-SEAADE), Vietnam.